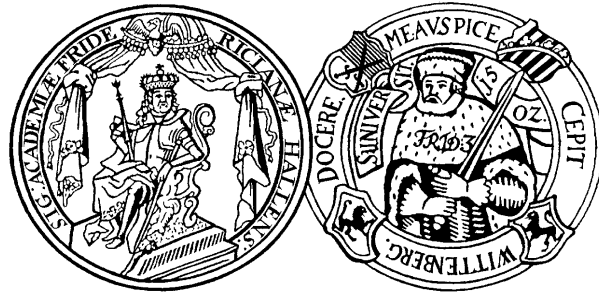


# Synthesis, EPR characterization and chitosan labelling of triarylmethyl radicals



## Dissertation

Zur Erlangung des akademischen Grades  
Doctor rerum naturalium (Dr. rer. nat.)

vorgelegt der

Naturwissenschaftlichen Fakultät I

Biowissenschaften

der Martin-Luther-Universität Halle-Wittenberg

von

**M.Sc. Marwa Aly El-metwaly Mohamed Elewa**

Geboren am 16. August 1982 in Port Said, Ägypten

Gutachter:

1. Prof. Dr. habil. Peter Imming
2. Prof. Dr. habil. Karsten Mäder
3. Prof. Dr. habil. Klaus Müller

Halle (Saale), den 30.07.2015

Verteidigt am 06.11.2015



*TO MARYAM &  
TAMER*



---

**Table of contents**

<b><i>Table of contents</i></b>	<b>A</b>
<b><i>List of abbreviations</i></b>	<b>E</b>
<b><i>Abstract</i></b>	<b>G</b>
<b>English version</b>	<b>G</b>
<b>German version</b>	<b>I</b>
<b>1. Introduction</b>	<b>1</b>
<b>1.1. Electron paramagnetic resonance (EPR)</b>	<b>1</b>
<b>1.2. Spin probes</b>	<b>5</b>
1.2.1. Tetrathia-TAM radicals as spin probes for oxygen, pH, redox status and thiol concentration measurements	7
1.2.1.1. Tetrathia-TAM radicals and oxygen mapping	7
1.2.1.2. Tetrathia-TAM radicals metabolism and reactions	11
1.2.1.3. Tetrathia-TAM radicals and interaction with biological macromolecules	15
1.2.1.4. Tetrathia-TAM radicals as pH-sensitive spin probes	16
1.2.1.5. Tetrathia-TAM radicals and redox status determination	19
1.2.1.6. Tetrathia-TAM radicals and thiol concentration measurement	20
1.2.1.7. Tetrathia-TAM radicals and superoxide radical measurement	21
1.2.2. Tetrachloro-TAM radicals	22
1.2.2.1. Synthesis of tetrachloro-TAM radicals	22
1.2.2.2. Stability of tetrachloro-TAM radicals	24
1.2.2.3. Reactivity of tetrachloro-TAM radicals	24
1.2.2.4. Different derivatives of tetrachloro-TAM radicals	25
1.2.2.5. Tetrachloro-TAM radicals as spin probes for various pharmaceutical applications	27
<b>1.3. Aim of the work</b>	<b>31</b>
<b>2. Tetrathiatriarylmethyl radicals</b>	<b>32</b>
<b>2.1. Introduction</b>	<b>32</b>
<b>2.2. Experimental</b>	<b>33</b>
2.2.1. Materials and general methods for synthesis and analytical characterization	33
2.2.2. Sample preparation for EPR spectroscopic characterization.	33
2.2.3. EPR spectroscopy	33
<b>2.3. Results and Discussion</b>	<b>33</b>

## Table of contents

---

2.3.1. Synthesis of different tetrathia-TAM radicals	33
2.3.2. Characterization of hydrophilic trityl radicals in aqueous solutions	35
2.3.2.1. Influence of ion strength, osmolarity, and pH value	35
2.3.2.2. Impact of viscosity	35
2.3.3. EPR spectroscopic characterization of lipophilic tetrathia-TAM radicals in an oily solution	36
2.3.4. Oxygen sensitivity	37
2.3.5. Encapsulation of tetrathia-TAM esters and properties of the resulting nanocapsules (NCs)	38
<b>2.4. Conclusion</b>	<b>39</b>
<b>2.5. Syntheses</b>	<b>39</b>
<b>3. Tetrachlorotriarylmethyl radicals</b>	<b>51</b>
<b>3.1. Introduction</b>	<b>51</b>
<b>3.2. Experimental</b>	<b>51</b>
3.2.1. Materials and general methods for synthesis and analytical characterization	51
3.2.2. Sample preparation for EPR spectroscopic characterization	51
3.2.3. EPR spectroscopy	51
<b>3.3. Results and Discussion</b>	<b>52</b>
3.3.1. Synthesis of different tetrachloro-TAM radicals	52
3.3.2. EPR characterization	53
3.3.3. Oxygen calibration of radicals 24 and 25 in an oily solution	55
3.3.4. Spin labelling of a nucleoside	56
<b>3.4. Syntheses</b>	<b>64</b>
<b>4. PTMTC and <sup>13</sup>C-PTMTC</b>	<b>83</b>
<b>4.1. Introduction</b>	<b>83</b>
<b>4.2. Experimental</b>	<b>83</b>
4.2.1. Materials and general methods for synthesis and analytical characterization	83
4.2.2. Sample preparation for EPR spectroscopic characterization	83
4.2.3. Continuous wave (CW-EPR) spectra	84
4.2.4. Pulse X-band EPR	84
<b>4.3. Results and discussion</b>	<b>84</b>
4.3.1. Synthesis of tetrachlorotriarylmethyl tricarboxylic acid (PTMTC) and its <sup>13</sup> C labelled analog ( <sup>13</sup> C-PTMTC)	84
4.3.2. EPR characterization	85
4.3.3. CW-EPR spectrum	86

## Table of contents

---

4.3.4. Influence of pH value on $^{13}\text{C}$ -PTMTC line width	87
4.3.5. Influence of viscosity on $^{13}\text{C}$ -PTMC line width	88
4.3.6. Influence of oxygen on PTMTC line width	89
4.3.7. Influence of temperature on $^{13}\text{C}$ -PTMTC line width	91
4.3.8. The accelerated aging (by increasing temperature) method	93
4.3.9. Cell lysate study	95
<b>4.4. Conclusion</b>	<b>95</b>
<b>4.5. Syntheses</b>	<b>96</b>
<b>5. Spin labelling of polymers (chitosan and carboxymethyl chitosan)</b>	<b>100</b>
<b>5.1. Introduction</b>	<b>100</b>
5.1.1. Structure of CS and CMC	100
5.1.2. Properties of CS and CMC	102
<b>5.2. Experimental</b>	<b>103</b>
5.2.1. Materials and general methods for synthesis and analytical characterization	103
5.2.2. Characterization of CS and CMC conjugates	103
5.2.2.1. UV-Vis spectroscopy	103
5.2.2.2. EPR measurements	103
<b>5.3. Results and discussion</b>	<b>103</b>
5.3.1. Preparation of CS and CMC conjugates	103
5.3.2. UV-Vis spectroscopy	104
5.3.3. EPR spectroscopy	106
<b>5.4. Conclusion</b>	<b>107</b>
<b>5.5. Syntheses</b>	<b>107</b>
<b>6. Tetraoxatriarylmethyl radicals</b>	<b>109</b>
<b>6.1. Introduction</b>	<b>109</b>
<b>6.2. Results and Discussion</b>	<b>110</b>
<b>6.3. Syntheses</b>	<b>114</b>
<b>7. Summary and Outlook</b>	<b>118</b>
<b>8. References</b>	<b>128</b>
<b>9. Appendices</b>	<b>1</b>

## Table of contents

---

<b>9.1. Materials</b>	<b>I</b>
<b>9.2. General methods for synthesis and analytical characterization</b>	<b>I</b>
<b>9.3. LDH-release and cell activity/proliferation</b>	<b>II</b>
<b>9.4. Acknowledgement</b>	<b>III</b>
<b>9.5. Curriculum vitae</b>	<b>IV</b>
<b>9.6. List of publications</b>	<b>V</b>
9.6.1. Research articles	V
9.6.2. Conference contributions	V
<b>9.7. Selbständigkeitserklärung</b>	<b>VI</b>



**List of abbreviations**

<b>BAECs</b>	Bovine aortic endothelial cells
<b>BMC</b>	Ballester/Molinet/Castañer reagent
<b>BSA</b>	Bovine serum albumin
<b>calcd.</b>	Calculated
<b>CW-EPR</b>	Continues wave electron paramagnetic resonance
<b>DCE</b>	Dichloroethane
<b>DCM</b>	Dichloromethane
<b>DiBoc</b>	Di- <i>tert</i> -butyl dicarbonate
<b>DLS</b>	Dynamic light scattering
<b>DMAP</b>	4-Dimethylaminopyridine
<b>DMSO</b>	Dimethyl sulfoxide
<b>DMTCI</b>	4,4'-Dimethoxytrityl chloride
<b>EA</b>	Ethyl acetate
<b>EDC</b>	1-(3-Dimethylaminopropyl)-3-ethylcarbodiimide hydrochloride
<b>EI</b>	Electron impact ionization
<b>EPR</b>	Electron paramagnetic resonance
<b>ESI</b>	Electron spray ionization
<b>Et<sub>2</sub>O</b>	Diethylether
<b>HFB</b>	Hexafluorobenzene
<b>Hunig's base</b>	<i>N,N</i> -Diisopropylethylamine
<b>IPM</b>	Isopropyl myristate
<b>IR</b>	Infrared spectra
<b>MCT</b>	Medium-chain triglycerides
<b>Mp</b>	Melting point
<b>MPLC</b>	Middle pressure liquid chromatography
<b>MS</b>	Mass spectrometry
<b><i>n</i>-BuLi</b>	<i>n</i> -Butyllithium
<b>NC</b>	Nanocapsules
<b>NHS</b>	<i>N</i> -Hydroxylsuccinimide
<b>NMR</b>	Nuclear magnetic resonance
<b>PB</b>	Phosphate buffer
<b>PBS</b>	Phosphate buffer saline

## List of abbreviations

---

<b>PdI</b>	Polydispersity index
<b>PE</b>	Petroleum ether, bp 40–60 °C
<b>PEG</b>	poly(ethylene glycol)
<b>PFCs</b>	Perfluorinated solvents
<b>PFOB</b>	Perfluorooctyl-bromide
<b>PLE</b>	Porcine liver esterase
<b>PPTS</b>	Pyridinium <i>p</i> -toluenesulfonate
<b>PVAc</b>	Poly(vinyl acetate)
<b>PyBob</b>	1 <i>H</i> -Benzotriazol-1-yloxytris(pyrrolidino)phosphonium hexafluorophosphate
<b>RT</b>	Room temperature
<b>TEA</b>	Triethylamine
<b>TEM</b>	Freeze-fracture transmission electron microscopy
<b>TFA</b>	Trifluoroacetic acid
<b>THF</b>	Tetrahydrofuran
<b>TLC</b>	Thin layer chromatography
<b>TMA</b>	Trimethylaluminium
<b>TMEDA</b>	Tetramethylethylenediamine
<b>UV</b>	Ultraviolet
<b>ΔB<sub>PP</sub></b>	Peak-to-peak line width

## Abstract

### English version

Electron paramagnetic resonance (EPR), also known as electron spin resonance (ESR), is a non-destructive analytical technique that can detect paramagnetic species with one or more unpaired electrons. Very useful information regarding the microenvironment of the spin probe can be extracted from EPR spectra with high sensitivity, *e.g.* molecular oxygen concentrations, micropolarity, microviscosity, pH values, and the distribution of the spin probe between different environments. EPR imaging (EPRI) is widely used in biomedical research to detect the distribution of free radicals in biological systems. EPR detection of endogenous paramagnetic species in biological systems is limited by the very low concentration as well as short half-life time of the spin probes. Therefore, exogenous spin probes are introduced into biological systems to enable EPR detection. Spin probes that are suitable for the EPR biological applications should be non-toxic, and stable in the biological systems. Additionally, they should have a good spectral response to the physiological parameters, and their half-life time is sufficient for the measurement. During the last few years, significant progress has been made to develop spin probes that cover the above-mentioned requirements with narrow and intense EPR signal. Triarylmethyl (TAM or trityl) radicals are paramagnetic spin probes, which are used in EPR spectroscopy and imaging. TAM radicals are known to be difficult to prepare. The aim of the project was to develop new and stable TAM radicals. The EPR signals of the synthesized radicals were characterized under different conditions (*e.g.* different pH values, oxygen contents and viscosities). Furthermore, the introduction of functional groups such as carboxylate prepared the radicals for further applications, for example, spin labelling of polymers and nucleotides.

Different derivatives of tetrathiatriarylmethyl (tetrathia-TAM) radicals were reproducibly synthesized. Hydrophilic radicals were investigated in aqueous environment in various viscosity and ionic strength, mimicking the different physiological conditions. In addition, lipophilic triesters were characterized in oily solution. The deuterated ethyl ester (radical **13**, **Fig. 2.1**) has an extremely narrow single EPR line under anoxic conditions, excellent oxygen sensitivity, and was used for further research focusing on the development of suitable pharmaceutical formulation. In addition, a variety of tetrachlorotriarylmethyl (tetrachloro-TAM) radicals were synthesized to investigate the substitution effect on the EPR signal. The hydrophilic 50%  $^{13}\text{C}$  labelled spin probe ( $^{13}\text{C}$ -PTMTC, **Fig. 4.1**) was prepared and EPR signal line width was investigated under different parameters of viscosity, oxygen content and pH.

The observed differential effects of oxygen content and viscosity on the line widths of the  $^{12}\text{C}$ -PTMTC and the  $^{13}\text{C}$ -PTMTC EPR signals suggest that this mixture of isotopic radicals could gain importance as a probe for both parameters. The hydrophilic radicals (**D-TAM** and **PTMTC**) were covalently attached to biopolymers of pharmaceutical interest, *e.g.* chitosan and carboxymethyl chitosan. EPR spectroscopy showed that the radical is still active after coupling with the biopolymer and that line widths after coupling with carboxymethyl chitosan were still narrow. Labelling of nucleoside with the trimethyl ester tetrachloro-TAM was achieved. However, EPR spectroscopy revealed that the radical was not active after coupling with nucleoside. Synthesis of triethyl ester of tetraoxatriarylmethane was optimized regarding to reaction conditions and yield. Nevertheless, conversion to the radical form was not successful and the carbocation was the formed product.

## German version

Die Elektronen Paramagnetisch Resonanz (EPR), auch als Elektronenspinresonanz (ESR) bekannt, ist eine nicht-destruktive analytische Technik. Mit Hilfe der EPR kann man paramagnetische Spezies (Spinsonden) mit einem oder mehreren ungepaarten Elektronen erkennen. Aus den gemessenen EPR-Spektren können mit hoher Empfindlichkeit sehr nützliche Informationen über die Mikroumgebung der Spinsonden erhalten werden. Beispiele hierfür sind die Konzentration von molekularem Sauerstoff, Micropolarität, Microviskosität, pH-Wert und die Verteilung der Spinsonden zwischen verschiedenen Umgebungen. EPR Imaging (EPRI) ist weit verbreitet in der biomedizinischen Forschung und wird eingesetzt, um die Verteilung von freien Radikalen in biologischen Systemen nachzuweisen. Die EPR-Erkennung von endogenen paramagnetischen Spezies in biologischen Systemen ist durch die sehr niedrige Konzentration sowie kurze Halbwertszeit dieser Spezies begrenzt. Daher werden exogene Spinsonden in biologische Systeme eingeführt, um einen EPR-Nachweis endogener paramagnetischer Substanzen zu ermöglichen. Spinsonden, die für biologische EPR Anwendungen geeignet sind, sollten nicht toxisch und stabil in den biologischen Systemen sein. Darüber hinaus sollten sie eine gute spektrale Reaktion auf die physiologischen Parameter zeigen und eine ausreichende Halbwertszeit für die Messungen haben. In den letzten Jahren wurde intensive Forschung betrieben, um Spinsonden zu entwickeln, die die oben genannten Anforderungen mit einem engen und intensiven EPR-Signal abdecken. Triarylmethylradikale (TAM-oder Trityl-Radikale) sind paramagnetisch Spinsonden, die für EPR-Spektroskopie und Bildgebung verwendet werden. TAM-Radikale sind für ihre schwierige Synthese bekannt. Ziel des Projekts war die Entwicklung von neuen und stabilen TAM-Radikalen. Die EPR-Signale der synthetisierten Radikale wurden unter verschiedenen Bedingungen charakterisiert (zB unterschiedliche pH-Werte, Sauerstoffgehalte und Viskositäten). Ferner wurden funktionelle Gruppen wie Carboxylat in die Radikale eingeführt, um diese für weitere Anwendungen, zB Spin-Labeling von Polymeren und Nukleotiden nutzbar zu machen.

Es konnten verschiedene Derivate von Tetrathiatriarylmethylradikalen (Tetrathia-TAM) reproduzierbar synthetisiert werden. Die hydrophilen Radikale wurden in wässriger Umgebung bei unterschiedlicher Viskosität und Ionenstärke untersucht, welche die verschiedenen physiologischen Bedingungen imitieren. Außerdem wurden die lipophilen Triester der entsprechenden TAM-Radikale in öliger Lösung charakterisiert. Der deuterierte Ethylester (Radikal **13**, **Abb. 2.1**) hat unter anoxischen Bedingungen eine extrem schmale Einzel EPR-Linie und eine sehr gute Sauerstoffempfindlichkeit. Daher wurde für die weitere Forschung der

Schwerpunkt auf der Entwicklung von geeigneten pharmazeutischen Formulierungen verwendet. Darüber hinaus wurden mehrere Tetrachlorotriarylmethylradikale (Tetrachloro-TAM) zur Untersuchung des Einflusses der Substitution auf das EPR-Signal synthetisiert. Die hydrophile 50%  $^{13}\text{C}$ -markierte Spinsonde ( $^{13}\text{C}$ -PTMTC, **Abb. 4.1**) wurde hergestellt und die Linienbreite des EPR-Signals wurde in Abhängigkeit der verschiedenen Parameter Viskosität, Sauerstoffgehalt und pH-Wert untersucht. Die beobachtete differentielle Effekte von Sauerstoffgehalt und Viskosität auf die Linienbreite der  $^{12}\text{C}$ -PTMTC und den  $^{13}\text{C}$ -PTMTC EPR-Signale deuten darauf hin, dass diese Mischung von isotopischen Radikalen als Sonde für beide Parameter verwendet werden könnten. Die hydrophilen Radikale (**D-TAM** und **PTMTC**) wurden kovalent an Biopolymere von pharmazeutischen Interesse, zB Chitosan und Carboxymethylchitosan gebunden. Die EPR-Spektroskopie zeigte, dass die Radikale nach Kopplung mit dem Biopolymer noch aktiv sind und, dass Linienbreiten nach Kopplung mit Carboxymethylchitosan weiterhin schmal blieb. Auch die Kopplung eines Nukleosids mit dem Trimethylester des Tetrachloro-TAM wurde erreicht. Jedoch ergab die EPR-Spektroskopie, dass die Radikale nach der Kopplung mit dem Nukleosid nicht mehr aktiv waren. Die Synthese der Triethylester aus Tetraoxatriarylmethan wurde hinsichtlich der Reaktionsbedingungen und des Ertrags optimiert. Allerdings war die Konversion des Triarylmethans zum freien Radikan nicht erfolgreich. Als Endprodukt wurde das Carbokation indentifiziert.

## 1. Introduction

### 1.1. Electron paramagnetic resonance (EPR)

Electron paramagnetic resonance (EPR), also known as electron spin resonance (ESR), is a non-destructive analytical technique that can detect paramagnetic species with one or more unpaired electrons. Paramagnetic species, spin probes, include free radicals and transition metal ions such as copper, iron, cobalt, molybdenum, manganese, and nickel. EPR study of a definite system depends on the presence of spin probes that are incorporated into the system either physically or through covalent binding (spin labelling technique).

Zavoisky discovered the EPR in 1944<sup>1</sup>, since then EPR has been involved in many research fields including chemistry, physics, biology and medicine as well as industrial research<sup>2,3</sup>.

#### EPR principles

A single electron is a negatively charged particle that is spinning around its own axis creating a magnetic field called spin magnetic moment. An unpaired electron acts as a tiny magnet (with north and south poles) with an electron spin quantum number of  $(S) = 1/2$ . Electron spins are randomly oriented in the absence of an external magnetic field, **Fig. 1.1A**. When an external magnetic field ( $B_0$ ) is applied, electron spins can either align parallel (magnetic quantum number  $(m_s) = -1/2$ ) or antiparallel ( $m_s = +1/2$ ) to the direction of the magnetic field, **Fig. 1.1B**. This phenomenon is known as Zeeman splitting.

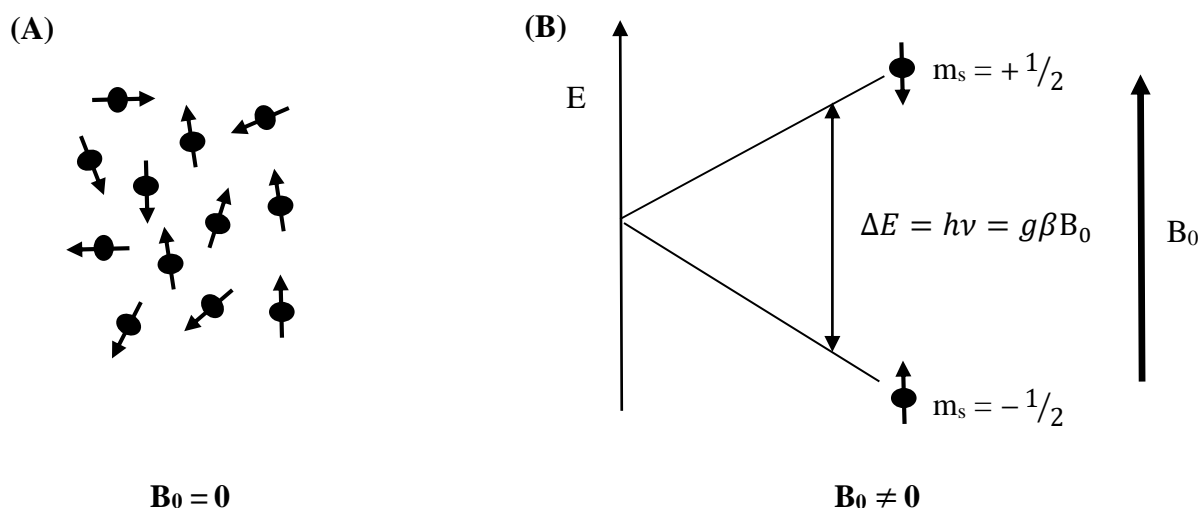


**Fig. 1.1** (A) Random orientation of electron spins in the absence of an external magnetic field ( $B_0 = 0$ ); (B) Zeeman splitting of energy levels for a single electron spin in the presence of external magnetic field ( $B_0 \neq 0$ ), lower energy level (parallel to the field) and upper energy level (antiparallel)<sup>4</sup>.

EPR is a type of absorption spectroscopy, where the energy absorption causes transition of electron spins from the ground to the excited state. According to Planck's law, the energy difference ( $\Delta E$ ) between the two states is proportional to the frequency of the applied magnetic field ( $\nu$ ) (**Equation 1**). The energy difference ( $\Delta E$ ) is dependent on the strength of the external applied magnetic field ( $B_0$ ).

**Equation 1** Planck's law of energy.

$$\Delta E = h\nu = g\beta B_0$$

Where  $h$  is the Planck's constant,  $g$  is the splitting factor or the g-factor that is indicating the contribution of spin and orbital movement of the electron to its total magnetic momentum (for a free electron,  $g = 2.00232$ ),  $\beta$  is the Bohr magneton, which is the unit of an electron's magnetic moment <sup>5</sup>.

Resonance condition, *i.e.* transition between lower and higher energy levels or  $180^\circ$  flipping of the electron spin, occurs when the absorbed energy is equal to the energy necessary for the transition between the two energy levels. Absorption is monitored and converted into a curve (**Fig. 1.2A**), phase sensitive detector in EPR spectrometers convert the absorption signal into the first derivative that is the commonly detected EPR signal, **Fig. 1.2B**.

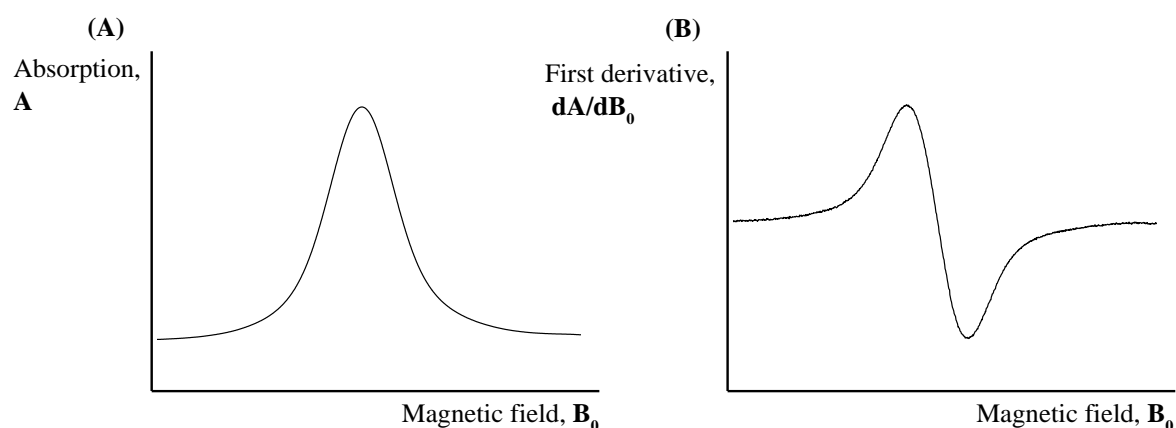


**Fig. 1.2** EPR signal: (A) Absorption curve; (B) Absorption first derivative curve.

Excited electrons at the higher energy level tend to turn back to the ground state with releasing the  $h\nu$  energy that is called spin relaxation process. There are two types of the spin relaxation process. The first is spin-lattice relaxation when the energy is released to the surrounding environment (lattice), and it is characterized by  $T_1$  relaxation time. The second is the spin-spin relaxation when the energy is exchanged to the nearby paramagnetic species, and



the process is characterized by  $T_2$  relaxation time. The width of the EPR line is inversely proportional to relaxation time  $T_2$ .

Interaction between the unpaired electron and the neighboring magnetic nuclei is known as hyperfine interaction, which results in splitting of the EPR spectrum that is called hyperfine splitting. Number of EPR spectrum lines ( $N$ ) is determined by the formula:  $N = 2nI + 1$ , where  $n$  is the number of nuclei, and  $I$  is the nuclear spin quantum number. **Table 1-1** shows  $I$  values of different isotopes.

**Table 1-1**  $I$  value of some isotopes

Isotope	$I$ value
$^1\text{H}$ , $^{13}\text{C}$ , $^{31}\text{P}$ , $^{15}\text{N}$ , $^{19}\text{F}$	$1/2$
$^2\text{H}$ , $^{14}\text{N}$	1
$^{12}\text{C}$ , $^{16}\text{O}$ , $^{32}\text{S}$	0

When unpaired electron couple with single nucleus ( $n = 1$ ) with nuclear spin ( $I = 1/2$ ), the spectrum shows splitting into two components with equal intensity separated by the hyperfine splitting constant ( $a$ ), **Fig. 1.3A**. When more than one nucleus ( $n > 1$ ) couple with the unpaired electron, the relative intensity of the spectrum lines follows a binomial distribution (**Table 1-2**).

**Table 1-2** Intensity ratio of EPR lines depending on nuclear spin ( $I$ ). (**Left**) when  $I = 1/2$ , (**Right**) when  $I = 1$ .

$n$	Relative intensity	$n$	Relative intensity
0	1	0	1
1	1 1	1	1 1 1
2	1 2 1	2	1 2 3 2 1
3	1 3 3 1	3	1 3 6 7 6 3 1
4	1 4 6 4 1	4	1 4 10 16 19 16 10 4 1
	$I = 1/2$		$I = 1$

As an example, one of the prepared radicals (radical **26**, section **3.3.1**) showed a quartet signal with internal ratio 1:3:3:1, due to coupling with three  $^{31}\text{P}$  (nuclear spin,  $I = 1/2$ ), **Fig. 1.3B**.

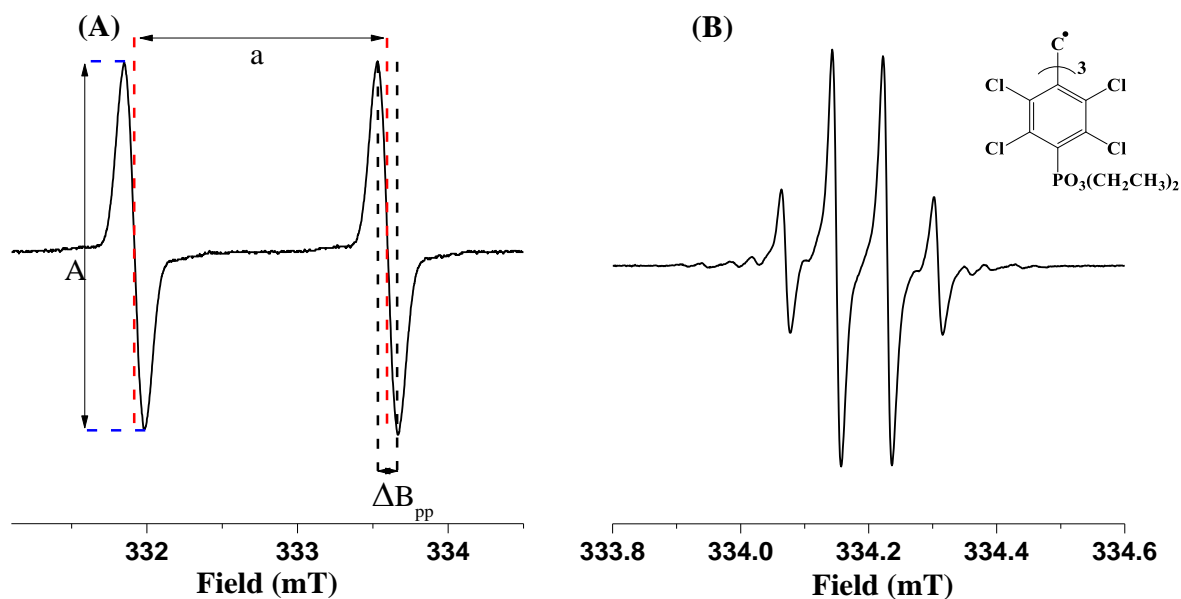


**Fig. 1.3** Hyperfine splitting of the EPR spectrum: **(A)**  $n = 1$  and  $I = 1/2$ . The spectrum appears as a doublet with equal intensities. The figure also shows the essential EPR spectral parameters: peak-to-peak line width ( $\Delta B_{PP}$ ), signal amplitude ( $A$ ), and hyperfine splitting constant ( $a$ ); **(B)**  $n = 3$ ,  $I = 1/2$ , the spectrum shows a quartet signal with internal ratio 1:3:3:1.

The most significant EPR parameters are: peak-to-peak line width ( $\Delta B_{PP}$ ), signal amplitude ( $A$ ), and hyperfine splitting constant (it is represented as  $a$  followed by a subscript of the splitting nucleus. In case of nitrogen the symbol is  $a_N$ , in case of phosphorus the symbol is  $a_P$ , etc.), **Fig. 1.3A**.

EPR spectroscopy is carried out either by continuous wave (CW-EPR) or pulsed spectrometers. In the CW-EPR, the most widely used method, low-intensity microwave radiation with a fixed frequency continuously irradiates the sample while the magnetic field is varied. In the pulsed-EPR, short high power microwave pulses are applied to the sample at constant magnetic field.

The sample to be studied is placed in the resonator cavity that is located between two magnets with variable magnetic field strength ( $B_0$ ). Microwave radiation with a fixed frequency is applied to the resonator, and the magnetic field strength is swept till resonance condition of the unpaired electron is reached. The energy absorption is detected, and EPR spectrum is displayed as the first derivative of the energy absorption with respect to the magnetic field.

**Fig. 1.4** represents a general layout of EPR spectrometer.

EPR spectrometers are classified according to the microwave frequency ranges into: L-band ( $\nu = 1\text{--}2$  GHz), S-band ( $\nu = 2\text{--}4$  GHz), X-band ( $\nu = 8\text{--}12$  GHz), K-band ( $\nu = 18\text{--}26$  GHz), Q-band ( $\nu = 30\text{--}50$  GHz) and W-band ( $\nu = 75\text{--}110$  GHz). By increasing frequency, the sensitivity

is increased but there are certain limitations, which are: the size of the resonator cavity is decreased, the penetration depth is decreased, and for water containing samples (such as biological samples) absorption of microwave radiation is increased. For biological studies only L-band and X-band are of interest.

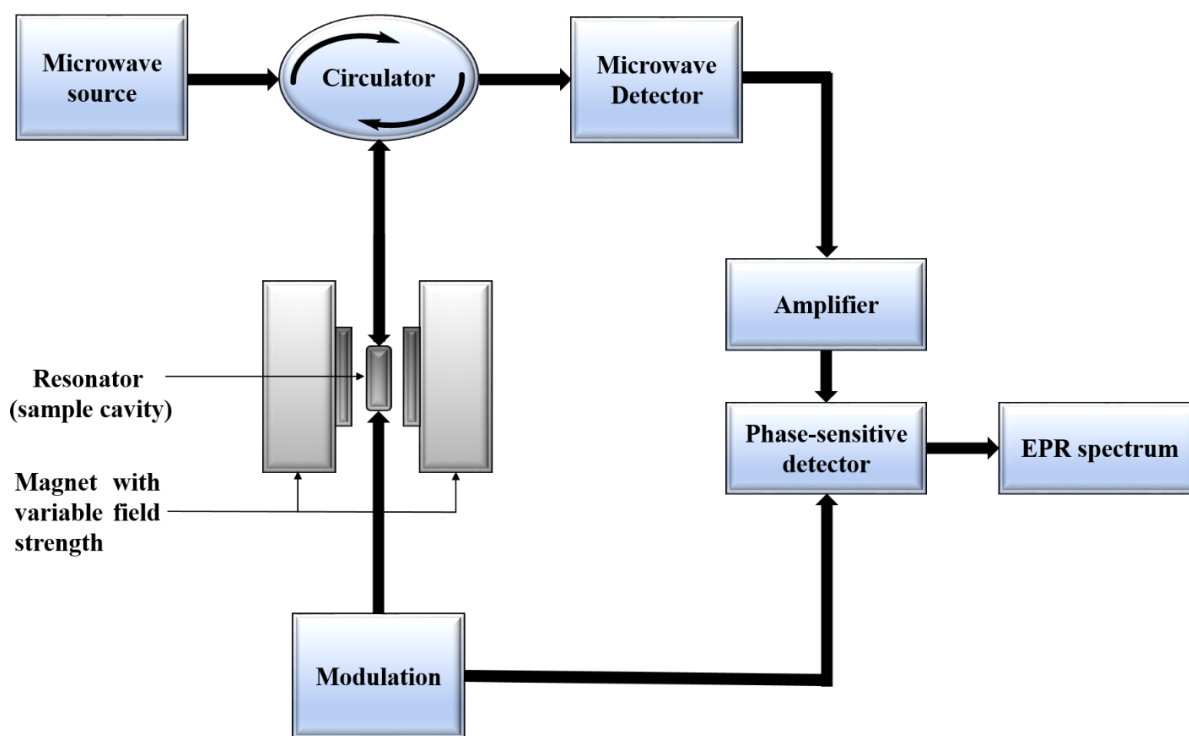


**Fig. 1.4** Schematic layout of the main components of an EPR spectrometer.

Very useful information regarding the microenvironment of the spin probe can be extracted from EPR spectra with high sensitivity, *e.g.* molecular oxygen concentrations, micropolarity, microviscosity, pH values, and the distribution of the spin probe between different environments<sup>6-11</sup>. EPR imaging (EPRI) is widely used in biomedical research to detect the distribution of free radicals in biological systems<sup>12,13</sup>. The effect of some of these parameters on the EPR spectrum is explained in the next sections.

## 1.2. Spin probes

EPR detection of endogenous paramagnetic species in biological systems is limited by its very low concentration as well as short half-life time. Therefore, exogenous spin probes are introduced into a biological system to enable EPR detection. Spin probes that are suitable for the biological applications of EPR should be harmless, stable in the biological system, have a good spectral response to the physiological parameters, and the half-life time is long enough for the measurement. During the last (few) years, significant progress has been made to develop

spin probes that cover the above-mentioned requirements with narrow and intense EPR signal. Triarylmethyl radicals are paramagnetic spin probes, which are used in EPR spectroscopy and imaging. The following sections will present different modification on the chemical structure of two families of triarylmethyl radicals, namely the tetrathiatriarylmethyl (tetrathia-TAM) radicals and tetrachlorotriarylmethyl (tetrachloro-TAM) radicals, and the subsequent EPR applications.

### Triarylmethyl radicals

Gomberg prepared the unsubstituted triarylmethyl radical in 1900<sup>14</sup>. Many limitations of the first triarylmethyl radical were reported such as: dimerization in solutions<sup>15,16</sup>, very fast reaction with oxygen and peroxide formation<sup>17,18</sup>, instability in presence of iodine or nitric oxide<sup>19</sup> in addition to hyperfine splitting resulted from interaction between aromatic hydrogen nuclei and the unpaired electron. In 1967, a new family of triarylmethyl radicals, the tetrachloro-TAM radicals where the aromatic hydrogen atoms were replaced with bulky chlorine atoms, was developed<sup>20</sup>. Steric shielding of the central (methyl) carbon by the six *ortho* chlorine atoms provides high chemical and thermal stability of these radicals<sup>21</sup>, **Fig. 1.5**.

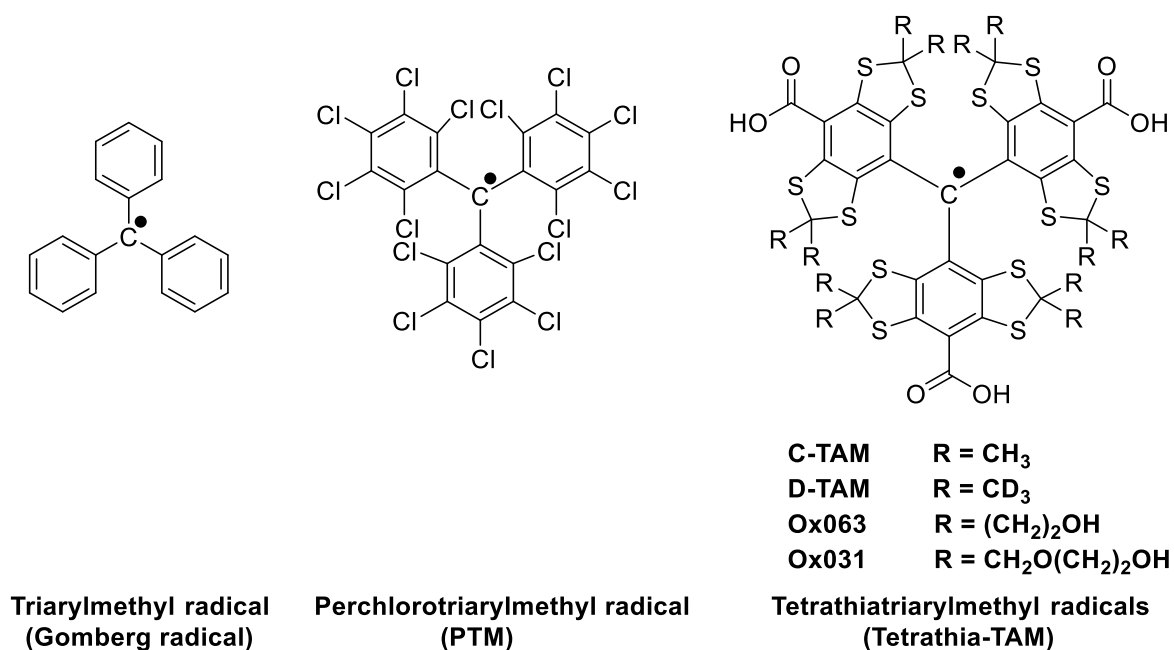


**Fig. 1.5** Chemical structure of different radicals.

The family of tetrathia-TAM radicals were first introduced by Nycomed innovation AB<sup>22-26</sup>. The chemical structure was designed to avoid hyperfine coupling of the unpaired electron with the hydrogen nuclei through replacement of hydrogen atoms that are close to the methyl radical center with alkylthio atoms, so that the hyperfine splitting and line broadening were

eliminated, and an extremely narrow line width was obtained allowing for higher sensitivity in the micromolar range. Furthermore, the methyl center of the unpaired electron is sterically protected to improve the stability of the radical. Tetrathia-TAM radicals display a propeller-like conformation because of steric hindrance <sup>27</sup>.

The most prominent members of this group are Finland TAM (also known as C-TAM), its deuterated analogue D-TAM, Ox063 and Ox031 bearing carboxylic acid groups, **Fig. 1.5**. The synthesis of this type of radicals was improved to enable large scale production of molar amounts <sup>28-31</sup>. Tetrathia-TAM radicals showed a very narrow single EPR signal, very good solubility in aqueous solutions (at neutral pH) in addition to - for a radical - relatively high stability in the presence of biological reducing reagents such as ascorbate and glutathione <sup>32,33</sup>.

These criteria enable the use of tetrathia-TAM radicals in many applications: *in-vivo* detection of radicals <sup>34</sup>, measurement of thiol concentrations <sup>35</sup>, measurement of extracellular <sup>36</sup> and intracellular <sup>6,37-39</sup> oxygen levels, specific detection of superoxide radical anion <sup>40-44</sup>, pH determination <sup>10,33,45-49</sup>, as well as analysis of redox status <sup>50,51</sup>. Tetrathia-TAM-based spin labels were used for distance measurement in nucleic acid <sup>52</sup>, site-directed spin labelling of proteins and nanometer distance measurements using pulsed dipolar EPR spectroscopy <sup>53,54</sup> and studies of molecular diffusion in microheterogeneous systems <sup>55</sup>. Tetrathia-TAM radicals were used for CW-EPRI applications <sup>56</sup>. Long relaxation times <sup>57,58</sup> made Tetrathia-TAM radicals attractive for pulsed EPRI <sup>59-63</sup>, proton-electron double-resonance imaging (PEDRI) <sup>49,64-67</sup>, hyperpolarized nuclear magnetic resonance (NMR) <sup>68</sup>, magnetic resonance imaging (MRI) <sup>25,69</sup>, and dynamic nuclear polarization (DNP) imaging <sup>65,70-72</sup>.

### **1.2.1. Tetrathia-TAM radicals as spin probes for oxygen, pH, redox status and thiol concentration measurements**

#### **1.2.1.1. Tetrathia-TAM radicals and oxygen mapping**

Molecular oxygen plays a critical role in cellular metabolism, and abnormal oxygen levels are involved in a number of diseases such as cancer and ischemic diseases <sup>73-75</sup>. As a result, the measurement of oxygen concentration *in-vitro* and *in-vivo* is essential to study many physiological and pathological processes. EPR spectroscopy is one of the various techniques for oxygen measurement using oxygen sensitive spin probes (EPR oximetry) <sup>76</sup>.

Molecular oxygen in its ground state has two unpaired electrons, which are responsible for its paramagnetic character <sup>77</sup>. However, dissolved oxygen can not be detected directly via EPR spectroscopy because of the very short relaxation time <sup>78</sup>. For this reason, EPR oximetry requires the use of an external oxygen-sensitive spin probe. Heisenberg spin exchange between

the paramagnetic oxygen and the spin probe shortens the relaxation time and the EPR signal becomes broader <sup>79</sup>. The extent of line width broadening is proportional to the oxygen content <sup>80</sup>. Therefore, the measured line width can be used to quantify the oxygen content, **Fig. 1.6**.

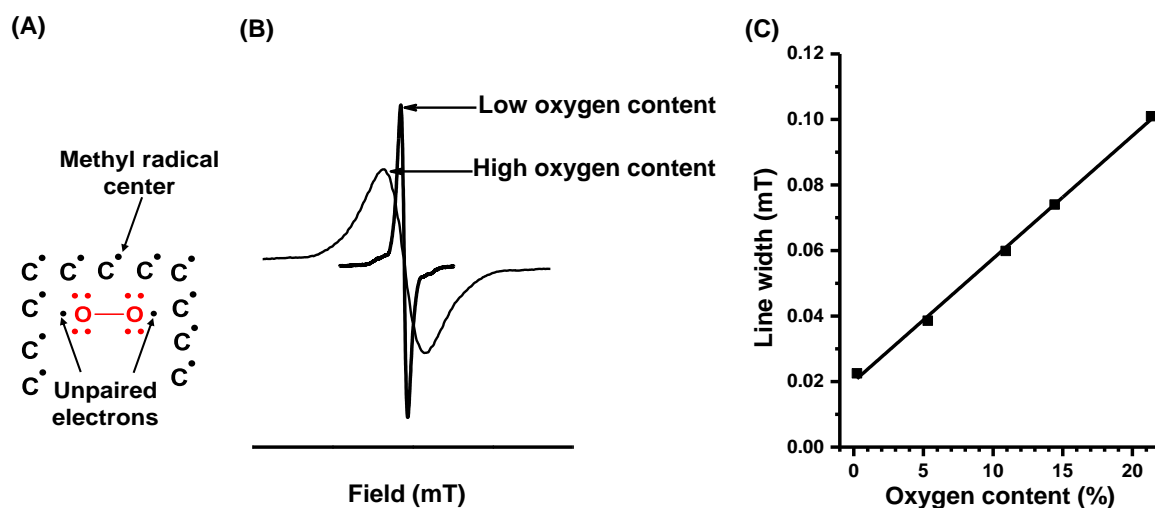


**Fig. 1.6** Oxygen interaction with radical spin probe: **(A)** Collision between oxygen molecule (with unpaired electrons) and the radical center; **(B)** EPR signal broadening at high oxygen content; **(C)** Linear relationship between line width and oxygen content, modified from Ref. <sup>5</sup>.

EPR oximetry enables oxygen quantification in biological systems without interference with the oxygen metabolism and with high selectivity, sensitivity, and non-invasiveness <sup>81,82</sup>.

Oximetric spin probes should have narrow line EPR signals, high oxygen sensitivity, stability, and low toxicity. There are two types of spin probes suitable for EPR oximetry: (1) particulate probes such as lithium phthalocyanine particles <sup>83,84</sup>, naphthalocyanine crystals <sup>85</sup>, carbonaceous materials (chars <sup>86</sup>, charcoals <sup>87,88</sup> and carbon blacks <sup>89</sup>) or India inks <sup>90</sup>; (2) soluble probes namely nitroxides <sup>91-94</sup> and tetrathia-TAM radicals <sup>22,65,95-100</sup>. Particulate probes were used for monitoring of oxygen partial pressure at the site of implantation with high sensitivity <sup>80,84</sup>.

Nitroxide radicals were used for oxygen mapping but their fast metabolic reduction into the EPR silent hydroxylamines (**Fig. 1.7**) as well as hyperfine splitting, and broad EPR signals limit their use <sup>101</sup>. The high water solubility (if they contain ionisable or polar groups), intracellular stability <sup>65</sup>, narrow line width and long relaxation time <sup>58</sup> as well as low toxicity <sup>70,96</sup> and oxygen dependent line width <sup>64,65</sup> make tetrathia-TAM radicals spin probes of choice for oximetric applications.

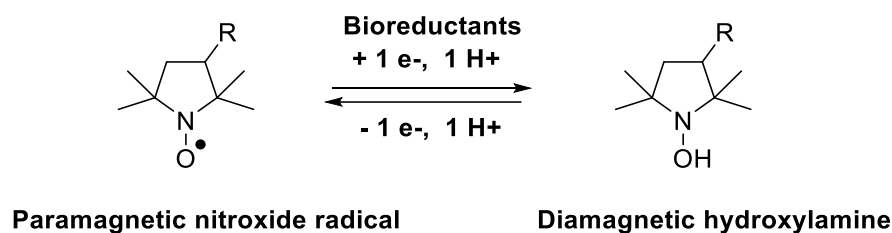


**Fig. 1.7** Bioreduction of nitroxide radical with bio-reductants (ascorbate, thiols, NADPH, etc.) into EPR silent hydroxylamine <sup>102</sup>.

Despite the high oxygen sensitivity, the presence of three carboxyl groups makes tetrathia-TAM radicals anionic at physiological pH values <sup>45</sup>. Consequently, intracellular permeability and *in-vivo* applications are limited. Different modifications of tetrathia-TAM structure were reported in order to overcome this limitation.

Liu et al. <sup>6</sup> prepared four tetrathia-TAM esters, **Fig. 1.8**. DMSO solutions of the esters showed broader line width (because of hyperfine coupling of the hydrogen atoms of the ester alkyl chain with the radical center) and higher oxygen sensitivity than C-TAM. Stability of the tetrathia-TAM esters against porcine liver esterase (PLE) was tested. Methyl and *tert*-butyl tetrathia-TAM esters (MT-03 and Bt-03) were stable while acetoxymethoxycarbonyl tetrathia-TAM esters (AMT-02 and AMT-03) showed enzymatic hydrolysis to the hydrophilic C-TAM. This means the ability of the hydrophobic radicals (AMT-02 and AMT-03) to cross the cell membrane and to be hydrolyzed into hydrophilic C-TAM that will be retained inside the cell allowed for intracellular oxygen concentration measurement. AMT-02 was evaluated as an intracellular oxygen sensitive spin probe in the presence of bovine aortic endothelial cells (BAECs) <sup>37</sup>. AMT-02 is a cell permeable spin probe with sharp and narrow signal because of intracellular hydrolysis into C-TAM, enabling intracellular oxygen measurement.

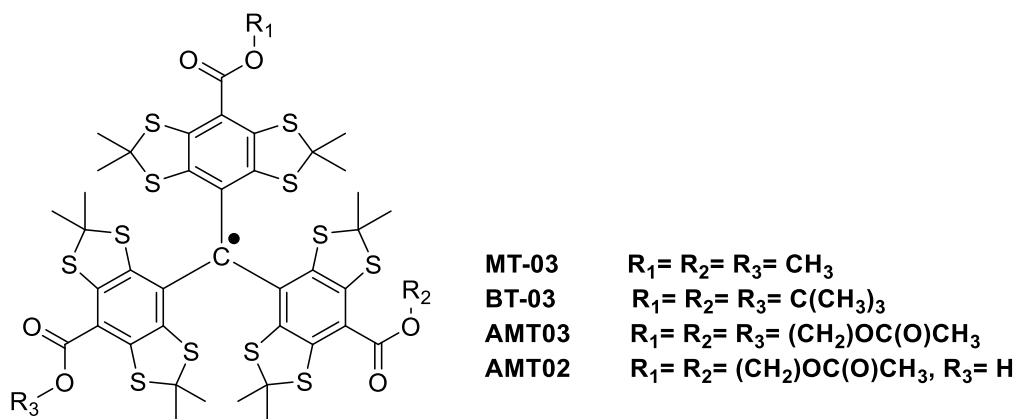


**Fig. 1.8** Chemical structure of tetrathia-TAM esters radicals <sup>6</sup>.

Perfluorinated solvents (PFCs) such as hexafluorobenzene (HFB) and perfluorooctylbromide (PFOB) are lipophilic solvents characterized by: lack of toxicity<sup>103</sup>, high oxygen solubility<sup>104</sup>, biocompatibility, and are used clinically as blood substitutes<sup>105</sup>. Sensitivity of line broadening induced by molecular oxygen is much higher in PFCs compared to water because of higher oxygen solubility<sup>106</sup>. The solubility of oxygen at atmospheric pressure (21% of oxygen) at 25 °C is 4.4 mM in HFB as compared to 0.27 mM in water<sup>107</sup>. Driesschaert et al.<sup>108</sup> designed two tetrathia-TAM structures (F15T-03 and F45T-03) with fluorinated side chains (15 or 45 fluorine atoms), **Fig. 1.9A**. F15T-03 and F45T-03 have high tendency to dissolve in PFCs. Nano-emulsions containing F15T-03 and F45T-03 dissolved in PFCs showed a substantial increase in oxygen sensitivity both *in-vitro* and *in-vivo* compared to C-TAM<sup>109</sup>.

Bobko et al.<sup>38</sup> described the synthesis of a new tetrathia-TAM radical (TAM-H) with one aldehyde and two carboxyl groups, **Fig. 1.9B**. The EPR spectroscopy showed a doublet signal because of the hyperfine interaction between the unpaired electrons with the aldehyde hydrogen directly attached to the *para* position of one of the aromatic rings. Comparing the oxygen sensitivity of Ox063 and TAM-H revealed that Ox063 is insensitive to oxygen partial pressures below 20 mm Hg while TAM-H is sensitive to very low concentration of oxygen down to 1 mm Hg. It was reported<sup>32</sup> that the presence of hydrogen on the aromatic ring decreases the stability of the trityl radical by making the intermediate more susceptible to O<sub>2</sub> addition at the aromatic carbon bearing the H. In case of TAM-H, the presence of aldehyde hydrogen did not interfere with the stability of the radical<sup>38</sup>.

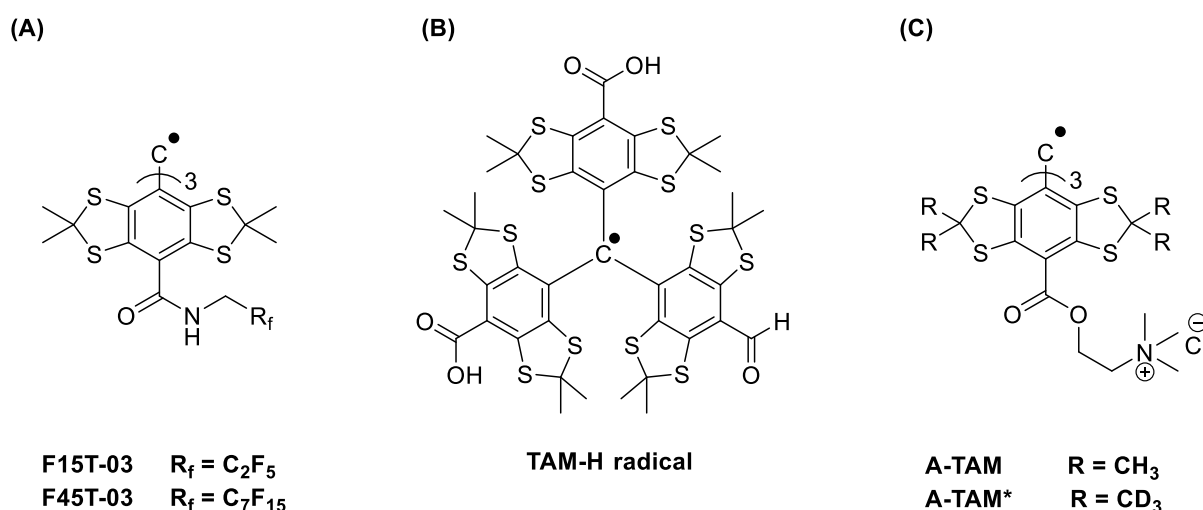


**Fig. 1.9** Chemical structure of tetrathia-TAM radicals: (A) with fluoride side chain<sup>108</sup>; (B) with two carboxyl and one aldehyde group (TAM-H radical)<sup>38</sup>; (C) with linkers<sup>110</sup>.

Substitution of 36 hydrogen atoms in C-TAM with deuterium in D-TAM was found to reduce the EPR signal line width and, hence, increase the EPR signal intensity. Although the



synthesis of D-TAM was described in patents <sup>22,65</sup>, the synthetic procedures were hard to reproduce. Dhimitruka et al. <sup>110</sup> described a modified scheme for the synthesis of D-TAM. In addition, the synthesis and EPR characterization of tetrathia-TAM derivatives with linkers was described, **Fig. 1.9C**. The presence of these linkers permits further structure modifications. In 2012, Komarov et al. <sup>39</sup> reported the first use of D-TAM for the non-invasive EPR oximetry of isolated perfused hearts.

Song et al. <sup>99</sup> described the synthesis of dendritic tetrathia-TAM derivatives (TG, TdG, dTdG and, dTdG-PEG). The authors used C-TAM and the deuterated analogue D-TAM as core, linked through non-deuterated or deuterated ester linkers with dendrons, **Fig. 1.10**. The design of these dendritic tetrathia-TAM derivatives aimed to reduce the EPR signal line width, enhance biological stability, and improve *in-vivo* oximetric applications. dTdG (with D-TAM core and deuterated ester linkers) has the smallest line width (62 mG under anaerobic conditions) and the highest oxygen sensitivity of 3.9 mG/% O<sub>2</sub>. Furthermore, dendritic tetrathia-TAM showed higher stability than C-TAM against several oxidants such as hydroxyl radical (HO•), peroxy radical, H<sub>2</sub>O<sub>2</sub>, peroxyxynitrite (ONOO), superoxide (O<sub>2</sub><sup>•-</sup>), iron(III) (Fe<sup>3+</sup>), and horse radish peroxidase (HRP)/H<sub>2</sub>O<sub>2</sub> as well as reducing agents such as iron(II) (Fe<sup>2+</sup>), glutathione (GSH), and ascorbic acid.

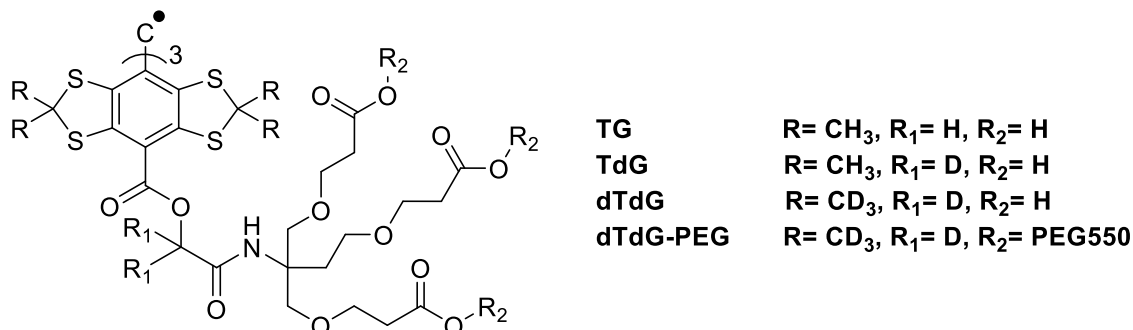


**Fig. 1.10** Chemical structure of dendritic tetrathia-TAM radicals <sup>99</sup>.

### 1.2.1.2. Tetrathia-TAM radicals metabolism and reactions

It was reported that Ox063 is stable in the presence of ascorbate, glutathione, or NADPH. However, disappearance of the EPR signal in the presence of superoxide (O<sub>2</sub><sup>•-</sup>) or alkylperoxyl (ROO•) was observed <sup>40</sup>. Decroos and co-authors reported the oxidative decarboxylation of C-TAM and Ox063 by O<sub>2</sub><sup>•-</sup> and ROO• with the formation of diamagnetic quinone-methide (QM) <sup>44</sup>. The reaction between C-TAM and O<sub>2</sub><sup>•-</sup> was monitored with UV-Vis spectroscopy. The characteristic band of C-TAM at 469 nm decayed with the formation of a new band at 542 nm. The new product was extracted and found to be a QM, **Fig. 1.11**.

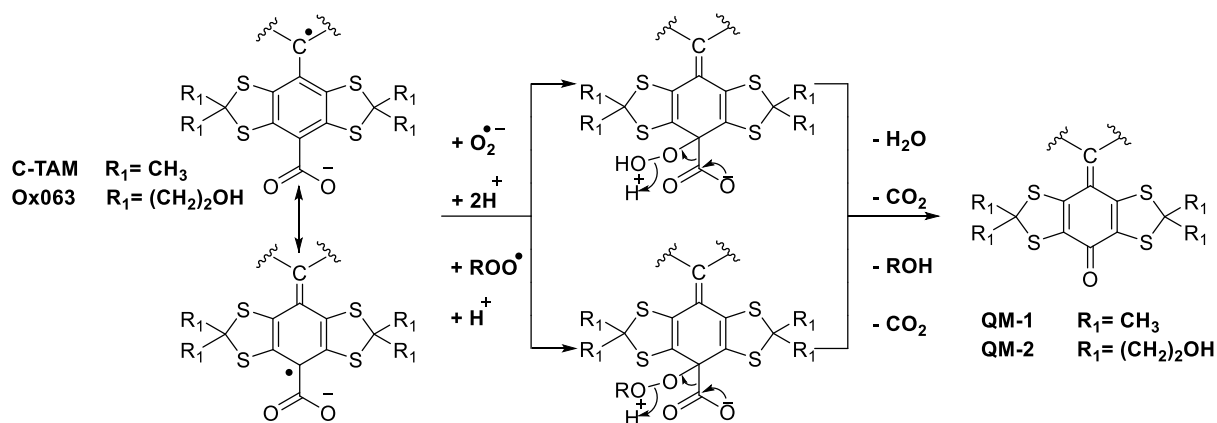


**Fig. 1.11** Oxidative decarboxylation of tetrathia-TAM radical with  $O_2^{\bullet-}$  or  $ROO^{\bullet}$ .<sup>44</sup>

Later, Decroos et al.<sup>111</sup> described the metabolic transformation of both C-TAM and Ox063 by liver microsomes/NADPH. Under aerobic conditions, liver microsomes/NADPH/ $O_2$  catalyzed the oxidative decarboxylation of tetrathia-TAM radicals into the corresponding diamagnetic QM. Under anaerobic conditions, liver microsomes/NADPH catalyzed the reduction of TAM radicals into the corresponding diamagnetic triarylmethane derivatives. In a subsequent publication, Decroos et al.<sup>112</sup> reported the ability of peroxidases to induce oxidative decarboxylation of C-TAM and Ox063 to QM by hydrogen peroxide ( $H_2O_2$ ) or alkylhydroperoxides. The reaction mechanism involved oxidation of the radical into the intermediate cation ( $TAM^+$ ) which has a characteristic UV-Vis band at 744 nm. The nucleophilic attack of deprotonated  $ROOH$  on aromatic carbon attached to a carboxylate group gave an intermediate, decarboxylation of this intermediate gave the QM, **Fig. 1.12**. The generation of the intermediate cation was chemically induced with potassium hexachloroiridate(IV) ( $K_2IrCl_6$ ).

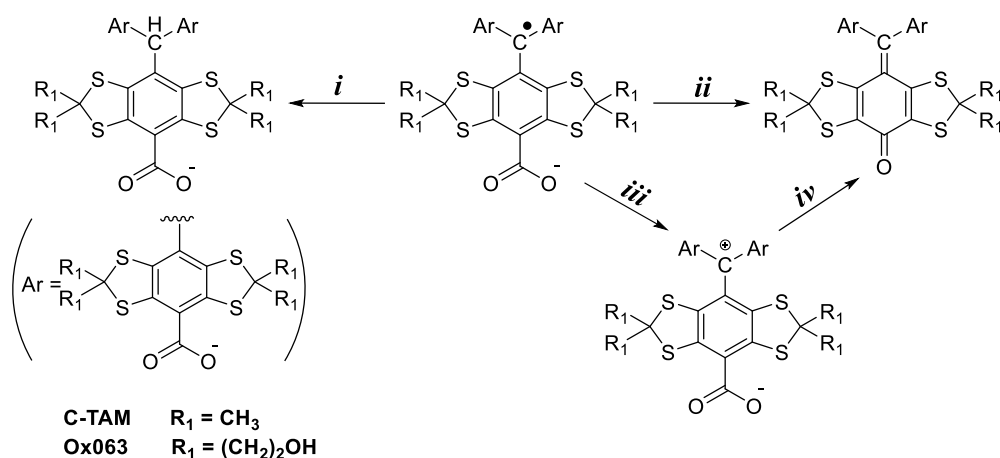


**Fig. 1.12** Biological and chemical metabolism of tetrathia-TAM radicals. **(i)** Liver microsomes/NADPH/anaerobic conditions. **(ii)**  $O_2^{\bullet-}$ ,  $ROO^{\bullet}$  or liver microsomes/NADPH/aerobic conditions. **(iii)** Peroxidases/ $H_2O_2$  or  $K_2IrCl_6$ . **(iv)**  $ROOH$ ,  $H_2O_2$  or  $H_2O$ <sup>111,112</sup>.

Better understanding of the oxidative decarboxylation of tetrathia-TAM radicals opened the way for further modification in the tetrathia-TAM structure. Decroos et al.<sup>113</sup> described the reaction of TAM<sup>+</sup> with some nucleophiles (NuH) such as phosphines, amines, imidazoles, or thiols. NuH attacked one aromatic carbon that was attached to a carboxylate group giving an intermediate. Decarboxylation of the formed intermediate gave an anion that was oxidized (either with K<sub>2</sub>IrCl<sub>6</sub> or TAM<sup>+</sup>) to the radical (TAM-Nu<sup>•</sup>), **Fig. 1.13**. TAM-Nu<sup>•</sup> is an asymmetric radical with one carboxylate group replaced with nucleophiles. With nitrite (NO<sub>2</sub><sup>•</sup>), the reaction with TAM<sup>+</sup> followed a different mechanism resulting in the formation of the trinitro radical.

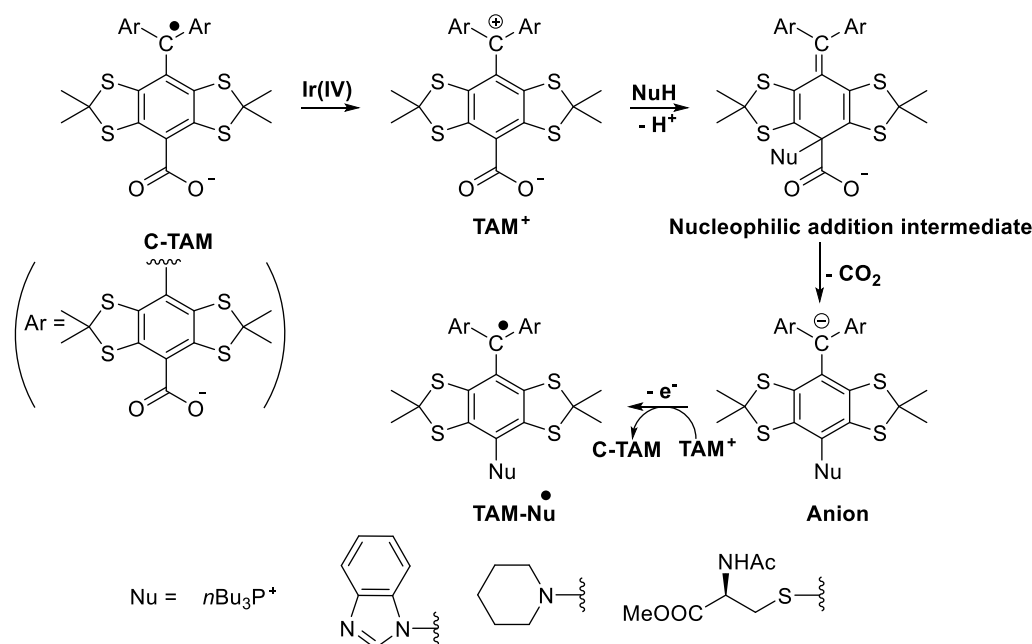


**Fig. 1.13** Reaction of TAM<sup>+</sup> with different nucleophiles<sup>113</sup>.

The mechanism of tetrathia-TAM radical release from the corresponding triarylmethanol through reaction with strong acids such as trifluoroacetic acid (TFA), was not clear<sup>29</sup>. Rogozhnikova et al.<sup>31</sup> proposed a mechanism of the reaction. The cation (TAM<sup>+</sup>) was generated from the triarylmethanol in the presence of TFA. TAM<sup>+</sup> reacted with water giving cyclohexadiene intermediate. Decarboxylation of the intermediate, followed by oxidation with TAM<sup>+</sup> gave TAM radical in addition to a transient trityl. The transient radical reacted fastly with TAM<sup>+</sup> giving QM and a second crop of the TAM radical, **Fig. 1.14**.

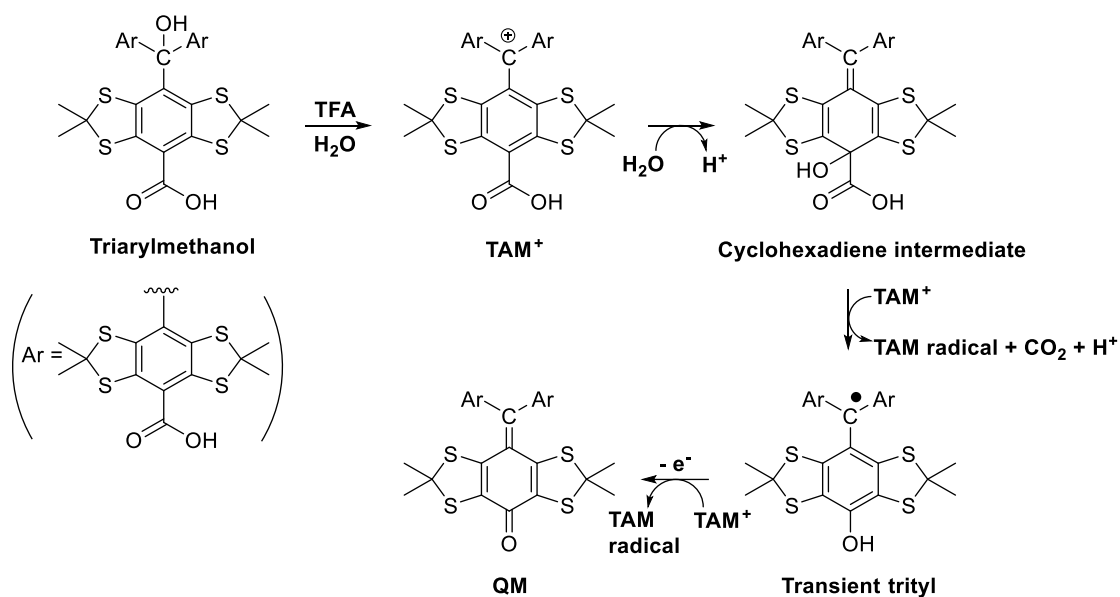


**Fig. 1.14** Mechanism of tetrathia-TAM radical release from triarylmethanol with the formation of Quinone methide<sup>31</sup>.

Decroos et al. concluded from the aforementioned literature<sup>31</sup> that decarboxylation is the main reason for metabolic instability. To overcome this problem, Decroos et al.<sup>114</sup> synthesized four ester tetrathia-TAM esters, which were soluble in water, **Fig. 1.15**. Stability of the most water-soluble esters **2** and **3** was tested and compared with the stability of C-TAM under the same conditions. They were found to be more oxidation resistant but were more easily reduced than C-TAM.

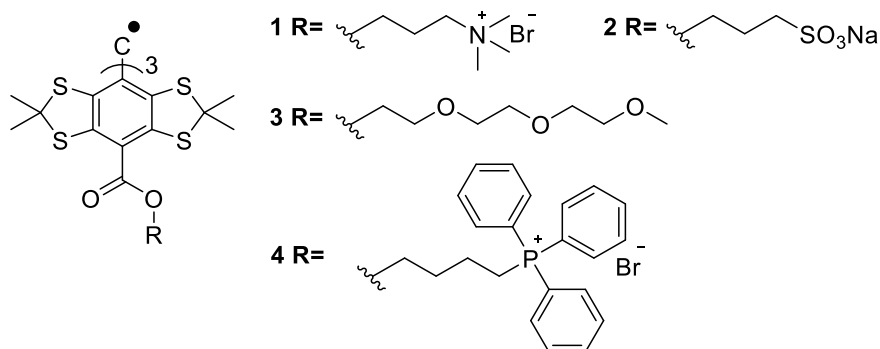


**Fig. 1.15** Chemical structure of different water-soluble esters<sup>114</sup>.

Tormyshev and co-authors<sup>115</sup> followed the same sequence of conversion of the triarylmethanol into a cation, followed by reaction with P-, O-, N-, or S-nucleophiles. Various asymmetrical tetrathia-TAM derivatives with one substitution on the *para* position of one aromatic ring were formed, **Fig. 1.16**.

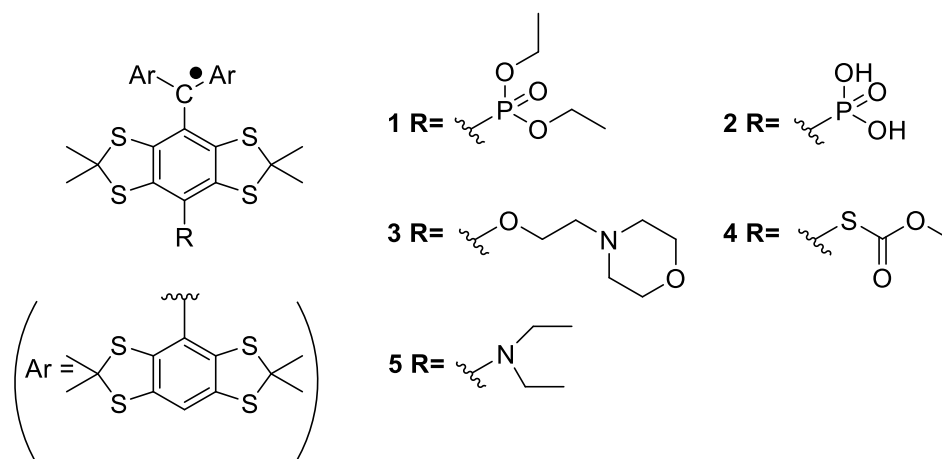


**Fig. 1.16** Chemical structure of different mono-substituted tetrathia-TAM radicals <sup>115</sup>.

### 1.2.1.3. Tetrathia-TAM radicals and interaction with biological macromolecules

Ardenkjaer-Larsen <sup>65</sup> suggested binding of tetrathia-TAM radicals to bovine serum albumin (BSA). Liu et al. <sup>37</sup> investigated the binding of C-TAM with BSA. A solution of C-TAM in phosphate buffer saline (PBS) ( $C = 20 \mu\text{M}$ ) has a  $\Delta B_{pp}$  of 192 mG. Addition of 100  $\mu\text{M}$  of BSA increased the  $\Delta B_{pp}$  to 285 mG. The increase in line width was attributed to binding of C-TAM to BSA, resulted in shorter relaxation time ( $T_2$ ) and consequently, the EPR oximetry might be limited <sup>99,116</sup>.

Song et al. <sup>99</sup> synthesized the promising dTdG (**Fig. 1.10**) that is soluble in aqueous media, has a higher oxygen sensitivity, and a better stability against many oxidizing and reducing agents compared to D-TAM. However, dTdG was found to bind to BSA, and broader EPR signals were recorded. Covalent binding of dTdG with poly(ethylene glycol) (PEG550) gave dTdG-PEG. The EPR signal of dTdG-PEG showed no change even at higher concentration of BSA. Binding of dTdG-PEG to BSA was prevented and dTdG-PEG retained its high oxygen sensitivity (3.3 mG/%  $\text{O}_2$ ).

Tetrathia-TAM radicals undergo oxidative decarboxylation into the corresponding QM with  $\text{O}_2^{\cdot-}$  or  $\text{ROO}^{\cdot}$  <sup>44</sup>, liver microsomes/NADPH/ $\text{O}_2$  <sup>111</sup>, or peroxidase/ $\text{H}_2\text{O}_2$  <sup>112</sup>. The mechanism of oxidative metabolism involved the formation of  $\text{TAM}^+$  as an intermediate. Conversion of tetrathia-TAM radical into  $\text{TAM}^+$  was chemically induced with  $\text{K}_2\text{IrCl}_6$ .  $\text{TAM}^+$  can react with many nucleophiles <sup>31,113,115</sup> giving asymmetric tetrathia-TAM radicals. Reaction of  $\text{TAM}^+$  with biological nucleophiles from proteins or nucleic acid might cause modifications of cellular components. In order to understand this possibility, Decroos et al. <sup>117</sup> allowed  $\text{TAM}^+$  to react with different natural amino acids or small peptides. Three different types of products were obtained according to nucleophilic groups.  $\text{TAM}^+$  bind with glutathione and L- $\alpha$ -Amino acids

with strong nucleophilic thiol group (such as L-cysteine, L-cysteine derivatives, and L-histidine) giving TAM-Nu<sub>1</sub> (Nu<sub>1</sub> = SG, Cys or His) as major product and small amount of QM (~5%) as minor product, **Fig. 1.17A**. TAM-Nu<sub>1</sub> exist as (50:50) mixture of two diastereoisomers, because of the chiral properties of TAM<sup>•+</sup><sup>27,118</sup>.

Reaction of TAM<sup>+</sup> with L-lysine, N<sup>α</sup>-acetyl-lysine or L-proline gave a type of quinone structure called iminoquinone methide (IQM-Nu<sub>2</sub>, Nu<sub>2</sub> = Lys, N<sup>α</sup>-AcLys, or Pro). The reaction occurred through nucleophilic attack of NH<sub>2</sub> group from the amino acid to the aromatic carbon atom at the *para* position giving TAM-Nu<sup>•</sup> as intermediate. In this case, TAM-Nu<sup>•</sup> favored losing the amino-NH proton giving IQM-Nu<sub>2</sub>, **Fig. 1.17B**.

TAM<sup>+</sup> reacted with less nucleophilic amino acids, L-arginine, L-serine, L-threonine, L-tyrosine, L-aspartate, as well as the tetrapeptide H-(Gly)<sub>4</sub>-OH, with the formation of iminoquinone methide (IQM), **Fig. 1.17C**.

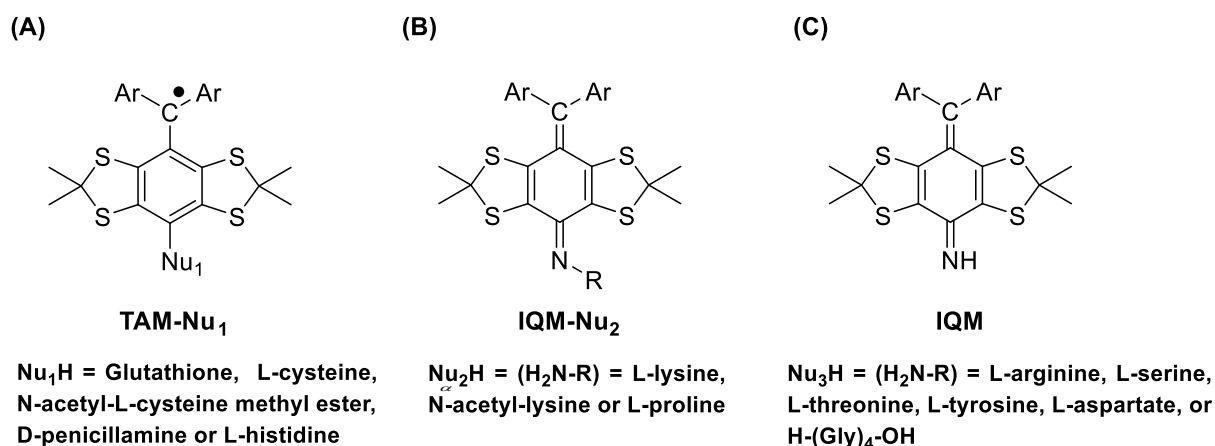


**Fig. 1.17** Products of reactions of TAM<sup>+</sup> with glutathiones, L- $\alpha$ -amino acids, or small peptide<sup>117</sup>.

#### 1.2.1.4. Tetrathia-TAM radicals as pH-sensitive spin probes

Proton concentration or pH status was found to play a critical role in the physiology of the living organism<sup>119</sup>. Deviations from normal tissue pH are associated with a number of pathological conditions such as neurodegenerative disease<sup>120</sup>, myocardial ischemia<sup>39</sup>, or cancer<sup>121</sup>.

pH sensitivity of the spin probe is based on monitoring of EPR parameters: hyperfine splitting (a), and g factor. To begin with an example taken from nitroxide radicals, imidazoline and imidazolidine nitroxide radicals, with an ionizable group, are used as pH sensitive spin probes<sup>122,123</sup>. Reversible protonation of the nitrogen atom causes an equilibrium of the two forms R<sup>•</sup> and RH<sup>•+</sup> (**Fig. 1.18**) depending on the pH value of the media. At low pH value,

protonation of the imidazolidine nitrogen atom resulted in pushing the unpaired electron to the oxygen atom. Consequently, the spin density at the nitrogen atom and the hyperfine splitting ( $a_N$ ) are decreased. Protonation results in a significant change in hyperfine splitting ( $a_N$ ) and  $g$ -factor ( $\Delta a_N \approx 1$  G and  $\Delta g \approx 0.0002$ ) between  $R^\cdot$  and  $RH^{+\cdot}$  forms <sup>124</sup>.

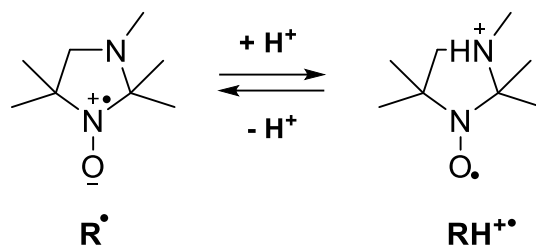


**Fig. 1.18** Reversible protonation of the nitrogen atom at imidazolidine nitroxide radical.

C-TAM and Ox063 bearing three ionizable carboxyl groups can exist in neutral [RH] form or deprotonated [ $R^-$ ] form, depending on protonation of the carboxyl group. The pH sensitivity of tetrathia-TAM radicals was studied <sup>45</sup>. Tetrathia-TAM derivatives with carboxyl groups supported the concept and demonstrated pH-sensitive EPR spectra in acidic aqueous solutions (*i.e.* changes in  $g$  factor value upon protonation of carboxyl groups,  $\Delta g \approx 0.00014$ ).

However, the pH measurement applications were limited to the pH range from 2 to 4 because of the low  $pK_a$  value ( $pK_a \approx 2.6$  for Ox063,  $pK_a \approx 4$  for C-TAM) in addition to low aqueous solubility when the molecule is in neutral form with protonated carboxyl groups. Dhimitruka et al. <sup>29</sup> found that C-TAM has a weak and broad EPR signal at acidic pH ( $pH < 4$ ) because of self-aggregation. Therefore, EPR sensitivity and imaging applications at lower pH values were restricted.

In order to improve pH sensitivity, Dhimitruka et al. <sup>47</sup> synthesized five tetrathia-TAM derivatives (aTAM1–5) with ionizable amino groups, **Fig. 1.19**.

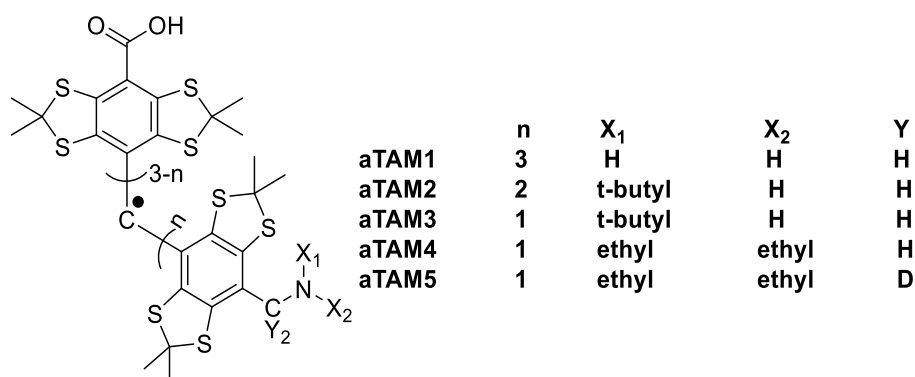


**Fig. 1.19** Chemical structure of aTAM derivatives including amino group to improve pH sensitivity <sup>47</sup>.

The asymmetrical derivative aTAM4 with both amino and carboxyl groups showed improved pH sensitivity in a pH range from 6.8 to 8.8, better solubility, and stability. In addition, aTAM4 had high oxygen sensitivity (6 mG/% O<sub>2</sub>) permitting concurrent measurement of both O<sub>2</sub> and pH in one spectrum.

Liu et al.<sup>33</sup> prepared dendritic tetrathia-TAM derivatives. C-TAM was linked through amide bond to highly symmetrical and branched dendrimers, and the carboxylate groups were located on the surface, **Fig. 1.20**. The dendritic structure provides shielding protection for the radical core. As a result, dendritic TAMs showed greater stability in the presence of reactive oxygen species (ROO<sup>•</sup>, O<sub>2</sub><sup>•-</sup>, or HO<sup>•</sup>) and higher solubility over a wide pH range (2.0–7.8) compared to C-TAM.

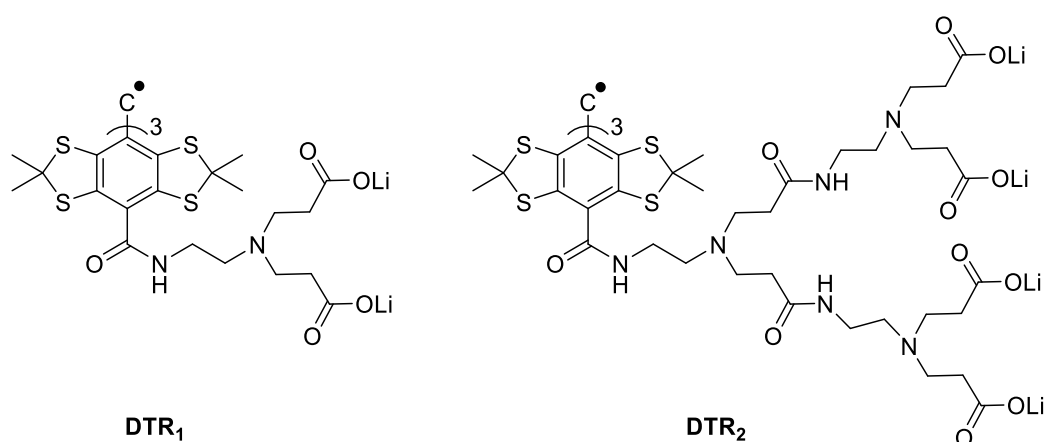


**Fig. 1.20** Chemical structure of dendritic tetrathia-TAM radicals<sup>33</sup>.

Bobko et al.<sup>45</sup> found that tetrathia-TAM derivatives, which include one or more atoms with nuclear spin ( $I \neq 0$ ) such as hydrogen ( $I = 1/2$ ), nitrogen ( $I = 1$ ), or phosphorus ( $I = 1/2$ ), showed splittings in the EPR spectra and that the determination of hyperfine splitting constant allowed the measurement of pH values.

In 2012, Driesschaert et al.<sup>10</sup> developed a promising tetrathia-TAM radical (Ph-TAM) including three ionizable phosphonic acid groups (**Fig. 1.21**) with excellent water solubility up to 10 mM. Coupling with <sup>31</sup>P ( $I = 1/2$ ) splitted the EPR signal into a quartet. The determination of the phosphorus hyperfine splitting constant ( $a_p$ ) provided pH sensitivity of the EPR spectra. Ph-TAM radical has two pK<sub>a</sub> values (pK<sub>a1</sub> = 1.3 and pK<sub>a2</sub> = 7.1). Although the second pK<sub>a</sub> is more attractive because it enables pH measurements within the physiological range, the first is also useful to avoid self-aggregation at lower pH compared to C-TAM.

Ph-TAM has an individual line width of 170 mG. Substitution of the 36 methyl protons of Ph-TAM with deuterons in the perdeuterated analog (P-TAM) (**Fig. 1.21**) decreased the



individual line width down to 40 mG. The narrow line width enabled better analysis of oxygen-induced line broadening and, hence, improved the oxygen sensitivity of the radical <sup>46</sup>.

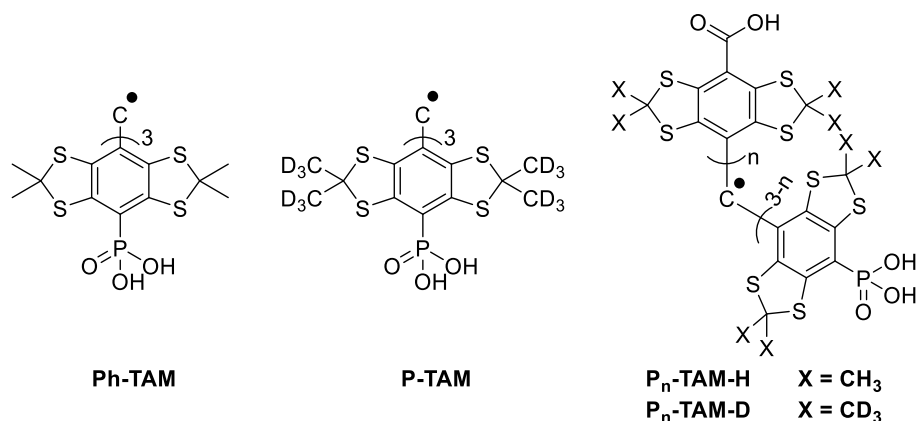


**Fig. 1.21** Chemical structures of different phosphonated tetrathia-TAM radicals <sup>10,46</sup>.

Asymmetrical derivatives of phosphonated tetrathia-TAM including both carboxylic acid and phosphonic acid groups were synthesized <sup>48</sup>. P<sub>1</sub>-TAM with one phosphonic acid and two carboxylic acid groups (**Fig. 1.21**) showed the simplest doublet EPR spectra. The EPR spectra of the perdeuterated structure P<sub>1</sub>-TAM-D showed narrower individual lines consequently higher sensitivity for pH and oxygen measurements in addition to higher water solubility and, hence, make it ideal for *in-vivo* applications. Long relaxation time of P<sub>1</sub>-TAM allowed the use of Fourier Transform EPR (FT-EPR) to extract useful information about the microenvironmental parameters such as pH, pO<sub>2</sub>, concentration of the radical and concentration of inorganic phosphate <sup>63</sup>. Further applications of the multifunctional P<sub>1</sub>-TAM using proton-electron double resonance imaging (PEDRI) enabled *in-vivo* pH mapping <sup>49</sup>. PEDRI provides reducing radiofrequency (RF) power and so avoid sample overheating, which is very important for *in-vivo* application.

#### 1.2.1.5. Tetrathia-TAM radicals and redox status determination

A normal cellular redox status is needed for the maintenance of normal physiological processes <sup>125</sup>. Abnormal redox balance may result in oxidative stress that is related to many pathological conditions such as cancer, aging, or neurologic disorders <sup>126</sup>. There are many endogenous redox species, such as oxygen, glutathione (GSH), ascorbate anion, thioredoxins, NADH, and NADPH that contribute to the redox environment of cells <sup>127</sup>.

Nitroxide paramagnetic spin probes interact with these redox species giving diamagnetic EPR-silent hydroxylamines as illustrated in **Fig. 1.7**. Monitoring the rate of decay of the nitroxide EPR signal can provide information about the redox status of tissues <sup>128,129</sup>. Although bio-reduction of nitroxides enabled measurement of redox status, it limited the EPR oximetry

and imaging applications. On the other hand, tetrathia-TAM radicals have very narrow line width and high oxygen sensitivity. The inertness of tetrathia-TAM radicals towards biological reductants such as ascorbate or glutathione limits their application as redox probes.

In order to combine the advantages of the two classes of spin probes, novel trityl-nitroxide biradicals (**Fig. 1.22**) were designed<sup>50,51</sup> allowing for measurement of redox status and oxygen content. The intramolecular spin-spin interaction between the nitroxide and trityl radicals resulted in a very broad EPR signal. Upon the reduction of the nitroxide moiety to the diamagnetic hydroxylamine, the trityl-hydroxylamine monoradical had a much sharper singlet signal stemming from trityl moiety.

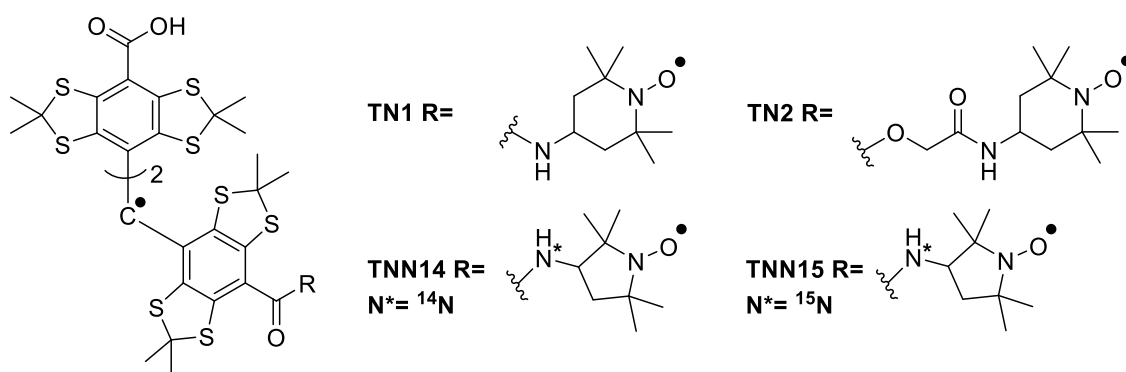


**Fig. 1.22** Chemical structure of trityl-nitroxide biradicals<sup>50,51</sup>.

#### 1.2.1.6. Tetrathia-TAM radicals and thiol concentration measurement

Glutathione is the major intracellular thiol present in all tissues<sup>130</sup>. The redox couple glutathione (GSH) and glutathione disulfide (GSSG) are the major regulator of tissue redox status<sup>131</sup>.

Disulfide nitroxyl bi-radicals (RS-SR) were used to determine the GSH concentration<sup>132-134</sup>. The EPR spectrum of RS-SR consists of the typical triplet mono-nitroxide signal plus the bi-radical spectral component (resulting from spin-spin interaction between two radical species)<sup>124</sup>. GSH interacts with RS-SR, which results in splitting of the disulfide bond and a significant increase of the triplet signal of the mono-nitroxide. The concentration of GSH could be determined from a standard titration curve with known concentrations of GSH under similar conditions<sup>135</sup>.

Liu et al.<sup>35</sup> applied the same principle to develop two new tetrathia-TAM radicals. The C-TAM radical was linked through a disulfide bond with either a nitroxide radical (TSSN) or another unit of C-TAM radical (TSST), **Fig. 1.23**. EPR spectra showed a broad signal because of intramolecular spin-spin interaction between the two radicals. GSH caused cleavage of the disulfide bond in the bi-radicals. EPR spectra showed a concomitant decrease in the bi-radical

signal and an increase in the signals of both mono-radicals. The rate of decline of bi-radical signal can be used to indicate GSH concentration. The mono-radical signal related to TAM has a very narrow line width, intracellular stability, and high oxygen sensitivity, which further enable EPR oximetry.

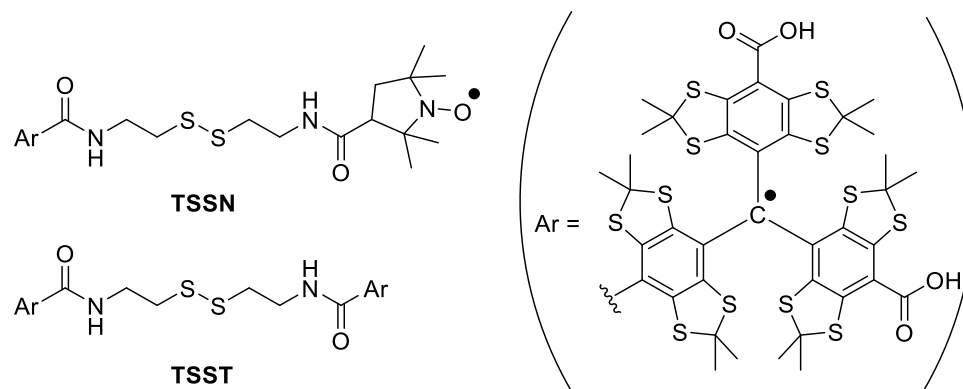


**Fig. 1.23** Chemical structure of trityl radical-conjugated disulfide bi-radicals <sup>35</sup>.

#### 1.2.1.7. Tetrathia-TAM radicals and superoxide radical measurement

Superoxide radical anion ( $O_2^{\cdot-}$ ) is one of the reactive oxygen species, resulting from one electron reduction of molecular oxygen <sup>136</sup>.  $O_2^{\cdot-}$  is implicated in a number of physiological disorders such as chronic inflammation <sup>137</sup>, reperfusion injury and ischemia <sup>138</sup>, diabetes <sup>139</sup>, or cancer incidence <sup>140</sup>.

As mentioned before, the Ox063 EPR signal decayed in the presence of  $O_2^{\cdot-}$  and alkylperoxyl ( $ROO^{\cdot}$ ) radicals <sup>40</sup>. Tetrathia-TAM reacted specifically with  $O_2^{\cdot-}$  to give a diamagnetic product. The quantification of  $O_2^{\cdot-}$  was achieved by following the changes in the EPR signal <sup>40,43</sup> or UV-Vis absorbance <sup>41</sup> of Ox063. The reaction mechanism of tetrathia-TAM radicals with  $O_2^{\cdot-}$  was reported (**Fig. 1.11**) <sup>44</sup> and the corresponding QM products were identified <sup>32,44</sup>.

Recently, Liu et al. <sup>42</sup> prepared an analog of C-TAM with one hydrogen atom instead of one carboxyl group (CT02-H), **Fig. 1.24**. The EPR spectrum appeared as a doublet because of hyperfine interaction between unpaired electrons and proton nuclei. Sensitivity towards  $O_2^{\cdot-}$  was tested for both C-TAM and CT02-H under the same conditions. In case of C-TAM, 45% of the EPR signal intensity was still detectable after 15 min. In contrast, EPR signal intensity of CT02-H showed a fast decrease, and it was completely lost after 10 min. Specificity of CT02-H for  $O_2^{\cdot-}$  was also studied. CT02-H was stable in the presence of ascorbate, glutathione, Fe(II),  $H_2O_2$  or Fe(III). Investigation of the product of the interaction between CT02-H and  $O_2^{\cdot-}$  indicated the formation of QM through oxidative dehydrogenation. In conclusion, CT02-H had

higher sensitivity to  $O_2^{\bullet -}$  compared to C-TAM with short biostability and high oxygen sensitivity.

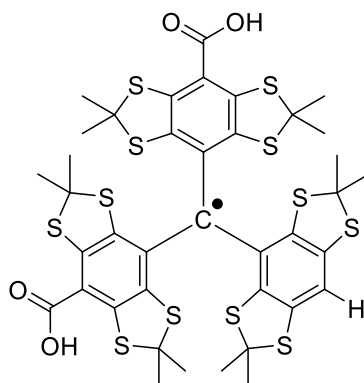


**Fig. 1.24** Chemical structure of CT02-H as superoxide sensitive spin probe <sup>42</sup>.

### 1.2.2. Tetrachloro-TAM radicals

In 1967, a new family of triarylmethyl radicals, the tetrachloro-TAM where the aromatic hydrogen atoms were wholly or partially replaced by bulky chlorine atoms, was developed <sup>20</sup>. Bulky chlorine atoms restrict the rotation around the three carbon-carbon bonds (that are connecting the three aryl groups to the central carbon) giving tetrachloro-TAM a propeller shape. This geometrical arrangement allows the radical to exist in two enantiomeric forms, namely the Plus (*P*) and the Minus (*M*) conformations <sup>141</sup>, **Fig. 1.25**. These two enantiomeric forms interconvert at high temperature (45 °C) with an energy barrier of 23 kcal/mol <sup>142</sup>.

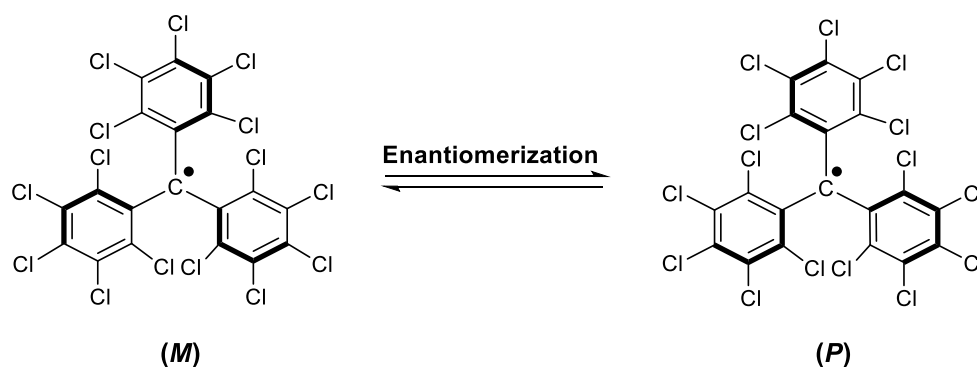


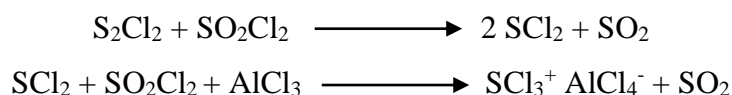
**Fig. 1.25** Two enantiomeric conformations of PTM radical.

#### 1.2.2.1. Synthesis of tetrachloro-TAM radicals

Different derivatives of tetrachloro-TAM radicals were synthesized from the corresponding  $\alpha$ H-tetrachlorotriarylmethane ( $\alpha$ H-tetrachloro-TAM). The synthesis of  $\alpha$ H-tetrachloro-TAM was achieved through two methods. The first is perchlorination of the corresponding

triarylmethane<sup>21,143</sup> with BMC (Ballester/Molinet/Castañer) reagent. BMC reagent is a solution of aluminum trichloride (AlCl<sub>3</sub>) and sulfur monochloride (S<sub>2</sub>Cl<sub>2</sub>) in sulfuryl chloride (SO<sub>2</sub>Cl<sub>2</sub>)<sup>144,145</sup>. The actual chlorinating species is supposed to be the trichlorosulfonium ion (SCl<sub>3</sub><sup>+</sup>) (Equation 2)<sup>146</sup>.

**Equation 2** Suggested mechanism for the generation of the BMC reagent.



The second method is Friedel-Crafts alkylation of chlorobenzene with chloroform (CHCl<sub>3</sub>) in the presence of AlCl<sub>3</sub> at high temperature<sup>147</sup>. Radical release involved the formation of carbanions (tetrachloro-TAM<sup>-</sup>) in the presence of a base followed by oxidation with a mild oxidant into the radical. The commonly used mixtures for radical formation are NaOH/DMSO/Et<sub>2</sub>O and I<sub>2</sub> or tetrabutylammonium hydroxide (Bu<sub>4</sub>NOH) and *p*-chloranil<sup>148</sup>. UV-Vis can monitor the steps of tetrachloro-TAM radical release.  $\alpha$ H-tetrachloro-TAM, tetrachloro-TAM<sup>-</sup> and tetrachloro-TAM radicals are characterized by three different absorption bands around 280-300 nm, 510 nm, and 374 nm, respectively<sup>149</sup>. The synthesis of PTM radical is given as an example, **Fig. 1.26**.

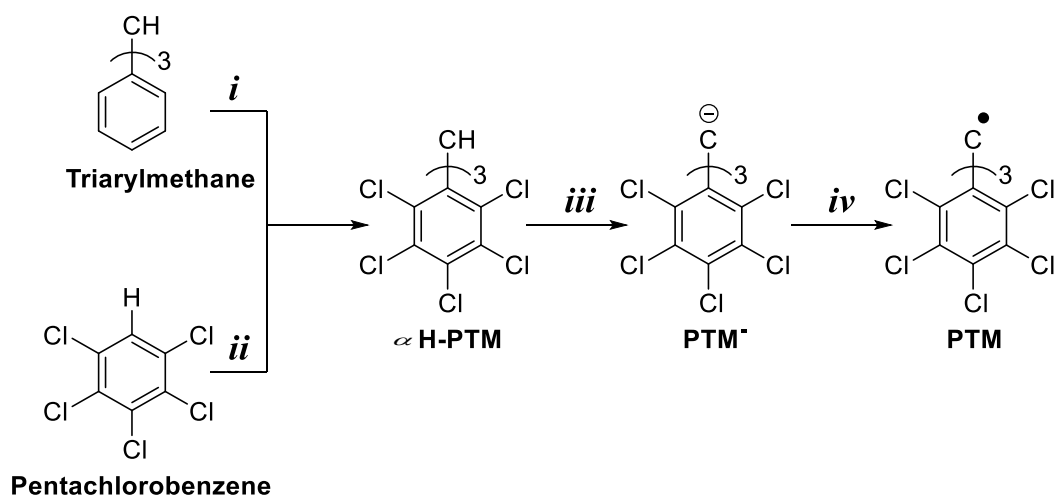


**Fig. 1.26** Synthesis of PTM radical. Reagents and conditions. **(i)** S<sub>2</sub>Cl<sub>2</sub>/SO<sub>2</sub>Cl<sub>2</sub>/AlCl<sub>3</sub>; **(ii)** CHCl<sub>3</sub>/AlCl<sub>3</sub>/160 °C; **(iii)** NaOH/DMSO/Et<sub>2</sub>O or Bu<sub>4</sub>NOH; **(iv)** I<sub>2</sub> or *p*-chloranil.

The EPR spectra of the tetrachloro-TAM radicals showed a single peak, in addition to three symmetrical pairs of satellites because of spin coupling with naturally abundant <sup>13</sup>C. There was no evidence of interaction with aromatic chlorines other than band broadening<sup>21,150</sup>.

### 1.2.2.2. Stability of tetrachloro-TAM radicals

Tetrachloro-TAM radicals are unreactive to typical radical reagents and scavengers such as nitrous oxide, nitric oxide, quinones, and boiling toluene. They are also stable against aggressive chemicals like concentrated sulfuric acid, concentrated nitric acid, chlorine (in the dark) and bromine. In addition, tetrachloro-TAM radicals have high thermal stability up to 300 °C<sup>21,143,151-153</sup>. High chemical and thermal stability of these radicals are attributed to steric shielding of the central methyl carbon by the six *ortho* chlorine atoms. However, some of these inert radicals, such as PTM radical, are light sensitive in solution<sup>20,151</sup>. PTM radical undergoes cyclization with irreversible loss of two of the *ortho* chlorine atoms, giving perchloro-9-phenylfluorenyl (PPF) radical, **Fig. 1.27**<sup>154</sup>. Later, Ballester et al.<sup>155</sup> reported the thermolysis of PTM radical at 310–320 °C into PPF radical. Similar reactions were observed with the unsubstituted triarylmethyl radical<sup>156,157</sup>.

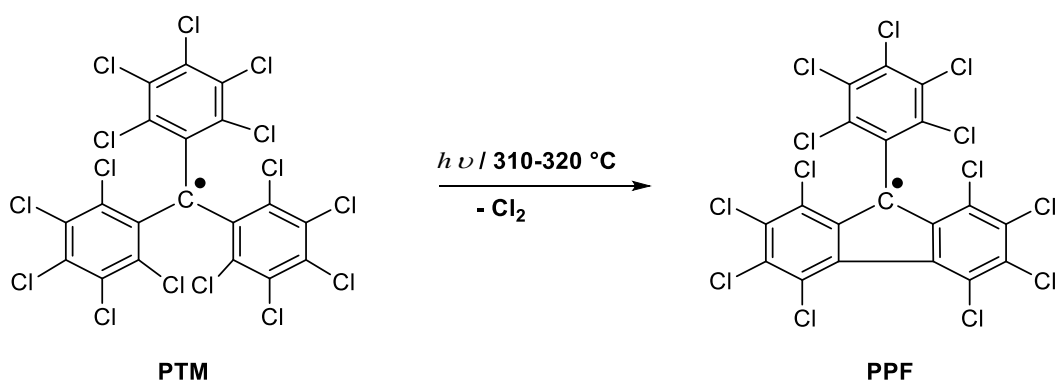


**Fig. 1.27** Photo- or thermolysis of PTM radical.

### 1.2.2.3. Reactivity of tetrachloro-TAM radicals

Tetrachloro-TAM radicals undergo single electron transfer (SET), acting either as electron donors or electron acceptors yielding the corresponding carbocations or carboanions<sup>158</sup>. Oxidation of PTM radical with antimony pentachloride ( $\text{SbCl}_5$ ) in sulfuryl chloride ( $\text{SO}_2\text{Cl}_2$ ) gave the perchlorotriphenylcarbenium hexachloroantimonate salt<sup>159</sup>. Oxidation of PTM radical with  $\text{AlCl}_3/\text{SO}_2\text{Cl}_2$ <sup>152</sup> or  $\text{AlCl}_3/\text{CH}_2\text{Cl}_2$ <sup>160</sup> afforded the perchlorocarbocation (tetrachloro-TAM<sup>+</sup>). Although the salt could be isolated, the PTM-carbocation is very reactive in solutions. Nucleophilic attack of water, alcohol or amines gave perchlorofuchsones instead of the expected perchlorotriphenylcarbinol. The steric shielding of the  $\alpha$ -carbon protects it from being attacked, and the nucleophilic attack occurs at the less shielded carbon atom in *para* position of one aromatic ring of tetrachloro-TAM<sup>+</sup><sup>161</sup>. Perchlorofuchsones were used as a precursor for the synthesis of some monosubstituted radicals.

Ballester et al.<sup>20,21</sup> reported the reduction of PTM radical with alkaline metals (potassium in ethyl ether) or hydroxide ion in DMSO mixtures into perchlorocarbanions (PTM-carbanion). PTM-carbanion is stable towards water and EtOH but in the presence of diluted hydrochloric acid gave  $\alpha$ H-PTM<sup>162</sup>. Ascorbic acid was also found to reduce PTM radical to  $\alpha$ H-PTM. One mole of  $\alpha$ H-PTM requires at least 0.5 mole of ascorbic acid for complete reduction<sup>163</sup>. **Fig. 1.28** shows the reactivity of the PTM radical.

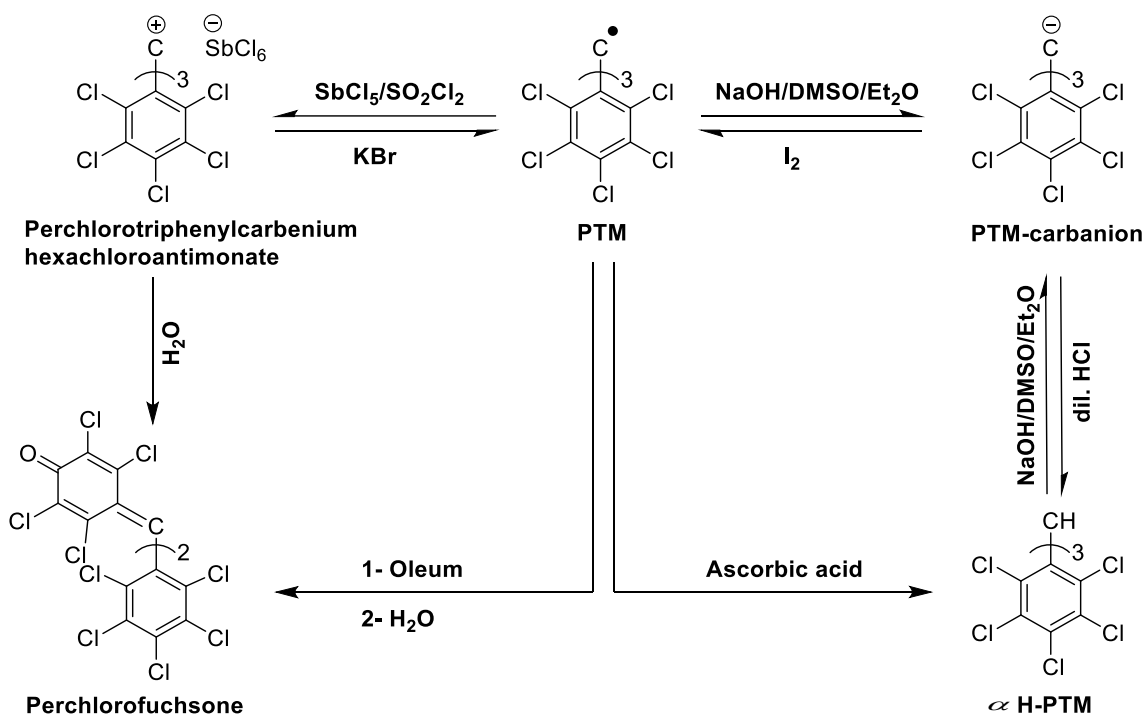


**Fig. 1.28** Reactivity of PTM radical.

#### 1.2.2.4. Different derivatives of tetrachloro-TAM radicals

Synthesis of tetrachloro-TAM radicals with different functional groups can be achieved starting from  $\alpha$ H-tetrachloro-TAM as precursor. Oftentimes, tetrachloro-TAM radicals react at the functional group without impairment of the radical character<sup>164-166</sup>.

Various derivatives of tetrachloro-TAM radicals were developed in order to study the effect of substitution on the paramagnetic character. Derivatives that are mono-substituted in *para* position of one of the aromatic rings were reported, **Fig. 1.29A**<sup>21,151,152,164,167,168</sup>. Introduction of functional groups such as carboxyl, amino or hydroxyl groups, enabled labelling of amino acids and peptides<sup>169-171</sup> as well as the conjugation with D-maltose<sup>172</sup>. Derivatives of tetrachloro-TAM radicals with different substitution at 3 and 5 positions of one of the aromatic rings were also described, **Fig. 1.29B**<sup>166</sup>. Juliá et al.<sup>165</sup> reported the synthesis of tetrachloro-TAM radicals with heteroaromatic ring for the first time, **Fig. 1.29C**.

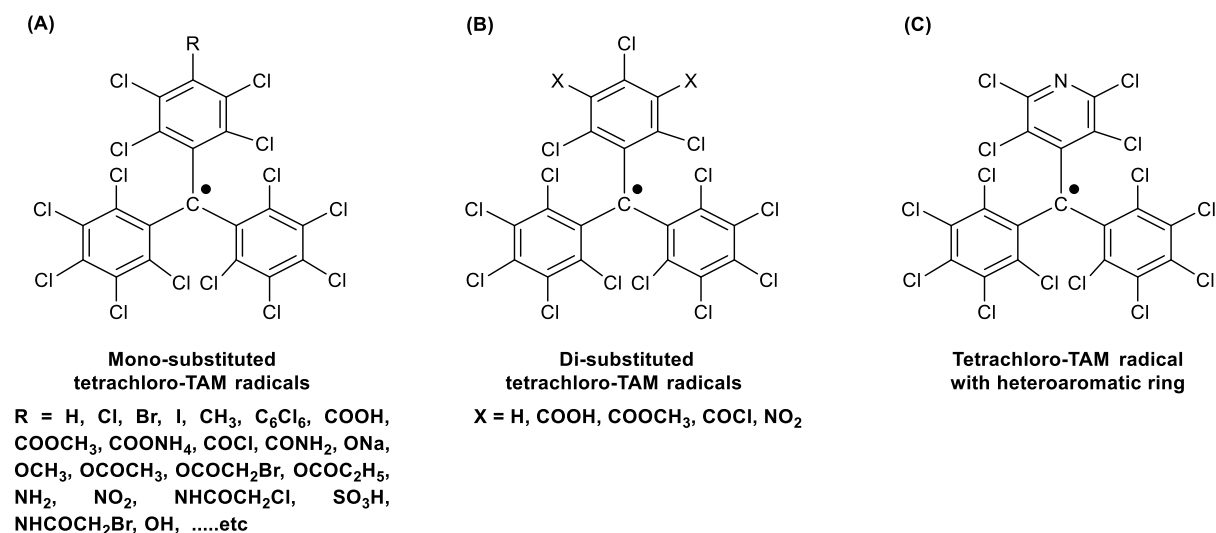


**Fig. 1.29** Chemical structure of different derivatives of tetrachloro-TAM radicals: (A) Mono-substituted tetrachloro-TAM radicals; (B) Di-substituted tetrachloro-TAM radicals; (C) Tetrachloro-TAM radical with heteroaromatic ring.

Other tetrachloro-TAM radicals were designed to study the influence of the radical character on the reactivity of the non-radical substituents (reverse effect)<sup>173</sup>. For example, 4-bromomethyl-PTM radical decomposes at 110 °C while its  $\alpha$ H analogue does not decompose up to 180 °C<sup>164,174</sup>. Another example is the reaction between PTM radical and dimethylamine (Me<sub>2</sub>NH) that resulted in the substitution of one or two chlorine atoms and the formation of dimethylamino radicals. Under the same conditions,  $\alpha$ H-PTM did not react at all suggesting that radical character enhanced the nucleophilic aromatic substitution<sup>175</sup>. Moreover, the synthesis of symmetrical trisubstituted<sup>176-179</sup> or hexasubstituted PTM radicals<sup>180-183</sup> (**Fig. 1.30**) was reported.

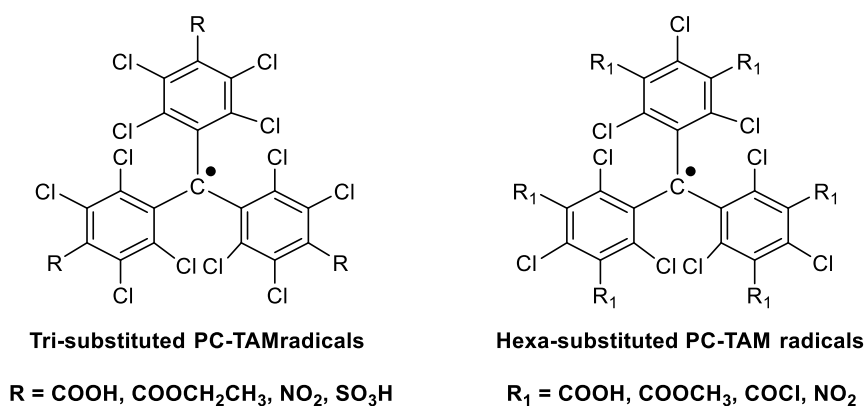


**Fig. 1.30** Chemical structure of symmetrical tetrachloro-TAM radicals

Tetrachloro-TAM radicals were involved in many applications such as dynamic nuclear polarization (DNP)<sup>184-187</sup> and material science that is reviewed in details in<sup>141,188</sup>. For the scope



of this thesis, the synthesis and EPR pharmaceutical applications of some tetrachloro-TAM spin probes were mentioned in some detail.

### 1.2.2.5. Tetrachloro-TAM radicals as spin probes for various pharmaceutical applications

#### 1.2.2.5.1. Tetrachlorotriarylmethyl triethyl ester radical (PTMTE)

The synthesis of PTMTE is outlined in **Fig. 1.31**. Perchlorotriarylmethane was synthesized by Friedel-Crafts alkylation of 1,2,4,5-tetrachlorobenzene with  $\text{CHCl}_3$  in the presence of  $\text{AlCl}_3$ . Reaction of perchlorotriarylmethane with an excess of *n*-butyllithium (*n*-BuLi) and tetramethylethylenediamine (TMEDA) in THF at low temperature gave the corresponding trianion. With ethyl chloroformate the perchlorotriarylmethane triethyl ester ( $\alpha$ H-PTMTE) was formed, which was converted into the triester radical (PTMTE) by a two-step process: Conversion into the triarylcabanion with NaOH, followed by oxidation with iodine<sup>178</sup>.

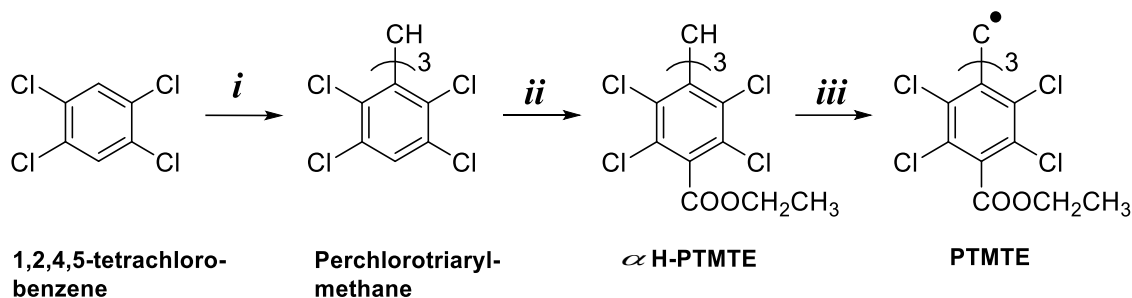
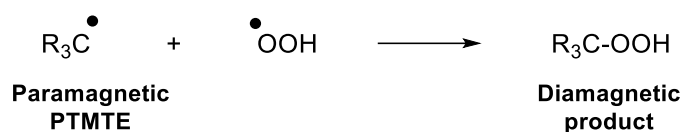


**Fig. 1.31** Synthesis of PTMTE radical. Reagents and conditions: **(i)**  $\text{CHCl}_3/\text{AlCl}_3/160\text{ }^\circ\text{C}$ ; **(ii)** *n*-BuLi, TMEDA, ethyl chloroformate; **(iii)** 1. NaOH, DMSO/ $\text{Et}_2\text{O}$ , 2.  $\text{I}_2/\text{Et}_2\text{O}$ <sup>178</sup>.

PTMTE showed a single narrow EPR peak ( $\Delta B_{\text{PP}} = 0.054\text{ mT}$  for 100  $\mu\text{M}$  solution in DMSO at ambient conditions), very good solubility in hexafluorobenzene (HFB) up to 12 mM without spin-spin line broadening, high oxygen sensitivity (1.8  $\mu\text{T}/\text{mmHg}$  in HFB, 0.16  $\mu\text{T}/\text{mmHg}$  in DMSO) and no significant effect on microwave power saturation up to 200 mW<sup>178</sup>. Bratasz et al.<sup>106</sup> developed an injectable formulation consisting of PTMTE dissolved in HFB, for *in-vivo* imaging of oxygen concentration in tissue, which showed good stability in tumor tissue (half-life: 3.3 h). Recently, Meenakshisundar et al.<sup>189</sup> incorporated PTMTE in an oxygen-permeable polymer matrix, polydimethyl siloxane (PDMS). High oxygen sensitivity as well as high *in-vitro* stability of the formed PTMTE/PDMS chips make them suitable as spin probes for EPR oximetry.

PTMTE can react with superoxide radical anion ( $\text{O}_2^{\bullet-}$ ) with complete loss of the EPR signal. Dang et al.<sup>178</sup> suggested that PTMTE reacted with the protonated form of superoxide ( $\text{}^{\bullet}\text{OOH}$ ) with the formation of a diamagnetic product (**Equation 3**).

**Equation 3** Reaction of PTMTE with superoxide radical <sup>178</sup>.



The conjugation of a fluorescent chromophore moiety to the radical spin probe permitted the detection of the conjugate by both fluorescence and/or EPR spectroscopy. Fluorophore-conjugated PTM radicals (FPTM 1–3) (**Fig. 1.32**) were reported for  $\text{O}_2^{\bullet-}$  detection by both fluorescence and EPR technique <sup>190</sup>. The principle of the dual property of the conjugate is based on the fact that the paramagnetic activity of the radical fragment quench the fluorescence of the chromophore fragment. Interaction of the radical part with  $\text{O}_2^{\bullet-}$  gave a diamagnetic product. As a result, the EPR signal decayed and the fluorescence emission enhanced. The use of FPTM radicals allowed accurate and reliable quantification of  $\text{O}_2^{\bullet-}$ .

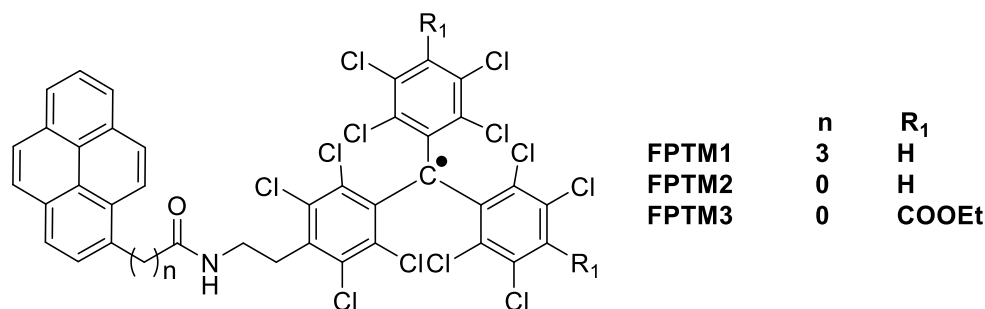


**Fig. 1.32** Chemical structure of fluorophore-conjugated tetrachloro-TAM radicals <sup>190</sup>.

#### 1.2.2.5.2. Tetrachlorotriarylmethyl tricarboxylic acid radical (PTMTC)

The synthesis of PTMTC is represented in **Fig. 1.33**. Friedel-Crafts alkylation of perchlorotriarylmethane with  $\text{CHCl}_3$  in the presence of  $\text{AlCl}_3$  afforded 4-dichloromethyl-perchlorotriarylmethane, which was further heated with oleum at  $150^\circ\text{C}$  to give the perchlorotriarylmethane tricarboxylic acid ( $\alpha\text{H-PTMTC}$ ). Conversion into PTMTC radical was completed with  $\text{NaOH}/\text{Et}_2\text{O}/\text{DMSO}$  followed by  $\text{I}_2$  addition <sup>179</sup>.

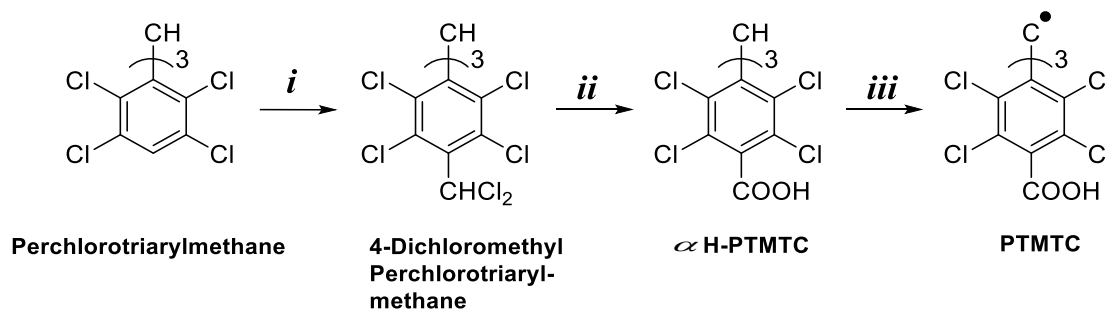
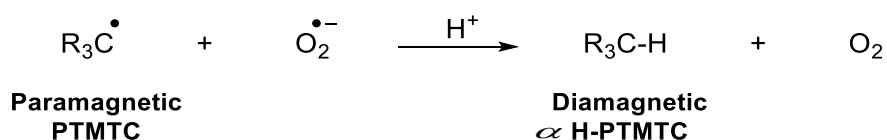


**Fig. 1.33** Synthesis of PTMTC radical. Reagents and conditions: (i)  $\text{CHCl}_3/\text{AlCl}_3/160^\circ\text{C}$ ; (ii) 20% oleum/ $150^\circ\text{C}$ ; (iii) 1.  $\text{NaOH}$ ,  $\text{DMSO}/\text{Et}_2\text{O}$ , 2.  $\text{I}_2/\text{Et}_2\text{O}$  <sup>179</sup>.

PTMTC is soluble in aqueous solutions, shows a single sharp EPR signal ( $\Delta B_{PP} = 0.055$  mT of  $1\mu\text{M}$  solution in tris-HCl buffer at  $37^\circ\text{C}$ , under aerated conditions,  $\Delta B_{PP} = 0.051$  mT under anoxic conditions) and a characteristic UV absorption at  $380\text{ nm}$  <sup>191</sup>. PTMTC has two enantiomers; Plus and Minus conformations <sup>192</sup>.

PTMTC is stable towards hydrogen peroxide ( $500\ \mu\text{M}$ ), alkyl peroxy radicals, hydroxyl radicals, nitric oxide, glutathione ( $1\text{ mM}$ ), and ascorbate ( $100\ \mu\text{M}$ ). PTMTC reacts specifically with  $\text{O}_2^{\bullet-}$  causing decrease in both EPR signal intensity and the absorbance band at  $380\text{ nm}$ . The reaction with  $\text{O}_2^{\bullet-}$  involved a reduction of PTMTC radical into  $\alpha\text{H-PTMTC}$  (**Equation 4**) unlike the reaction with tetrathia-TAM radicals, which is an oxidation process into the cation <sup>191</sup>. As an application for PTMTC radical's sensitivity to  $\text{O}_2^{\bullet-}$ , Warwar et al. <sup>193</sup> reported the use of PTMTC to examine superoxide generated in the plant roots.

**Equation 4** Reaction of PTMTC with superoxide radical.



Stability of PTMTC radical in the presence of human blood or plasma was investigated. A 40% decrease in the signal intensity was observed after 30 min suggesting that PTMTC is unsuitable for *in-vivo* applications because of higher concentration of oxido-reductants <sup>191</sup>.

#### 1.2.2.5.3. Tetrachlorotriarylmethyl trisulfonic acid radical (PTMTS) and its tripotassium salt ( $3\text{K}^+ \text{PTMTS}_3^-$ )

The synthesis of PTMTS is represented in **Fig. 1.34**. Perchlorotriarylmethane is stirred with 65% oleum at  $95\text{--}110^\circ\text{C}$  for five days to give perchlorotriarylmethane trisulfonic acid ( $\alpha\text{H-PTMTS}$ ). Conversion into PTMTS radical was done with KOH/chloranil/ $\text{H}_3\text{O}^+$  <sup>177</sup>. Treatment of  $\alpha\text{H-PTMTS}$  with KOH/chloranil resulted in the formation of tripotassium neutral salt <sup>194</sup>.

PTMTS shows very good solubility in aqueous solutions and its aqueous solutions are very acidic because of the three sulfonic acid groups. EPR spectra of  $1\text{mM}$  aqueous solution at room temperature (RT) showed a single sharp EPR signal with  $\Delta B_{PP} = 0.07$  mT. PTMTS has two characteristic UV-Vis absorption bands at  $385$  and  $503\text{ nm}$ .

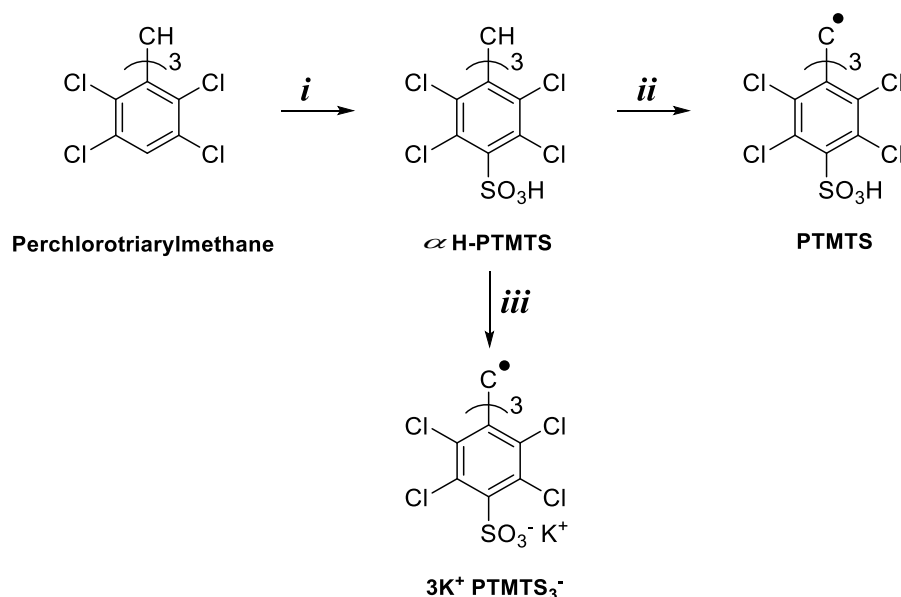


**Fig. 1.34** Synthesis of PTMTS and  $3K^+ PTMTS_3^{3-}$  radicals. Reagents and conditions: (i) 65% oleum/90–110 °C; (ii) KOH/chloranil/ $H_3O^+$ ; (iii) KOH/chloranil<sup>177,194</sup>.

Polyphenols (ArOH) such as pyrogallol or catechol act as antioxidants and they can scavenge radicals through two mechanisms: hydrogen atom donation or single-electron transfer from ArOH or the deprotonated form (ArO<sup>-</sup>)<sup>195</sup>. PTMTS in acidic (pH~3) aqueous solutions is reduced with ascorbic acid and pyrogallol (electron transfer process) into the carbanion that has UV-Vis absorption band at 535 nm and is further protonated to give  $\alpha$ H-PTMTS.

The radical scavenging activity of polyphenols with a number of dissociable OH groups is affected with pH of the medium. At higher pH values ArO<sup>-</sup> predominates and because of its higher electron donating properties, higher radical scavenging activity is expected. The neutral tripotassium salt of PTMTS ( $3K^+ PTMTS_3^-$ ) is water-soluble and stable at different pH values.  $3K^+ PTMTS_3^-$  is used to study the impact of pH on the antioxidant activity of a number of polyphenols<sup>194</sup>.  $3K^+ PTMTS_3^-$  is also used to detect hydroxyl radical (OH<sup>•</sup>) in water<sup>196</sup>. Nucleophilic attack of OH<sup>•</sup> radical to one of the *para* phenyl carbon atoms resulted in the formation of quinonemethide (QM), **Fig. 1.35**. QM had a characteristic UV-Vis absorption band at 410 nm and was identified by MS spectroscopy.

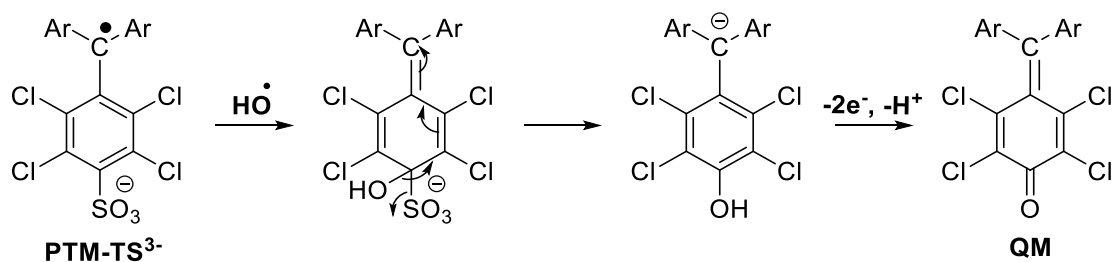


**Fig. 1.35** Reaction of  $3K^+ PTMTS_3^-$  with OH<sup>•</sup> in water with the formation of diamagnetic QM.

#### 1.2.2.5.4. Tetrachlorotriarylmethyl trinitro radical

It is another trisubstituted radical of tetrachloro-TAM with three nitro groups at the *para* positions that is also used to detect the antioxidant activity of polyphenols <sup>176</sup>.

### 1.3. Aim of the work

EPR spectroscopy is a non-destructive analytical tool, which permits assessment of certain physiological parameters such as molecular oxygen concentrations, pH values, redox status, etc. Triarylmethyl radicals (TAM or trityl) radicals are paramagnetic spin probes, which are used in EPR spectroscopy and imaging. The aim of this project was to reproducibly synthesize different trityl radicals, which should conform to the following criteria: a) stable, b) show good EPR spectral properties, and c) have a good response to the changes in the physiological parameters.

This thesis will address the synthesis of different tetrathia- and tetrachloro-TAM radicals. The EPR properties of the synthesized radicals under different parameters (*e.g.* different pH values, oxygen contents and viscosities) will be characterized. Based on the EPR properties, promising spin probe(s) will be selected for the development of biocompatible nanosensors for EPR oximetry.

Spin labelling of oligonucleotides to be used for distance measurement will be assessed. Radicals are generally toxic and unsuitable for direct administration, in high concentrations. Being linked to polymer scaffold, the toxicity may be reduced and the properties for the non-invasive monitoring of oxygen and pH gradients by EPRI may be optimized. Therefore, covalent binding of the hydrophilic radicals **PTMTC** and **D-TAM** with polymers of pharmaceutical interest such as chitosan or the water-soluble carboxymethyl chitosan will be attempted.

The synthesis of the isotopic mixture <sup>13</sup>C-**PTMTC** (with 50% <sup>13</sup>C labelling at the methyl radical center) will be described. The differential effect of oxygen content and viscosity on the line widths of the <sup>12</sup>C and the <sup>13</sup>C EPR signals will be explored.

The tetraoxatriarylmethyl radicals (tetraoxa-TAM) are structurally related to tetrathia-TAM radicals, with oxygen instead of sulfur. Optimization of the reaction conditions for the sake of triethyl ester tetraoxa-TAM radical synthesis will be discussed.

## 2. Tetrathiatriarylmethyl radicals\*

### 2.1. Introduction

As mentioned before in section 1.2.1.1, the quantification of oxygen levels *in-vitro* and *in-vivo* is crucial for understanding of many physiological and pathological processes. EPR oximetry provides oxygen measurement with high selectivity, sensitivity, and non-invasiveness. Tetrathia-TAM radicals (**Fig. 1.5**) are carbon-centered radicals, which are characterized by extremely narrow line width and long relaxation times<sup>57,58</sup>. Tetrathia-TAM radicals are commonly used for EPR oximetry<sup>36,39</sup> and pH measurement<sup>46,48</sup>.

The EPR line widths of the hydrophilic tetrathia-TAM radicals (**C-TAM** and **D-TAM**) are oxygen-dependent<sup>64,65</sup>. The presence of three carboxyl groups makes tetrathia-TAM radicals anionic at physiological pH. Consequently, intracellular permeability and *in-vivo* applications are limited<sup>45</sup>. Lui et al.<sup>6</sup> found that lipophilic ester derivatives of **C-TAM** have sharp, single and relatively narrow EPR signals as well as higher oxygen sensitivities than the hydrophilic **C-TAM**. **D-TAM** has a narrower line width compared to its undeuterated analog **C-TAM**<sup>22,65,110</sup>. Partial deuteration of ester protons was found to narrow the line width further<sup>110</sup>. Based on these outcomes, a spin probe of the tetrathia-TAM series was envisioned which possesses narrow line width and high sensitivity towards variation in oxygen content. Different types of tetrathia-TAM radicals were synthesized (**Fig. 2.1**) that: (1) were hydrophilic (**9** and **10**) or lipophilic (**7**, **8**, **11** and **13**), (2) had a very narrow EPR line widths (**8** and **13**), and (3) radicals that displayed hyperfine coupling (*e.g.* with <sup>1</sup>H) as a second signal parameter next to line width, but still having narrow lines (**7** and **11**). The EPR properties of the prepared radicals were explored under different conditions (*e.g.* different ion strengths and viscosities for the hydrophilic radicals or different solvent and different oxygen content for the lipophilic radicals). Radical **13** showed a very narrow line width (13  $\mu$ T, 1 mM solution in IPM under anaerobic condition) as well as high oxygen sensitivity ( $\approx 3.7 \mu$ T/% O<sub>2</sub>, 1 mM solution in IPM). Radical **13** was incorporated into oily-core nanocapsules (NCs). The NCs were investigated regarding their physical properties, oxygen-sensitivity and ability to protect the incorporated spin probe from reduction by ascorbic acid.

---

\* These results were published:

(197) Frank, J.; Elewa, M.; Said, M. M.; El Shihawy, H. A.; El-Sadek, M.; Müller, D.; Meister, A.; Hause, G.; Drescher, S.; Metz, H.; Imming, P.; Mäder, K. *J. Org. Chem.* **2015**, *80*, 6754..

## 2.2. Experimental

### 2.2.1. Materials and general methods for synthesis and analytical characterization

See section 9.1 and 9.2.

### 2.2.2. Sample preparation for EPR spectroscopic characterization.

Radical **9** was dissolved ( $c = 50 \mu\text{M}$ ) in four different buffer systems listed in **Table 2-1**.

**Table 2-1** Buffer systems used to investigate the impact of different ion strengths and pH values on the EPR line width of radical **9**.

Buffer system	Buffer salts	I (mmol/L)	$c_{\text{osm}}$ (mosmol/L)	pH
<b>PBS 7.4</b>	$\text{Na}_2\text{HPO}_4$ , $\text{KH}_2\text{PO}_4$ and NaCl	189	327	7.4
<b>PB 7.4</b>	$\text{Na}_2\text{HPO}_4$ , $\text{KH}_2\text{PO}_4$	49	55	7.4
<b>PBS 6.2</b>	$\text{Na}_2\text{HPO}_4$ , $\text{KH}_2\text{PO}_4$ and NaCl	180	349	6.2
<b>PB 6.2</b>	$\text{Na}_2\text{HPO}_4$ , $\text{KH}_2\text{PO}_4$	52	86	6.2

Additionally, radical **9** was dissolved ( $c = 50 \mu\text{M}$ ) in mixtures of PBS 7.4 and freshly opened absolute glycerol with a glycerol content ranging from 0% to 90% (m/m). Radical **10** was dissolved ( $c = 50 \mu\text{M}$ ) in PBS 7.4. The lipophilic spin probes (radicals **7**, **8**, **11** and **13**) were dissolved ( $c = 1 \text{ mM}$ ) in MCT as well as IPM. All solutions were measured by EPR spectroscopy.

### 2.2.3. EPR spectroscopy

Samples were measured under defined oxygen contents using an EPR spectrometer at 1.3 GHz (Magnettech, Berlin, Germany). The NCs reduction assay was conducted using an X-band EPR spectrometer at 9.30–9.55 GHz (Miniscope MS 200, Magnettech, Berlin, Germany). The measurement parameters, the oxygen content calibration and data fitting are described in Ref. <sup>197</sup>.

## 2.3. Results and Discussion

### 2.3.1. Synthesis of different tetrathia-TAM radicals

The tetrathia-TAM radicals are known to be very difficult to prepare. The synthesis of tetrathia-TAM radicals is shown in **Fig. 2.1** based on protocols that worked reproducibly.

The main hurdle to obtain tetrathia-TAM radicals lies right at the beginning of the synthesis, *i.e.* the preparation of molar amounts of tetrakis(*tert*-butylthio)benzene (**1**) because of the necessity to use the very odoriferous *tert*-butyl thiol that is added to city gas to detect leakages. A manageable technique to obtain **1** was published<sup>198</sup>. The subsequent steps towards the preparation of the tetrathia-TAM radicals shown in **Fig. 2.1** mainly followed published procedures<sup>22-26,28-32,55,72,95,110,198,199</sup>. Modifications regarding the synthetic procedures are mentioned in (section **2.5**).

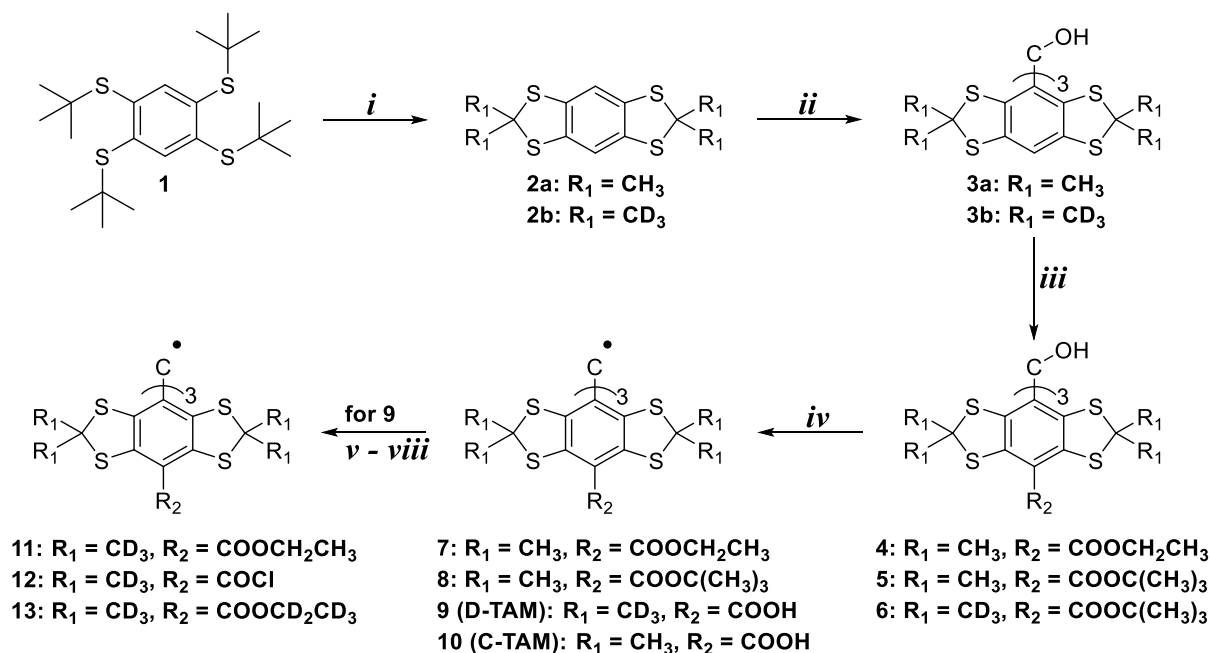


**Fig. 2.1** Synthesis of tetrathia-TAM radicals (**7–13**). Reagents and conditions: **(i)**  $HBF_4$ , acetone or acetone- $d_6$ ; **(ii)**  $n$ -BuLi, methyl chloroformate; **(iii)**  $n$ -BuLi, TMEDA, and diethyl carbonate or DiBoc; **(iv)**  $BF_3 \cdot Et_2O/SnCl_2$ , TFA; **(v)** **9**, TEA, acetonitrile, ethyl chloroformate, DMAP; **(vi)** **9**,  $SOCl_2$ , TEA; **(vii)** **12**,  $EtOH-d_6$ , reflux; **(viii)** **9**, TEA, acetonitrile, ethyl chloroformate- $d_5$ , DMAP.

Compound **1** was converted into the cyclized arene (**2a, b**) by tetrafluoroboric acid ( $HBF_4$ ) 54% in  $Et_2O$ , toluene and acetone or acetone- $d_6$ . The triarylmethanols (**3a, b**) were prepared by treatment of **2a** or **2b** with  $n$ -BuLi and the subsequent addition of methyl chloroformate. Reaction of **3a** or **3b** with ten equivalents of  $n$ -BuLi and TMEDA resulted in the formation of the corresponding trianion. Different derivatives (compounds **4–6**) were prepared through reaction of the appropriate anion with diethyl carbonate (**4**) or di-*tert*-butyldicarbonate (DiBoc) (**5,6**). The conversion of compounds **4** and **5** by Boron trifluoride diethyl etherate ( $BF_3 \cdot Et_2O$ ) into the carbocation followed by reduction with stannous chloride ( $SnCl_2$ ) gave the lipophilic trityl radicals **7** and **8**, respectively. Esters **5** and **6** were subsequently hydrolyzed with



trifluoroacetic acid (TFA) overnight at RT to give the tricarboxylic acid (hydrophilic) radicals **9** and **10**, respectively. A mixture of radical **9** and triethylamine (TEA) in acetonitrile was kept at 0 °C. Ethyl chloroformate was added followed by the addition of 4-dimethylaminopyridine (DMAP) to afford the ethyl ester (**11**) with 80% yield. Formation of the fully deuterated ethyl ester analogue **13** was achieved through two methods. Method A involved the esterification of **9** through a two-step reaction: The formation of the corresponding acid chloride **12** with the help of thionyl chloride (SOCl<sub>2</sub>) and TEA followed by reflux with EtOH-d<sub>6</sub> to give radical **13** with 73% yield. Method B included the synthesis of ethyl chloroformate-d<sub>5</sub> and reaction with a mixture of **9** and TEA followed by addition of DMAP as described before.

### 2.3.2. Characterization of hydrophilic trityl radicals in aqueous solutions †

In this section, the EPR characterization of the hydrophilic tetrathia-TAM radical (radical **9**) and its oxygen sensitivity in aqueous solution are summarized.

#### 2.3.2.1. Influence of ion strength, osmolarity, and pH value

The hydrophilic radicals were studied under several conditions to mimic environments in drug formulations or *in-vivo*. Aerated solutions of radical **9** in the different buffer systems (**Table 2-1**) showed similar line widths ( $\Delta B_{PP} = (13.7 \pm 0.2) \mu\text{T}$ ) as well as similar EPR line width narrowing ( $\Delta B_{PP} = (3.1 \pm 0.1) \mu\text{T}$ ) after deoxygenation of the samples. Therefore, under physiologically relevant limits of ionic strength, osmolarity and pH value, there was negligible effect on the EPR line width of radical **9**.

#### 2.3.2.2. Impact of viscosity

Radical **9** was insoluble in absolute glycerol. Hence, it was dissolved ( $c = 50 \mu\text{M}$ ) in different glycerol-water mixtures (0%–90% glycerol in water, m/m). Increasing the percentage of glycerol results in decreasing the oxygen solubility<sup>200</sup>. Therefore, the EPR signal line width was decreased upon increasing the glycerol content (0%-50% (m/m)). A sharp increase in the line width caused by the strong increase of viscosity of the glycerol-water-mixtures above 50 % (m/m) glycerol content was observed, **Fig. 2.2**. The measurements were repeated under deoxygenated conditions. It was found that up to 40 % (m/m) of glycerol, the impact of viscosity on the EPR line width was negligible if compared to the effect of oxygen. A sharp increase in the EPR line width followed, similar to the aerated samples.

---

† This part of the work will be reported in detail in an ongoing thesis by Juliane Frank (research group Prof. Mäder) the other first author of our publication (Ref. 196).

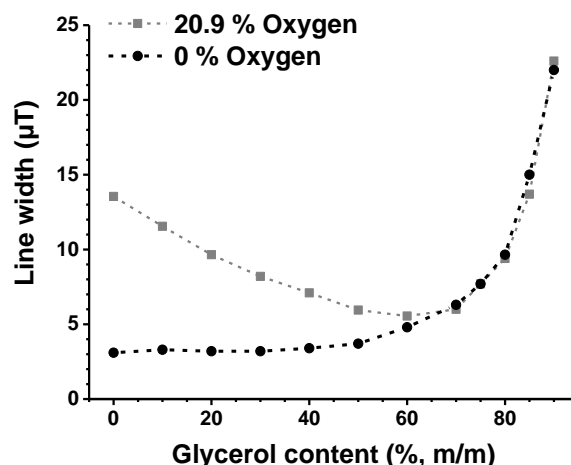


**Fig. 2.2** Change in the EPR line width of radical **9** ( $c = 50 \mu\text{M}$ ) on different glycerol-water mixtures.

### 2.3.3. EPR spectroscopic characterization of lipophilic tetrathia-TAM radicals in an oily solution ‡

The triesters of the tetrathia-TAM radicals (**7**, **8**, **11** and **13**, **Fig. 2.1**) proved to be very lipophilic. When these radicals were distributed between octanol and water or MCT and PBS ( $\text{pH} = 7.4$ ) for 2 h at  $37^\circ\text{C}$ , the EPR signal resided in the lipophilic solvent exclusively.

Solutions of the lipophilic radicals **7**, **8**, **11**, and **13** ( $c = 1 \text{ mM}$ ) in MCT and IPM were investigated in air (20.9%  $\text{O}_2$ ) and after flushing with nitrogen ( $\sim 0\% \text{ O}_2$ ). **Fig. 2.3** shows the EPR spectra in IPM under anoxic conditions.

As predicted from the higher viscosity, the EPR lines under anoxic conditions were broader in MCT. In air, however, the lines were broader in IPM. This is attributed to the higher oxygen solubility and correspondingly higher oxygen content, overruling the effect of viscosity. Under anaerobic conditions, the signal of radical **11** displayed superhyperfine coupling with the six equivalent protons of the three methylene groups of the ethyl ester moieties resulting in seven equidistant lines with relative intensities of  $1 : 6 : 15 : 20 : 15 : 6 : 1$  and a coupling constant of  $a = 11.3 \mu\text{T}$ . The coupling pattern was much better resolved in the less viscous IPM. The same ester, but with protonated instead of deuterated methyl groups in the ketal moiety (radical **7**, **Fig. 2.1**), resonated with slightly broader EPR line widths compared to the radical **11**. The additional superhyperfine coupling with the the protons of the methyl groups affected the signal

‡ This part of the work will be reported in detail in an ongoing thesis by Juliane Frank (research group Prof. Mäder) the other first author of our publication (Ref. <sup>196</sup>).

pattern in the deoxygenated solutions, **Fig. 2.3**. In MCT, only the envelope of the coupling pattern was visible. Deuterium ( $I = 1$ ) of course also couples with the electron, but the coupling constant is much smaller compared to the coupling constant of hydrogen.

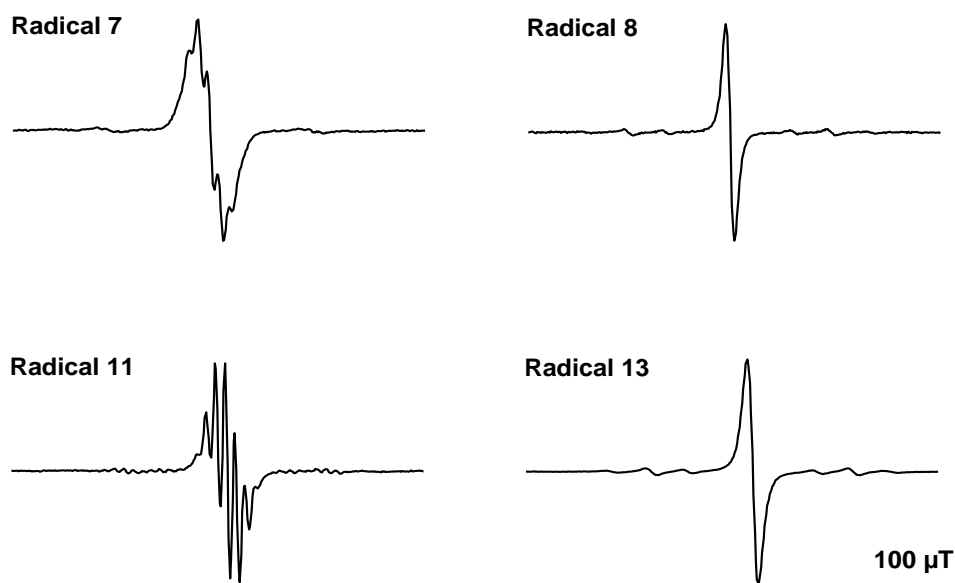


**Fig. 2.3** EPR signals of radicals **7**, **8**, **11** and **13** under anaerobic conditions ( $\approx 0\%$   $O_2$ ) in IPM.

The *tert*-butyl ester of the non-deuterated trityl radical (**8**) displayed the narrowest single EPR line among the investigated lipophilic esters. As expected, due to the small unresolved hfs with the protons of the *tert*-butyl moieties, the line width in anoxic IPM was slightly broader when compared to the hfs lines of radical **11**. Fully deuterated ethyl ester and methyl ketal groups (radical **13**, **Fig. 2.1**), displayed a very narrow single line especially in deoxygenated solutions. Compared to radicals **8** and **11**, the lines were slightly broader in anoxic solutions caused by the unresolved coupling with deuterium nuclei. However, because radical **13** had a better synthetic accessibility than **8**, it was chosen for the following oxygen calibration measurements and encapsulation investigations.

#### 2.3.4. Oxygen sensitivity

For atmospheric pressure and *in-vivo* applications, only the data between approx. 0 and 20.9 % (0–156 mmHg) oxygen are of interest. Solutions of the hydrophilic radicals **9** and **10** ( $c = 50 \mu\text{M}$ ) in PBS (pH = 7.4) showed a linear relationship between the EPR line width and oxygen concentration with similar oxygen sensitivities as reported<sup>32,65</sup>. As expected, radical **9** had a narrower line width ( $\Delta B_{PP} \sim 13.6 \mu\text{T}$  at 20.9%  $O_2$ ) than its undeuterated analogue **10** ( $\Delta B_{PP} \sim$

16.5  $\mu\text{T}$  at 20.9%  $\text{O}_2$ ), which is in accordance with Dhimitruka et al.<sup>110</sup>. The slope of the curves, *i.e.*, the oxygen sensitivity of 0.5  $\mu\text{T}/\% \text{O}_2$  (0.07  $\mu\text{T}/\text{mmHg}$ ), was quite small.

The oxygen sensitivities of the lipophilic radical **13** ( $c = 1 \text{ mM}$ ) was about 1.7  $\mu\text{T}/\% \text{O}_2$  (0.2  $\mu\text{T}/\text{mmHg}$ ) in MCT and 3.7  $\mu\text{T}/\% \text{O}_2$  (0.5  $\mu\text{T}/\text{mmHg}$ ) in IPM. Oxygen solubility in oil is generally higher than in water at a given temperature and pressure<sup>201</sup>, such that the concentration of dissolved oxygen rises noticeably with increasing oxygen partial pressure. Accordingly, the slopes were steeper than in water. The different slopes in MCT and IPM were probably caused by the different polarity and especially viscosity of the oils.

Radical **13** had the steepest slope with the smallest  $y$ -intercept. Hence, it combined both a excellent oxygen sensitivity and a good signal-to-noise-ratio. The high oxygen sensitivity in IPM is comparable with widely used particulate oxygen-sensitive spin probes, such as Lithium phthalocyanine (LiPc) or Lithium octabutoxynaphthalocyanine (LiNc-BuO)<sup>83,202</sup> and, thus, very promising for future applications in the field of EPR oximetry as an alternative to particulate materials. Trityl radicals have been employed in lipophilic formulations *e.g.*, microspheres<sup>203</sup>, hexafluorobenzene nanoemulsions or solutions<sup>106,177</sup>, and polydimethyl siloxane chips<sup>189</sup>.

### **2.3.5. Encapsulation of tetrathia-TAM esters and properties of the resulting nanocapsules (NCs)**

Based on the aforementioned results, radical **13** was incorporated into NCs. The preparation and characterization of the NCs are discussed in Ref.<sup>197</sup>. Briefly, being dissolved in the oily core of these NCs, the spin probes are located in a constant microenvironment without being affected by changes of the outer pH value or viscosity. Thereby, the NCs can also be used in acidic conditions, where hydrophilic tetrathia-TAM radicals would precipitate. Moreover, oxygen molecules can penetrate the capsule shell, turning NCs into oxygen sensors. Since the oxygen solubility in oils is higher than in water, the oxygen sensitivity of the spin probes is improved (section 2.3.4). Highly lipophilic encapsulated probes would stay inside the NCs without being partitioned to the outer aqueous phase, shielding them from oxidoreductants<sup>204</sup>. It is known that suitable formulations are needed to prevent spin probe-tissue interactions in long-term *in-vivo* studies<sup>205</sup>. Consequently, not only the oxygen-responsiveness of the spin probes would be preserved, but also their bio-compatibility could be improved.

The prepared NCs had similar oxygen sensitivities as the unencapsulated solutions. Thus, the encapsulation of the spin probes did not compromise their oxygen sensitivity. To investigate the stability of encapsulated radicals against reduction, an ascorbic acid reduction assay was

carried out. The result proves that the capsule shell was capable to sterically shield the incorporated radical from reductants.

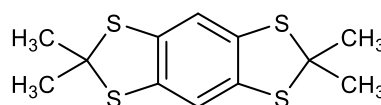
## 2.4. Conclusion

Reproducible protocols for the synthesis of different derivatives of tetrathia-TAM radicals are described. Moreover, a new trityl derivative (radical **13**) with deuterated core and deuterated ethyl ester groups was devised. The EPR properties of the synthesized radicals were investigated in either aqueous media (hydrophilic radicals) or MCT and IPM (lipophilic radicals). It was shown that within physiological limits of osmolarity, viscosity, and pH value, there was, for practical purposes, no impact on the EPR line widths of the hydrophilic radicals. The non-deuterated lipophilic triethyl esters of C-TAM or D-TAM (radicals **7** and **11**) showed hyperfine splitting in deoxygenated solutions. Other triesters exhibited single EPR lines with line widths directly proportional to the oxygen concentration, rendering them candidates for oxygen measurements. The fully deuterated triethyl ester of D-TAM (radical **13**) had the most promising EPR properties, especially when dissolved in IPM. It had a very narrow EPR line under anaerobic conditions and a high oxygen sensitivity ( $\sim 3.7 \mu\text{T}/\% \text{O}_2$ ). Therefore, solutions of radical **13** in MCT and IPM were encapsulated into NCs. The oxygen responsiveness of the incorporated tetrathia-TAM radicals was retained. Using IPM for encapsulation, a high oxygen sensitivity of the NCs could be ensured, especially suitable for measuring low oxygen contents. MCT provided stable NCs for long-term measurements. In addition, encapsulated lipophilic trityl radicals were protected against reducing agents such as ascorbic acid. Hydrophilic trityl radicals were shown to be useful EPR oximetry probes, but lack high oxygen sensitivity. Encapsulation of lipophilic trityl radicals offers potential for nanosensors with high oxygen sensitivity, specificity, and stability, particularly suitable for EPR oximetry in complex biological systems.

## 2.5. Syntheses

### 2,2,6,6-tetramethylbenzo[1,2-*d*:4,5-*d'*]bis[1,3]dithiole (**2a**)<sup>28,29,31</sup>.

$\text{HBF}_4$  (54% in  $\text{Et}_2\text{O}$ , 10 mL, 37.0 mmol) was added to a solution of 1,2,4,5-tetra(*tert*-butylthio)benzene (**1**) (16.0 g, 37.2 mmol) in toluene (500 mL). The mixture was stirred for 30 min at RT. Acetone (10 mL, 136 mmol) was added, the reaction mixture was stirred for 4 h at RT, and then heated to reflux overnight. After cooling, a saturated  $\text{NaHCO}_3$  solution (100 mL) was added carefully; the organic layer was separated and the aqueous layer was extracted



three times with EA. The combined organic layers were dried over  $\text{MgSO}_4$  and concentrated in vacuum. EtOH (50 mL) was added to the brown solution. The pure product was crystallized off, separated by filtration, washed several times with EtOH and dried.

**Yield:** 7.2 g (68%)

**Colour:** White crystals

**Molecular formula:**  $\text{C}_{12}\text{H}_{14}\text{S}_4$

**Molar mass:** 286 g/mol

**Mp:** 145–147 °C

**R<sub>f</sub>:** 0.32 (heptane)

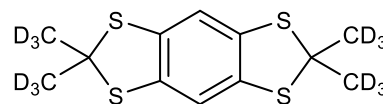
**$^1\text{H}$  NMR:** (400 MHz,  $\text{CDCl}_3$ )  $\delta$  7.02 (s, 2H), 1.88 (s, 12H)

**$^{13}\text{C}$  NMR:** (100 MHz,  $\text{CDCl}_3$ )  $\delta$  135.7, 116.8, 65.7, 31.3

**HRMS (ESI):** calcd. for  $\text{C}_{12}\text{H}_{14}\text{S}_4$   $[\text{M}]^+$  285.998; found 285.997

**2,2,6,6-tetra( $^2\text{H}_3$ -methyl)benzo[1,2-*d*:4,5-*d'*]bis[1,3]dithiole (2b)**<sup>22,25,110</sup>.

$\text{HBF}_4$  (54% in  $\text{Et}_2\text{O}$ , 10 mL, 37.0 mmol) was added to a solution of compound **1** (16.0 g, 37.2 mmol) in toluene (500 mL). The mixture was stirred for 30 min at RT. Acetone- $\text{D}_6$  (10



mL, 148 mmol) was added, the reaction mixture was stirred for 4 h at RT, and then heated to reflux overnight. After cooling, a saturated solution of  $\text{NaHCO}_3$  (100 mL) was added carefully, the organic layer was separated and the aqueous layer was extracted three times with EA. The combined organic layers were dried over  $\text{MgSO}_4$  and concentrated in vacuum. EtOH (50 mL) was added to the brown solution. The pure product was crystallized off, separated by filtration, washed several times with EtOH and dried.

**Yield:** 7.8 g (70%)

**Colour:** White solid

**Molecular formula:**  $\text{C}_{12}\text{H}_2\text{D}_{12}\text{S}_4$

**Molar mass:** 298.07 g/mol

**Mp:** 143–145 °C

**R<sub>f</sub>:** 0.35 (heptane)

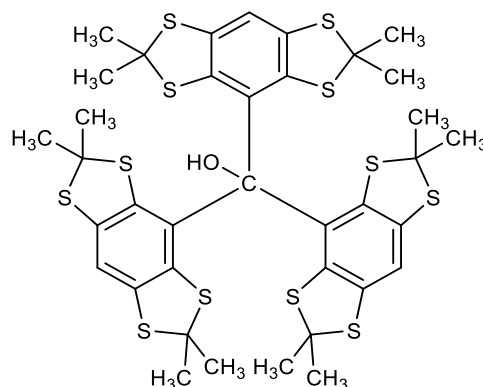
**$^1\text{H}$  NMR:** (400 MHz,  $\text{CDCl}_3$ )  $\delta$  7.02 (s, 2H)

**$^{13}\text{C}$  NMR:** (400 MHz,  $\text{CDCl}_3$ )  $\delta$  135.7, 116.8, 65.7, 31.3

**HRMS (ESI):** calcd. for  $\text{C}_{12}\text{H}_2\text{D}_{12}\text{S}_4$   $[\text{M}]^+$  298.073; found 298.073

**Tris[2,2,6,6-tetramethylbenzo[1,2-*d*:4,5-*d'*]bis([1,3]dithiole)-4-yl]methanol (3a)**<sup>28,29,31</sup>.

Compound **2a** (3.5 g, 12.2 mmol) was dissolved in dry Et<sub>2</sub>O (150 mL) under argon atmosphere. A solution of 2.5 M *n*-BuLi in *n*-hexane (4.88 mL, 12.2 mmol) was added dropwise, and the reaction mixture was stirred for 2 h at RT. Methyl chloroformate (0.32 mL, 4.0 mmol) was mixed with Et<sub>2</sub>O (40 mL), and the mixture was added slowly via perfusion pump (flow rate 1 mL/h). Saturated NaHCO<sub>3</sub> solution (100 mL)



was added, and the reaction mixture was allowed to stir till the formed precipitate completely dissolves. The organic layer was separated and the aqueous layer was extracted with EA. The combined organic layers were dried over MgSO<sub>4</sub> and solvent was evaporated to dryness in vacuum. The resulting solid was heated at reflux in a mixed solvent of CCl<sub>4</sub> and *n*-hexane (1:1 v/v) for 15 min. After cooling the yellow solid was collected, washed with CCl<sub>4</sub>/*n*-hexane mixture (1:1 v/v), and dried in vacuum.

**Yield:** 1.7 g (47%)

**Colour:** Yellowish solid

**Molecular formula:** C<sub>37</sub>H<sub>40</sub>OS<sub>12</sub>

**Molar mass:** 883.97 g/mol

**Mp:** 250–255 °C

**R<sub>f</sub>:** 0.32 (heptane)

**<sup>1</sup>H NMR:** (400 MHz, CDCl<sub>3</sub>) δ 7.17 (s, 3H), 6.20 (s, 1H), 1.82 (s, 9H), 1.80 (s, 9H), 1.72 (s, 9H), 1.68 (s, 9H)

**<sup>13</sup>C NMR:** (100 MHz, CDCl<sub>3</sub>) δ 139.2, 138.3, 137.8, 137.2, 131.8, 118.1, 83.6, 64.0, 63.3, 34.8, 32.2, 29.1, 27.6

**IR (KBr):** ν = 3364, 2954, 2921, 1451, 1147, 756 cm<sup>-1</sup>

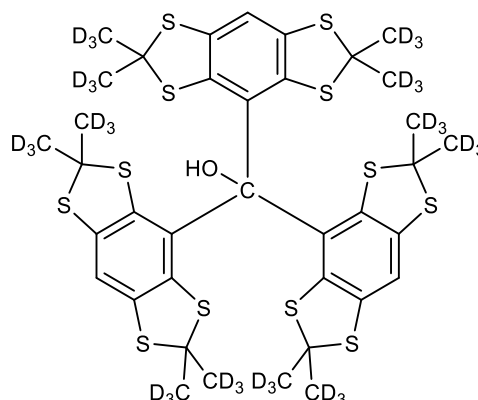
**MS (ESI):** *m/z* 906.91 [M+Na]<sup>+</sup>, 882.90 [M-H]<sup>-</sup>

**HRMS (ESI):** calcd. for C<sub>37</sub>H<sub>40</sub>OS<sub>12</sub> [M]<sup>+</sup> 883.973; found 883.973

**Tris[2,2,6,6-(<sup>2</sup>H<sub>3</sub>-tetramethyl)benzo[1,2-*d*:4,5-*d'*]bis([1,3]dithiole)-4-yl]methanol (3b)**

22,25,110

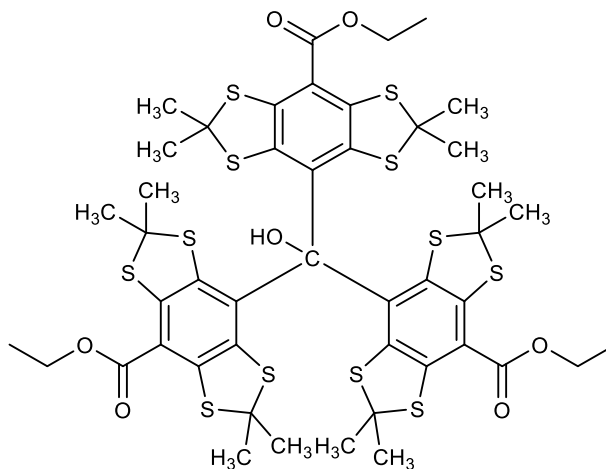
Compound **2b** (3.49 g, 11.7 mmol) was dissolved in dry Et<sub>2</sub>O (150 mL) under argon atmosphere. A solution of 2.5 M *n*-BuLi in *n*-hexane (4.7 mL, 11.7 mmol) was added dropwise, and the reaction mixture was stirred for 2 h at RT. Methyl chloroformate (0.3 mL, 3.9 mmol) was mixed with Et<sub>2</sub>O (40 mL), and the mixture was added slowly via perfusion pump (flow rate 1 mL/h). Saturated solution of NaHCO<sub>3</sub> (100 mL) was added, and the reaction mixture was allowed to stir till the formed precipitate completely dissolves. The organic layer was separated, and the aqueous layer was extracted with EA. The combined organic layers were dried over MgSO<sub>4</sub> and solvent was evaporated to dryness in vacuum. The resulting solid was heated at reflux in a mixed solvent of CCl<sub>4</sub> and *n*-hexane (1:1 v/v) for 15 min. After cooling the yellow solid was collected, washed with CCl<sub>4</sub>/*n*-hexane mixture (1:1 v/v), and dried in vacuum.

**Yield:** 1.62 g (45%)**Colour:** White to yellow solid**Molecular formula:** C<sub>37</sub>H<sub>4</sub>D<sub>36</sub>OS<sub>12</sub>**Molar mass:** 920.20 g/mol**Mp:** 250–255 °C**R<sub>f</sub>:** 0.35 (heptane)**<sup>1</sup>H NMR:** (400 MHz, CDCl<sub>3</sub>) δ 7.17 (s, 3H), 6.21 (s, 1H)**<sup>13</sup>C NMR:** (100 MHz, CDCl<sub>3</sub>) δ 139.5, 138.6, 138.1, 137.6, 132.2, 118.5, 83.9, 63.9, 63.6, 63.2**IR (KBr):** ν = 3360, 2953, 2922, 2217, 1374, 1247, 1182, 1003, 861, 754 cm<sup>-1</sup>**MS (ESI):** *m/z* 943.12 [M+Na]<sup>+</sup>, 919.03 [M-H]<sup>-</sup>



**Tris[8-ethoxycarbonyl-2,2,6,6-tetramethylbenzo[1,2-*d*:4,5-*d'*]bis([1,3]dithiole)-4-yl]methanol (4)**<sup>31,32</sup>.

Compound **3a** (500 mg, 0.57 mmol) and TMEDA (0.85 mL, 5.7 mmol) were mixed in dry *n*-hexane (5 mL) under argon atmosphere and cooled to 0 °C. A solution of 2.5 M *n*-BuLi in *n*-hexane (2.3 mL, 5.7 mmol) was added dropwise over 30 min and the mixture was stirred at RT for 3.5 h. Anhydrous toluene (10 mL) was added and the reaction mixture was allowed to stir for an additional hour, afterwards it was added slowly via syringe to cold (−25 °C, cooling bath temperature) diethyl carbonate (3.42 mL, 28.3 mmol) diluted with toluene (5 mL). The reaction mixture was allowed to reach RT and stirred overnight. Saturated NaH<sub>2</sub>PO<sub>4</sub> solution (10 mL) was added, the organic layer was separated and the aqueous layer was extracted three times with Et<sub>2</sub>O (10 mL). The combined organic layers was washed with water, dried over MgSO<sub>4</sub>, and the filtrate was passed through short silica plug. The residue was purified with silica gel eluting with (heptane/EA, 9/1).



**Yield:** 301.4 mg (48%)

**Colour:** Yellow solid

**Molecular formula:** C<sub>46</sub>H<sub>52</sub>O<sub>7</sub>S<sub>12</sub>

**Molar mass:** 1100.04 g/mol

**Mp:** > 280 °C

**R<sub>f</sub>:** 0.4 (heptane/EA, 7/3)

**<sup>1</sup>H NMR:** (400 MHz, CDCl<sub>3</sub>) δ 6.77 (s, 1H), 4.50 – 4.36 (m, 6H), 1.77 (s, 9H), 1.75 (s, 9H), 1.66 (s, 18H), 1.46 (t, *J* = 7.1 Hz, 9H)

**<sup>13</sup>C NMR:** (100 MHz, CDCl<sub>3</sub>) δ 166.2, 141.8, 141.4, 140.3, 139.2, 134.0, 121.3, 84.4, 62.3, 60.9, 60.9, 33.8, 31.9, 29.2, 28.7, 14.3

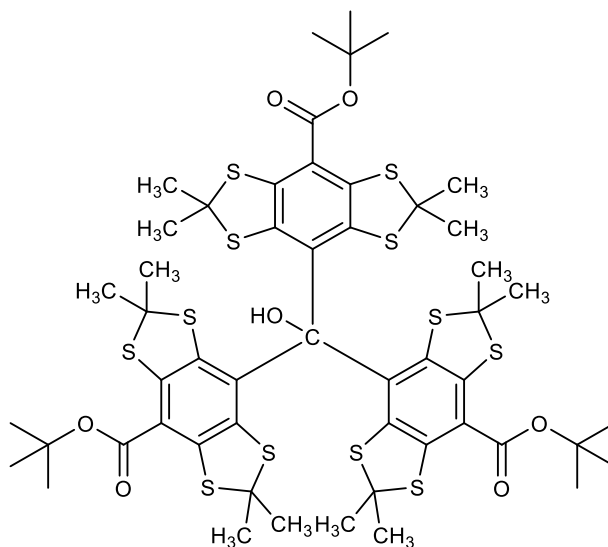
**IR (KBr):** ν = 3339, 2975, 1705, 1244, 1221, 1022, 754 cm<sup>-1</sup>

**MS (ESI):** *m/z* 1122.85 [M+Na]<sup>+</sup>, 1098.93 [M-H]<sup>-</sup>

**HRMS (ESI):** calcd. for C<sub>46</sub>H<sub>52</sub>O<sub>7</sub>S<sub>12</sub> [M]<sup>+</sup> 1100.035; found 1100.036

**Tris[8-*tert*-butoxycarbonyl-2,2,6,6-tetramethylbenzo[1,2-*d*:4,5-*d'*]bis([1,3]dithiole)-4-yl)methanol (5)**<sup>6,29,47</sup>.

Compound **3a** (1 g, 1.13 mmol) and TMEDA (1.7 mL, 11.3 mmol) were mixed in dry *n*-hexane (10 mL) under argon atmosphere and cooled to 0 °C. A solution of 2.5 M *n*-BuLi in *n*-hexane (4.52 mL, 11.3 mmol) was added dropwise over 30 min and the mixture was stirred at RT for 3.5 h. Anhydrous toluene (20 mL) was added and the reaction mixture was allowed to stir for an additional 1 h, afterwards it was added slowly via syringe to cold (−10 °C, cooling bath temperature) DiBoc (24.66 g, 113 mmol) soaked with toluene (10 mL). The reaction mixture was allowed to reach RT and stirred for 2 days. The reaction was quenched with 20 mL of MeOH added portionwise until no more gas release was observed. The resulting mixture was evaporated and the thick residue obtained was partitioned between aqueous HCl (2 M) and EA. The organic phase was separated, washed with water and dried over Na<sub>2</sub>SO<sub>4</sub>. Solvent was evaporated, and the residue was purified with silica gel eluting with (heptane/EA, 9/1).



**Yield:** 522 mg (39%)

**Colour:** Yellow solid

**Molecular formula:** C<sub>52</sub>H<sub>64</sub>O<sub>7</sub>S<sub>12</sub>

**Molar mass:** 1184.13 g/mol

**Mp:** 200–210 °C

**R<sub>f</sub>:** 0.5 (heptane/EA, 7/3)

**<sup>1</sup>H NMR:** (400 MHz, CDCl<sub>3</sub>) δ 6.72 (s, 1H), 1.77 (s, 9H), 1.74 (s, 9H), 1.65 (s, 45H)

**<sup>13</sup>C NMR:** (100 MHz, CDCl<sub>3</sub>) δ 165.3, 141.2, 140.8, 140.2, 139.1, 133.8, 122.8, 84.2, 60.90, 34.0, 31.9, 29.3, 28.6, 28.4

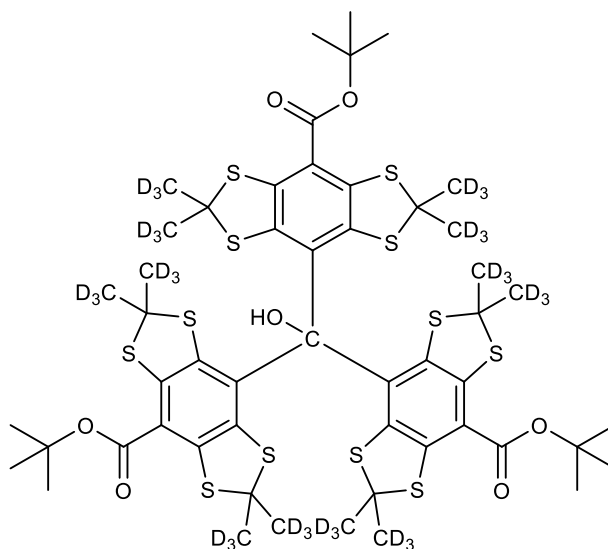
**IR (KBr):** ν = 3347, 2977, 2923, 2863, 1698, 1506, 1453, 1365, 1315, 1253, 1220, 1160, 1103, 1011, 845, 755 cm<sup>-1</sup>

**MS (ESI):** *m/z* 1206.71 [M+Na]<sup>+</sup>, 1183.04 [M-H]<sup>-</sup>

**HRMS (ESI):** calcd. for C<sub>52</sub>H<sub>64</sub>O<sub>7</sub>S<sub>12</sub> [M]<sup>+</sup> 1184.129; found 1184.131

**Tris[8-*tert*-butoxycarbonyl-2,2,6,6-(<sup>2</sup>H<sub>3</sub>-tetramethyl)benzo[1,2-*d*:4,5-*d'*]bis([1,3]dithiole)-4-yl]methanol (6)**<sup>110</sup>.

Compound **3b** (1 g, 1.08 mmol) and TMEDA (1.64 mL, 10.85 mmol) were mixed in dry *n*-hexane (10 mL) under argon atmosphere and cooled to 0 °C. A solution of 2.5 M *n*-BuLi in *n*-hexane (4.34 mL, 10.85 mmol) was added dropwise over 30 min and the mixture was stirred at RT for 3.5 h. Anhydrous toluene (20 mL) was added and the reaction mixture was allowed to stir for an additional hour, afterwards the mixture



was added slowly via syringe to cold (−10 °C, cooling bath temperature) di-*tert*-butyl dicarbonate (DiBoc) (23.68 g, 108.5 mmol) soaked with toluene (10 mL). The reaction mixture was allowed to reach RT and stirred for 2 days. The reaction was quenched with 20 mL of MeOH added portionwise until no more gas release was observed. The resulting mixture was evaporated, and the thick residue obtained was partitioned between aqueous HCl (2 M) and EA. The organic phase was separated, washed with water and dried over Na<sub>2</sub>SO<sub>4</sub>. Solvent was evaporated, and the residue was purified with silica gel eluting with (heptane/EA, 9/1).

**Yield:** 528 mg (40%)

**Colour:** Yellow solid

**Molecular formula:** C<sub>52</sub>H<sub>28</sub>D<sub>36</sub>O<sub>7</sub>S<sub>12</sub>

**Molar mass:** 1220.36 g/mol

**Mp:** 200–210 °C

**R<sub>f</sub>:** 0.3 (heptane/EA, 5/1)

**<sup>1</sup>H NMR:** (400 MHz, CDCl<sub>3</sub>) δ 6.70 (s, 1H), 1.65 (s, 27H)

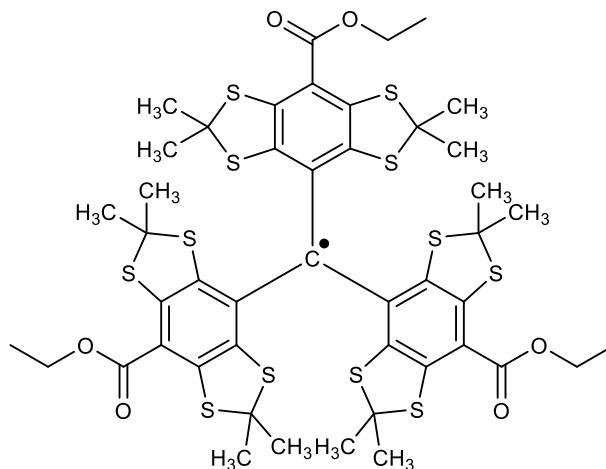
**<sup>13</sup>C NMR:** (100 MHz, CDCl<sub>3</sub>) δ 165.7, 141.5, 141.2, 140.6, 139.4, 134.1, 123.2, 84.5, 60.8, 28.7

**IR (KBr):** ν = 3351, 2978, 2927, 1701, 1506, 1476, 1455, 1393, 1368, 1314, 1253, 1221, 1161, 1124, 1023, 987, 896, 845 cm<sup>-1</sup>

**MS (ESI):** *m/z* 1243.00 [M+Na]<sup>+</sup>

**Tris[8-ethoxycarbonyl-2,2,6,6-tetramethylbenzo[1,2-*d*:4,5-*d'*]bis([1,3]dithiole)-4-yl]methyl radical (7)**<sup>28,32</sup>.

BF<sub>3</sub>.Et<sub>2</sub>O (73 μl, 0.58 mmol) was added dropwise to a solution of compound **4** (80 mg, 0.073 mmol) in DCM (10 mL) at RT. The mixture was stirred in the dark for 1 h. A solution of SnCl<sub>2</sub> (234 mg, 1.23 mmol) dissolved in THF was added to the dark green-blue reaction mixture. The mixture was stirred for 10 min and a saturated solution of KH<sub>2</sub>PO<sub>4</sub> was added. The organic layer was separated, dried over Na<sub>2</sub>SO<sub>4</sub>, and concentrated in vacuum.



**Yield:** 73 mg (92%)

**Colour:** Green-brown solid

**Molecular formula:** C<sub>46</sub>H<sub>51</sub>O<sub>6</sub>S<sub>12</sub>

**Molar mass:** 1083.03 g/mol

**Mp:** > 280 °C

**R<sub>f</sub>:** 0.4 (heptane/EA, 7/3)

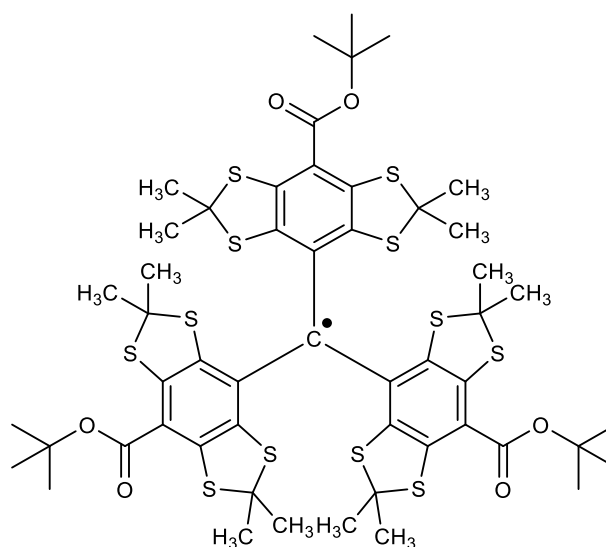
**IR (KBr):** ν = 2957, 2922, 2861, 1703, 1490, 1452, 1365, 1233, 1109, 1043, 792 cm<sup>-1</sup>

**MS (ESI):** *m/z* 1105.83 [M+Na]<sup>+</sup>, 1083.07 [M]<sup>-</sup>

**HRMS (ESI):** calcd. for C<sub>46</sub>H<sub>51</sub>O<sub>6</sub>S<sub>12</sub> [M]<sup>+</sup> 1083.033; found 1083.034

**Tris[8-*tert*-butoxycarbonyl-2,2,6,6-tetramethylbenzo[1,2-*d*:4,5-*d'*]bis([1,3]dithiole)-4-yl]methyl radical (8)**<sup>6</sup>.

BF<sub>3</sub>.Et<sub>2</sub>O (85 μl, 0.67 mmol) was added to a solution of compound **5** (100 mg, 0.084 mmol) in DCM (10 mL) dropwise at RT. The mixture was stirred in the dark for 1 h. A solution of SnCl<sub>2</sub> (271.81 mg, 1.43 mmol) dissolved in THF was added to the dark green reaction mixture. The mixture was stirred for 10 min. The mixture was stirred for 10 min and a saturated solution of KH<sub>2</sub>PO<sub>4</sub> was added. The organic layer was separated,



dried over  $\text{Na}_2\text{SO}_4$ , and concentrated in vacuum. The resulting residue was purified on silica gel eluting with (heptane/EA, 9/1).

**Yield:** 72 mg (73%)

**Colour:** Green solid

**Molecular formula:**  $\text{C}_{52}\text{H}_{63}\text{O}_6\text{S}_{12}$

**Molar mass:** 1167.13 g/mol

**Mp:** 200–210 °C

**R<sub>r</sub>:** 0.5 (heptane/EA, 7/3)

**IR (KBr):**  $\nu = 2957, 2923, 1696, 1489, 1454, 1366, 1306, 1280, 1240, 1163, 1135, 1111, 1034, 845 \text{ cm}^{-1}$

**MS (ESI):**  $m/z$  1189.76  $[\text{M}+\text{Na}]^+$ , 1167.08  $[\text{M}]^-$

**HRMS (ESI):** calcd. for  $\text{C}_{52}\text{H}_{63}\text{O}_6\text{S}_{12}$   $[\text{M}]^+$  1167.127; found 1167.126

**Tris[8-carboxy-2,2,6,6-( $^2\text{H}_3$ -tetramethyl)benzo[1,2-*d*:4,5-*d'*]bis([1,3]dithiole)-4-yl]methyl radical (9)**<sup>110</sup>.

Compound **6** (100 mg, 82  $\mu\text{mol}$ ) was treated with TFA (3 mL) and stirred at RT overnight. The reaction mixture was concentrated and dried.

**Yield:** 82.2 mg (97%)

**Colour:** Green-brown solid

**Molecular formula:**  $\text{C}_{40}\text{H}_3\text{D}_{36}\text{O}_6\text{S}_{12}$

**Molar mass:** 1035.17 g/mol

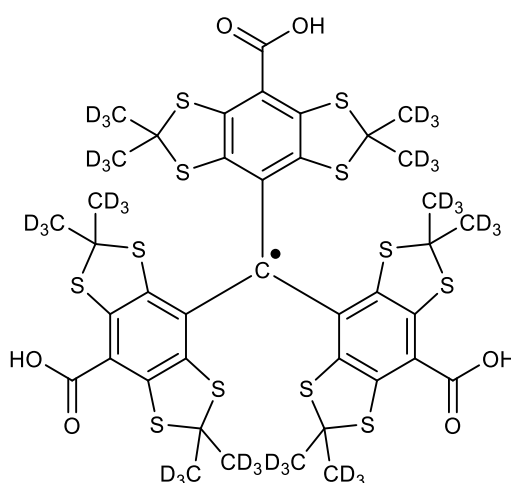
**Mp:** > 280 °C

**R<sub>r</sub>:** 0.20 ( $\text{CHCl}_3/\text{MeOH}$ , 7/3)

**IR (KBr):**  $\nu = 3541\text{--}2730, 1666, 1576, 1401, 1345, 1239, 1050 \text{ cm}^{-1}$

**MS (ESI):**  $m/z$  1035.11  $[\text{M}]^+$ , 990.23  $[\text{M}-\text{COOH}]^-$

**HRMS (ESI):** calcd. for  $\text{C}_{40}\text{H}_4\text{D}_{36}\text{O}_6\text{S}_{12}$   $[\text{M}+\text{H}]^+$  1036.173; found 1036.172, calcd. for  $\text{C}_{40}\text{H}_3\text{D}_{36}\text{O}_6\text{S}_{12}\text{Na}$   $[\text{M}+\text{Na}]^+$  1058.155; found 1058.153



**Tris[8-carboxy-2,2,6,6-tetramethylbenzo[1,2-*d*:4,5-*d'*]bis([1,3]dithiole)-4-yl]methyl radical (10)**<sup>29,31</sup>.

Compound **5** (100 mg, 84  $\mu\text{mol}$ ) was treated with TFA (3 mL) and stirred at RT overnight. The reaction mixture was concentrated and dried.

**Yield:** 79.7 mg (95%)

**Colour:** Green-brown solid

**Molecular formula:**  $\text{C}_{40}\text{H}_{39}\text{O}_6\text{S}_{12}$

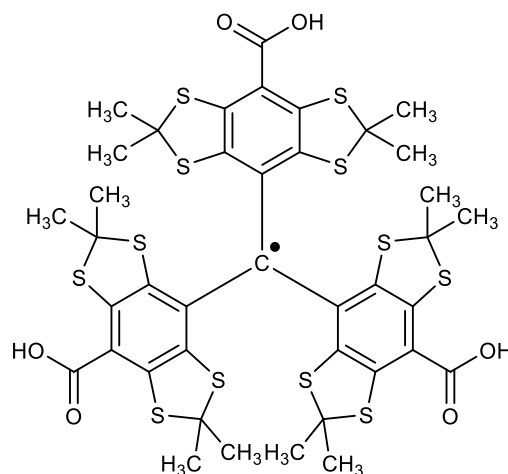
**Molar mass:** 998.94 g/mol

**Mp:** > 280 °C

**R<sub>f</sub>:** 0.20 ( $\text{CHCl}_3/\text{MeOH}$ , 7/3)

**IR (KBr):**  $\nu = 2956, 2921, 1674, 1485, 1451, 1385, 1365, 1226, 1167, 1148, 1111, 866, 725 \text{ cm}^{-1}$

**HRMS (ESI):** calcd. for  $\text{C}_{40}\text{H}_{39}\text{O}_6\text{S}_{12} [\text{M}]^+$  998.939; found 998.940

**Tris[8-ethoxy-2,2,6,6-(<sup>2</sup>H<sub>3</sub>-tetramethyl)benzo[1,2-*d*:4,5-*d'*]bis([1,3]dithiole)-4-yl]methyl radical (11)**<sup>22,25</sup>.

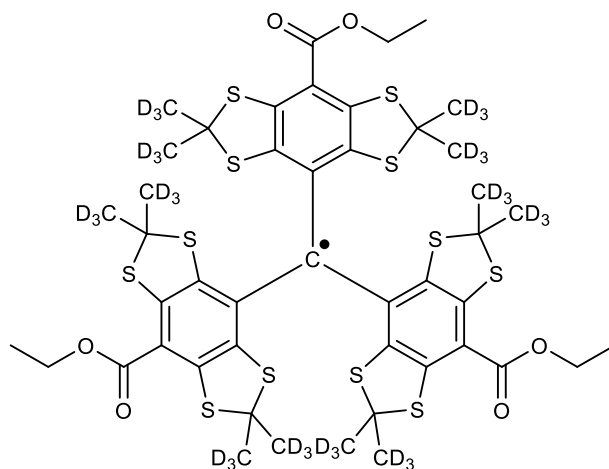
Compound **9** (50 mg, 48.3  $\mu\text{mol}$ , 1 eq.) and TEA (7  $\mu\text{l}$ , 48.3  $\mu\text{mol}$ , 1 eq.) were dissolved in acetonitrile (5 mL) under argon atmosphere and cooled to 0 °C. Ethyl chloroformate (0.23 mL, 2.4 mmol, 50 eq.) diluted with acetonitrile (2.5 mL) was added dropwise. The mixture was stirred for further 5 min, then a solution of DMAP (147.5 mg, 1.21 mmol, 25 eq.) dissolved in acetonitrile (2 mL) was added. The reaction mixture was allowed to reach RT and stir overnight. The reaction mixture was concentrated in vacuum, and the residue was treated with  $\text{CHCl}_3$  (10 mL), and washed with saturated  $\text{NaHCO}_3$  solution. The organic layer was separated, washed with HCl (0.1 M, 5 mL) and water (5 mL), dried over  $\text{MgSO}_4$  and concentrated in vacuum.

**Yield:** 43 mg (79.4%)

**Colour:** Green-brown solid

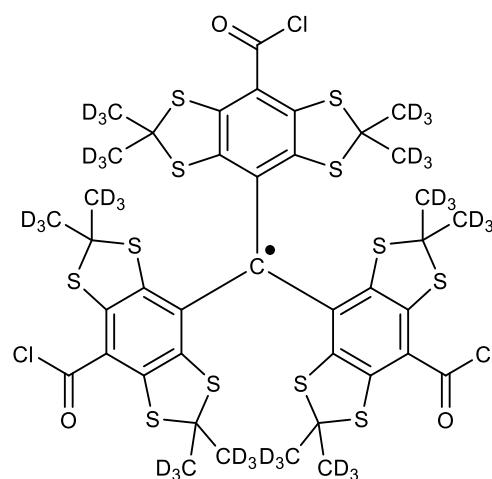
**Molecular formula:**  $\text{C}_{46}\text{H}_{15}\text{D}_{36}\text{O}_6\text{S}_{12}$

**Molar mass:** 1119.26 g/mol



**Mp:** > 280 °C**R<sub>f</sub>:** 0.4 (heptane/EA, 7/3)**IR (KBr):**  $\nu = 3326, 2925, 2850, 1702, 1627, 1575, 1232, 979 \text{ cm}^{-1}$ **MS (ESI):**  $m/z$  1142.32 [M+Na]<sup>+</sup>, 1119.37 [M]<sup>-</sup>**HRMS (ESI):** calcd. for C<sub>46</sub>H<sub>15</sub>D<sub>36</sub>O<sub>6</sub>S<sub>12</sub> [M]<sup>+</sup> 1119.259; found 1119.259**Tris[8-chloro-carbonyl-2,2,6,6-(<sup>2</sup>H<sub>3</sub>-tetramethyl)benzo[1,2-*d*:4,5-*d'*]bis([1,3]dithiole)-4-yl]methyl radical (12)**<sup>31,33</sup>.

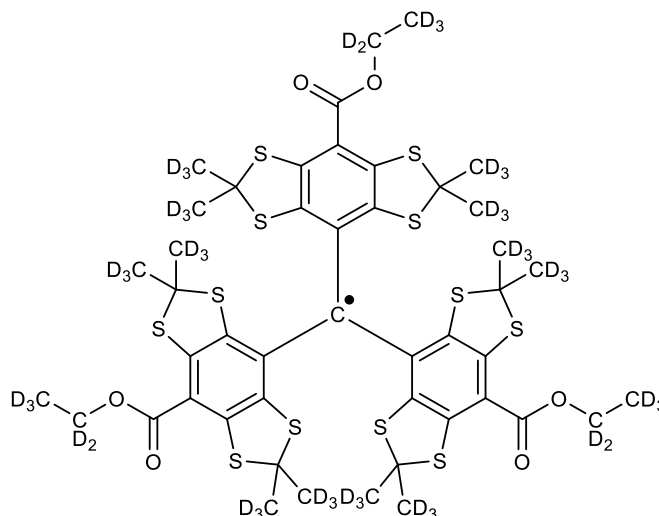
Compound **9** (150 mg, 0.14 mmol) and dry TEA (121  $\mu\text{L}$ , 0.87 mmol) were dissolved in anhydrous CHCl<sub>3</sub> (5 mL) and the mixture was stirred for 10 min at RT. A solution of SOCl<sub>2</sub> (105  $\mu\text{L}$ , 1.45 mmol) in CHCl<sub>3</sub> (2 mL) was added dropwise over 20 min. The mixture was refluxed for 2.5 h, stirred overnight at RT, and then concentrated to dryness to give a red solid, which was directly used in the next step without further purification.

**Molecular formula:** C<sub>40</sub>D<sub>36</sub>Cl<sub>3</sub>O<sub>3</sub>S<sub>12</sub>**Molar mass:** 1091.06 g/mol**R<sub>f</sub>:** 0.37 (heptane/EA, 7/3)**IR (KBr):**  $\nu = 2978, 2945, 2738, 2620, 2602, 2531, 2496, 1699, 1475, 1444, 1398, 1383, 1230, 1172, 1037, 921, 850, 808 \text{ cm}^{-1}$ **MS (ESI):**  $m/z$  1091.00 [M]<sup>+</sup>**HRMS (ESI):** calcd. for C<sub>40</sub>D<sub>36</sub>Cl<sub>3</sub>O<sub>3</sub>S<sub>12</sub> [M]<sup>+</sup> 1091.061; found 1091.061

**Tris[8-(<sup>2</sup>H<sub>3</sub>-ethoxy)-2,2,6,6-(<sup>2</sup>H<sub>3</sub>-tetramethyl)benzo[1,2-*d*:4,5-*d'*]bis([1,3]dithiole)-4-yl]methyl radical (13).**

**Method A:**

Compound **12** was dissolved in CHCl<sub>3</sub> (5 mL). EtOH-*d*<sub>6</sub> (0.72 mL, 12.32 mmol) and pyridine (19 μL, 0.24 mmol) were added. The reaction mixture was stirred at 60 °C for 4 h and then overnight at RT. The solvent was evaporated and the formed residue was dissolved in CHCl<sub>3</sub> washed with water, HCl (0.1 M) and water again three times. The



separated organic layer was dried over MgSO<sub>4</sub> and filtered through short silica plug and dried.

**Yield:** 120 mg (73%)

**Molecular formula:** C<sub>46</sub>D<sub>51</sub>O<sub>6</sub>S<sub>12</sub>

**Molar mass:** 1134.35 g/mol

**R<sub>r</sub>:** 0.40 (heptane/EA, 7/3)

**Mp:** > 280 °C

**IR (KBr):** ν = 3337, 2956, 2923, 2717, 2220, 1699, 1489, 1364, 1309, 1280, 1238, 1190, 1139, 1093, 1057, 1022, 980, 791, 753 cm<sup>-1</sup>

**MS (ESI):** *m/z* 1158.16 [M+Na]<sup>+</sup>

**HRMS (ESI):** calcd. for C<sub>46</sub>D<sub>51</sub>O<sub>6</sub>S<sub>12</sub> [M]<sup>+</sup> 1134.353; found 1134.355

**Method B:**

**Synthesis of ethyl chloroformate-*d*<sub>5</sub>:**

To a 2 M solution of phosgene in toluene (5 mL, 9.97 mmol) at 0 °C, pyridine (0.83 mL, 10.31 mmol) was added dropwise and the temperature should be kept between (0–5 °C). EtOH-*d*<sub>6</sub> (0.6 mL, 9.97 mmol) was added dropwise. The reaction mixture was allowed to reach RT, stirred for 2 h and filtered. The filtrate was used to the next step<sup>206</sup>.

The same procedure used for the synthesis of radical **11** was applied for the synthesis of radical **13**. Compound **9** (50 mg, 48.3 μmol, 1 eq.), TEA (7 μL, 48.3 μmol, 1 eq.), ethyl chloroformate-*d*<sub>5</sub> (272.5 mg, 0.24 mL, 2.4 mmol, 50 eq.) and DMAP (147.5 mg, 1.21 mmol, 25 eq.) were used to give 31 mg (56% yield) of the titled radical as green solid. The analytical data of **13** are in accordance with data mentioned above.



### 3. Tetrachlorotriarylmethyl radicals

#### 3.1. Introduction

Tetrachloro-TAM radicals are characterized by high chemical and thermal stability with good EPR properties of single and sharp EPR signal. Tetrachloro-TAM radicals show broader EPR lines due to coupling with the chlorine nuclei in close vicinity, but are distinguished by better synthetic accessibility than tetrathia-TAM radicals. The aim of this work was to synthesize a variety of trisubstituted tetrachloro-TAM radicals to investigate the substitution effect on the EPR signal. In addition, introduction of functional groups, such as carboxylate prepares the radicals for further applications, for example spin labelling of polymers, (poly)nucleotides, and proteins. The influences of pH, viscosity, oxygen concentration, and solvent parameters on the EPR signal were studied in detail.

#### 3.2. Experimental

##### 3.2.1. Materials and general methods for synthesis and analytical characterization

See section 9.1 and 9.2.

##### 3.2.2. Sample preparation for EPR spectroscopic characterization

Radicals (**23–26**) were dissolved ( $c = 1$  mM) in DMSO, radical **28** in ( $c = 1$  mM) DCM. For hydrophilic radicals **27** and **29**, solutions in PB pH 7.4 with a buffer strength of 50 mM ( $c = 1$  mM) were used. Samples were loaded into 50  $\mu$ L micropipettes that were sealed with clay. If not stated, measurements were taken in air and at ambient temperature. Radicals **24** and **25** were dissolved ( $c = 1$  mM) in MCT as well as IPM in order to investigate their oxygen sensitivity.

##### 3.2.3. EPR spectroscopy

EPR activity was investigated with a 9.3–9.55 GHz X-band spectrometer (Miniscope MS 200, Berlin, Germany). General instrument settings were: Modulation amplitude, 100 G; microwave attenuation, 20 dB; sweep time, 120 s.

Measurements under defined oxygen content were performed in glass vials using an EPR spectrometer at 1.3 GHz (Magnettech, Berlin, Germany) equipped with a re-entrant resonator.

### 3.3. Results and Discussion

Although the preparation of some tetrachloro-TAM radicals has been published (section 1.2.2.5), in this chapter new protocols for the synthesis that are reproducible with high yield are presented. In addition, introduction of functional groups that can be modified to permit the production of derivatives of tetrachloro-TAM radicals is described.

#### 3.3.1. Synthesis of different tetrachloro-TAM radicals

The synthesis of different derivatives of tetrachloro-TAM radicals is shown in **Fig. 3.1**.

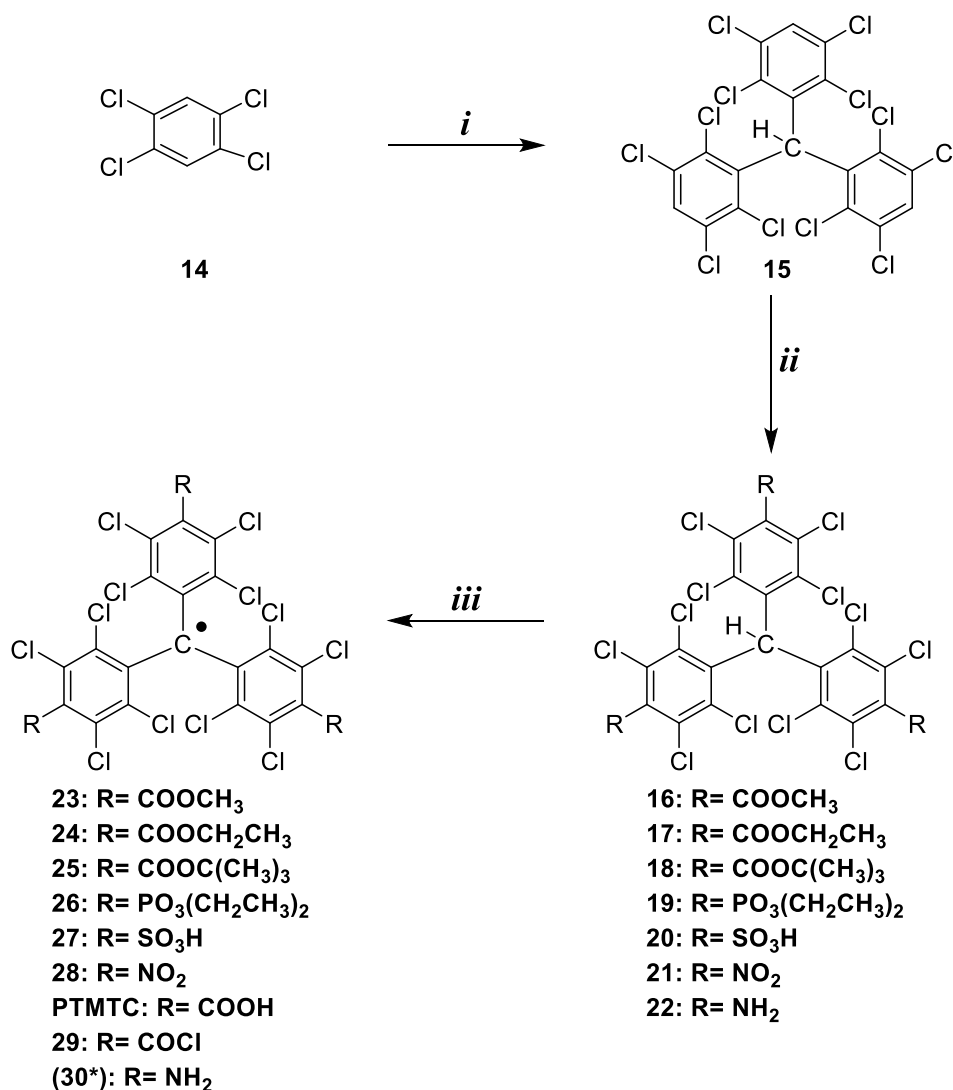


**Fig. 3.1** Synthesis of tetrachloro-TAM radicals. Reagents and conditions: **(i)** CHCl<sub>3</sub>/ AlCl<sub>3</sub>/160 °C; **(ii)** *n*-BuLi, TMEDA, methyl chloroformate, ethyl chloroformate, DiBoc or diethyl chlorophosphate, conc. HNO<sub>3</sub>/reflux, Pd/C 10%/H<sub>2</sub>, 40% oleum/110 °C; **(iii)** Bu<sub>4</sub>NOH, *p*-chloranil in THF or 95% conc. H<sub>2</sub>SO<sub>4</sub>. \* Compound **30** is not a radical, it was assumed to be the carbocation.

Perchlorotriarylmethane (**15**) was synthesized by Friedel-Crafts alkylation of 1,2,4,5-tetrachlorobenzene (**14**) with  $\text{CHCl}_3$  in the presence of  $\text{AlCl}_3$ <sup>147</sup>. Reaction of **15** with an excess of *n*-BuLi and TMEDA in THF at low temperature gave the corresponding trianion. Different ester derivatives (**16–19**) were prepared through reaction with methyl chloroformate, ethyl chloroformate<sup>178</sup>, DiBoc or di-ethyl chlorophosphate. A variation of a literature synthesis<sup>177</sup> - heating of **15** with 40% oleum at 110 °C for 4 days - reproducibly gave the trisulfonic acid **20**. An 18 h reflux of **15** with 100% fuming nitric acid yielded the trinitro derivative **21**<sup>176</sup>. Reduction of **21** with hydrogen in the presence of palladium (10% wt. on activated carbon) gave the triamino derivative **22**. Radicals (**23–28**) release from the corresponding methane derivatives was achieved through the commonly used reaction mixture  $\text{Bu}_4\text{NOH}$  and *p*-chloranil in THF<sup>183</sup>. In case of **24**, heating in 95% sulphuric acid for 18 h yielded the corresponding triacid radical (**PTMTC**)<sup>207</sup>. The free acid **PTMTC** was converted to the acid chloride **29** through reflux with  $\text{SOCl}_2$ .

The incorporation of an ionizable amino group improves the pH sensitivity of the radicals, (section 1.2.1.4). The preparation of the corresponding radical (**30**) from **22** with  $\text{Bu}_4\text{NOH}/p$ -chloranil was attempted. EPR of the reaction mixture showed the presence of a signal. After work up and column purification two fractions were separated: the first was found to be the educt **22**. The second, more polar fraction did not give an EPR signal. This finding is in accordance with what had been found for the triamino tetrathia-TAM radical<sup>208</sup>. The triamino radical, when compared with the tricarboxylate, trichloro or triethoxycarbonyl tetrathia-TAM radicals, showed the lowest stability. This may be related to the ionization potential (IP) value, which was calculated to be highest for the tricarboxylate radical and lowest for the triamino radical<sup>208</sup>. Therefore, the tricarboxylate is the most stable in an aerobic (oxidizing) environment, and the triamino is the least stable one. The EPR signal of the crude product indicated that it was formed, but decomposed during purification to give the carbocation (represented by the polar fraction of column chromatography).

### 3.3.2. EPR characterization

The EPR spectra of the tetrachloro-TAM radicals showed a single peak, in addition to three symmetrical pairs of satellites (**PTMTC**, Fig. 3.2) because of spin coupling with naturally abundant  $^{13}\text{C}$ . There was no evidence of interaction with aromatic chlorines other than band broadening<sup>150</sup>.

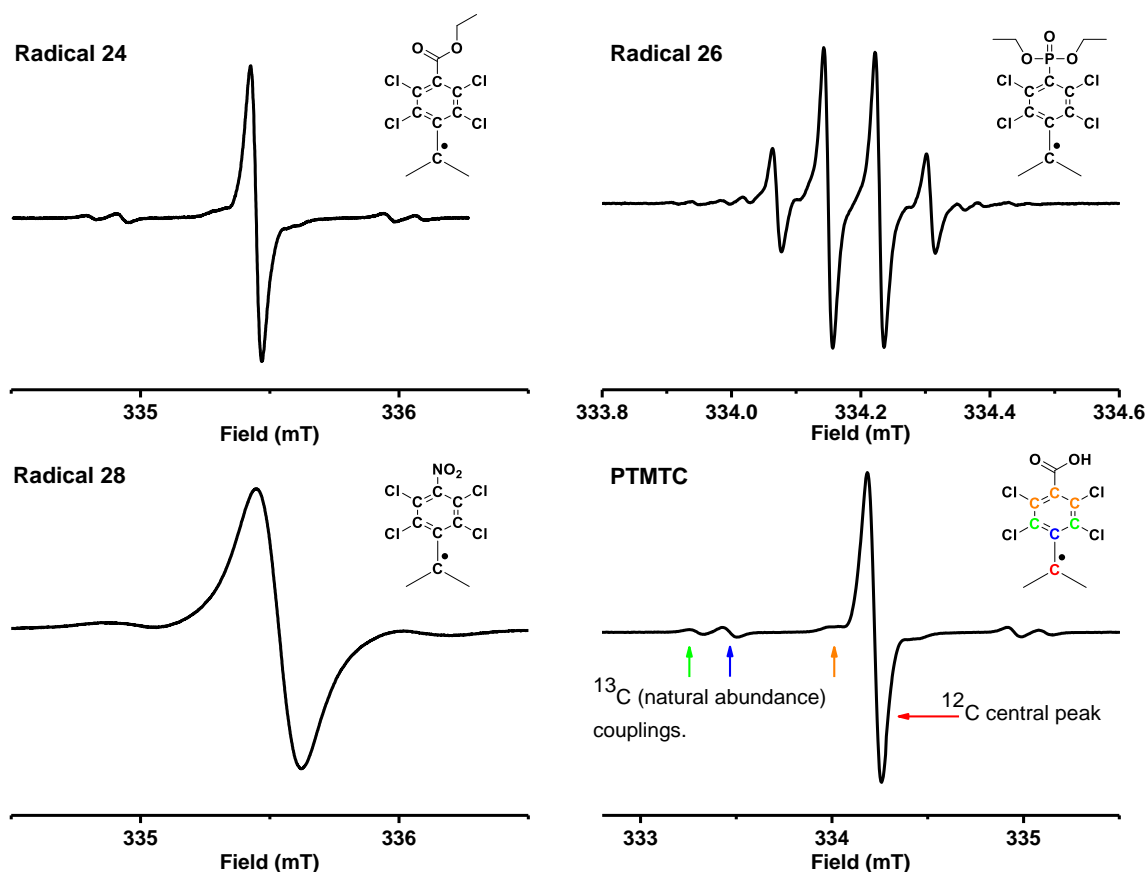


**Fig. 3.2** EPR signals of radicals **24**, **26**, **28** and **PTMTC** under aerobic conditions (20.9%  $\text{O}_2$ ).

Neither increasing the number of alkoxy protons, *i.e.* 3 protons in case of **23** or 5 protons in case of **24**, nor increasing their relative distance from the ester (**25**) caused significant effects on line width through electron-nuclei coupling. Radical **26** showed a quartet signal (internal ratio 1:3:3:1) with line widths of approx. 0.044 mT due to coupling with  $^{31}\text{P}$  ( $I = 1/2$ ). Radical **28** exhibited a broad singlet only ( $\Delta B_{\text{PP}} = 0.16$  mT) due to unresolved coupling with the quadrupolar  $^{14}\text{N}$  ( $I = 1$ , 99.63% natural abundance), which usually has a short  $T_1$  value, and because steric crowding forces the nitro groups out of conjugation with the aromatic ring<sup>176</sup>. The hydrophilic radical **PTMTC** showed a single narrow EPR peak ( $\Delta B_{\text{PP}} = 0.046$  mT) and very good solubility in PB up to 10 mM without spin-spin line broadening.

Moreover, solutions of radicals **27** and **PTMTC** (1 mM in PB) were stored under different conditions, and the EPR signal was monitored for 5 weeks. The trisulfonate radical **27** was stable in the dark at 37 °C for only 2 weeks, while radical **PTMTC** showed stability for more than 5 weeks. However, if ambient light was allowed into the solutions, the EPR signal of radical **PTMTC** showed broadening and very low intensity after 3 days and completely

disappeared after approx. 1 week, whereas **27** was less affected by light, retaining the 2-week stability it had in the dark.

To conclude, very promising EPR spin probes with different hydrophilic and lipophilic properties were synthesized. Radicals **24** and **25** were used for further research, focus on the development of suitable pharmaceutical formulation. Oxygen sensitivity of radicals **24** and **25** in different solvents (MCT and IPM) was investigated, and results are given in section 3.3.3. The use of radical **23** for spin labelling of nucleotide is discussed in section 3.3.4. Synthesis and a comprehensive study of the impact of different parameters (*e.g.* pH value, viscosity and oxygen content) on the EPR spectra of radical **PTMTC** and its  $^{13}\text{C}$  labelled analog ( $^{13}\text{C}$ -**PTMTC**) are discussed in section **PTMTC and  $^{13}\text{C}$ -PTMTC**. Moreover, **PTMTC** and radical **29** were used for spin labelling of polymers (chitosan and carboxymethylchitosan) as it is explained in section **Spin labelling of polymers (chitosan and carboxymethyl chitosan)**.

### 3.3.3. Oxygen calibration of radicals **24** and **25** in an oily solution <sup>‡‡</sup>

Solutions of radical **24** and **25** in either MCT or IPM ( $c = 1 \text{ mM}$ ) were tested under aerobic conditions (20.9%  $\text{O}_2$ ) and after flushing with nitrogen ( $\sim 0\% \text{ O}_2$ ). As it was found before for solutions in DMSO, line widths of both radicals were quite similar in both solvents (MCT and IPM).

**Table 3-1** EPR line widths of radicals **24** and **25** in MCT and IPM (1mM, under aerobic (20.9%  $\text{O}_2$ ) and deoxygenated ( $\sim 0\% \text{ O}_2$ ) conditions).

Radical	MCT				IPM			
	$\Delta B_{PP}$ ( $\mu\text{T}$ )		Oxygen sensitivity		$\Delta B_{PP}$ ( $\mu\text{T}$ )		Oxygen sensitivity	
	0% $\text{O}_2$	20.9% $\text{O}_2$	$\mu\text{T}/\% \text{O}_2$	$\mu\text{T}/\text{mmHg}$	0% $\text{O}_2$	20.9% $\text{O}_2$	$\mu\text{T}/\% \text{O}_2$	$\mu\text{T}/\text{mmHg}$
<b>24</b>	51	82	1.67	0.23	23	98	3.83	0.51
<b>25</b>	53	90	1.84	0.25	23	98	3.75	0.52

Due to the chlorine splitting, tetrachloro-TAM radicals have generally broader EPR lines than the tetrathia-TAM derivatives. The triethyl ester (**24**) in MCT solution has EPR line widths of 84  $\mu\text{T}$  (at 20.9% oxygen) and 51  $\mu\text{T}$  (at  $\sim 0\%$  oxygen), as well as in IPM solution 104  $\mu\text{T}$  (at

<sup>‡‡</sup> This part of the work will be reported in detail in an ongoing thesis by Juliane Frank (research group Prof. Mäder) the other first author of our publication (Ref. <sup>196</sup>).

20.9% oxygen) and 23  $\mu\text{T}$  (at  $\sim 0\%$  oxygen). The tri-*tert*-butyl ester (**25**) has comparable line widths (**Table 3-1**). The different slopes in MCT and IPM were probably caused by the different polarity and especially viscosity of the oils.

### 3.3.4. Spin labelling of a nucleoside

Site-directed spin labeling combined with EPR spectroscopy is used to study structure and function of biomolecules (such as proteins and oligonucleotides)<sup>209,210</sup>. The general idea is that the biomolecule is spin labelled with two paramagnetic center at selected positions and the distance determination with EPR spectroscopy depends on the magnetic dipole-dipole interaction between the magnetic moments of the two spins<sup>52,211</sup>. Continuous wave and pulsed EPR methods can measure the magnetic dipole coupling between two unpaired electrons reliably and precisely up to 80 Å<sup>211</sup>. Nitroxide radicals were used as spin labels for peptides and proteins<sup>212-214</sup> as well as DNA and RNA<sup>215-219</sup>. Recently, tetrathia-TAM radicals were used as spin labels for distance measurements<sup>52-54,220</sup>.

The aim was to synthesize a spin labelled nucleoside that could be converted into an oligonucleotide through phosphoramidite method as described in Ref.<sup>221</sup>.

The first trial to synthesize a spin labelled nucleoside (**38**) is shown in **Fig. 3.3**. The nucleoside (**34**) was synthesized through Sonogashira coupling<sup>222-224</sup> between 2'-deoxy-5-iodouridine (**33**) and *N*-propynyltrifluoroacetamide (**32**). The amino group was protected<sup>225</sup> to avoid interference with the subsequent catalytic process. 5'-hydroxy group of **34** was protected with 4,4'-dimethoxytrityl chloride (DMTCl, **35**)<sup>226,227</sup> to give the nucleoside **36**. Deprotection of the amino group was accomplished in concentrated aqueous ammonia (conc.  $\text{NH}_3$ )<sup>228</sup> to afford the nucleoside **37** with free amino group.

Compound **37** was allowed to react with radical **PTMTC** in the presence of 1*H*-benzotriazol-1-yloxytris(pyrrolidino)phosphonium hexafluoro-phosphate (PyBob) and *N,N*-Diisopropylethylamine (Hunig's base) in DMF as solvent<sup>229</sup>. Mass spectroscopy of the product mixture indicated the formation of the target spin labelled nucleoside (**38**). Several trials of purification through column chromatography were attempted. However, the separation of the pure product could not be achieved. This complicated purification may be attributed to the presence of three carboxyl groups in the structure of **PTMTC**. Accordingly, mono, di or triamides might be developed upon their reaction with the amino group from compound **37**. Therefore, a series of side product that are closely related and are difficult to be separated, were formed.

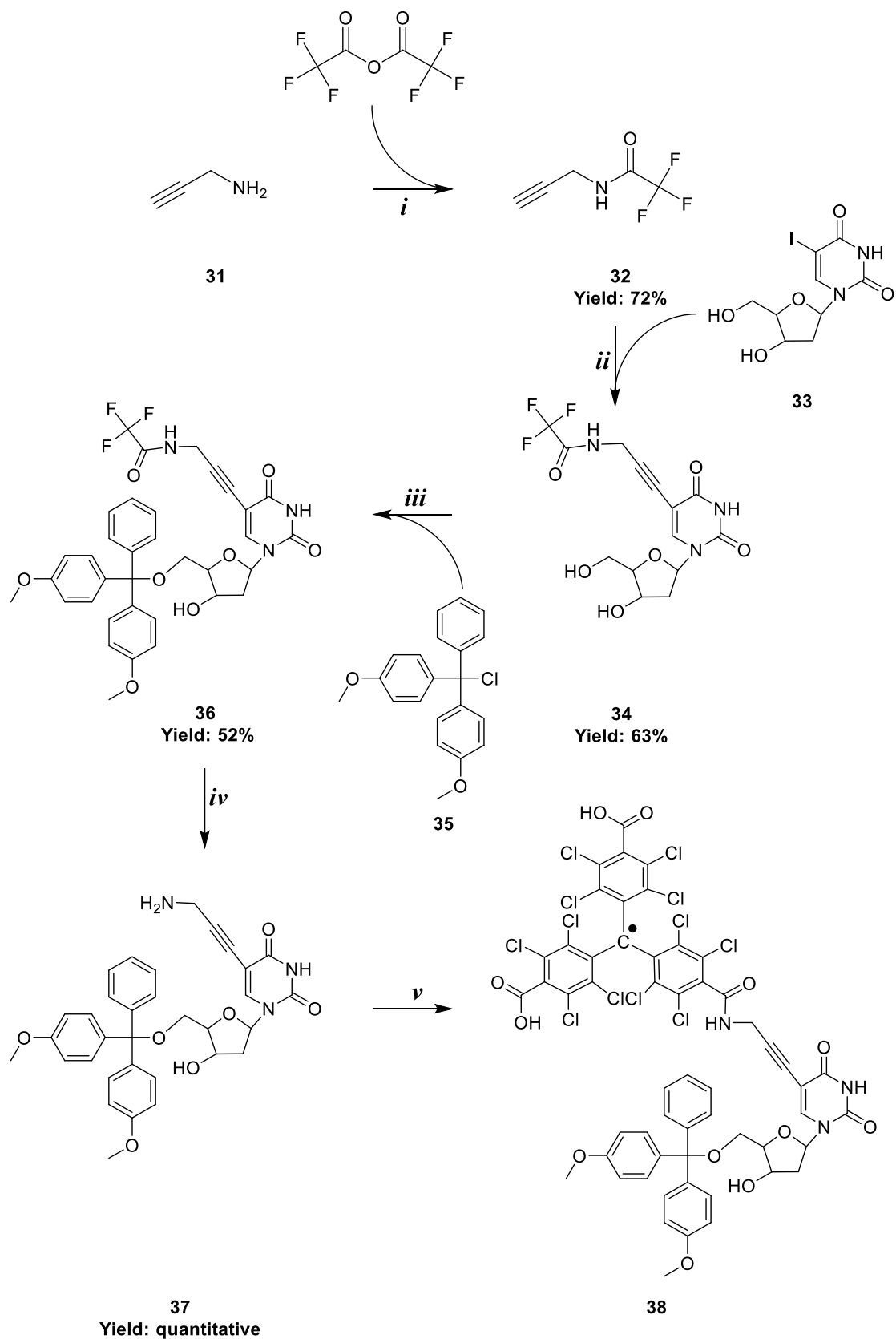
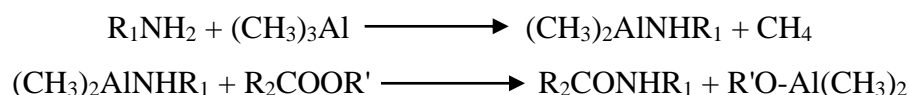


**Fig. 3.3** Synthesis of spin labelled nucleoside **38**. Reagents and conditions: **(i)** trifluoroacetic anhydride/DCM/0 °C; **(ii)** 2'-deoxy-5-iodouridine/CuI/TEA/tetrakis(triphenylphosphine)-palladium(0)/DMF; **(iii)** DMTCI/TEA/pyridine; **(iv)** Conc. NH<sub>3</sub>; **(v)** PyBob/Hunig's base/DMF/PTMTC.

Based on the fact that the ester derivatives of tetrachloro-TAM are very stable towards hydrolysis and the free carboxyl groups made the purification of nucleoside **38** problematic, a modification towards the synthesis of spin labelled nucleoside was suggested, **Fig. 3.4**. The idea was to prepare a tetrachloro-TAM derivative protected with two ester groups and coupled with nucleoside **41** at one *para* position (radical **42**, **Fig. 3.4**).

The trimethoxycarbonyl tetrachloro-TAM (**16**) was reacted with propargylamine in the presence of trimethylaluminium (TMA) to give tetrachloro-TAM derivative with terminal alkyne group (**39**). TMA can react with ammonia as well as primary and secondary amines to produce dimethylaluminum-amide complexes. These complexes can further react with esters under mild conditions producing amides with a high yield<sup>230,231</sup>, (**Equation 5**).

**Equation 5** Suggested mechanism for amide formation in the presence of TMA as catalyst<sup>232</sup>.



The reaction between propargylamine (acts as Lewis base) and TMA (acts as Lewis acid) was reported, and the aluminium-amide complex was separated and characterized<sup>233</sup>. In order to optimize the reaction conditions, some modifications of the solvent and the molar ratio were carried out (**Table 3-2**). Trial **D** has provided the highest yield of **39** (31%). In this trial, dichloroethane (DCE)<sup>108</sup> (higher boiling point) was used instead of DCM as solvent and 10 equivalents of propargylamine/TMA were used. Further increase of the molar equivalents of propargylamine/TMA to compound **16** resulted in the formation of di and triamide with lowering the yield of **39**.

**Table 3-2** Modification to improve the yield of **39**.

	Solvent	Molar ratio Compound 16 : Propargylamine/TMA	Result
<b>A</b>	DCM	1 : 1.2	Starting was recovered
<b>B</b>	DCM	1 : 3.4	Starting was recovered
<b>C</b>	DCE	1 : 3.4	3% of compound <b>39</b>
<b>D</b>	DCE	1 : 10	31% of compound <b>39</b>
<b>E</b>	DCE	1 : 20	11% of compound <b>39</b> + 22% of dialkyne derivative + 13 % of trialkyne derivative



Compound **39** was converted to the corresponding radical (**40**) through the reaction mixture Bu<sub>4</sub>NOH/*p*-chloranil in THF<sup>183</sup>. Sonogashira coupling<sup>234</sup> between **40** and compound **41** - with protected 5'-hydroxy group<sup>235</sup> - resulted in the formation of two types of products, the cross-coupling product (**42**) and the homocoupling product (**43**).

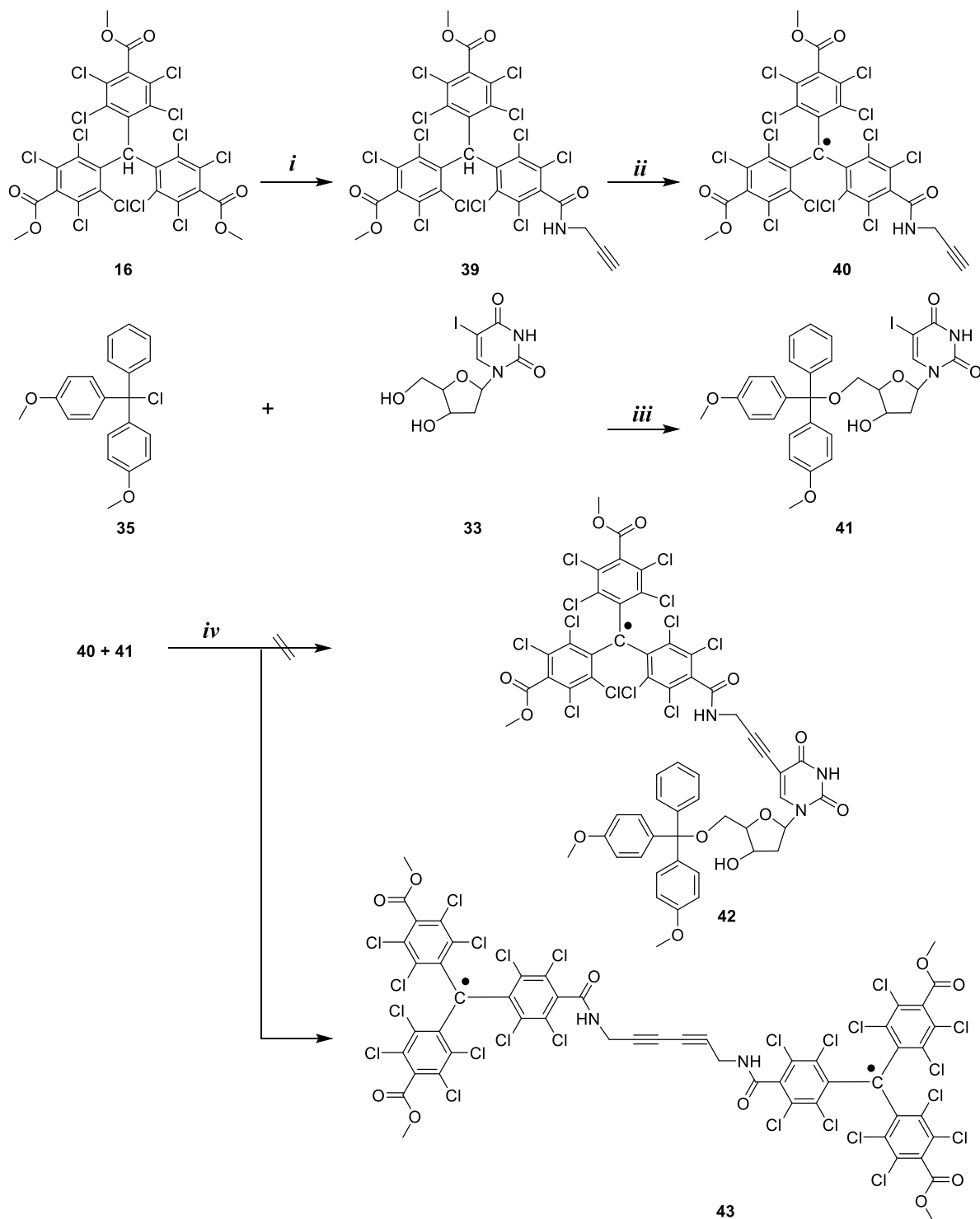


**Fig. 3.4** Synthesis of spin labelled nucleoside **42** and diradical **43**. Reagents and conditions: (i) propargylamine/TMA/DCE; (ii) Bu<sub>4</sub>NOH/*p*-chloranil; (iii) DMTCl/TEA/pyridine; (iv) CuI/TEA/tetrakis(triphenylphosphine)palladium(0)/DMF.

Sonogashira coupling reaction is one of the most important carbon-carbon bond formation reactions in organic synthesis. Sonogashira coupling is the coupling of aryl or vinyl halides with terminal alkynes catalyzed by palladium with or without the presence of copper(I)<sup>236</sup>. In 1975, Kenkichi Sonogashira et al.<sup>237</sup> reported for the first time the palladium catalyzed carbon-carbon bond formation in the presence of a catalytic amount of CuI.

### Mechanism of the reaction:

Cu-catalysed Sonogashira coupling is expected to take place through the path outlined in **Fig. 3.5**.

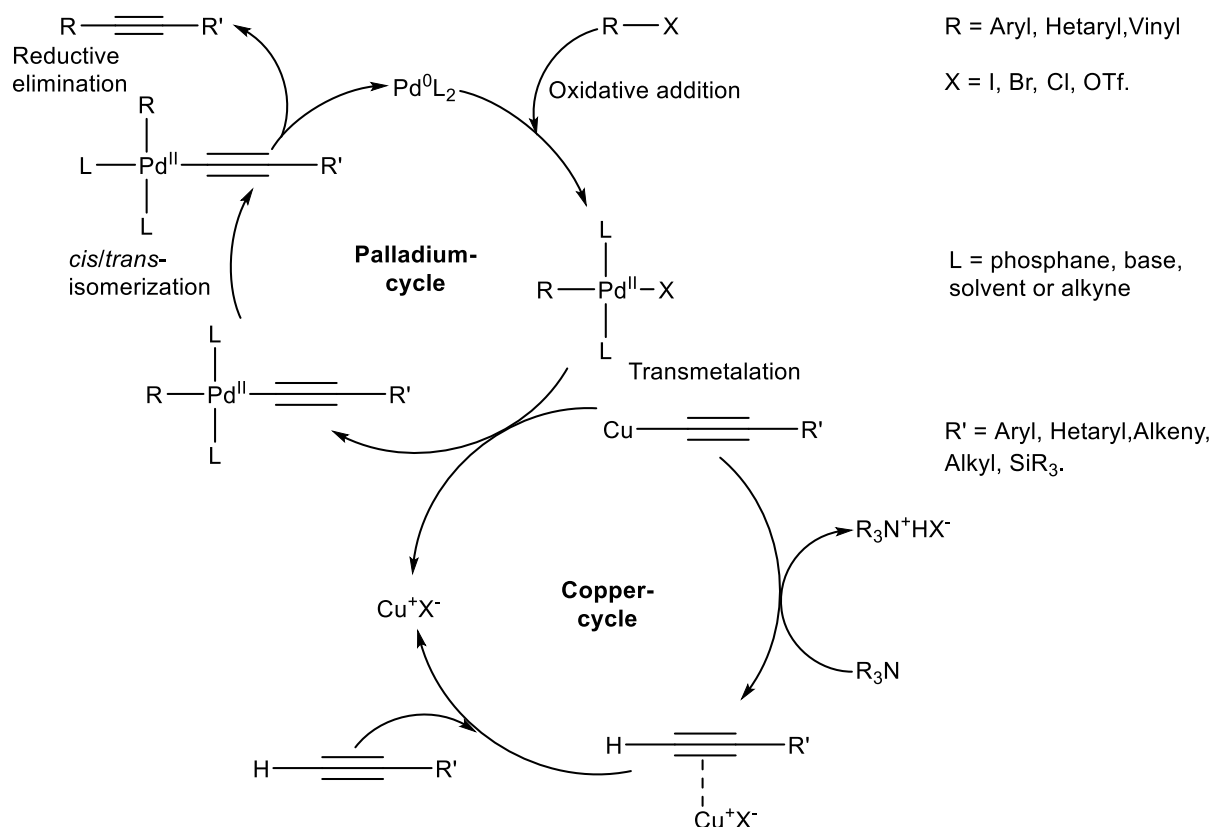


**Fig. 3.5** Schematic representation of Cu-catalysed Sonogashira coupling, modified from Ref.<sup>236</sup>.

The main drawback of Cu-catalyzed Sonogashira coupling is that the copper acetylide undergoes homocoupling with itself, when exposed to air or oxidative agents, producing the homocoupling product ( $R'-C\equiv C-C\equiv C-R'$ ) along with the desired cross-coupling product ( $R-C\equiv C-R'$ )<sup>238</sup>. This causes wasting of the valuable terminal alkynes that may be expensive to purchase or must be synthesized through a complicated reaction. Different modifications in the Sonogashira reaction conditions were reported to diminish the homocoupling and to increase the efficiency of the reaction. These modifications include:

working under anaerobic conditions, working under reductive atmosphere of hydrogen or a mixture of hydrogen and nitrogen<sup>239</sup>, slow addition of the acetylene and more recently working without copper salt, the so-called Cu-free Sonogashira coupling<sup>240-242</sup>. More details about Sonogashira cross-coupling improvements are discussed in details on reviews<sup>236,243</sup>.

Glasswares were carefully dried, and the used solvents (DMF and TEA) were freshly distilled. In addition, working cautiously under argon atmosphere was considered. However, the homocoupling was unavoidable. During the first trial of synthesis (**Fig. 3.4**), MS and TLC indicated the presence of the two products (**42** and **43**), but during purification on silica gel eluting with a mixture of (heptane/acetone) the homocoupling product (**43**) was separated with (heptane/acetone: 78/22) as pale red solid. Afterwards, the polarity was increased till 100% acetone, and the desired cross-coupling product did not elute. For better understanding of the reaction, a second trial was performed using the  $\alpha$ H-derivative (**39**), **Fig. 3.6**. Both  $\alpha$ H products (**44** and **45**) were separated and characterized. Radical (**43**) release from  $\alpha$ H precursor **45** was achieved with the mixture Bu<sub>4</sub>NOH/*p*-chloranil in THF.

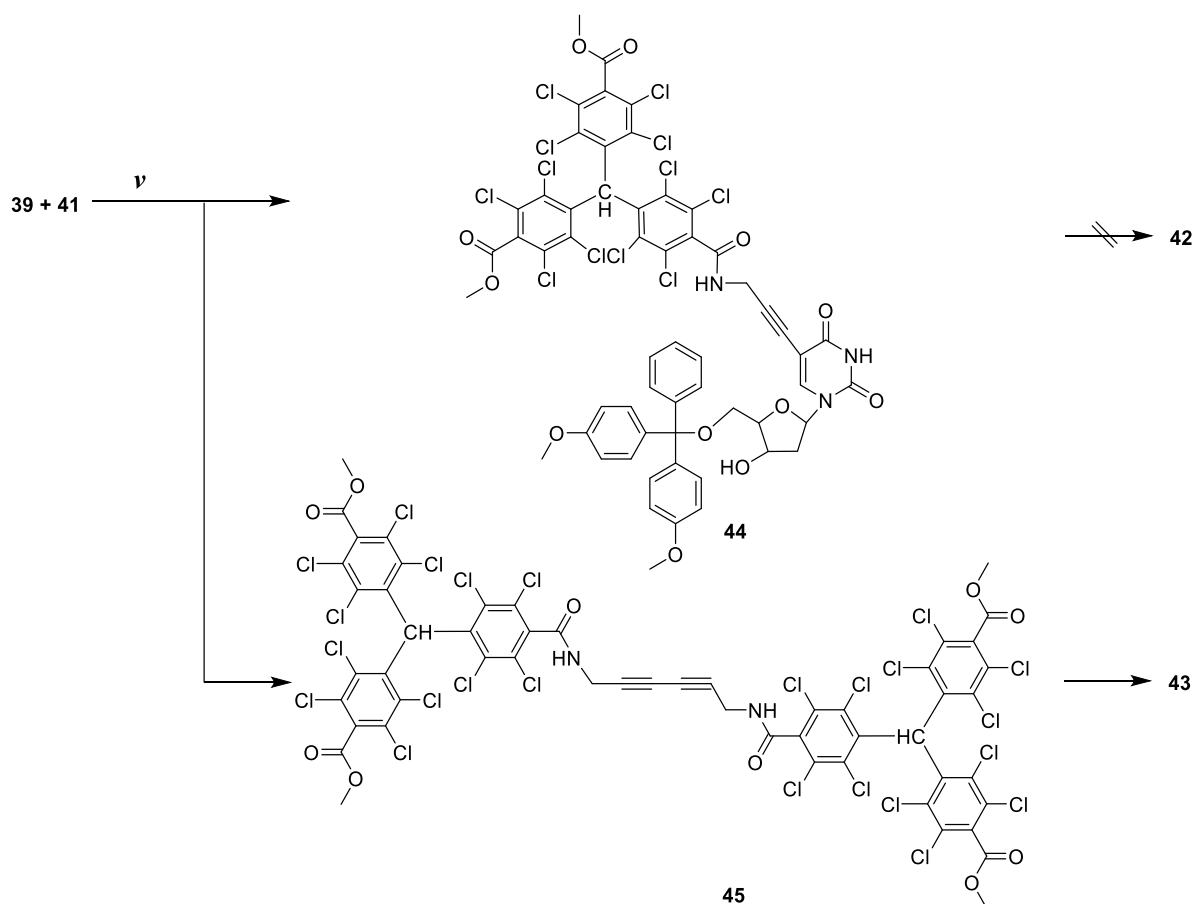


**Fig. 3.6** Sonogashira coupling between  $\alpha$ H-derivative (compound **39**) and nucleoside **41** (with protected 5'-hydroxy group). Reagents and conditions: **(v)** CuI/TEA/tetrakis(triphenylphosphine)palladium(0)/DMF.

Release of radical **42** from its  $\alpha$ H precursor **44** was attempted with the commonly used mixture Bu<sub>4</sub>NOH/*p*-chloranil in THF. EPR spectroscopy of the reaction mixture revealed the presence of a signal. After conventional workup and purification on silica eluting with (heptane/EA/TEA: 45/50/5) to separate the excess unreacted *p*-chloranil. Then the polarity was increased to (EA/MeOH/TEA: 65/30/5) and a purple fraction was eluted. MS indicated that this purple fraction has the same molar mass of the desired product **42**, but no EPR signal was detected for this product. It was supposed that in the presence of excess *p*-chloranil and atmospheric oxygen, the radical was oxidized into carbocation that is much more polar than the radical itself. The same procedure was repeated using only one equivalent of *p*-chloranil. The crude mixture (without further purification) showed EPR signal that had disappeared when the mixture was kept at ambient conditions for one day.

Another trial to synthesize spin labelled nucleoside **47** was carried out, **Fig. 3.7**. Sonogashira coupling between **39** and 2'-deoxy-5-iodouridine (compound **33**) resulted in the formation of both homocoupling product (**45**) along with the cross-coupling product (**46**). The radical **47** was not stable as observed before for radical **42**.

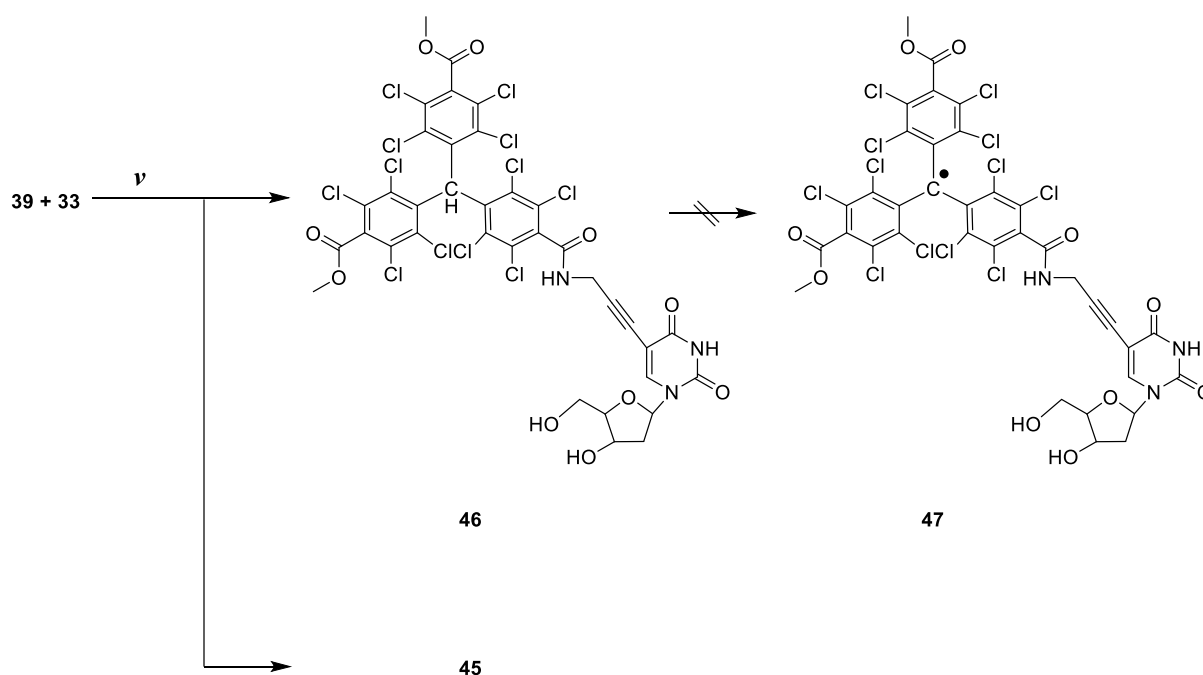


**Fig. 3.7** Sonogashira coupling between compound **39** and nucleoside **33**. Reagents and conditions: ( $\nu$ ) CuI/TEA/tetrakis-(triphenylphosphine)palladium(0)/DMF.

It worth to mention that Rosaria Carmela Perone was able to react  $\alpha$ H-acid chloride with 2',3'-O-isopropylidene-guanosine under mild conditions to synthesize  $\alpha$ H-PTM-Gace, **Fig. 3.8**. However, the acid chloride radical did not react with 2',3'-O-isopropylidene-guanosine either under the same reaction conditions or different conditions. Moreover, conversion of  $\alpha$ H-PTM-Gace into the corresponding radical (PTM-Gace radical) was not successful <sup>149</sup>.

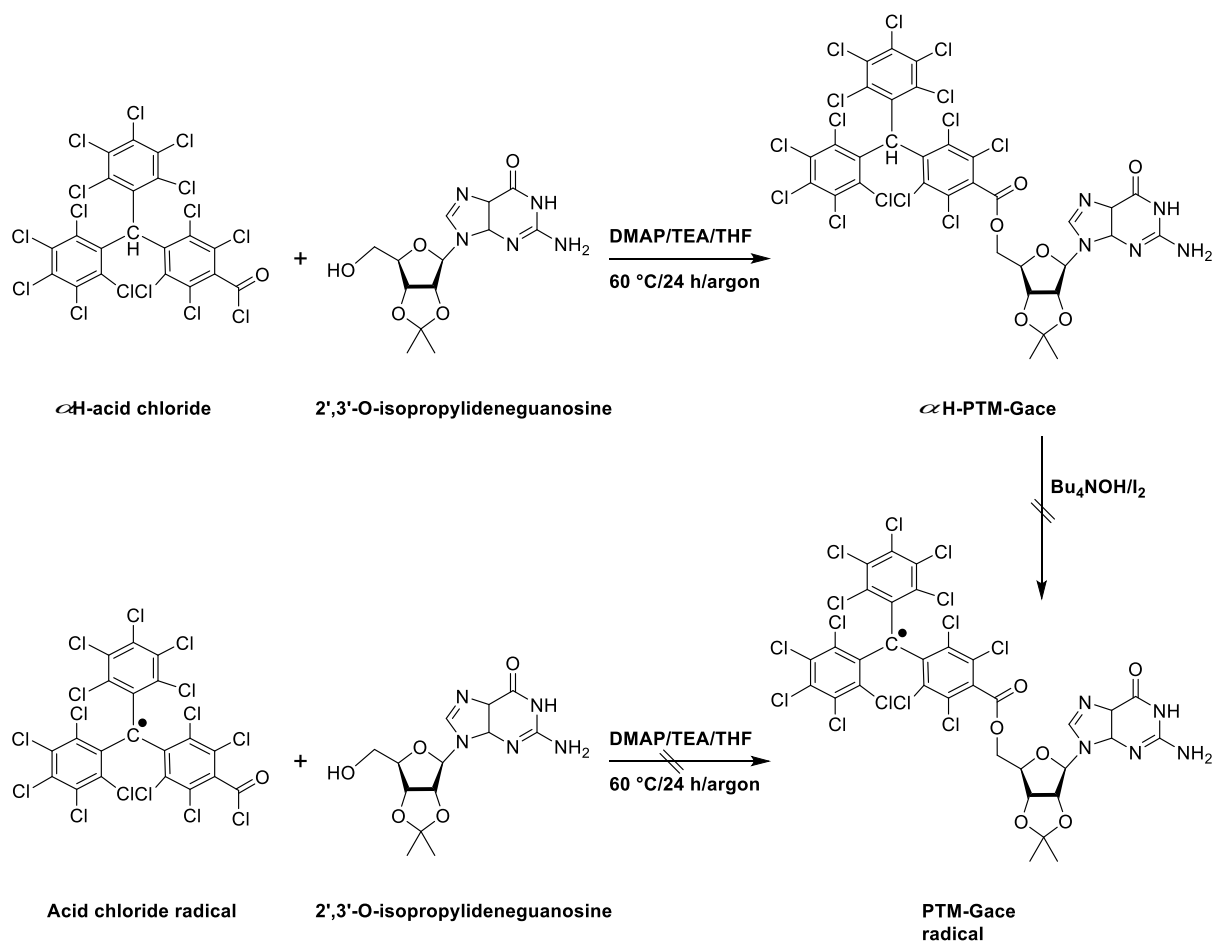


**Fig. 3.8** Synthesis of PTM-Gace radical <sup>149</sup>.

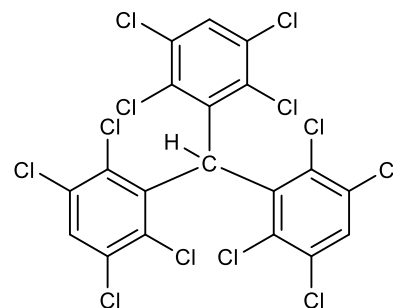
### Conclusion and outlook

Tetrachloro-TAM radicals may be unstable when directly connected to the nucleoside moiety. The reaction can be repeated with one of the tetrathia-TAM radicals. Even though development of a radical suitable for distance measurement was unsuccessful, radical (**40**) with a terminal alkyne group, was prepared. Radical **40** may open the way for the synthesis of more tetrachloro-TAM derivatives through click chemistry reactions.

### 3.4. Syntheses <sup>§§</sup>

#### Tris(2,3,5,6-tetrachlorophenyl)methane (**15**) <sup>147</sup>.

1,2,4,5-tetrachlorobenzene (**14**) (9.6 g, 44 mmol), AlCl<sub>3</sub> (0.73 g, 5.2 mol) and CHCl<sub>3</sub> (0.4 mL, 4.9 mmol) were mixed in a glass pressure vessel, and were heated in an oil bath at 160 °C for 45 min. The mixture was then poured onto ice and HCl (1M, 50 mL) and extracted three times with CHCl<sub>3</sub>. The organic layer was washed with water, aqueous NaHCO<sub>3</sub> and dried over Na<sub>2</sub>SO<sub>4</sub>. After evaporation, the residue was purified on silica gel eluting with heptane.



**Yield:** 1.3 g (40%, based on CHCl<sub>3</sub>).

**Colour:** White crystals

**Molecular formula:** C<sub>19</sub>H<sub>4</sub>Cl<sub>12</sub>

**Molar mass:** 657.65 g/mol

**Mp:** > 280 °C

**R<sub>f</sub>:** 0.67 (heptane)

**<sup>1</sup>H NMR:** (400 MHz, CDCl<sub>3</sub>) δ 7.65 (s, 3H), 6.98 (s, 1H)

**<sup>13</sup>C NMR:** (100 MHz, CDCl<sub>3</sub>) δ 138.0, 134.3, 133.6, 133.3, 132.4, 130.3, 56.1

**IR (KBr):** ν = 3112, 3067, 2926, 1547, 1409, 1387, 1348, 1322, 1235, 1199, 1164, 1099, 975, 866, 844, 782, 759, 704, 690 cm<sup>-1</sup>

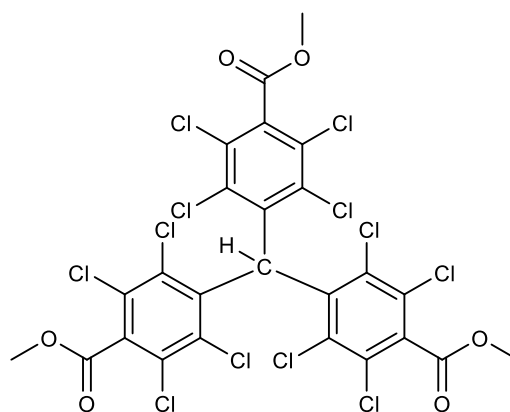
**MS (EI):** 658 (C<sub>19</sub>H<sub>4</sub>Cl<sub>12</sub>), 621 (C<sub>19</sub>H<sub>4</sub>Cl<sub>11</sub>), 586 (C<sub>19</sub>H<sub>4</sub>Cl<sub>10</sub>), 551 (C<sub>19</sub>H<sub>4</sub>Cl<sub>9</sub>), 516 (C<sub>19</sub>H<sub>4</sub>Cl<sub>8</sub>), 479 (C<sub>19</sub>H<sub>4</sub>Cl<sub>7</sub>), 444 (C<sub>19</sub>H<sub>4</sub>Cl<sub>6</sub>), 409 (C<sub>19</sub>H<sub>4</sub>Cl<sub>5</sub>)

**HRMS (ESI):** calcd. for C<sub>19</sub>H<sub>3</sub>Cl<sub>12</sub> [M-H]<sup>-</sup> 656.642; found 656.639

<sup>§§</sup> Syntheses of compound **20** and radical **27** were discussed in another thesis PhD thesis in the research group of Prof. Imming, Diana Müller. Martin-Luther-Universität Halle-Wittenberg, 2013. The synthesis of PTMTC radical will be discussed later (section 4.5).

**Tris(4-methoxy-carbonyl-2,3,5,6-tetrachlorophenyl)methane (16).**

Compound **15** (980 mg, 1.49 mmol) and TMEDA (2.25 mL, 14.49 mmol) were dissolved in dry THF (100 mL) under argon atmosphere and cooled to  $-78$  °C. A solution of 2.5 M *n*-BuLi in *n*-hexane (6 mL, 14.49 mmol) was added in one portion, and the mixture was stirred at this temperature for 1 h. Methyl chloroformate (1.15 mL, 14.49 mmol) was added, and the reaction mixture was allowed to reach



RT overnight. Solvent was evaporated, and the residue was dissolved in DCM. The organic layer was washed with water and dried over MgSO<sub>4</sub>. Solvent was evaporated under vacuum and residue was purified on silica gel eluting with (heptane/EA, 10/1).

**Yield:** 1.48 g (83 %)

**Colour:** white solid

**Molecular formula:** C<sub>25</sub>H<sub>10</sub>Cl<sub>12</sub>O<sub>6</sub>

**Molar mass:** 831.67 g/mol

**Mp:** 260–263 °C

**R<sub>f</sub>:** 0.2 (heptane/EA, 10/1)

**<sup>1</sup>H NMR:** (400 MHz, CDCl<sub>3</sub>) δ 7.01 (s, 1H), 4.01 (s, 9 H)

**<sup>13</sup>C NMR:** (400 MHz, CDCl<sub>3</sub>) δ 163.7, 138.5, 135.4, 135, 134, 130.6, 129.6, 56.3, 53.6

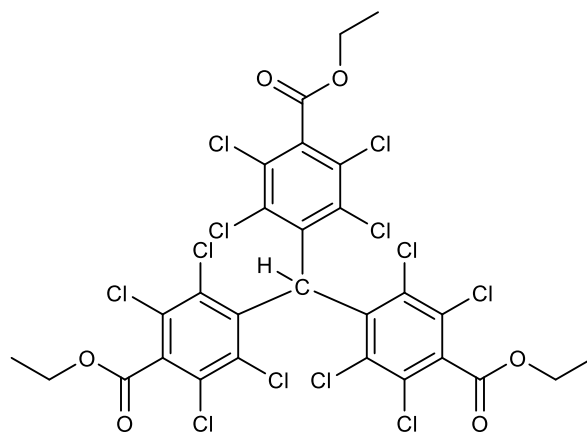
**IR (KBr):** ν = 3024, 2953, 1745, 1555, 1436, 1370, 1342, 1324, 1300, 1264, 1226, 1208, 1182, 1120, 1012, 953, 900, 854, 826, 797, 756 cm<sup>-1</sup>

**MS (EI):** 831.7 (C<sub>25</sub>H<sub>10</sub>Cl<sub>12</sub>O<sub>6</sub>)

**HRMS (ESI):** calcd. for C<sub>25</sub>H<sub>11</sub>Cl<sub>12</sub>O<sub>6</sub> [M+H]<sup>+</sup> 832.673; found 832.676

**Tris(4-ethoxy-carbonyl-2,3,5,6-tetrachlorophenyl)methane (17)** <sup>178</sup>.

Compound **15** (950 mg, 1.44 mmol) and TMEDA (2.18 mL, 14.44 mmol) were dissolved in dry THF (100 mL) under argon atmosphere and cooled to  $-78$  °C. A solution of 2.5 M *n*-BuLi in *n*-hexane (5.8 mL, 14.44 mmol) was added in one portion, and the mixture was stirred at this temperature for 1 h. Ethyl chloroformate (1.37 mL, 14.44 mmol)



was added, and the reaction mixture was allowed to reach RT overnight. Solvent was evaporated, and the residue was dissolved in DCM. The organic layer was washed with water and dried over MgSO<sub>4</sub>. Solvent was evaporated under vacuum and residue was purified on silica gel eluting with (heptane/EA, 12/1).

**Yield:** 1 g (81%)

**Colour:** Colorless solid

**Molecular formula:** C<sub>28</sub>H<sub>16</sub>Cl<sub>12</sub>O<sub>6</sub>

**Molar mass:** 873.71 g/mol

**Mp:** 173–175 °C

**R<sub>f</sub>:** 0.26 (heptane/EA, 10/1)

**<sup>1</sup>H NMR:** (400 MHz, CDCl<sub>3</sub>) δ 7.01 (s, 1H), 4.5 (q, *J* = 7.1 Hz, 6H), 1.42 (t, *J* = 7.1 Hz, 9H)

**<sup>13</sup>C NMR:** (100 MHz, CDCl<sub>3</sub>) δ 163.1, 138.4, 135.5, 135, 134, 130.5, 129.5, 63.1, 56.3, 14

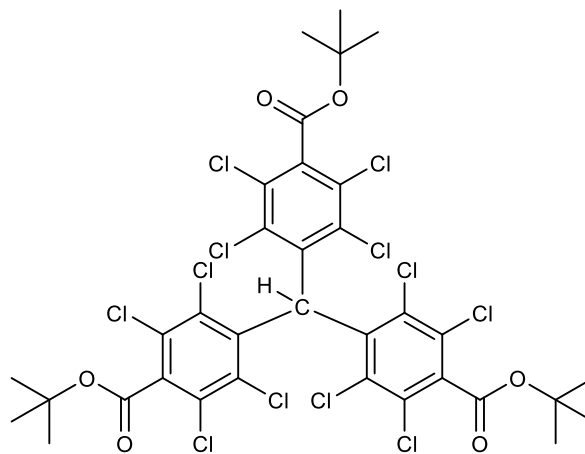
**IR (KBr):** ν = 2958, 2926, 1744, 1555, 1465, 1445, 1372, 1341, 1329, 1299, 1263, 1225, 1207, 1121, 1095, 1019, 859 cm<sup>-1</sup>

**MS (EI):** 874 (C<sub>28</sub>H<sub>16</sub>Cl<sub>12</sub>O<sub>6</sub>)

**HRMS (ESI):** calcd. for C<sub>28</sub>H<sub>17</sub>Cl<sub>12</sub>O<sub>6</sub> [M+H]<sup>+</sup> 874.720; found 874.719

### Tris(4-*tert*-butoxy-carbonyl-2,3,5,6-tetrachlorophenyl)methane (18).

Compound **15** (500 mg, 0.76 mmol) and TMEDA (1.15 mL, 7.6 mmol) were dissolved in dry THF (50 mL) under argon atmosphere and cooled to -78 °C. A solution of 2.5 M *n*-BuLi in *n*-hexane (3 mL, 7.6 mmol) was added in one portion, and the mixture was stirred at this temperature for 1 h. The reaction mixture was added slowly via syringe to DiBoc (8.3 gm, 38 mmol), previously charged in a dry



flask and placed on ice bath. After the addition was complete, the reaction mixture was allowed to reach RT and stirred for 2 days. The reaction was quenched with MeOH (20 mL) added portionwise until no more gas release was observed. The resulting mixture was evaporated, and the thick residue obtained was partitioned between aqueous HCl and CHCl<sub>3</sub>. The organic phase was separated, washed with water and dried over MgSO<sub>4</sub>. Solvent was evaporated, and the residue was purified on silica gel eluting with (heptane/EA, 10/1).

**Yield:** 356.7 mg (49%)



**Colour:** Sticky yellow solid

**Molecular formula:** C<sub>34</sub>H<sub>28</sub>Cl<sub>12</sub>O<sub>6</sub>

**Molar mass:** 957.81 g/mol

**R<sub>f</sub>:** 0.33 (heptane/EA, 10/1)

**<sup>1</sup>H NMR:** (400 MHz, CDCl<sub>3</sub>) δ 6.99 (s, 1H), 1.62 (s, 27H)

**<sup>13</sup>C NMR:** (400 MHz, CDCl<sub>3</sub>) δ 162, 138, 136.2, 134.9, 133.9, 130.2, 129.2, 85.1, 56.2, 27.8

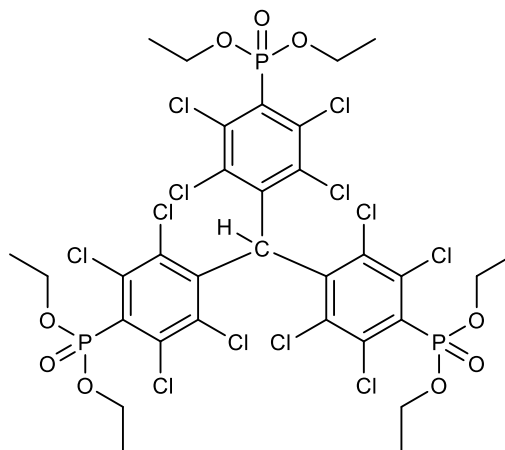
**IR (KBr):** ν = 2979, 2932, 1736, 1553, 1457, 1394, 1369, 1337, 1274, 1255, 1232, 1157, 1121 cm<sup>-1</sup>

**MS (ESI):** *m/z* 958.82 [M+H]<sup>+</sup>

**HRMS (ESI):** calcd. for C<sub>29</sub>H<sub>19</sub>Cl<sub>12</sub>O<sub>4</sub> [M-COOC(CH<sub>3</sub>)<sub>3</sub>]<sup>-</sup> 856.746; found 856.743

### Tris(4-diethoxyphosphoryl-2,3,5,6-tetrachlorophenyl)methane (19).

Compound **15** (560 mg, 0.85 mmol) and TMEDA (1.3 mL, 8.5 mmol) were dissolved in dry THF (50 mL) under argon atmosphere and cooled to -78 °C. A solution of 2.5 M *n*-BuLi in *n*-hexane (3.4 mL, 8.5 mmol) was added in one portion, and the mixture was stirred at this temperature for 1 h. Diethyl chlorophosphate (6.15 mL, 42.6 mmol) was added dropwise over 30 min. After the addition was



completed the reaction mixture was allowed to reach RT and stirred for 2 days. The resulting mixture was evaporated, and the thick residue obtained was dissolved in DCM, washed with water and dried over Na<sub>2</sub>SO<sub>4</sub>. Solvent was evaporated, and the residue was purified on silica gel eluting with (DCM/EA, 80/20).

**Yield:** 35% of the starting was recovered, 23% (150 mg) of mono-substituted, 27% (218 mg) of di-substituted, 11% (100 mg) of trisubstituted.

**Colour:** brown oil

**Molecular formula:** C<sub>31</sub>H<sub>31</sub>Cl<sub>12</sub>O<sub>9</sub>P<sub>3</sub>

**Molar mass:** 1065.74 g/mol

**R<sub>f</sub>:** 0.27 (DCM/EA, 80/20)

**<sup>1</sup>H NMR:** (400 MHz, CDCl<sub>3</sub>) δ 7.09 (s, 1H), 4.39 – 4.12 (m, 12H), 1.37 (t, *J* = 7.1 Hz, 18H)

**<sup>13</sup>C NMR:** (100 MHz, CDCl<sub>3</sub>) δ 140.9, 137.6, 136.6, 136.3, 135.4, 130.6, 128.7, 63.3, 58.2, 16.3

**IR (KBr):**  $\nu = 3472, 2981, 2930, 2869, 1772, 1526, 1477, 1443, 1391, 1368, 1347, 1304, 1285, 1259, 1163, 1117, 1097, 1045, 1017, 975, 797, 690 \text{ cm}^{-1}$

**MS (ESI):**  $m/z$  1064.79  $[M]^-$  (80%), 994.90  $[M-2Cl]^-$  (100%)

**HRMS (ESI):** calcd. for  $C_{31}H_{32}Cl_{12}O_9P_3$   $[M+H]^+$  1066.743; found 1066.744

### Tris(4-nitro-2,3,5,6-tetrachlorophenyl)methane (**21**)<sup>176</sup>.

A mixture of compound **15** (800 mg, 1.22 mmol) and 100% fuming nitric acid (50 mL) was refluxed for 18 h. After cooling down, the mixture was carefully added to ice cold water. The formed precipitate separated by filtration, dried under reduced pressure and purified through passing in silica gel column eluting with  $CHCl_3$ .

**Yield:** 58 %

**Colour:** white solid

**Molecular formula:**  $C_{19}HCl_{12}N_3O_6$

**Molar mass:** 792.60 g/mol

**Mp:** > 280 °C

**R<sub>f</sub>:** 0.4 (heptane/ $CHCl_3$ , 7/3)

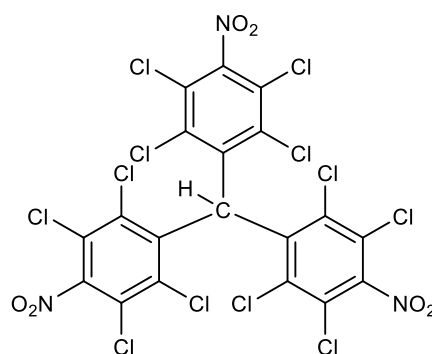
**<sup>1</sup>H NMR:** (400 MHz,  $CDCl_3$ )  $\delta$  7.01(s, 1H)

**<sup>13</sup>C NMR:** (400 MHz,  $CDCl_3$ )  $\delta$  138.3, 135.7, 134.7, 126.0, 125.1, 56.1

**IR (KBr):**  $\nu = 1555, 1379, 1362, 1344, 1304, 1234, 1134, 883, 830, 781, 760, 733 \text{ cm}^{-1}$

**MS (EI):** 792.6 ( $C_{19}HCl_{12}N_3O_6$ )

**HRMS (ESI):** calcd. for  $C_{19}Cl_{12}N_3O_6$   $[M-H]^-$  791.596; found 791.592

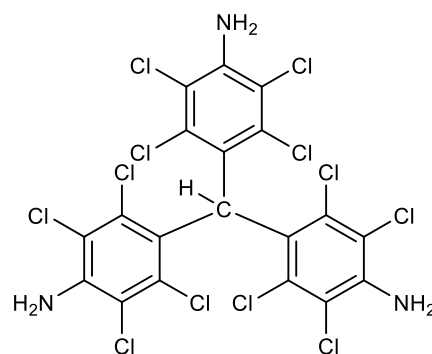


### Tris(4-amino-2,3,5,6-tetrachlorophenyl)methane (**22**).

A solution of compound **21** (500 mg, 0.76 mmol) in EtOH was mixed with palladium (10% wt. on activated carbon) in a hydrogenation pressure vessel. Hydrogen pressure was adjusted to 20 bar. After stirring for 18 h, the solution was filtered through celite. Solution was evaporated, and the residue was purified on silica gel eluting with (heptane/DCM, 3/7).

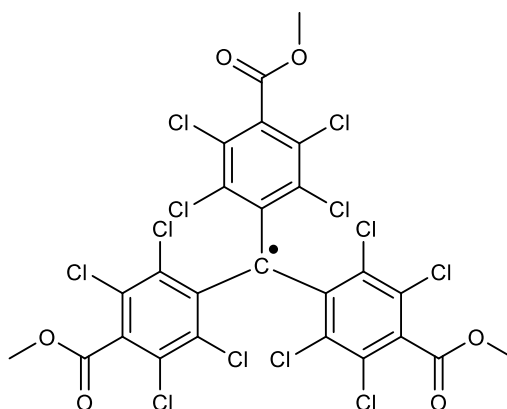
**Yield:** 87 %

**Colour:** white solid



**Molecular formula:** C<sub>19</sub>H<sub>7</sub>Cl<sub>12</sub>N<sub>3</sub>**Molar mass:** 702.68 g/mol**Mp:** > 280 °C**Rf:** 0.6 (heptane/DCM, 3/7)**<sup>1</sup>H NMR:** (400 MHz, CDCl<sub>3</sub>) δ 6.81 (s, 1H), 4.76 (s, 6H)**<sup>13</sup>C NMR:** (400 MHz, CDCl<sub>3</sub>) δ 141.0, 134.3, 133.2, 127.0, 117.9, 116.9, 54.3**IR (KBr):** ν = 3494, 3394, 1602, 1552, 1440, 1389, 1368, 1241, 1151, 1100, 911, 821, 753 cm<sup>-1</sup>**MS (EI):** 702.7 (C<sub>19</sub>H<sub>7</sub>Cl<sub>12</sub>N<sub>3</sub>)**HRMS (MALDI-TOF):** calcd. for C<sub>19</sub>H<sub>7</sub>Cl<sub>12</sub>N<sub>3</sub> [M]<sup>+</sup> 702.682; found 702.688**HRMS (ESI):** calcd. for C<sub>19</sub>H<sub>8</sub>Cl<sub>12</sub>N<sub>3</sub> [M+H]<sup>+</sup> 703.689; found 703.690**Tris(4-methoxy-carbonyl-2,3,5,6-tetrachlorophenyl)methyl radical (23).**

A solution of 1 M Bu<sub>4</sub>NOH in MeOH (0.72 mL, 0.72 mmol, 1.2 eq.) was added to a solution of compound **16** (500 mg, 0.60 mmol, 1 eq.) in freshly distilled THF (50 mL) under argon atmosphere. The mixture was stirred in the dark for 1 h. *p*-chloranil (591.3 mg, 2.40 mmol, 4 eq.) was added as a solid. The mixture was stirred overnight. Solvent was removed giving a purple residue, which was purified on silica gel eluting with (heptane/EA, 80/20).

**Yield:** 85 %**Colour:** Red crystals**Molecular formula:** C<sub>25</sub>H<sub>9</sub>Cl<sub>12</sub>O<sub>6</sub>**Molar mass:** 830.66 g/mol**Mp:** 255–260 °C**Rf:** 0.2 (heptane/EA, 10/1)**EPR:** (1mM in DMSO) single peak, ΔB<sub>pp</sub>= 0.043 mT**IR (KBr):** ν = 2953, 1747, 1536, 1435, 1360, 1343, 1332, 1319, 1285, 1230, 1136, 1042, 961, 762, 721 cm<sup>-1</sup>**MS (EI):** 830.8 (C<sub>25</sub>H<sub>9</sub>Cl<sub>12</sub>O<sub>6</sub>)**HRMS (ESI):** calcd. for C<sub>25</sub>H<sub>9</sub>Cl<sub>12</sub>O<sub>6</sub> [M]<sup>-</sup> 830.657; found 830.668

**Tris(4-ethoxy-carbonyl-2,3,5,6-tetrachlorophenyl)methyl radical (24)**<sup>178</sup>.

A solution of 1 M Bu<sub>4</sub>NOH in MeOH (0.69 mL, 0.69 mmol, 1.2 eq.) was added to a solution of compound **17** (500 mg, 0.57 mmol, 1 eq.) in freshly distilled THF (50 mL) under argon atmosphere. The mixture was stirred in the dark for 1 h. *p*-chloranil (562.7 mg, 2.29 mmol, 4 eq.) was added as a solid. The mixture was stirred overnight. Solvent was removed giving a purple residue, which was purified on silica gel eluting with (heptane/EA, 80/20).

**Yield:** 432.8 mg (87%)

**Colour:** Red solid

**Molecular formula:** C<sub>28</sub>H<sub>15</sub>Cl<sub>12</sub>O<sub>6</sub>

**Molar mass:** 872.720 g/mol

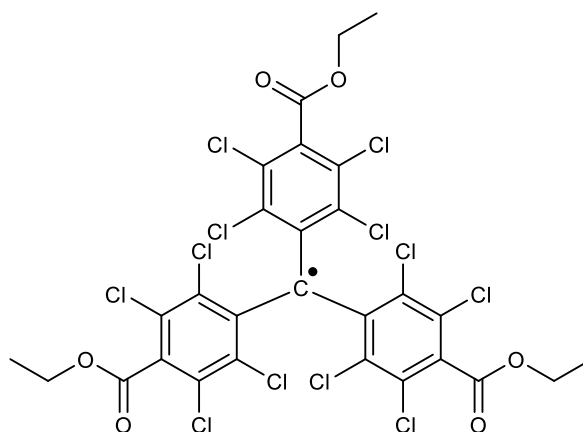
**Mp:** 158–160 °C

**R<sub>f</sub>:** 0.26 (heptane/EA, 10/1)

**IR (KBr):**  $\nu$  = 2981, 1742, 1688, 1679, 1572, 1456, 1445, 1373, 1342, 1329, 1260, 1224, 1136, 1111, 1017, 857, 755 cm<sup>-1</sup>

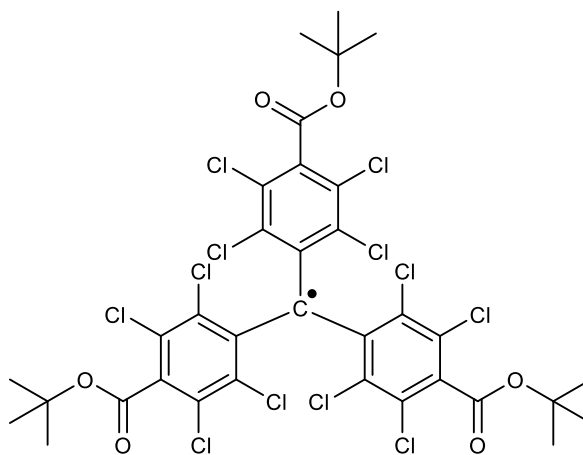
**HRMS (MALDI-TOF):** 872.761

**HRMS (ESI):** calcd. for C<sub>28</sub>H<sub>15</sub>Cl<sub>12</sub>O<sub>6</sub> [M]<sup>+</sup> 872.720; found 872.725

**Tris(4-tert-butoxy-carbonyl-2,3,5,6-tetrachlorophenyl)methyl radical (25)**<sup>183</sup>.

A solution 1 M Bu<sub>4</sub>NOH in MeOH (0.3 mL, 0.25 mmol, 1.2 eq.) was added to a solution of compound **18** (200 mg, 0.21 mmol, 1 eq.) in freshly distilled THF (20 mL) under argon atmosphere. The mixture was stirred in the dark for 1 h. *p*-chloranil (205 mg, 0.84 mmol, 4 eq.) was added as a solid. The mixture was stirred overnight. Solvent was removed giving a purple residue, which was purified on silica gel eluting with (heptane/EA, 80/20).

**Yield:** 160.7 mg (80%)



**Colour:** Red solid

**Molecular formula:** C<sub>34</sub>H<sub>27</sub>Cl<sub>12</sub>O<sub>6</sub>

**Molar mass:** 956.80 g/mol

**Mp:** 80–83 °C

**R<sub>f</sub>:** 0.33 (heptane/EA, 10/1)

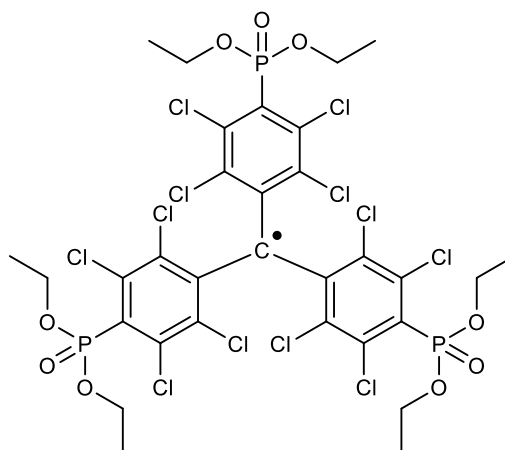
**IR (KBr):**  $\nu$ = 2980, 2956, 2918, 2850, 1737, 1687, 1573, 1457, 1394, 1370, 1334, 1288, 1240, 1159, 1137, 839, 756 cm<sup>-1</sup>

**MS (ESI):**  $m/z$  956.99 [M]<sup>-</sup>

**HRMS (ESI):** calcd. for C<sub>34</sub>H<sub>27</sub>Cl<sub>12</sub>O<sub>6</sub> [M]<sup>-</sup> 956.799; found 956.795

**Tris(4-diethoxyphosphoryl-2,3,5,6-tetrachlorophenyl)methyl radical (26).**

A solution 1 M Bu<sub>4</sub>NOH in MeOH (61  $\mu$ l, 1.2 eq.) was added to a solution of compound **19** (54 mg, 51  $\mu$ mol, 1 eq.) in freshly distilled THF (5 mL) under argon atmosphere. The mixture was stirred in the dark for 1 h. *p*-chloranil (562.7 mg, 0.29 mmol, 4 eq.) was added as a solid. The mixture was stirred overnight. Solvent was removed giving a purple residue, which was purified on silica gel eluting with (DCM/EA, 80/20).



**Yield:** 42 %

**Colour:** Red sticky solid

**Molecular formula:** C<sub>31</sub>H<sub>30</sub>Cl<sub>12</sub>O<sub>9</sub>P<sub>3</sub>

**Molar mass:** 1064.73 g/mol

**R<sub>f</sub>:** 0.26 (DCM/EA, 80/20)

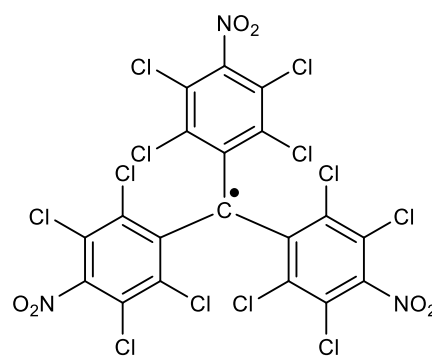
**EPR:** (1mM in DMSO, aerated conditions (20.9% O<sub>2</sub>)): Quartet signal (internal ratio, 1:3:3:1) with  $\Delta B_{pp} \approx 0.044$  mT. At deoxygenated condition ( $\approx 0\%$  O<sub>2</sub>),  $\Delta B_{pp} = 0.026$  mT.

**MS (ESI):**  $m/z$  1064.84 [M]<sup>-</sup>

**HRMS (ESI):** calcd. for C<sub>31</sub>H<sub>31</sub>Cl<sub>12</sub>O<sub>9</sub>P<sub>3</sub> [M+H]<sup>+</sup> 1065.736; found 1065.737

**Tris(4-nitro-2,3,5,6-tetrachlorophenyl)methyl radical (28)** <sup>176</sup>.

Compound **21** (300 mg, 0.38 mmol) was dissolved in THF (50 mL), an aqueous solution of Bu<sub>4</sub>NOH (40%, 0.32 mL, 0.49 mmol) was added under argon and in the dark. The mixture was stirred at 0 °C for 2 h and *p*-chloranil (372 mg, 1.51 mmol) was then added. The reaction mixture was stirred at 0 °C for 1 h and the overnight at RT. The solvent was evaporated, and the residue was purified on silica gel eluting with (heptane/CHCl<sub>3</sub>, 3/1).



**Yield:** 76 %

**Colour:** Red solid

**Molecular formula:** C<sub>19</sub>Cl<sub>12</sub>N<sub>3</sub>O<sub>6</sub>

**Molar mass:** 791.6

**Mp:** > 280 °C

**R<sub>f</sub>:** 0.4 (heptane/CHCl<sub>3</sub>, 7/3)

**EPR:** (1mM in DMSO) single peak, ΔB<sub>pp</sub>= 0.104 mT

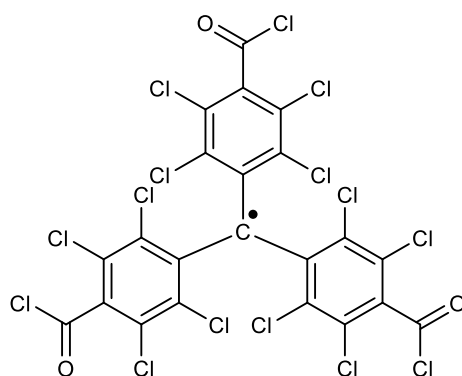
**IR (KBr):** ν = 1744, 1688, 1679, 1662, 1553, 1510, 1359, 1300, 1258, 1230, 1126, 1110, 1023, 750, 731 cm<sup>-1</sup>

**MS (ESI):** *m/z* 791.79 [M]<sup>-</sup>

**HRMS (ESI):** calcd. for C<sub>19</sub>Cl<sub>12</sub>N<sub>3</sub>O<sub>6</sub> [M]<sup>-</sup> 791.597; found 791.598

**Tris(2,3,5,6-tetrachloro-4-chlorocarbonyl-phenyl)methyl radical (29)**

A solution of **PTMTC** radical (200 mg, 0.25 mmol) in SOCl<sub>2</sub> (20 mL) was refluxed for 24 h. After cooling to RT, the mixture was poured onto water, treated with excess NaHCO<sub>3</sub> and extracted with CHCl<sub>3</sub>. The organic layer was washed with water, dried over Na<sub>2</sub>SO<sub>4</sub> and the solvent was evaporated. The residue was purified on silica gel eluting with (EA/MeOH, 10/1).



**Yield:** 78 %.

**Colour:** dark red crystals.

**Molecular formula:** C<sub>22</sub>Cl<sub>15</sub>O<sub>3</sub>.

**Molar mass:** 844.51 g/mol.

**Mp:** > 280 °C.

**R<sub>r</sub>**: 0.6 (EA/MeOH: 10/1).

**IR (KBr)**:  $\nu = 2924, 1826, 1785, 1748, 1531, 1436, 1324, 1238, 1214, 1165, 1129, 1062, 987, 961, 764, 719, 686 \text{ cm}^{-1}$ .

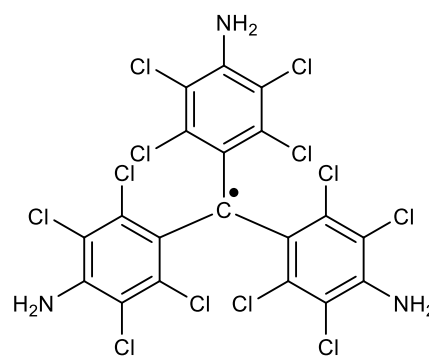
**EPR**: (1 Mm solution in CHCl<sub>3</sub>): single peak,  $\Delta B_{pp} = 0.06 \text{ mT}$ .

**MS (EI)**: 844.2 (C<sub>22</sub>Cl<sub>15</sub>O<sub>3</sub>), 809 (C<sub>22</sub>Cl<sub>14</sub>O<sub>3</sub>), 773 (C<sub>22</sub>Cl<sub>13</sub>O<sub>3</sub>), 738 (C<sub>22</sub>Cl<sub>12</sub>O<sub>3</sub>), 710 (C<sub>21</sub>Cl<sub>12</sub>O<sub>2</sub>), 682 (C<sub>20</sub>Cl<sub>12</sub>O<sub>1</sub>), 654 (C<sub>19</sub>Cl<sub>12</sub>), 582 (C<sub>19</sub>Cl<sub>10</sub>), 547 (C<sub>19</sub>Cl<sub>9</sub>), 511 (C<sub>19</sub>Cl<sub>8</sub>), 475 (C<sub>19</sub>Cl<sub>7</sub>), 405 (C<sub>19</sub>Cl<sub>5</sub>), 369 (C<sub>19</sub>Cl<sub>4</sub>), 334 (C<sub>19</sub>Cl<sub>3</sub>).

**HRMS (ESI)**: calcd. for C<sub>22</sub>Cl<sub>15</sub>O<sub>3</sub> [M]<sup>-</sup> 842.508; found 842.506.

### Tris(4-amino-2,3,5,6-tetrachlorophenyl)methyl radical (30).

A solution 1 M Bu<sub>4</sub>NOH in MeOH (0.2 mL, 0.17 mmol, 1.2 eq.) was added to a solution of compound **22** (100 mg, 0.14 mmol) in freshly distilled THF (5 mL) under nitrogen atmosphere. The mixture was stirred in the dark for 1 h. *p*-chloranil (140 mg, 0.57 mmol, 4 eq.) was added as a solid. The mixture was stirred overnight. Formation of the radical was confirmed through EPR spectroscopy.



Solvent was removed giving brownish residue which was purified on silica gel eluting with (heptane/DCM: 3/7). 37% of the starting was recovered, increasing the eluent polarity to (heptane/DCM: 15/85) gave 48% of yellow solid. EPR signal of the yellow solid was re-investigated; surprising disappearance of the EPR signal was observed. As mentioned in the discussion section, the more polar fraction is most likely the carbocation.

**Molecular formula**: C<sub>19</sub>H<sub>6</sub>Cl<sub>12</sub>N<sub>3</sub>

**Molar mass**: 701.67

**Mp**: > 280 °C

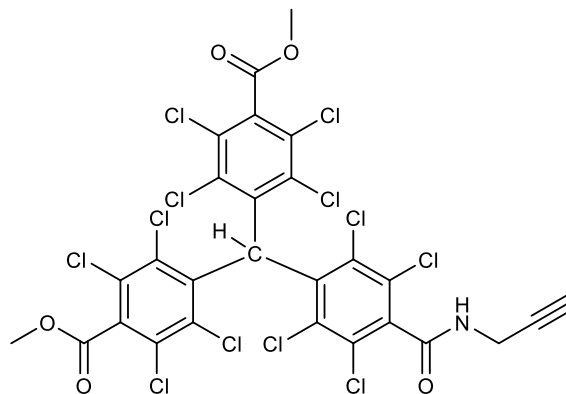
**R<sub>r</sub>**: 0.4 (heptane/DCM, 3/7)

**MS (ESI)**:  $m/z$  701.69 [M]<sup>-</sup>

**HRMS (ESI)**: calcd. for C<sub>19</sub>H<sub>7</sub>Cl<sub>12</sub>N<sub>3</sub> [M+H]<sup>+</sup> 702.681; found 702.683

**Di(4-methoxy-carbonyl-2,3,5,6-tetrachlorophenyl)-(2,3,5,6-tetrachloro-4-N-prop-2-yn-1-ylbenzamide)methane (39).**

A solution of propargylamine (0.31 mL, 4.8 mmol) in DCE (10 mL) was introduced into 100 mL 2-necked flask, which was attached to a condenser and under argon atmosphere. A solution of TMA (2 M in *n*-hexane) was added dropwise, and the mixture was stirred for 10 min. Compound **16** (400 mg, 0.48 mmol) dissolved in DCE (10 mL) was added. The mixture was stirred at RT for 1 h and refluxed for 18 h. After cooling to RT, the resulting brown solution was diluted with DCM (20 mL) and carefully treated with MeOH (5 mL). The mixture was partitioned between HCl (1M, 10 mL) and DCM (10 mL), layers were separated and the aqueous layer was extracted twice with 15 mL of DCM. The combined organic layers were dried over Na<sub>2</sub>SO<sub>4</sub> and concentrated in vacuum. The brownish residue was purified on silica gel eluting with (heptane/EA, 7/3). 104 mg (26%) of the starting material was recovered.



**Yield:** 31%

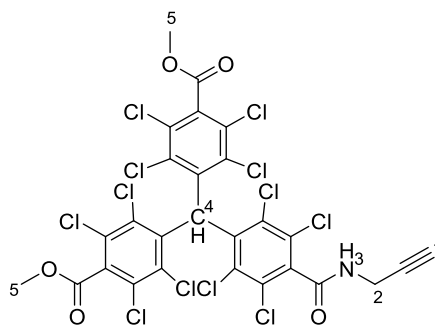
**Colour:** White powder

**Molecular formula:** C<sub>27</sub>H<sub>11</sub>Cl<sub>12</sub>NO<sub>5</sub>

**Molar mass:** 854.68 g/mol

**Mp:** 160–165 °C

**R<sub>f</sub>:** 0.31 (heptane/EA, 7/3)



**<sup>1</sup>H NMR:** (400 MHz, CDCl<sub>3</sub>) δ 7.00 (s, 1H, H<sup>4</sup>), 5.99 (t, J = 5.2 Hz, 1H, H<sup>3</sup>), 4.29 (dd, J = 5.3, 2.5 Hz, 2H, H<sup>2</sup>), 4.01 (s, 6H, H<sup>5</sup>), 2.32 (t, J = 2.5 Hz, 1H, H<sup>1</sup>)

**<sup>13</sup>C NMR:** (400 MHz, CDCl<sub>3</sub>) δ 163.7, 162.6, 138.6, 136.9, 135.4, 135.2, 135, 134.1, 134, 133.9, 131.1, 130.6, 130.1, 129.6, 77.9, 72.8, 56.4, 53.6, 29.9



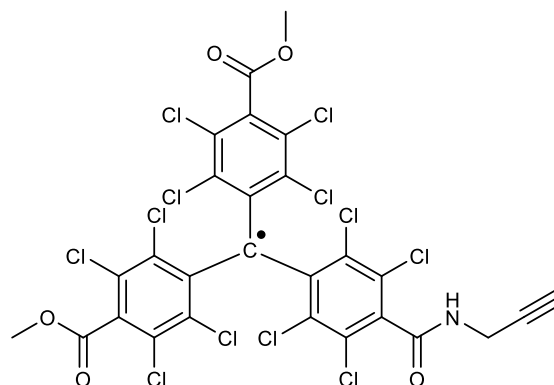
**IR (KBr):**  $\nu = 3306, 3012, 2953, 2924, 2853, 1747, 1662, 1556, 1527, 1437, 1370, 1326, 1267, 1228, 1209, 1183, 1116, 1012, 953, 827, 795, 758, 732 \text{ cm}^{-1}$

**MS (ESI):**  $m/z$  853.74  $[\text{M}-\text{H}]^-$  (70%), 772.69  $[\text{M}-\text{C}_4\text{H}_4\text{NO}]^-$  (100%)

**HRMS (ESI):** calcd. for  $\text{C}_{27}\text{H}_{12}\text{Cl}_{12}\text{NO}_5$   $[\text{M}+\text{H}]^+$  855.689; found 855.692

**Di(4-methoxy-carbonyl-2,3,5,6-tetrachlorophenyl)-(2,3,5,6-tetrachloro-4-N-prop-2-yn-1-ylbenzamide)methyl radical (40).**

A solution 1 M  $\text{Bu}_4\text{NOH}$  in MeOH (0.14 mL, 0.14 mmol, 1.2 eq.) was added to a solution of compound **39** (100 mg, 0.12 mmol, 1 eq.) in freshly distilled THF (10 mL) under argon atmosphere. The mixture was stirred in the dark for 1 h. *p*-chloranil (115 mg, 0.45 mmol, 4 eq.) was added as a solid. The mixture was stirred overnight. Solvent was removed giving a purple residue, which was purified on silica gel eluting with (heptane/EA, 7/3).



**Yield:** 81%

**Colour:** Red powder

**Molecular formula:**  $\text{C}_{27}\text{H}_{10}\text{Cl}_{12}\text{NO}_5$

**Molar mass:** 853.67 g/mol

**Mp:** 160–162 °C

**Rf:** 0.3 (heptane/EA, 7/3)

**EPR:** (1mM in DMSO) single peak  $\Delta B_{pp} = 0.047 \text{ mT}$

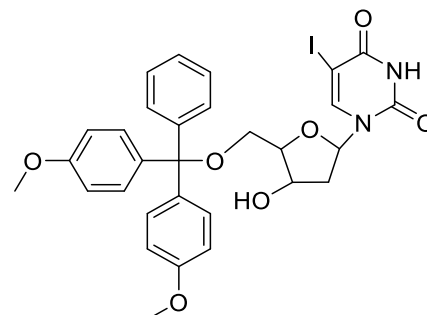
**IR (KBr):**  $\nu = 3306, 2954, 2924, 2868, 1747, 1662, 1539, 1436, 1377, 1343, 1332, 1286, 1233, 1136, 1121, 1041, 960, 858, 797, 762, 721 \text{ cm}^{-1}$

**MS (ESI):**  $m/z$  876.42  $[\text{M}+\text{Na}]^+$ , 853.80  $[\text{M}]^-$

**HRMS (ESI):** calcd. for  $\text{C}_{27}\text{H}_{11}\text{Cl}_{12}\text{NO}_5$   $[\text{M}+\text{H}]^+$  854.681; found 854.681

**2'-Deoxy-5'-O-(4,4'-dimethoxytrityl)-5-iodouridine (41).**

2'-deoxy-5-iodouridine (**33**) (500 mg, 1.41 mmol) was dissolved in a solution of anhydrous pyridine (12 mL) and TEA (1.4 mL), 4,4'-dimethoxytritylchloride (**35**) (0.62 g, 1.83 mmol) was then added. The mixture was stirred at RT for 5 h and then the reaction was quenched by the addition of MeOH (2 mL). The reaction mixture was diluted with



DCM and washed with 10% NaHCO<sub>3</sub> solution (3 × 20 mL). The organic phase was separated and dried over Na<sub>2</sub>SO<sub>4</sub>. The solvent was removed, and the residue was purified on silica gel, which was pre-treated with eluent containing 5% TEA, eluting with (heptane/acetone/TEA, 40/55/5).

**Yield:** 79 %

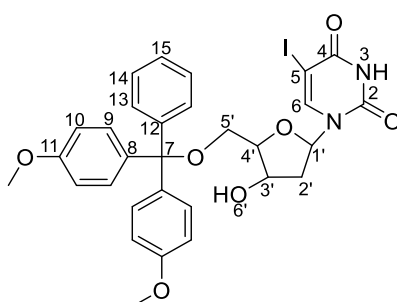
**Colour:** white solid

**Molecular formula:** C<sub>30</sub>H<sub>29</sub>IN<sub>2</sub>O<sub>7</sub>

**Molar mass:** 656.1 g/mol

**Mp:** 92–95 °C

**R<sub>f</sub>:** 0.4 (heptane/acetone/TEA, 40/55/5)



**<sup>1</sup>H NMR:** (400 MHz, d<sub>6</sub>-DMSO) δ 11.68 (s, 1H, NH), 7.99 (s, 1H, H<sup>6</sup>), 7.38 (d, *J* = 7.5 Hz, 2H, H<sup>13</sup>), 7.33 – 7.18 (m, 7H, H<sup>9</sup>, H<sup>14</sup>, H<sup>15</sup>), 6.88 (d, *J* = 8.8 Hz, 1H, H<sup>10</sup>), 6.08 (t, *J* = 6.7 Hz, 1H, H<sup>11</sup>), 5.27 (d, *J* = 4.5 Hz, 1H, OH), 4.24 – 4.17 (m, 1H, H<sup>3'</sup>), 3.90 – 3.85 (m, *J* = 3.5 Hz, 1H, H<sup>4'</sup>), 3.72 (s, 6H, OCH<sub>3</sub>), 3.20 – 3.11 (m, 2H, H<sup>5'</sup>), 2.27 – 2.19 (m, 1H, H<sup>2'</sup>), 2.18 – 2.11 (m, 1H, H<sup>2'</sup>)

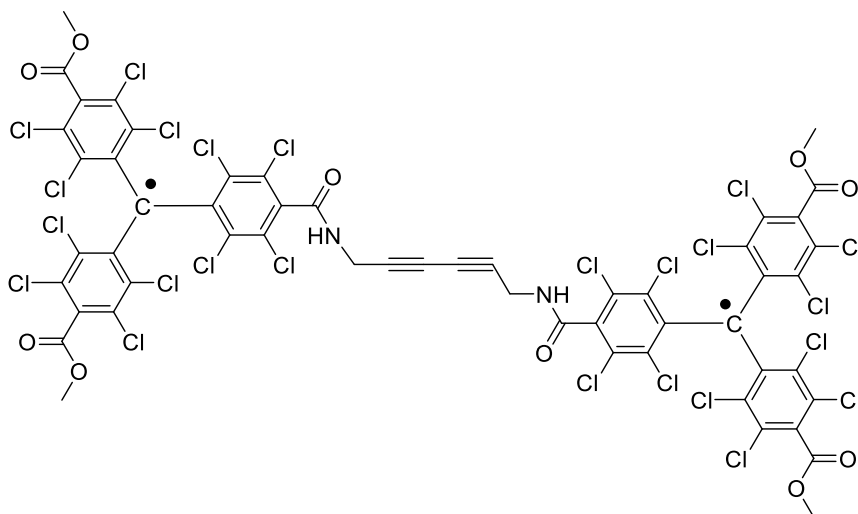
**<sup>13</sup>C NMR:** (100 MHz, d<sub>6</sub>-DMSO) δ 160.5, 158.1, 150.0, 144.7, 144.2, 135.41, 129.7, 127.9, 127.6, 126.7, 113.3, 85.8, 84.9, 70.5, 69.8, 63.7, 55.0, 45.7, 39.9

**IR (KBr):** ν = 3424, 3190, 3059, 2931, 2835, 1690, 1608, 1509, 1445, 1349, 1301, 1272, 1251, 1177, 1153, 1091, 1060, 1032, 986, 962, 828, 791, 755, 726, 702, 598, 584 cm<sup>-1</sup>

**MS (ESI):** *m/z* 678.97 [M+Na]<sup>+</sup>

**HRMS (ESI):** calcd. for C<sub>30</sub>H<sub>29</sub>IN<sub>2</sub>O<sub>7</sub> [M+Na]<sup>+</sup> 679.092; found 679.091

**N,N'-(hexa-2,4-diyne-1,6-diyl)di(dimethyl4,4'-((2,3,5,6-tetrachlorophenyl)methylene)bis(2,3,5,6-tetrachlorobenzoate))amide radical (43).**



A solution of compound **41** (33 mg, 0.09 mmol) in DMF (5 mL) was introduced in oven-dried 50 mL 2-necked flask. The solution was degassed in vacuum and the flask was flushed with argon 5 times. Then, TEA (63  $\mu$ l, 0.45 mmol), compound **40** (240 mg, 0.28 mmol), tetrakis(triphenylphosphine)palladium (11 mg, 9  $\mu$ mol), and CuI (4 mg, 19.7  $\mu$ mol) were added. In each case, the mixture was stirred until a clear solution was obtained before the next compound was added. Stir at RT overnight. The resulting solution was diluted with EA (10 mL) and washed with aqueous EDTA solution (5%, 10 mL  $\times$  3) and brine (10 mL). The organic layer was dried over Na<sub>2</sub>SO<sub>4</sub> and the solvent was removed in vacuum. Mass spectroscopy indicated the presence of both the cross-coupled product and the homocoupling side product. The residue was purified on silica gel eluting with (heptane/acetone, 78/22) to separate the homocoupling product (**43**) (27%, based on the terminal alkyne) as pale red solid. The polarity was increased till 100% acetone; the desired cross-coupling product (**42**) could not be separated.

**Molecular formula:** C<sub>54</sub>H<sub>18</sub>Cl<sub>24</sub>N<sub>2</sub>O<sub>10</sub>

**Molar mass:** 1705.33 g/mol

**Mp:** > 260 °C

**R<sub>f</sub>:** 0.12 (heptane/EA, 7/3)

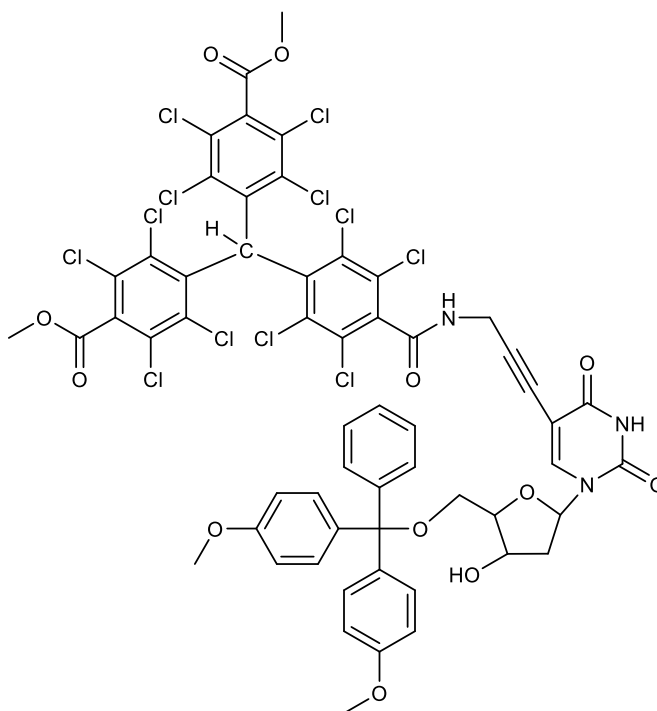
**EPR:** (1mM in DMSO) single peak,  $\Delta B_{pp}$  = 0.052 mT

**IR (KBr):**  $\nu$  = 3312, 2953, 2925, 2852, 1748, 1554, 1520, 1436, 1371, 1343, 1325, 1266, 1228, 1209, 1183, 1134, 1119, 1043, 1012, 954, 722 cm<sup>-1</sup>

**MS (ESI):**  $m/z$  1704.34 [M-H]<sup>-</sup> (100%), 930.38 [C<sub>31</sub>H<sub>13</sub>Cl<sub>12</sub>N<sub>2</sub>O<sub>6</sub>]<sup>-</sup> (35%), 770.67 [C<sub>23</sub>H<sub>6</sub>Cl<sub>12</sub>O<sub>4</sub>]<sup>-</sup> (55 %)

**5-(Di(2,3,5,6-tetrachloro-4-methoxy-carbonyl-phenyl)-(2,3,5,6-tetrachloro-4-N-prop-2-yn-1-ylbenzamide)methane)- 5'-O-(4,4'-dimethoxytrityl)-2'-deoxyuridine (44).**

A solution of compound **41** (77.3 mg, 0.12 mmol) in DMF (10 mL) was introduced in oven-dried 50 mL 2-necked flask. The solution was degassed in vacuo and the flask was flushed with argon 5 times. Then, TEA (0.11 mL, 0.8 mmol), compound **39** (300 mg, 0.35 mmol), tetrakis(triphenylphosphine) palladium (19 mg, 17  $\mu$ mol), and CuI (7 mg, 0.04 mmol) were added. In each case, the mixture was stirred until a clear solution was obtained before the next compound was added. Stir at RT



overnight. The resulting orange solution was diluted with EA (25 mL) and washed with aqueous EDTA solution (5%, 10 mL  $\times$  3) and brine (10 mL). The organic layer was dried over Na<sub>2</sub>SO<sub>4</sub> and the solvent was removed in vacuum. The residue was purified on silica gel, which was pre-treated with eluent containing 5% TEA, eluting with (heptane/acetone/TEA, 60/35/5) to separate the titled product.

**Yield:** 25 % (based on the terminal alkyne)

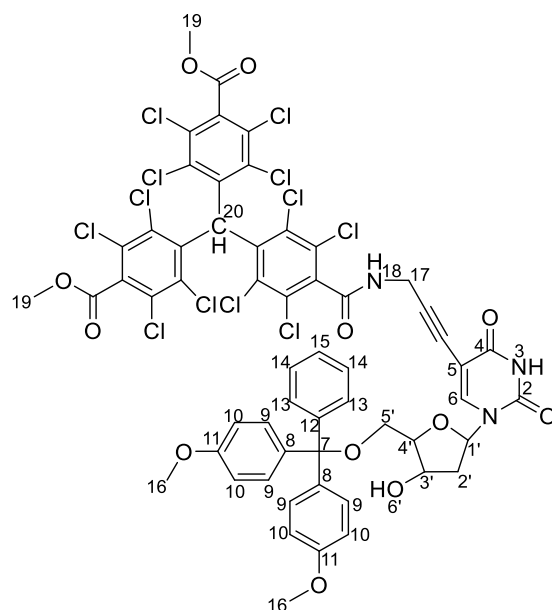
**Colour:** light brownish solid

**Molecular formula:** C<sub>57</sub>H<sub>39</sub>Cl<sub>12</sub>N<sub>3</sub>O<sub>12</sub>

**Molar mass:** 1382.87 g/mol

**Mp:** 178–182 °C

**R<sub>f</sub>:** 0.47 (DCM/ EA/TEA, 50/45/5) or 0.6 (EA/TEA, 95/5)



**<sup>1</sup>H NMR:** (400 MHz, d<sub>6</sub>-DMSO) δ 11.64 (s, 1H, H<sup>3</sup>), 9.33 (s, 1H, H<sup>18</sup>), 7.92 (s, 1H, H<sup>6</sup>), 7.40 (d, *J* = 7.4 Hz, 2H, H<sup>13</sup>), 7.35 – 7.16 (m, 7H, H<sup>9</sup>, H<sup>14</sup>, H<sup>15</sup>), 6.93 (s, 1H, H<sup>20</sup>), 6.89 (d, *J* = 7.9 Hz, 4H, H<sup>10</sup>), 6.09 (t, *J* = 6.7 Hz, 1H, H<sup>1</sup>), 5.32 (d, *J* = 4.2 Hz, 1H, OH<sup>6'</sup>), 4.30 – 4.22 (m, 1H, H<sup>3'</sup>), 4.11 (d, *J* = 5.0 Hz, 2H, H<sup>17</sup>), 3.98 (s, 6H, H<sup>19</sup>), 3.94 – 3.86 (m, 1H, H<sup>4</sup>), 3.72 (s, 6H, H<sup>16</sup>), 3.28 – 3.20 (m, 1H, H<sup>5'</sup>), 3.15 – 3.04 (m, 1H, H<sup>5</sup>), 2.34 – 2.22 (m, 1H, H<sup>2</sup>), 2.22 – 2.13 (m, 1H, H<sup>2'</sup>)

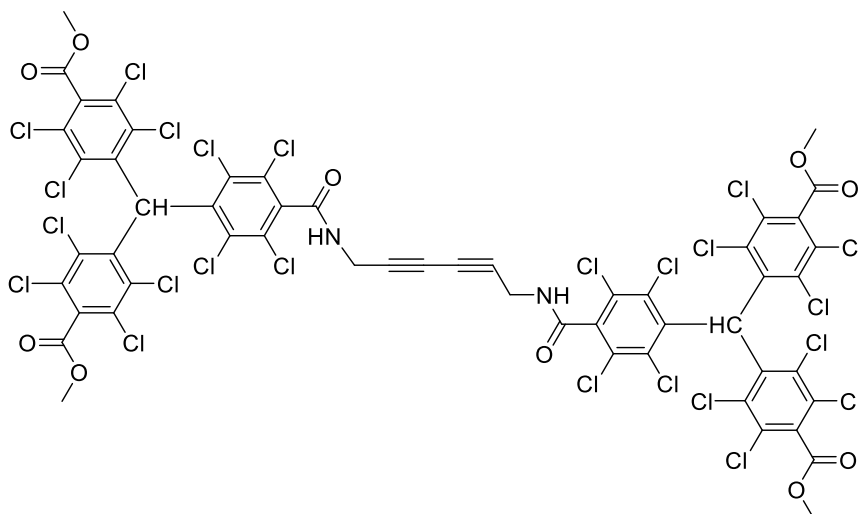
**<sup>13</sup>C NMR:** (400 MHz, CDCl<sub>3</sub>) δ 163.5, 162.0, 158.5, 150.0, 145.3, 138.9, 136.1, 135.4, 134.1, 133.5, 130.2, 130.1, 130.0, 129.2, 128.4, 128.0, 127.1, 113.7, 86.3, 70.9, 64.2, 56.3, 55.5, 54.5, 46.2, 31.7, 22.5

**IR (KBr):** ν = 3387, 3061, 2953, 2930, 2837, 1748, 1689, 1608, 1556, 1509, 1459, 1446, 1370, 1343, 1271, 1230, 1210, 1179, 1115, 1093, 1034, 953, 828, 792, 775, 758, 727, 702, 659, 584 cm<sup>-1</sup>

**MS (ESI):** *m/z* 1405.64 [M+Na]<sup>+</sup>

**HRMS (ESI):** calcd. for C<sub>57</sub>H<sub>39</sub>Cl<sub>12</sub>N<sub>3</sub>O<sub>12</sub> [M+Na]<sup>+</sup> 1405.862; found 1405.861

**N,N'-(hexa-2,4-diyne-1,6-diyl)di(dimethyl4,4'-((2,3,5,6-tetrachlorophenyl)methylene)bis(2,3,5,6-tetrachlorobenzoate))amide (homocoupling product, 45).**



**Molecular formula:** C<sub>54</sub>H<sub>20</sub>Cl<sub>24</sub>N<sub>2</sub>O<sub>10</sub>

**Molar mass:** 1707.35 g/mol

**Mp:** 250–258 °C

**R<sub>f</sub>:** 0.15 (heptane/ EA, 7/3)

**<sup>1</sup>H NMR:** (400 MHz, CDCl<sub>3</sub>) δ 7.01 (s, 2H), 6.06 (t, *J* = 5.2 Hz, 2H), 4.36 (d, *J* = 5.2 Hz, 4H), 4.01 (s, 12H)

**<sup>13</sup>C NMR:** (400 MHz, CDCl<sub>3</sub>) δ 163.7, 162.6, 138.7, 138.5, 136.7, 135.4, 135.2, 134.2, 134, 131, 130.5, 130, 129.5, 73.1, 68.3, 56.4, 53.6, 29.7

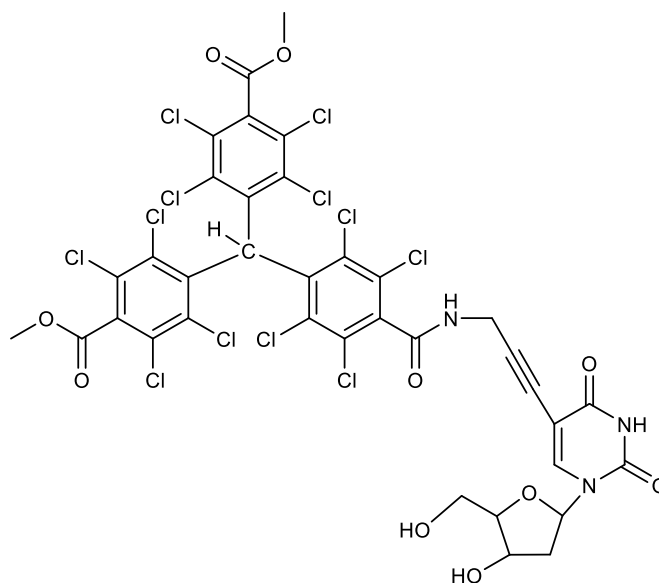
**IR (KBr):** ν = 3674, 3350, 2953, 2924, 2853, 1750, 1693, 1556, 1509, 1437, 1370, 1343, 1326, 1268, 1229, 1184, 1117, 1012, 954, 827, 797, 760, 733, 659, 577, 528 cm<sup>-1</sup>

**MS (ESI):** *m/z* 1730.3 [M+Na]<sup>+</sup>, 1707.55 [M]<sup>-</sup> (70%), 931.96 [C<sub>31</sub>H<sub>13</sub>Cl<sub>12</sub>N<sub>2</sub>O<sub>6</sub>]<sup>-</sup> (40%), 772.71 [C<sub>23</sub>H<sub>7</sub>Cl<sub>12</sub>O<sub>4</sub>]<sup>-</sup> (100%)

**HRMS (ESI):** calcd. for C<sub>54</sub>H<sub>20</sub>Cl<sub>24</sub>N<sub>2</sub>O<sub>10</sub> [M+Na]<sup>+</sup> 1730.337; found 1730.336

**5-(Di(2,3,5,6-tetrachloro-4-methoxy-carbonyl-phenyl)-(2,3,5,6-tetrachloro-4-*N*-prop-2-yn-1-ylbenzamide)methane)-2'-deoxyuridine (46).**

A solution of 5-iodo-2'-deoxyuridine (**33**) (28 mg, 0.08 mmol) in DMF (5 mL) was introduced in oven-dried 50 mL 2-necked flask. The solution was degassed in vacuo and the flask was flushed with argon 5 times. TEA (52  $\mu$ L, 0.37 mmol), compound **39** (200 mg, 0.23 mmol), tetrakis- (triphenylphosphine)palladium (9 mg, 8  $\mu$ mol), and copper iodide (CuI) (3 mg, 20  $\mu$ mol) were added. In each case, the mixture was stirred until a clear



solution was obtained before the next compound was added. The reaction mixture was stirred at RT overnight. The resulting orange solution was diluted with EA (10 mL) and washed with aqueous EDTA solution (5%, 10 mL  $\times$  3) and brine (10 mL). The organic layer was dried over Na<sub>2</sub>SO<sub>4</sub>, and the solvent was removed in vacuum. The residue was purified on silica gel eluting with (heptane/acetone, 80/20) to separate the homocoupling product (**45**) (23%, based on the terminal alkyne) as white solid. The polarity was increased to (heptane/acetone, 55/45) to separate the titled cross-coupling product (**46**) (21%, based on the terminal alkyne) as yellow solid.

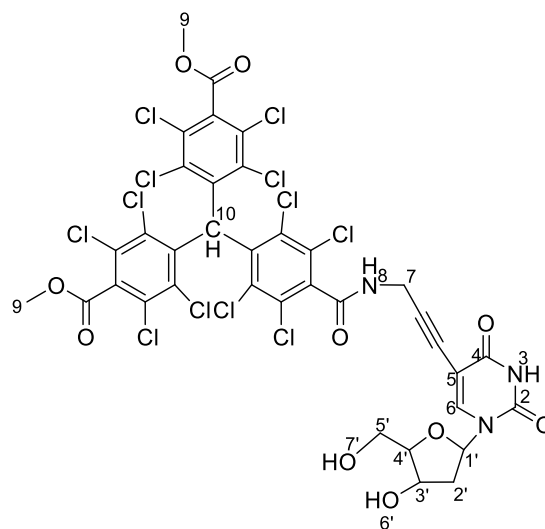
**Molecular formula:** C<sub>36</sub>H<sub>21</sub>Cl<sub>12</sub>N<sub>3</sub>O<sub>10</sub>

**Molar mass:** 1080.74

**Mp:** 260–265 °C

**R<sub>f</sub>:** 0.4 (DCM/ MeOH, 95/5)

**<sup>1</sup>H NMR:** (400 MHz, d<sub>6</sub>-DMSO)  $\delta$  11.62 (s, 1H, H<sup>3</sup>), 9.40 (s, 1H, H<sup>8</sup>), 8.17 (s, 1H, H<sup>6</sup>), 6.94 (s, 1H, H<sup>10</sup>), 6.11 (t,  $J = 6.7$  Hz, 1H, H<sup>1'</sup>), 5.22 (d,  $J = 4.2$  Hz, 1H, OH<sup>6'</sup>), 5.07 (t,  $J = 5.1$  Hz, 1H, OH<sup>7'</sup>), 4.31 (d,  $J = 5.0$  Hz, 2H, H<sup>7</sup>), 4.28–4.18 (m, 1H, H<sup>3'</sup>), 3.98 (s, 6H, H<sup>9</sup>), 3.80 (m, 1H, H<sup>4'</sup>), 3.67–3.46 (m, 2H, H<sup>5'</sup>), 2.19–2.01 (m, 2H, H<sup>2'</sup>)



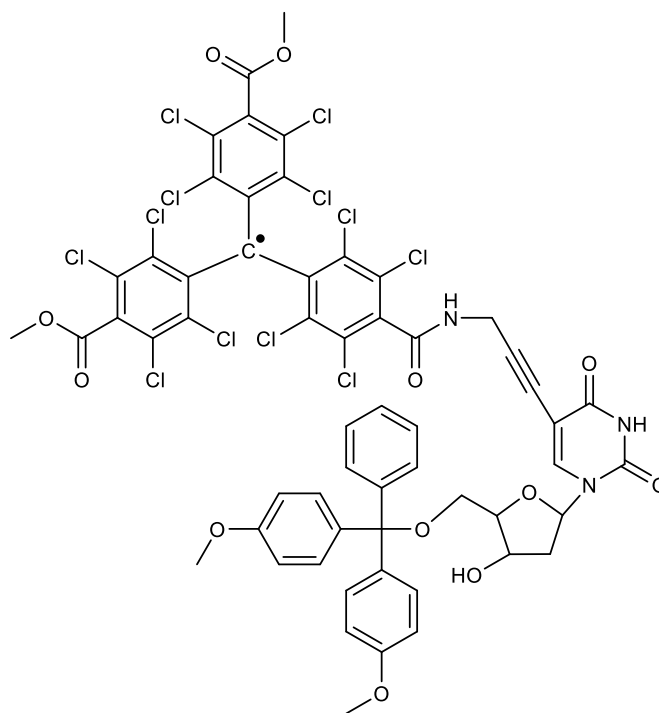
**IR (KBr):**  $\nu = 3422, 3060, 2954, 2927, 1748, 1691, 1556, 1459, 1437, 1343, 1326, 1275, 1230, 1210, 1184, 1096, 1054, 953, 855, 827, 797, 776, 760, 659, 579, 525, \text{cm}^{-1}$

**MS (ESI):**  $m/z$  1103.52  $[\text{M}+\text{Na}]^+$

**HRMS (ESI):** calcd. for  $\text{C}_{36}\text{H}_{22}\text{Cl}_{12}\text{N}_3\text{O}_{10}$   $[\text{M}+\text{H}]^+$  1081.748; found 1081.749

**5-(Di(2,3,5,6-tetrachloro-4-methoxy-carbonyl-phenyl)-(2,3,5,6-tetrachloro-4-*N*-prop-2-yn-1-ylbenzamide)methyl)-5'-O-(4,4'-dimethoxytrityl)-2'-deoxyuridine radical (42).**

A solution 1 M  $\text{Bu}_4\text{NOH}$  in MeOH (71  $\mu\text{l}$ , 0.07 mmol, 1.2 eq.) was added to a solution of compound **44** (82 mg, 0.06 mmol, 1 eq.) in freshly distilled THF (10 mL) under dry argon atmosphere. The mixture was stirred in the dark for 1 h. *p*-chloranil (58 mg, 0.24 mmol, 4 eq.) was added as a solid. The mixture was stirred overnight. Solvent was removed giving a purple residue. EPR indicates the presence of the radical signal (1mM solution of the product mixture in DMSO): single peak,  $\Delta\text{Bpp} = 0.047$  mT).



TLC showed 3 spots (the less polar is the unreacted *p*-chloranil, followed by the titled radical spot R<sub>f</sub>: 0.6 (EA/TEA: 95/5) in addition to another spot near the base line). Purification was tried on silica gel eluting with (heptane/EA/TEA, 45/50/5) to separate the excess unreacted *p*-chloranil, then the polarity was increased to (EA/TEA, 95/5) followed by (EA/MeOH/TEA, 65/30/5) a purple fraction was eluted. MS indicated that this purple fraction has the same molar mass of the desired product **42**, but with no EPR activity. The same procedure was repeated using only one eq. of *p*-chloranil. The crude mixture was used without further purification for EPR characterization.

**Molecular formula:**  $\text{C}_{57}\text{H}_{38}\text{Cl}_{12}\text{N}_3\text{O}_{12}$

**Molar mass:** 1381.86 g/mol

**R<sub>f</sub>:** 0.45 (DCM/EA/TEA, 50/45/5)

**EPR:** (1mM in DMSO) single peak,  $\Delta\text{Bpp} = 0.047$  mT

**MS (ESI):**  $m/z$  1405.48  $[\text{M}+\text{Na}]^+$ , 1381.88  $[\text{M}]^-$



## 4. PTMTC and $^{13}\text{C}$ -PTMTC<sup>††</sup>

### 4.1. Introduction

As mentioned in the general introduction, hyperfine interaction between the electronic and magnetic moments results in splitting of the EPR spectrum that is called hyperfine splitting. The hydrophilic tricarboxylic acid **PTMTC** showed very good aqueous solubility (up to 10 mM in PB, pH 7.4) without spin-spin line broadening and promising EPR properties of narrow line width, and sensitivity to variation in oxygen content. **PTMTC** radical showed a single peak, in addition to three symmetrical pairs of satellites because of spin coupling with naturally abundant  $^{13}\text{C}$  at the *ipso*, *ortho*, *para*, and *meta* positions of the phenyl rings, **Fig. 4.2A**. Coupling to the central carbon was not observed. Paniagua et al.<sup>186</sup> attributed this to the fast relaxation because of the slow tumbling rate of the radical in the used solvent system ( $\text{H}_2\text{O}/\text{DMSO}$ , 1/1). Enrichment of the methyl radical center with 50%  $^{13}\text{C}$  was expected to split the EPR spectrum to three components; central line related to the  $^{12}\text{C}$  containing radical in addition to high field and low field peaks related to  $^{13}\text{C}$ , **Fig. 4.2B**. The impact of different parameters mimicking physiological conditions, e.g., variation of viscosity, pH and oxygen content were studied.

### 4.2. Experimental

#### 4.2.1. Materials and general methods for synthesis and analytical characterization

See section **9.1** and **9.2**.

#### 4.2.2. Sample preparation for EPR spectroscopic characterization

The hydrophilic radicals **PTMTC** and  $^{13}\text{C}$ -**PTMTC** were dissolved ( $c = 1$  mM) in PB (50 mM, pH 7.4). Furthermore, 1 mM solutions of  $^{13}\text{C}$ -**PTMTC** in PB (50 mM, pH range from 0 to 14) were used to study the effect of pH changes. Solutions of radicals **PTMTC** and  $^{13}\text{C}$ -**PTMTC** ( $c = 1$  mM) prepared in a mixture of PB (50 mM, pH 7.4) and freshly opened commercial absolute glycerol, the glycerol content ranging from 0% to 80% (m/m) were used to investigate the impact of viscosity. Solutions of **PTMTC** and  $^{13}\text{C}$ -**PTMTC** radicals were prepared in a mixture of PB (50 mM, pH 7.4) and freshly opened absolute methanol with a methanol content ranging from 0% to 100% (v/v). A solution of  $^{13}\text{C}$ -**PTMTC** in 40/60

---

<sup>††</sup> This section was prepared in a co-operation with Dr. Nadica Maltar Strmecki in the research group of Prof. Dariush Hinderberger, Institut für Chemie - Physikalische Chemie, Martin-Luther-Universität Halle-Wittenberg.

glycerol/PB was selected to inspect the relation between the line width and the viscosity/temperature ratio. A solution of  $^{13}\text{C}$ -PTMTC in PB (50 mM, pH 7.4) was used to study both the thermal annealing at a temperature range (323–353 K) and stability against ascorbic acid ( $c = 1$  mM). Solution of PTMTC in PB (50 mM, pH 7.4) was used to perform cell-Lysate study ( $c = 0.5$  mM).

#### 4.2.3. Continuous wave (CW-EPR) spectra

CW-EPR spectra of  $^{13}\text{C}$ -PTMTC were recorded on the Miniscope MS 400 benchtop spectrometer (Magnetech, Berlin, Germany) working at X-band ( $\nu_{\text{mw}} \sim 9.4$  GHz). The microwave frequency was recorded with a Racal-Dana frequency counter, model 2101 (Racal Instruments, Neu-Isenburg, Germany). Temperature control unit TC H03 (Magnetech, Berlin, Germany) with nitrogen gas flow was used to control the temperature within  $\pm 1$  K. A manganese standard reference,  $\text{Mn}^{2+}$  in ZnS (Magnetech, Berlin, Germany) was used to calibrate the magnetic field of the spectrometer. The spectra were simulated with a custom-build program in MATLAB (The MathWorks, Inc.) using the EasySpin program package for EPR<sup>244</sup>.

#### 4.2.4. Pulse X-band EPR

Pulse X-band EPR studies were performed on X-band Bruker ELEXSYS 580 spectrometer. The temperature was controlled by a closed cycle cryostat (ARS AF204).  $T_2$  relaxation times were measured by using simple Hahn spin echo sequence:  $\pi/2$ -tau- $\pi$ -tau-echo.

### 4.3. Results and discussion

#### 4.3.1. Synthesis of tetrachlorotriarylmethyl tricarboxylic acid (PTMTC) and its $^{13}\text{C}$ labelled analog ( $^{13}\text{C}$ -PTMTC)

The preparation of PTMTC (**Fig. 3.1**) has been reported before (section 1.2.2.5.2)<sup>179</sup>. A new synthetic scheme that is easy, reproducible and worked with high yield, is depicted in **Fig. 4.1**. The same procedure was applied to prepare the  $^{13}\text{C}$ -PTMTC using perchlorotriarylmethane (**48**) that was enriched with  $^{13}\text{C}$  at the central carbon.

Friedel-Crafts alkylation of 1,2,4,5-tetrachlorobenzene (**14**) with a mixture of  $\text{CHCl}_3$  and  $^{13}\text{C}$ - $\text{CHCl}_3$  (1:1 ratio) in the presence of  $\text{AlCl}_3$ <sup>147</sup> gave compound **48**. Reaction of **48** with an excess of *n*-BuLi and TMEDA in THF at low temperature gave the corresponding trianion. With ethyl chloroformate the triethyl ester (**49**) was formed<sup>178</sup>, which was converted into the triester radical (**50**) by a two-step process: Conversion into the triaryl-carbanion with a 1 mM

solution of Bu<sub>4</sub>NOH in MeOH which served as a base, followed by oxidation with *p*-chloranil<sup>183</sup>. Heating **50** in conc. H<sub>2</sub>SO<sub>4</sub> yielded the tricarboxylic acid radical <sup>13</sup>C-PTMTC.

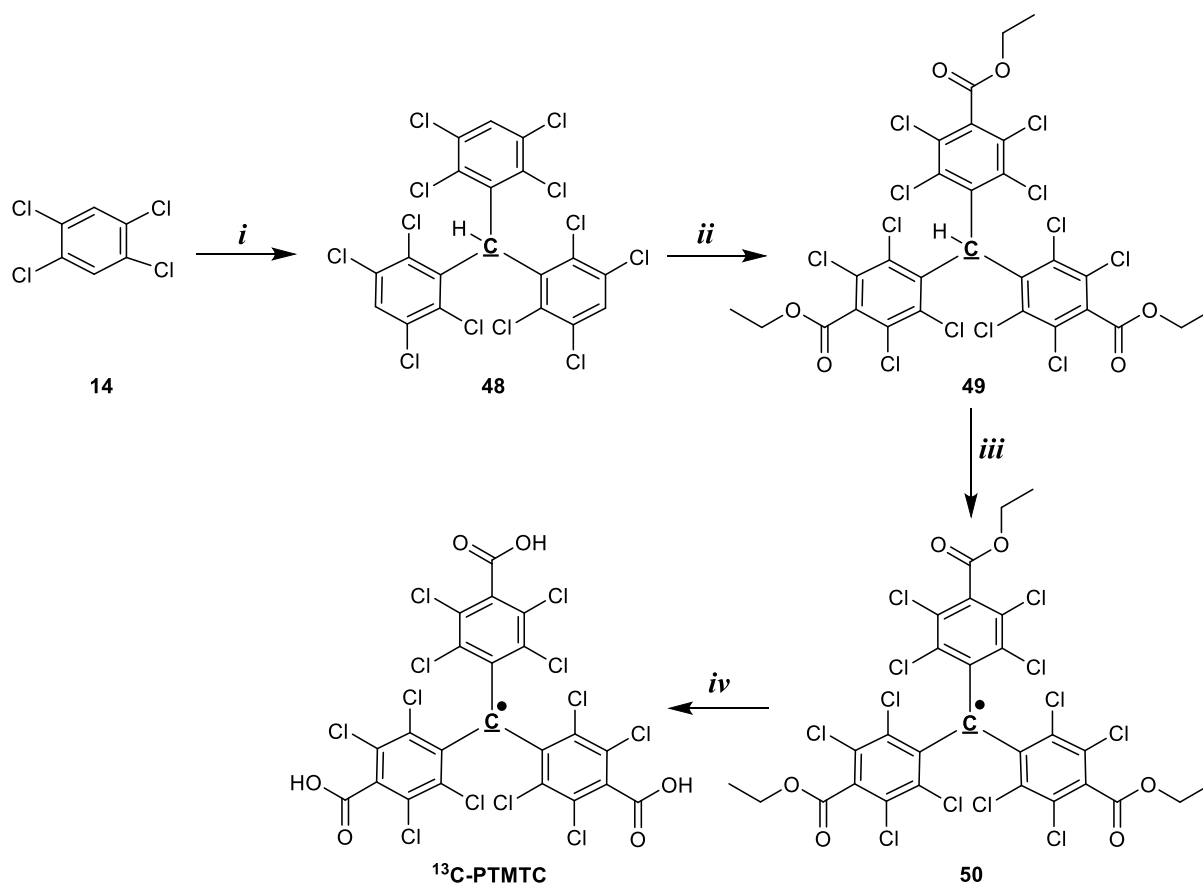


**Fig. 4.1** Synthesis of <sup>13</sup>C-PTMTC radical. Reagents and conditions: **(i)** CHCl<sub>3</sub>/<sup>13</sup>C-CHCl<sub>3</sub> (1:1 ratio)/AlCl<sub>3</sub>/160 °C; **(ii)** *n*-BuLi, TMEDA, ethyl chloroformate; **(iii)** 1. Bu<sub>4</sub>NOH, 2. *p*-chloranil; **(iv)** 95% H<sub>2</sub>SO<sub>4</sub>; central carbon C is the 50% <sup>13</sup>C labelled atom of <sup>13</sup>C-PTMTC.

#### 4.3.2. EPR characterization

The naturally abundant isotope of carbon, <sup>12</sup>C ( $I = 0$ ) caused no hyperfine splittings. The EPR spectrum of the PTMTC showed a single peak, in addition to three symmetrical pairs of satellites because of spin coupling with naturally abundant <sup>13</sup>C, **Fig. 4.2A**. The isotopically enriched analogue, <sup>13</sup>C-PTMTC, with 50% <sup>13</sup>C labelling at the methyl radical center, the EPR spectrum showed three lines. The central line was caused by PTMTC. <sup>13</sup>C ( $I = 1/2$ ) split the spectra into two components (high field and low field peaks), **Fig. 4.2B**. The same pattern of splitting was observed before for the un-substituted triarylmethyl radical with 50% <sup>13</sup>C labelling at the methyl radical center<sup>245</sup>.

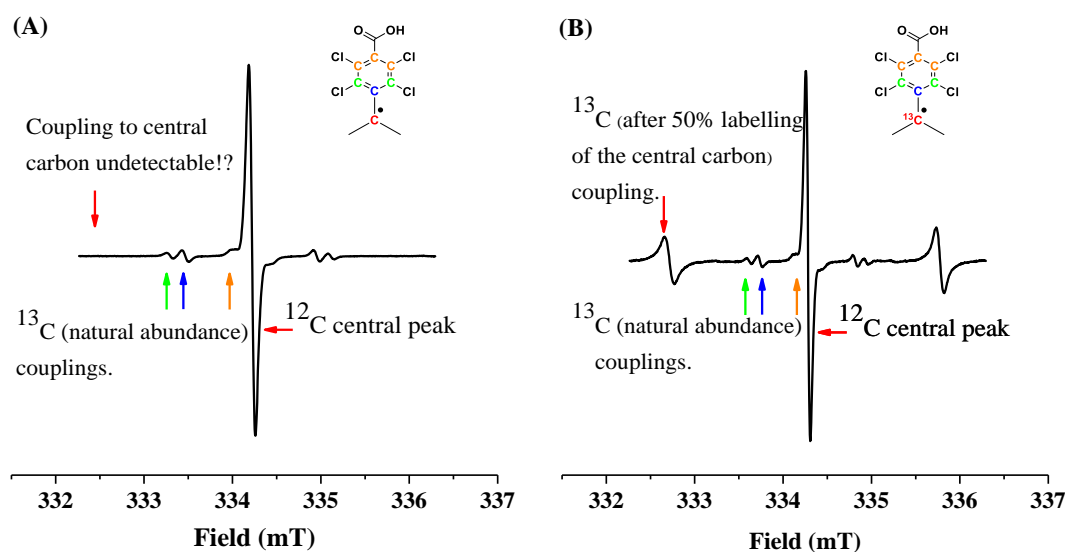


**Fig. 4.2** EPR spectra of PTMTC and  $^{13}\text{C}$ -PTMTC in PB pH 7.4 ( $c = 1$  mM). (A) PTMTC appears as a single line ( $^{12}\text{C}$  central peak); (B) The  $^{12}\text{C}$  central peak of PTMTC and the doublet of  $^{13}\text{C}$ -PTMTC because of the hyperfine coupling to the  $^{13}\text{C}$  nuclei ( $I = 1/2$ ).

#### 4.3.3. CW-EPR spectrum

**Fig. 4.3** shows an experimental CW-EPR spectrum (black) of a solution of  $^{13}\text{C}$ -PTMTC in DMSO ( $c = 1$  mM), recorded at RT, and the corresponding simulation (dashed red line). Hyperfine couplings were determined by simulation of the experimental spectra<sup>244</sup> and the obtained data are presented in **Table 4-1**. The obtained values are in accordance with data reported by Paniagua et al.<sup>186</sup>. Sabacky et al.<sup>246</sup> reported hyperfine coupling ( $a_c$ ) values of two radicals (the unsubstituted triarylmethyl and 2,6,2',6',2'',6''-Hexamethoxytriarylmethyl radicals) that were enriched with  $^{13}\text{C}$  (56% and 54% respectively) at the central carbon. Value of  $a_c$  for the unsubstituted triarylmethyl radical was 64.4575 MHz and for 2,6,2',6',2'',6''-Hexamethoxytriarylmethyl radical was 73.4255 MHz.

**Table 4-1**  $^{13}\text{C}$  hyperfine coupling values.

$^{13}\text{C}$ Hyperfine coupling (MHz)	
Central carbon	83.49
1-phenyl $^{13}\text{C}$ bridgehead ( <i>ipso</i> )	34.92
2,6-phenyl $^{13}\text{C}$ in <i>ortho</i> position	28.99
3,5-phenyl $^{13}\text{C}$ in <i>meta</i> position	5.88
<i>g</i> value	2.0028±0.0002

\*Hyperfine couplings were measured in absolute values.

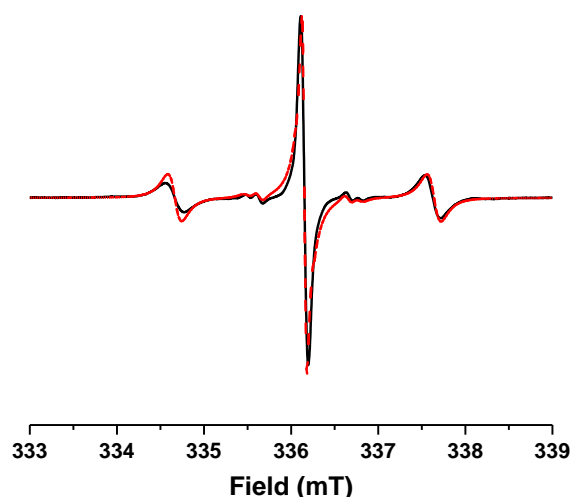


**Fig. 4.3** CW EPR spectrum of  $^{13}\text{C}$ -PTMTC (1 mM in DMSO) recorded at RT. The simulated spectrum (dashed red line) is superimposed onto the experimental one (solid black line).

#### 4.3.4. Influence of pH value on $^{13}\text{C}$ -PTMTC line width

PTMTC radical bearing ionizable carboxyl group was expected to show pH sensitivity. By varying pH, terminal groups are ionized from COOH (at low pH) to all  $\text{COO}^-$  (at high pH) and to a mixture of the COOH and  $\text{COO}^-$  (at intermediate pH values). Solutions of  $^{13}\text{C}$ -PTMTC ( $c = 1 \text{ mM}$ ) in PB (50 mM, pH 0–14) were used to investigate the impact of pH value on EPR line widths. Hyperfine splitting and line widths were found to be independent of pH changes. For the extreme values of pH, *i.e.*  $\text{pH} < 2$  the sample showed degradation and appearance of aggregates, **Fig. 4.4**. For applications at physiological pH values, it is assumed that the samples are stable.

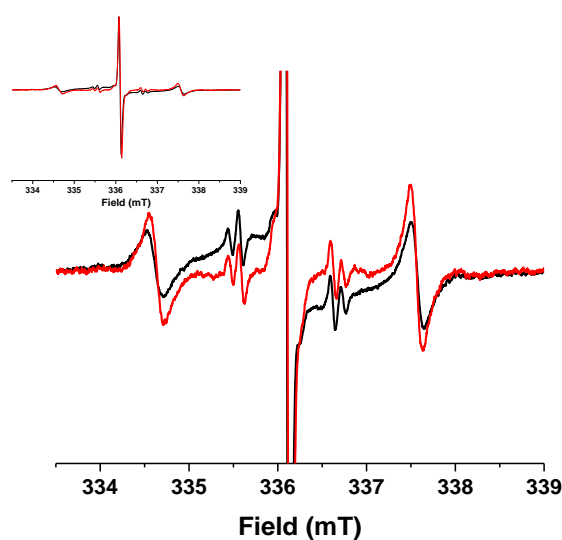


**Fig. 4.4** EPR X-band spectra of  $^{13}\text{C}$ -PTMTC recorded at 37 °C for  $\text{pH}=8.28$  (black line) and  $\text{pH}=1$  (red line). In the insert, the full range of the experimental spectrum is shown.

This can also be seen by following the ratio of the central  $^{12}\text{C}$  peak and the  $^{13}\text{C}$  doublet line intensities, at the low field (LF) and high field (HF) position, **Fig. 4.5**.

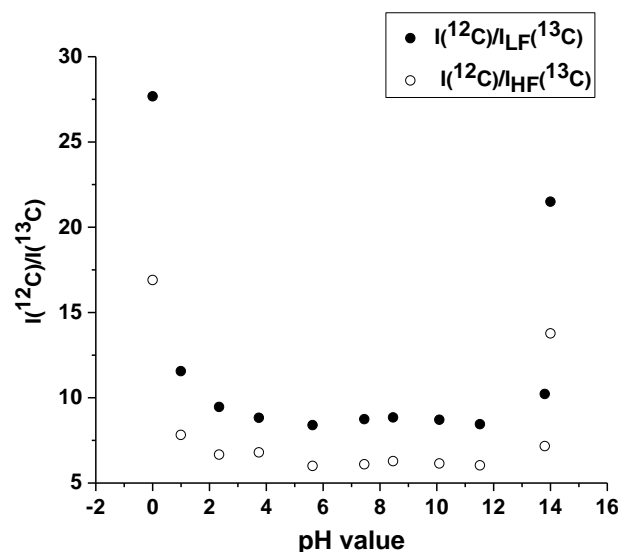


**Fig. 4.5** Dependence of the ratio of peak-to-peak intensities of the central  $^{12}\text{C}$  line and  $^{13}\text{C}$  doublet lines on the pH value.

#### 4.3.5. Influence of viscosity on $^{13}\text{C}$ -PTMC line width

Different glycerol-water mixtures (0%–80% glycerol in water, m/m) were used as solvents to prepare 1 mM solutions of PTMTC and  $^{13}\text{C}$ -PTMTC. For PTMTC, between 10 and 40% (m/m) glycerol content, a slight decrease in the EPR signal line width was detected. This could be due to a decrease in oxygen solubility with increasing percentage of glycerol<sup>247</sup>. The increase above 60% reflects the effect of increased viscosity by increasing glycerol content, **Fig. 4.6A**. Apparently, viscosity by itself up to the value of about 40% of glycerol has no effect on the EPR signal line width. This fact is important for *in-vivo* applications as blood has a viscosity of 3–4 mPa.s at 37 °C<sup>248</sup>, which is only reached at approx. 44 mass % of glycerol in water at 20 °C<sup>249</sup>. For  $^{13}\text{C}$ -PTMTC, the  $^{13}\text{C}$  doublets in buffer had fourfold broader lines than the  $^{12}\text{C}$  signal. Explanation: The comparatively small effect of oxygen on their width was overruled by the effect of viscosity increase with increasing glycerol concentration, **Fig. 4.6B**. The  $^{13}\text{C}$  atom provides a relaxation mechanism that is so fast as to override the relaxation effect of contacts with dissolved molecular oxygen. Thus, the doublet peak line widths were dominated by viscosity from the beginning and became too broad for the exact determination beyond approx. 30% glycerol.

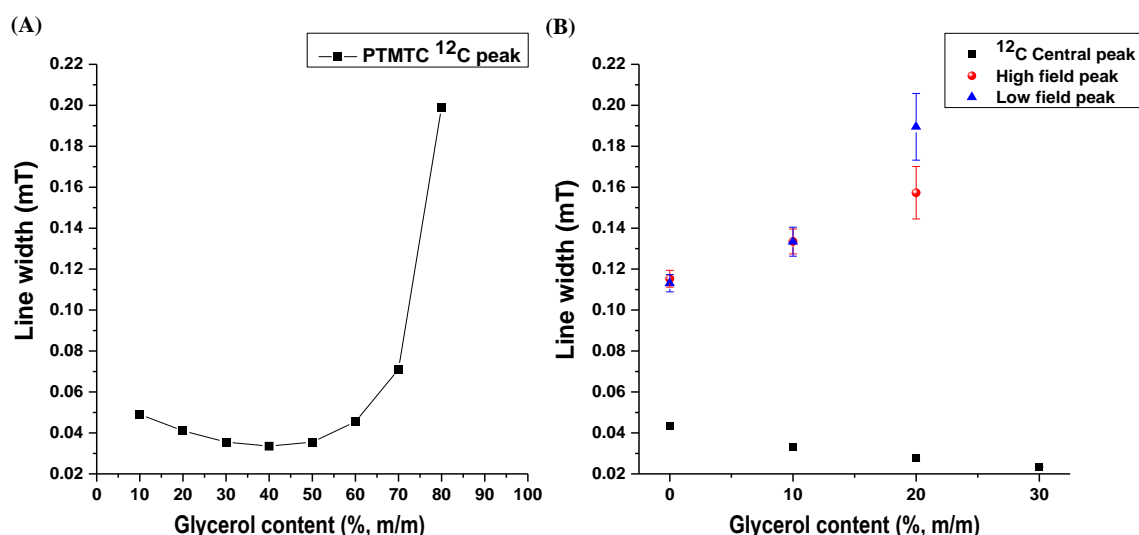


**Fig. 4.6** Line width changes at different glycerol concentrations. (A) PTMTC; (B)  $^{13}\text{C}$ -PTMTC.

Despite the fact that viscosity by itself up to a value of about 40% of glycerol has no effect on the EPR signal line width, the influence of viscosity can be observed through the ratio of the intensity of central  $^{12}\text{C}$  peak and intensity of  $^{13}\text{C}$  LF doublet line. The linear dependence can be observed for the different temperatures in the range from 293 K up to 363 K. In **Fig. 4.7** the dependence is shown only for two temperatures regarding the temperature limitation during the *in-vivo* application.

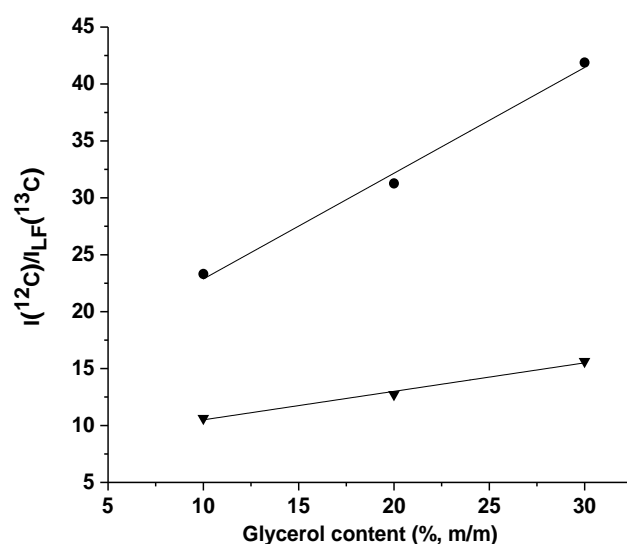


**Fig. 4.7** Ratio of the peak-to-peak intensities of central  $^{12}\text{C}$  line and  $^{13}\text{C}$  doublet lines at LF as a function of glycerol obtained at two different temperatures (●) 298.15 K and (▼) 310.15 K.

#### 4.3.6. Influence of oxygen on PTMTC line width

EPR signal line width increase is directly proportional to oxygen concentration<sup>250</sup>. A solution of PTMTC ( $c = 1$  mM) in PB (pH 7.4) shows a linear relationship between line width

and oxygen content, **Fig. 4.8**. The small slope of the curve is because of the fact that in aqueous solutions, dissolved oxygen concentration hardly increases with increasing oxygen partial pressure, a physicochemical fact that should be kept in mind for any oxygen determination in water <sup>5</sup>.

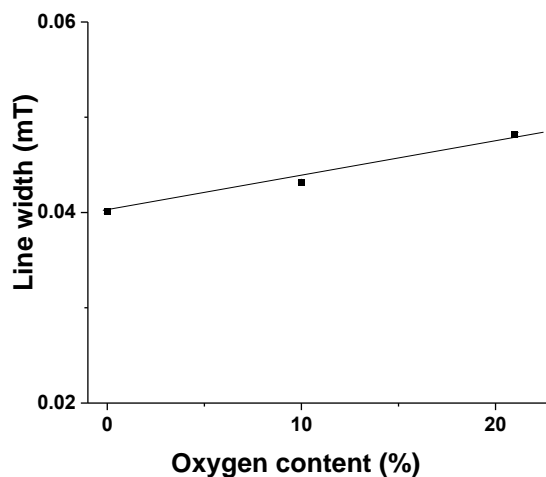


**Fig. 4.8** Line width of the EPR signal of PTMTC at different oxygen concentrations.

EPR spectra of methanol-water mixtures (10%–100% methanol in water, v/v) including 1 mM of <sup>13</sup>C-PTMTC were investigated. In aerated solutions (**Fig. 4.9A**), with increasing MeOH concentration the line width of both the <sup>12</sup>C central peak and the doublet peak (<sup>13</sup>C radical signal) increased. This may be explained as follows: (a) With increasing MeOH concentration, oxygen solubility increases <sup>200</sup>, leading to shorter relaxation times and thus broader lines because of the interaction between the paramagnetic oxygen with the spin probe. Under deoxygenated conditions (**Fig. 4.9B**), it was expected that the line width would not change because the oxygen effect was excluded. However, the line width of both <sup>13</sup>C-PTMTC doublet peaks increased up to approx. 50% MeOH and decreased beyond. This appears to follow the increase and decrease of viscosity of methanol-water mixtures <sup>250</sup>. The (slight) reduction, about 4%, of the line width for the <sup>12</sup>C-PTMTC signal follows the deviations reported for the water/methanol system such as volume contraction with maximum at 56% of MeOH <sup>251</sup> as well as parabolic entropy profile for both methanol and water in the methanol-water mixtures compared to the pure liquids <sup>252</sup>. The same behavior can be observed in **Fig. 4.10** where dependence of  $1/T_2$  relaxation rate ( $1/T_2$ ~line width) on water/methanol compositions recorded at RT is shown. This effect is not evident for the  $1/T_2$  relaxation rates of <sup>13</sup>C-PTMTC doublet peaks due to the stronger influence of other nuclear relaxation mechanisms.



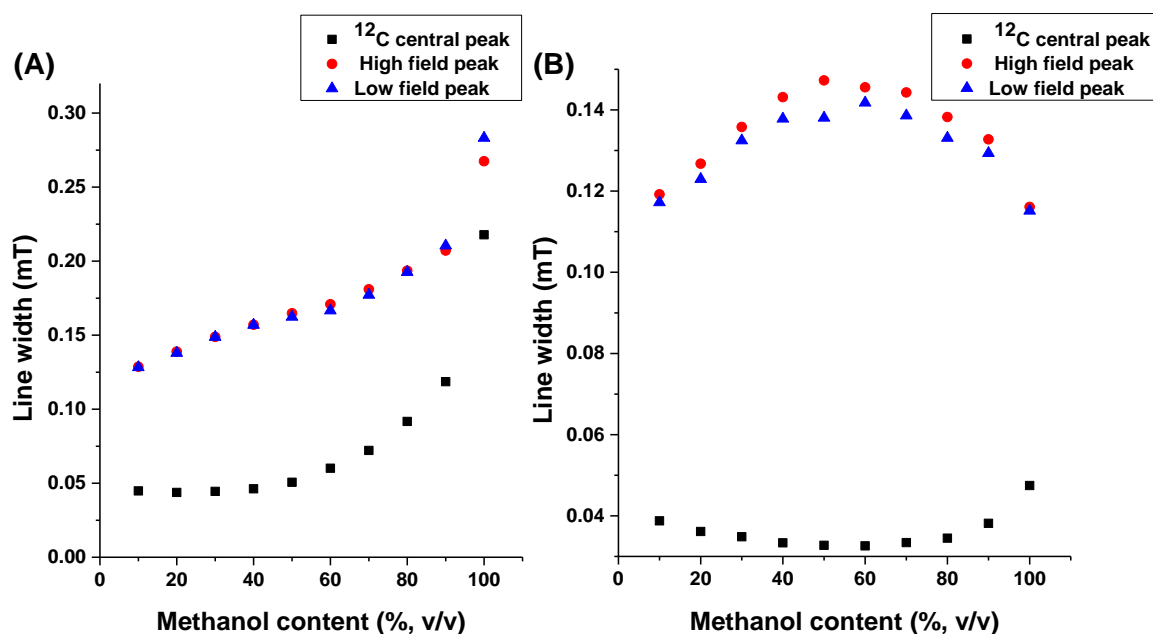


**Fig. 4.9** Effect of increasing methanol (MeOH) content on the line width of  $^{13}\text{C}$ -PTMTC (the central line and doublet peak). (A) Aerobic conditions (20.9%  $\text{O}_2$ ) (B) Deoxygenated conditions ( $\approx 0\%$   $\text{O}_2$ ).

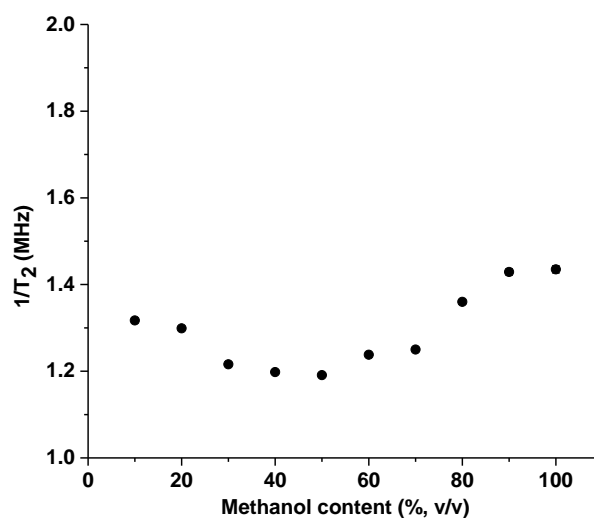


**Fig. 4.10** Dependence of  $1/T_2$  on water/methanol compositions for the  $^{12}\text{C}$ -PTMTC line.

#### 4.3.7. Influence of temperature on $^{13}\text{C}$ -PTMTC line width

The intensity of the EPR signal arising from the central line is inversely proportional to temperature according to the Curie law, whereas the intensity of EPR signals arising from the  $^{13}\text{C}$  doublet obeys a more complex relationship, **Fig. 4.11**. Non-Curie law behavior or the intensity enhancement is most marked with radicals where the electron spin is highly localized and isolated from nuclear interactions. This suggests that there are differential saturation where

the species that produces the main  $I_{\text{CF}}$  line in the spectrum has only weak relaxation mechanisms while the  $^{13}\text{C}$  labeled species have much stronger relaxation as a result of the nuclear hyperfine interaction.

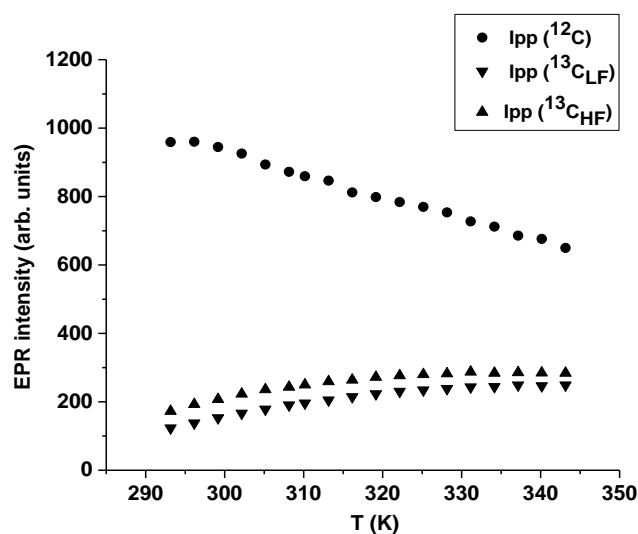


**Fig. 4.11** Temperature dependence of the EPR intensities.

Again, the effect of viscosity changes on the  $^{13}\text{C}$ -PTMTC signal is pronounced, leading concomitantly to an increase of the amplitude of both the high field and low field parts of the doublet by a factor of approx. 5 (data not shown) and a decrease of their line widths by a factor of approx. 3. **Fig. 4.12** depicts the linear relation between the line width and the viscosity/temperature ratio as described by the Stokes-Einstein equation. This linear behavior was not observed for the  $^{12}\text{C}$ -PTMTC line.

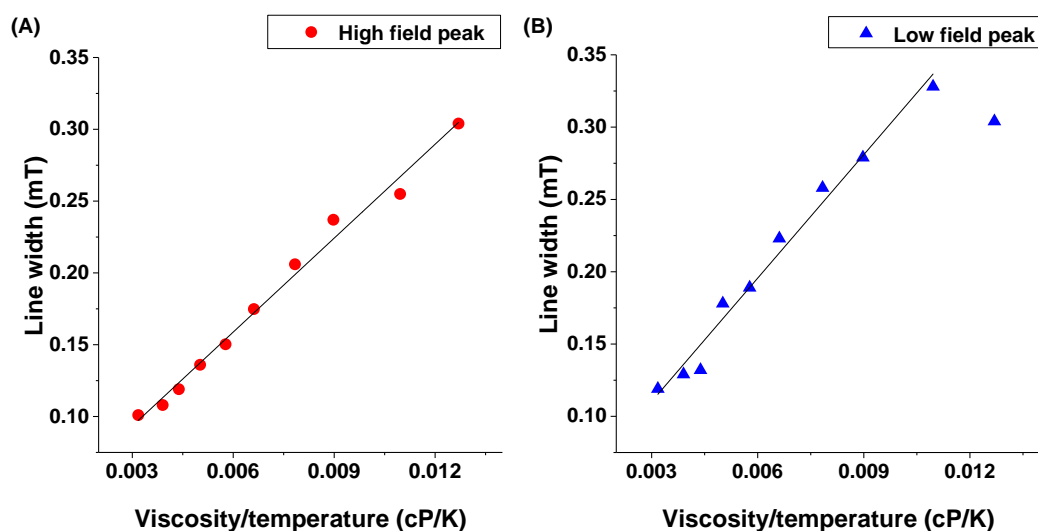


**Fig. 4.12** Effect of temperature. Solution of  $^{13}\text{C}$ -PTMTC ( $c = 1 \text{ mM}$ ) in 40/60 glycerol/buffer, 20–70 °C. **(A)** High field (HF) peak and **(B)** Low field (LF) peak.

The linear viscosity/temperature relation indicates that for  $^{13}\text{C-PTMTC}$ , the spin-rotational interaction is the dominant effect on line width<sup>253,254</sup>. In such cases, the movement of the nuclei and electrons is out of phase, resulting in a local magnetic field that interacts with the unpaired electron. This allows for measurements of viscosity even if other solvent parameters are also changed, *e.g.* oxygen content.

#### 4.3.8. The accelerated aging (by increasing temperature) method

A solution of  $^{13}\text{C-PTMTC}$  in PB (50 mM, pH 7.4) was used to study the stability of the samples<sup>255</sup>. Therefore, thermal annealing studies were performed in the temperature range 323–353 K. Peak-to-peak intensities of the central line were used to follow changes in the signal with time. As expected, the decrease in the EPR signal intensity was more pronounced at higher annealing temperatures. The EPR data presented in **Fig. 4.13** were analyzed in terms of the first-order kinetics.

$$I = I_o \cdot e^{-k(T)t} \quad (1)$$

where  $I$  is peak height of the central line obtained from the first derivative spectra,  $I_o$  is peak height of the central line obtained at time  $t=0$  from the first derivative spectra and  $k$  is the rate constant, which is function of absolute temperature,  $T$ . The kinetic parameters for the process ( $k_o$ ,  $\Delta E$ ) were derived by fitting the obtained rate constants  $k_i(T)$  to the Arrhenius equation,

$$k(T) = k_o \cdot e^{-\frac{\Delta E}{RT}} \quad (2)$$

Where  $k_o$  is, the frequency factor,  $\Delta E$  is the activation energy and  $R$  is the universal gas constant ( $R=8.314 \text{ Jmol}^{-1}\text{K}^{-1}$ ). **Fig. 4.14** shows the Arrhenius plot of the derived rate constants, from which the activation energies have been extracted. **Fig. 4.14** shows the Arrhenius diagram for this first-order process. The resulting activation energy ( $E$ ) is  $226.5 \pm 16.9 \text{ kJ/mol}$ , and the frequency factor ( $\ln k_o$ ) is  $73.4 \pm 6.0 \text{ min}^{-1}$ . The obtained data show long-term stability but only if the sample solution is stored in the dark.

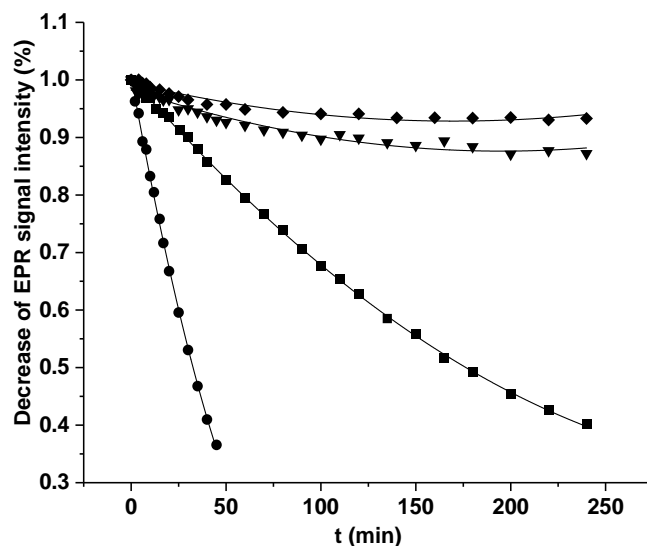


**Fig. 4.13** Thermal decay of  $^{13}\text{C}$ -PTMTC sample stored at different elevated temperatures: (●) 353.15 K; (■) 343.15 K; (▼) 333.15 K; (◆) 323.15 K. The solid lines are the monoexponential fits to Eq. 1.

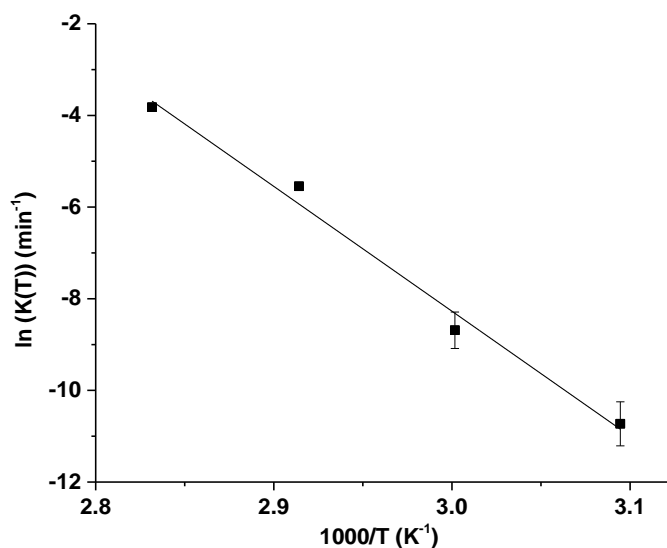


**Fig. 4.14** Rate of radical decay as a function of temperature.

Connected to the stability, the effect of the ascorbic acid as a reactive and commonly found biological substance was investigated. Aqueous solution of ascorbic acid ( $c = 10 \text{ mM}$ ) was added to  $1 \text{ mM}$  solution of the  $^{13}\text{C}$ -PTMTC radical in PB ( $50 \text{ mM}$ ,  $\text{pH } 7.4$ ). **Fig. 4.15** shows a decrease of the EPR signal intensity of 50% in an hour recorded at  $300 \text{ K}$ . The process of the interaction of the  $^{13}\text{C}$ -PTMTC and ascorbic acid is complex and can be influenced by solvent,

light and concentration of oxygen. Further investigation of these effects are indeed necessary, but they are beyond the scope of this paper.

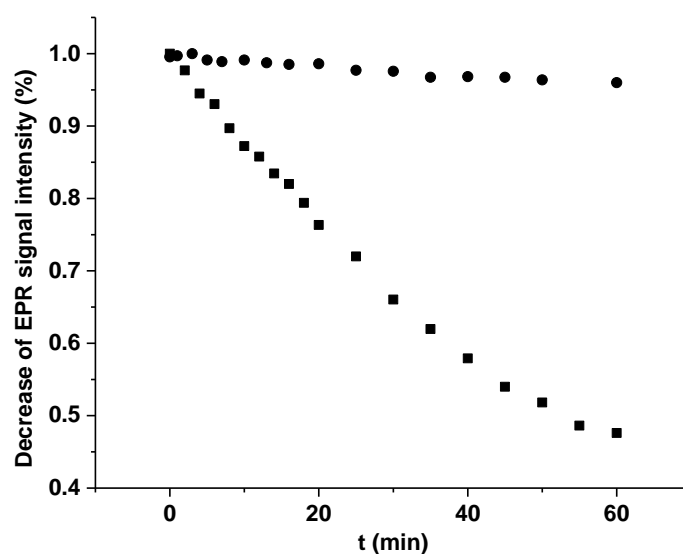


**Fig. 4.15** Decay of  $^{13}\text{C}$ -PTMTC recorded at 300 K (●) pure solution of  $^{13}\text{C}$ -PTMTC and (■) solution of  $^{13}\text{C}$ -PTMTC in the presence of ascorbic acid.

#### 4.3.9. Cell lysate study

With the help of cell lysate experiments, how fast substances are degraded reductively by enzymes can be identified. The experiments were carried out using a *Xenopus laevis* oocyte cell extract. The *Xenopus laevis* oocytes trial is an established and easy-to-use model system to perform microinjection experiments. 5  $\mu\text{l}$  of the 0.5 mM solution of PTMTC in PB (50 mM, pH 7.4) was mixed with 15  $\mu\text{l}$  of the cell lysate and was vortexed for 10 seconds. This mixture was measured in a capillary ring caps. PTMTC that has a half-life less than ten minutes appears to be unsuitable for *in-vivo* application. This result is in accordance with the instability of PTMTC radical in the presence of human blood or plasma (40% decrease of the signal intensity after 30 min) <sup>191</sup>. The stability can be possibly improved by access to a polymeric support; this, studies are underway. The cell lysate experiments confirm the statements of the redox potentials; the tetrachloro-TAM radicals are resistant to oxidation, but very easily reduced.

#### 4.4. Conclusion

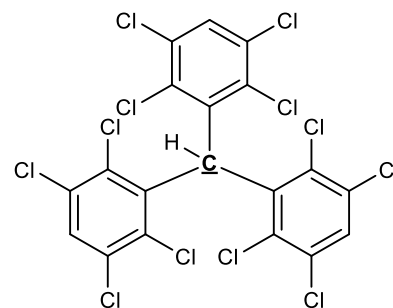
PTMTC is an interesting hydrophilic paramagnetic spin probe with favorable EPR spectroscopy and imaging characteristics (single EPR signal with narrow line width). The line width is affected by different parameters (viscosity, oxygen concentration and pH). Each of these parameters can be measured accurately when others are kept constant. In aqueous

solutions, viscosity and oxygen partial pressure do not have a pronounced effect on line width. The observed differential effects of oxygen content and viscosity on the line widths of the <sup>12</sup>C-PTMTC and the <sup>13</sup>C-PTMTC EPR signals suggest that this mixture of isotopic radicals could gain importance as a probe for both parameters.

#### 4.5. Syntheses

##### 50% <sup>13</sup>C-Tris(2,3,5,6-tetrachlorophenyl)methane (**48**)<sup>147</sup>.

1,2,4,5-tetrachlorobenzene (**14**) (9.6 gm, 44 mmol), AlCl<sub>3</sub> (0.73 gm, 5.2 mol), <sup>13</sup>C-CHCl<sub>3</sub> (0.2 mL, 2.45 mmol) and CHCl<sub>3</sub> (0.2 mL, 2.45 mmol) were mixed in a glass pressure vessel, and were heated in an oil bath at 160 °C for 45 min. The mixture was then poured onto ice and HCl (1M, 50 mL) and extracted three times with CHCl<sub>3</sub>. The organic layer was



washed with water, aqueous NaHCO<sub>3</sub> and dried over Na<sub>2</sub>SO<sub>4</sub>. After evaporation, the residue was purified on silica gel eluting with heptane.

**Yield:** 1.26 g (39%, based on chloroform)

**Colour:** White crystals

**Molecular formula:** C<sub>19</sub>H<sub>4</sub>Cl<sub>12</sub>

**Molar mass:** 657.65 g/mol

**Mp:** > 280 °C

**R<sub>f</sub>:** 0.67 (heptane)

**<sup>1</sup>H NMR:** (400 MHz, CDCl<sub>3</sub>) δ 7.65 (s, 3H), 6.99 (s, 1H, H<sup>12</sup>C), 6.83–7.13 (d, *J* = 122 Hz, 1H, H<sup>13</sup>C)

**<sup>13</sup>C NMR:** (100 MHz, CDCl<sub>3</sub>) δ 138.6, 134.4, 133.6, 133.3, 132.4, 130.4, 56.1

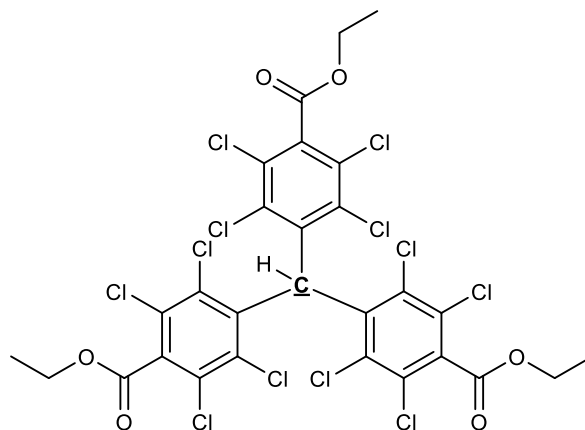
**IR (KBr):** ν = 3113, 3067, 2957, 2923, 1547, 1409, 1387, 1348, 1321, 1234, 1199, 1164, 1099, 974, 868, 843, 781, 758, 704, 690 cm<sup>-1</sup>

**MS (EI):** 657.6 (C<sub>19</sub>H<sub>4</sub>Cl<sub>12</sub>)

**HRMS (ESI):** calcd. for C<sub>19</sub>H<sub>3</sub>Cl<sub>12</sub> [M-H]<sup>-</sup> 656.642; found 656.642

**50% <sup>13</sup>C-Tris(4-ethoxy-carbonyl-2,3,5,6-tetrachlorophenyl)methane (49) <sup>178</sup>.**

Compound **48** (500 mg, 0.76 mmol) and TMEDA (1.15 mL, 7.6 mmol) were dissolved in dry THF (50 mL) under argon atmosphere and cooled to  $-78\text{ }^{\circ}\text{C}$ . A solution of 2.5 M *n*-BuLi in *n*-hexane (3 mL, 7.6 mmol) was added in one portion, and the mixture was stirred at this temperature for 1 h. Ethyl chloroformate (0.72 mL, 7.6 mmol) was added, and the reaction mixture was allowed to reach RT overnight. Solvent was evaporated, and the residue was dissolved in DCM. The organic layer was washed with water and dried over Na<sub>2</sub>SO<sub>4</sub>. Solvent was evaporated under vacuum and residue was purified on silica gel eluting with (heptane/EA, 12/1).



**Yield:** 525 mg (79 %)

**Colour:** Colourless solid

**Molecular formula:** C<sub>28</sub>H<sub>16</sub>Cl<sub>12</sub>O<sub>6</sub>

**Molar mass:** 873.71 g/mol

**Mp:** 170–172 °C

**R<sub>f</sub>:** 0.26 (heptane/EA, 10/1)

**<sup>1</sup>H NMR:** (400 MHz, CDCl<sub>3</sub>) δ 1.424 (t, 9H), 4.495 (q, 6H), 7.0 (s, 1H, H<sup>12</sup>C) 6.9–7.2 (d, *J* = 122 Hz, 1H, H<sup>13</sup>C)

**<sup>13</sup>C NMR:** (100 MHz, CDCl<sub>3</sub>) δ 163.2, 138.4, 135.5, 135, 134, 130.5, 129.5, 63.1, 56.3, 14

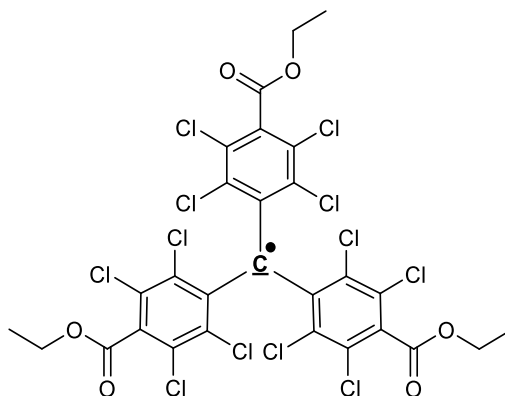
**IR (KBr):** ν = 2981, 1741, 1555, 1465, 1370, 1341, 1298, 1259, 1224, 1207, 1113, 858, 756 cm<sup>-1</sup>

**MS (EI):** 873.7 (C<sub>28</sub>H<sub>16</sub>Cl<sub>12</sub>O<sub>6</sub>)

**HRMS (ESI):** calcd. for C<sub>28</sub>H<sub>17</sub>Cl<sub>12</sub>O<sub>6</sub> [M+H]<sup>+</sup> 874.720; found 874.720

**50% <sup>13</sup>C-Tris(4-ethoxy-carbonyl-2,3,5,6-tetrachlorophenyl)methyl radical (50)** <sup>178,183</sup>.

A solution 1 M Bu<sub>4</sub>NOH in MeOH (0.5 mL, 0.48 mmol, 1.2 eq.) was added to a solution of compound **49** (350 mg, 0.4 mmol, 1 eq.) in freshly distilled THF (30 mL) under argon atmosphere. The mixture was stirred in the dark for 1 h. *p*-chloranil (394 mg, 1.6 mmol, 4 eq.) was added as a solid. The mixture was stirred overnight. Solvent was removed giving a purple residue, which was purified on silica gel eluting with (heptane/EA, 80/20).



**Yield:** 290 mg (83%)

**Colour:** Red solid

**Molecular formula:** C<sub>28</sub>H<sub>15</sub>Cl<sub>12</sub>O<sub>6</sub>

**Molar mass:** 872.70 g/mol

**Mp:** 160–165 °C

**R<sub>f</sub>:** 0.26 (heptane/EA, 10/1)

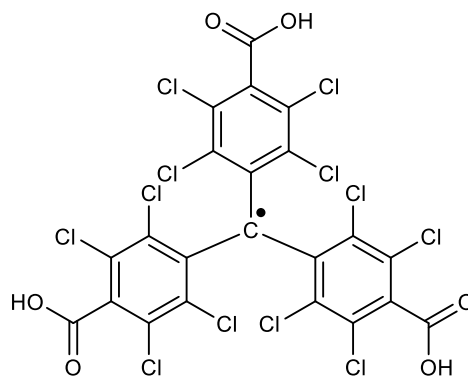
**IR (KBr):** ν = 2955, 2916, 2849, 1741, 1466, 1378, 1342, 1284, 1224, 1010, 756 cm<sup>-1</sup>

**MS (ESI):** *m/z* 872.81 [M]<sup>-</sup>

**HRMS (ESI):** calcd. for C<sub>28</sub><sup>13</sup>C<sub>1</sub>H<sub>16</sub>Cl<sub>12</sub>O<sub>6</sub> [M+H]<sup>+</sup> 874.712; found 874.724

**Tris(4-carboxy-2,3,5,6-tetrachloro-phenyl)methyl radical (PTMTC)** <sup>179</sup>.

Radical **11** (**Fig. 3.1**) (200 mg, 0.23 mmol) was mixed with conc. H<sub>2</sub>SO<sub>4</sub> (95%, 25 mL) and the mixture was heated at 90 °C for 12 h. The final solution was cooled and poured carefully onto cracked ice; the aqueous phase was extracted with Et<sub>2</sub>O. The organic phase was concentrated and extracted with aqueous Na<sub>2</sub>CO<sub>3</sub>. The resulting aqueous phase was acidified slowly with 5 M HCl and extracted several times with Et<sub>2</sub>O. The organic phase was dried over anhydrous Na<sub>2</sub>SO<sub>4</sub> and the solvent was removed under vacuum. The crude product was dissolved in Et<sub>2</sub>O (5 mL) and precipitated from *n*-hexane; this process was repeated 3 times.



**Yield:** 154.2 mg (85%)

**Colour:** Red powder

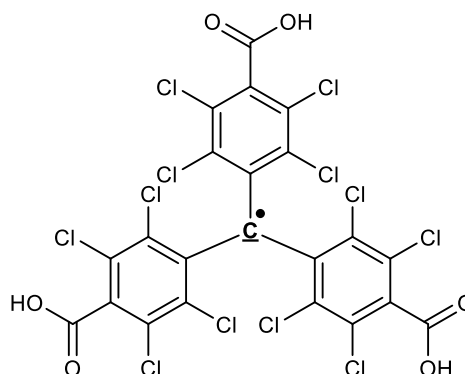
**Molecular formula:** C<sub>22</sub>H<sub>3</sub>Cl<sub>12</sub>O<sub>6</sub>

**Molar mass:** 788.61 g/mol



**Mp:** > 280 °C**R<sub>f</sub>:** 0.2 (EA/MeOH, 5/2)**IR (KBr):**  $\nu$ = 3702–2643, 1703, 1661, 1602, 1536, 1401, 1348, 1325, 1281, 1240, 1124, 1041, 859, 752, 724 cm<sup>-1</sup>**MS (ESI):**  $m/z$  788.83 [M]<sup>-</sup> (70%), 743.60 [M-CO<sub>2</sub>]<sup>-</sup> (100%), 698.82 [M-2CO<sub>2</sub>]<sup>-</sup> (60%)**HRMS (ESI):** calcd. for C<sub>22</sub>H<sub>4</sub>Cl<sub>12</sub>O<sub>6</sub> [M+H]<sup>+</sup> 789.618; found 789.618**50% <sup>13</sup>C-Tris(4-carboxy-2,3,5,6-tetrachlorophenyl)methyl radical (<sup>13</sup>C-PTMTC).**

Compound **50** (200 mg, 0.23 mmol) was mixed with conc. H<sub>2</sub>SO<sub>4</sub> (95%, 25 mL) and the mixture was heated at 90 °C for 12 h. The final solution was cooled and poured onto cracked ice; the aqueous phase was extracted with Et<sub>2</sub>O. The organic phase was concentrated and extracted with aqueous Na<sub>2</sub>CO<sub>3</sub>. The resulting aqueous phase was acidified slowly with 5 M HCl and extracted several times with Et<sub>2</sub>O. The organic phase was dried over anhydrous Na<sub>2</sub>SO<sub>4</sub> and the solvent was removed under vacuum. The crude product was dissolved in Et<sub>2</sub>O (5 mL) and precipitated from *n*-hexane, this process was repeated 3 times.

**Yield:** 159.6 mg (88%)**Colour:** Red solid**Molecular formula:** C<sub>22</sub>H<sub>3</sub>Cl<sub>12</sub>O<sub>6</sub>**Molar mass:** 788.61 g/mol**Melting point:** > 280 °C**R<sub>f</sub>:** 0.2 (EA/MeOH, 5/2)**EPR (1 mM in PBS pH 7.4):** The <sup>12</sup>C central peak,  $\Delta B_{pp}$ = 0.047 mT, and doublet peak of <sup>13</sup>C (LF:  $\Delta B_{pp}$ = 0.11 mT and HF:  $\Delta B_{pp}$ = 0.16 mT)**IR (KBr):**  $\nu$ = 3575–2414, 1698, 1660, 1601, 1394, 1323, 1240, 1143, 1037, 717 cm<sup>-1</sup>**MS (ESI):**  $m/z$  789 [M]<sup>-</sup>**HRMS (ESI):** calcd. for C<sub>21</sub><sup>13</sup>C<sub>1</sub>H<sub>4</sub>Cl<sub>12</sub>O<sub>6</sub> [M+H]<sup>+</sup> 790.621; found 790.627.

## 5. Spin labelling of polymers (chitosan and carboxymethyl chitosan)

### 5.1. Introduction

Chitosan (CS) is a natural biopolymer derived by partial N-deacetylation of chitin<sup>256,257</sup>. Chitin is a natural polysaccharide extracted from crustacean shells, such as prawns, crabs, insects, and shrimps<sup>258</sup>. CS is cationic in nature and has favorable biological properties such as low toxicity, good biocompatibility, and biodegradability<sup>259,260</sup>. CS has been used in various pharmaceutical applications including drug delivery systems<sup>261-263</sup>, tissue engineering<sup>264-266</sup>, wound healing<sup>267,268</sup>, gene delivery systems<sup>269,270</sup> and bioimaging applications<sup>271-273</sup>. However, CS applications are limited because of its poor aqueous solubility above pH ~ 6.5<sup>274,275</sup>.

Carboxymethyl chitosan (CMC) is a water-soluble CS derivatives, with carboxymethyl group linked to a nitrogen or oxygen atom<sup>276</sup>. The favorable properties, such as water solubility, non-toxicity, and good biocompatibility, make CMC an important derivative of CS<sup>277-280</sup>.

Radicals are generally toxic and unsuitable for direct administration, in high concentrations. By linking the spin probes with polymeric substrates, the properties of the polymer are transferred and the toxicity can be reversed. In this manner, the radicals can be made bioavailable, and analyzed with respect to the other of the modified spectra to a radical character. Polysaccharides such as hydroxyethyl starch or chitosan are usually used as carriers, because they are very well tolerated and can be modified easily. In this section, the hydrophilic radicals **D-TAM (Fig. 2.1)** and **PTMTC (Fig. 3.1)** were linked to CS and CMC. Loading was confirmed with UV-Vis spectroscopy and EPR spectroscopy. It is desirable to make such modified radicals of carrier materials to be used as pH and oxygen, as well as probes, for example, tumorous tissue capture.

#### 5.1.1. Structure of CS and CMC

CS is a cationic, linear copolymer consisting of repeating units of N-acetyl-2-amino-2-deoxy-d-glucopyranose and 2-amino-2-deoxy-d-glucopyranose that are linked by (1→4)-β-glycosidic linkages, **Fig. 5.1**<sup>281,282</sup>. 2-amino-2-deoxy-d-glucopyranose units are found to be randomly distributed and in different quantity throughout the polymer chain<sup>283</sup>.

The repeating glucosidic residue include two hydroxyl groups and one amino group, which enable further chemical modification of the structure such as acetylation, etherification, cross-linking, Schiff's base formation, or copolymerization<sup>284-288</sup>. These modification provide an improvement on the physico-chemical properties as well as biological activities of CS.

Three types of CMC (N-, O- or N,O-CMC) were prepared from CS under different reaction conditions and reagents, **Fig. 5.2**.

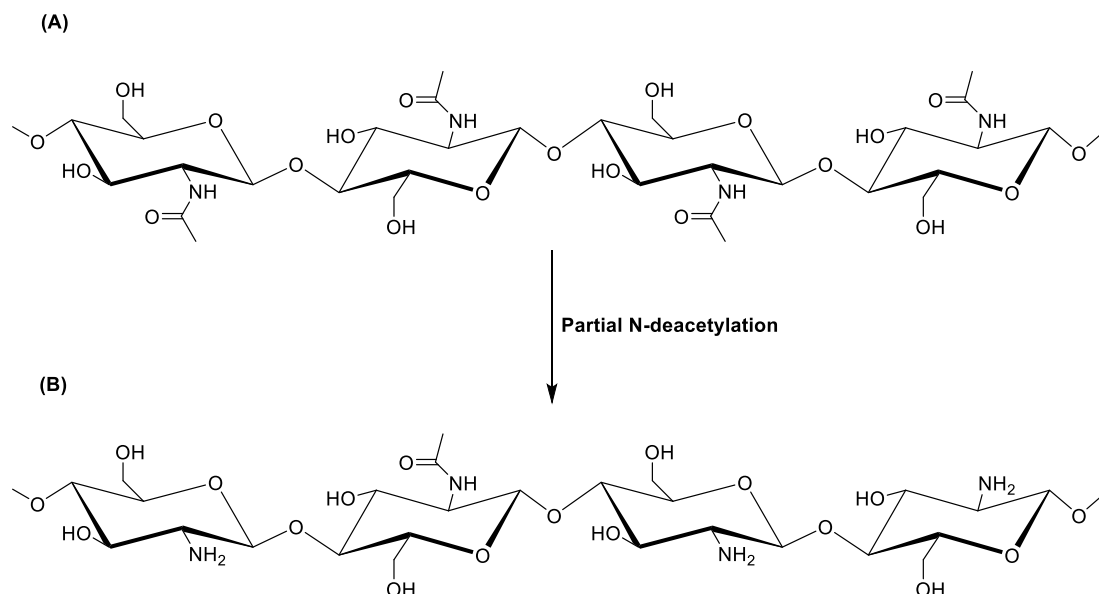


**Fig. 5.1** Structures of (A) chitin; (B) chitosan <sup>286</sup>.

Amino groups of CS are reacted with glyoxylic acid forming Schiff's base, which is hydrogenated with sodium cyanoborohydride ( $\text{NaBH}_3\text{CN}$ ) to give N-CMC <sup>289</sup>. Direct alkylation of CS with mono-chloroacetic acid in a mixture of aq. NaOH/*iso*-propanol at RT gave O-CMC. Increasing the temperature of the reaction ( $> 60\text{ }^\circ\text{C}$ ) resulted in carboxymethylation of some of the amino as well as primary hydroxyl groups with the formation of N,O-CMC <sup>280,290,291</sup>.

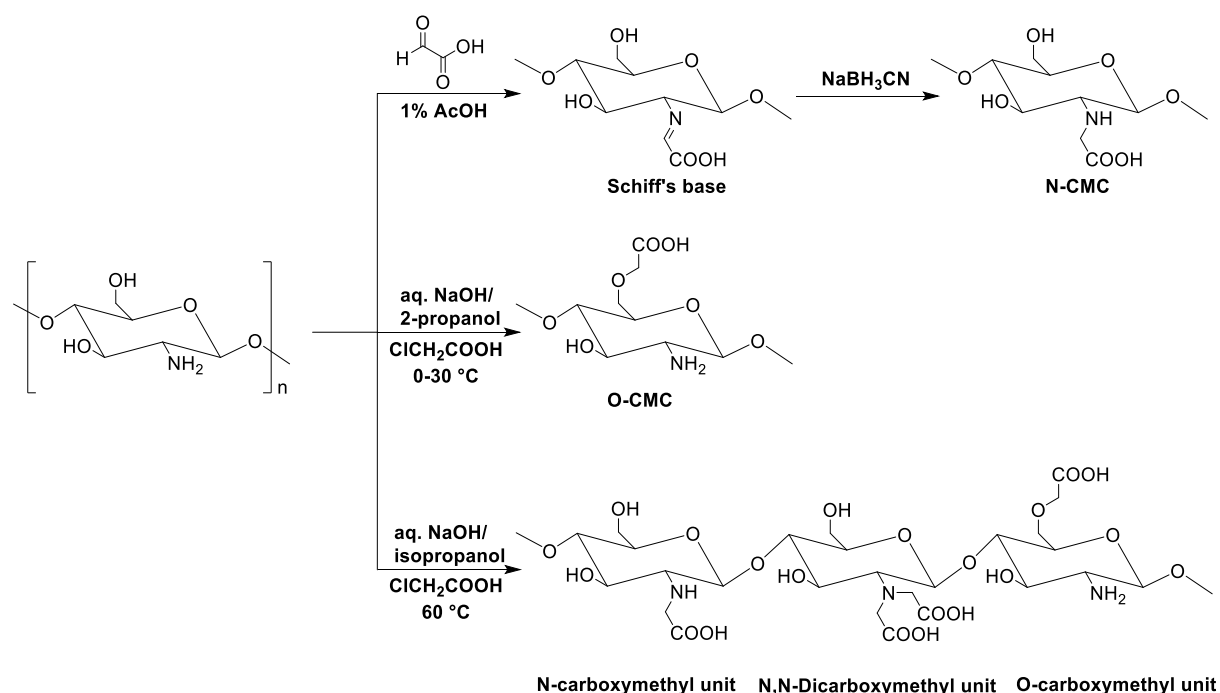


**Fig. 5.2** Carboxymethylation of chitosan <sup>286,290</sup>.

### 5.1.2. Properties of CS and CMC

CS is the product of partial N-deacetylation of chitin through alkaline hydrolysis (with NaOH, KOH or anhydrous hydrazine/hydrazine sulfate mixture<sup>292</sup>) or enzymatic hydrolysis in the presence of a chitin deacetylase<sup>285</sup>. CS has different molecular weights (50 kDa–2000 kDa), viscosity (1% CS in 1% acetic acid 200–2000 mPaS), and degree of deacetylation (DD), *i.e.* the ratio of 2-amino-2-deoxy-d-glucopyranose to N-acetyl-2-amino-2-deoxy-d-glucopyranose, (40%–98%)<sup>260,293</sup>. Molecular weight and DD are the main parameters that affect physical and chemical properties of the polymer such as solubility, viscosity, enzymatic hydrolysis and bioactivity<sup>276,294-297</sup>.

DD affects the pKa value of CS. Thus, solubility depends on DD as well as pH of the solvent. CSs with DD <40%, are soluble up to pH 9.0 while those with DD >85% are insoluble above pH 6.5<sup>260</sup>. The N-amino groups of CS have pKa value of 6.3, when dissolved in dilute acids (pH < pKa), the free amino groups (-NH<sub>2</sub>) become protonated (-NH<sub>3</sub><sup>+</sup>) making CS a water-soluble cationic polyelectrolyte<sup>298</sup>. In basic aqueous solution (pH > 7), the free amino groups lose their positive charge, and the polymer becomes insoluble<sup>256</sup>. CS is insoluble in most of the organic solvents because of the abundance of hydrophilic functional groups<sup>257</sup>. The addition of salts was found to interfere with the solubility. The higher the ionic strength is, the lower the solubility is, and salting-out effect may occur<sup>299</sup>.

The viscosity of CS solution increases with increasing CS concentration. DD was also found to affect the viscosity. At high DD, the polymer molecule is highly charged, and the polymer structure has extended conformation and flexible chain. In case of low DD, the molecule has a low charge and takes rod-like or coiled shape<sup>300</sup>.

CS is hydrolyzed by lysozymes that are non-specific proteolytic enzymes found in mammals<sup>301</sup>. DD affects the biodegradation of CS and it declines when DD > 70%<sup>294,302</sup>.

CMC is an amphoteric CS derivative bearing both anionic carboxymethyl group (-COOH) and cationic amino group (-NH<sub>2</sub>)<sup>303</sup>. Chen et al.<sup>304</sup> reported the effect of the reaction conditions of CS carboxymethylation on the water solubility of the formed CMC. CMCs prepared at temperatures of 0–10 °C were water-soluble whereas the CMCs prepared at 20–60 °C were water insoluble at near-neutral pH. The increase in the reaction temperature increases the degree of carboxymethylation. Accordingly, CMC solubility at lower pHs is decreased. Increasing the ratio of water/isopropanol in the reaction solvent decreased the degree of carboxymethylation and decreased the solubility at higher pHs.

## 5.2. Experimental

### 5.2.1. Materials and general methods for synthesis and analytical characterization

See section 9.1 and 9.2.

### 5.2.2. Characterization of CS and CMC conjugates

#### 5.2.2.1. UV-Vis spectroscopy

Tryl-CS conjugates were dissolved in a mixture of 1% acetic acid and methanol (100:85). Tryl-CMC conjugates were dissolved in PB (pH 7.4). The tryl contents in the polymer conjugates were assessed spectrophotometrically using a Spekol 1200 spectrometer (Analytik Jena GmbH, Jena, Germany).

Calibration curves of **PTMTC** and **D-TAM** were constructed (0.25 mg/100 mL–3.5 mL/100mL) in both media (PB and acetic acid/methanol). **PTMTC** samples were measured at 381 nm whereas **D-TAM** samples were measured at 468 nm (PB) and at 486 nm (acetic acid/methanol mixture). Blank media were used at reference. The absorbance of the polymers was subtracted from the conjugates absorbance at the measured wave length. The percentage of tryl was calculated on the basis of the tryl content of the final products.

#### 5.2.2.2. EPR measurements

EPR spectra were recorded by 9.3-9.55 GHz X-band spectrometer (Microscope MS200, Magnettech GmbH, Berlin, Germany). Instrumental settings are listed in **Table 5-1**.

**Table 5-1** The used parameters for the EPR measurements.

Parameter		Free acids	Conjugates
<b>Modulation</b>	mG	100	500
<b>MW attenuation</b>	dB	20	20
<b>Sweep time</b>	s	120	120
<b>Concentration</b>		20 $\mu$ M	1%

## 5.3. Results and discussion

### 5.3.1. Preparation of CS and CMC conjugates

**Fig. 5.3** shows activation of the carboxylic acid group with 1-(3-Dimethylaminopropyl)-3-ethylcarbodiimide hydrochloride (EDC) in the presence of *N*-Hydroxylsuccinimide (NHS) to form an active intermediate (succinimidyl ester), which is stable under aqueous conditions but

reactive towards primary amines <sup>305</sup>. The active intermediate was reacted with the primary amine of CS or CMC to form an amide bond. The mentioned procedure was applied for the activation of both **D-TAM** and **PTMTC** radicals.

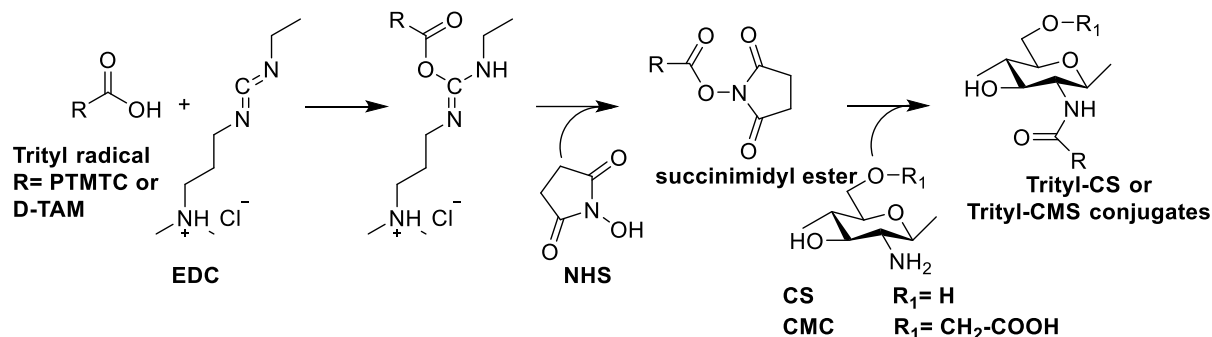


**Fig. 5.3** Activation of carboxylic acid group of **D-TAM** or **PTMTC** with EDC/NHS and coupling with CS or CMC.

The radical content in the polymer conjugates were determined via UV-Vis spectroscopy. In case of **PTMTC-CS** and **PTMTC-CMC** conjugates, lower percentage of **PTMTC** was observed. For this reason the more active acid chloride (radical **29**, **Fig. 3.1**) was used.

### 5.3.2. UV-Vis spectroscopy

The <sup>1</sup>HNMR did not show a difference between free polymer and polymer conjugates because of low percentage of radical in addition to the broad and strong proton signals of the CS and CMC residues. That's why, the percentage of loading of radicals was assessed by UV-Vis spectroscopy.

Calibration curves (0.25 mg/100mL - 3.5 mg/100 mL) of **D-TAM** and **PTMTC** were made in both mixture of 1% acetic acid and methanol (100:85) and PB (50 mM, pH 7.4). All solutions were measured directly after the preparation due to their light sensitivity. The effect of the light on the UV-spectrum of **PTMTC** radical is shown in **Fig. 5.4**. After 1 h exposure to light, the peak at 381 nm diminished with a formation of 2 extra peaks at 288 nm and 463 nm.

Changing the solvent did not affect the **PTMTC** UV-spectrum (**Fig. 5.5A** and **B**). On the other hand, **D-TAM** solutions showed a wave length shift from 468 nm in PB to 486 nm in the acetic acid/methanol mixture (**Fig. 5.5C** and **D**). In all cases, the absorbance of the pure polymer at these wave lengths was minimal (**Fig. 5.5**).

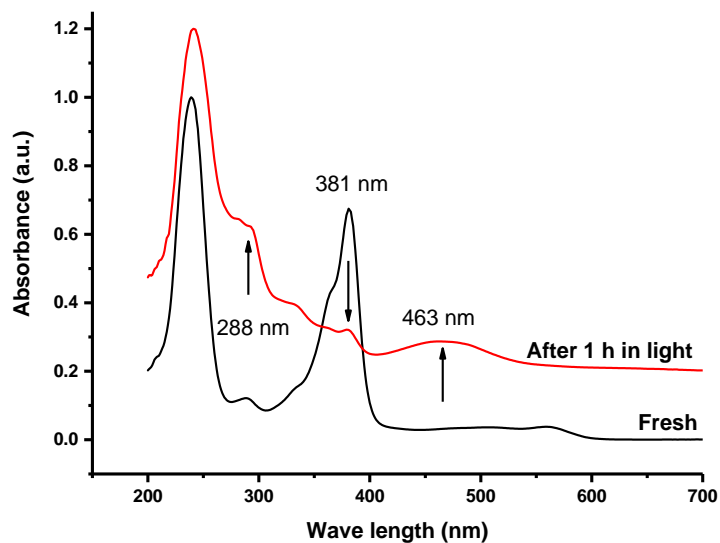


Fig. 5.4 Effect of light on the UV-spectrum of PTMTC radical.

In **D-TAM-CS** and **D-TAM-CMC** conjugates, the percentage of **D-TAM** ranged from 1 to 2%. On the other hand **PTMTC-CS** and **PTMTC-CMC** conjugates, the percentage of **PTMTC** was much lower (0.2%–0.5%). Therefore, the free acid **PTMTC** was converted to the acid chloride (radical **29**, Fig. 3.1) through reflux with  $\text{SOCl}_2$ .

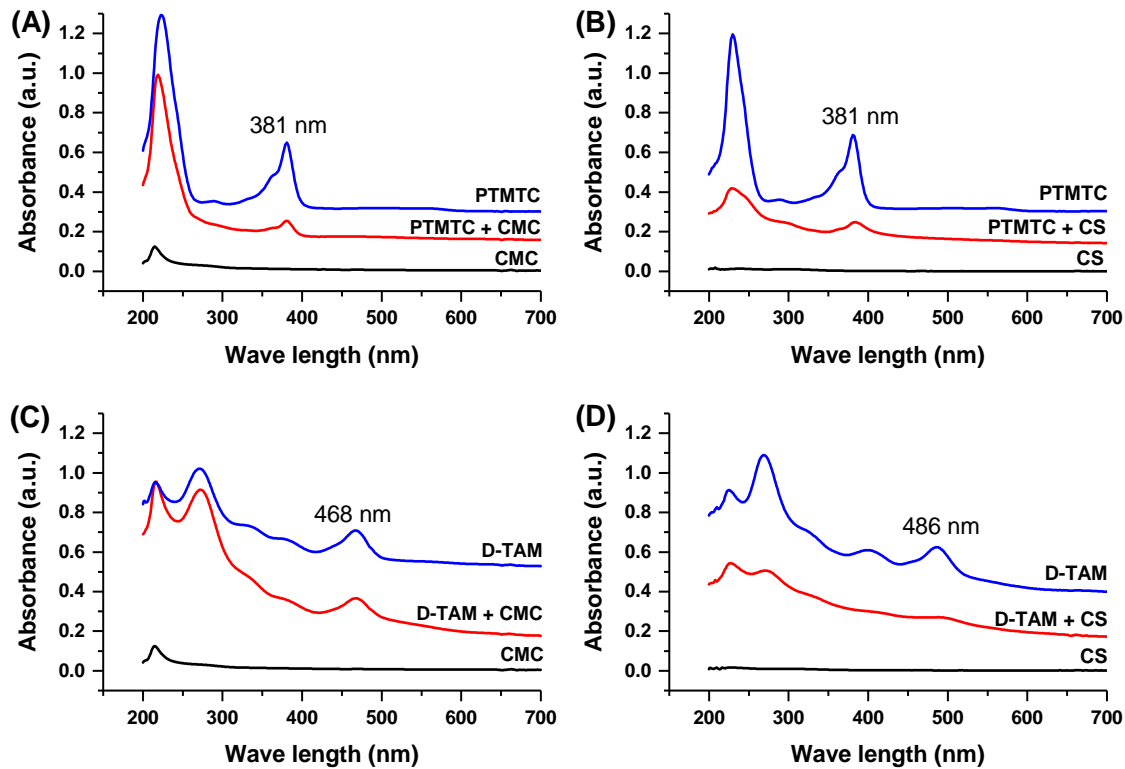


Fig. 5.5 UV-spectra of **PTMTC** and its CMC (A) and CS (B) conjugates as well as **D-TAM** and its CMC (C) and CS (D) conjugates. All spectra are compared to those of the pure polymers.

Radical **29** is dissolved in DMSO and a catalytic amount of TEA was added. After stirring at RT for 1 h, the mixture was added to CS or CMC solutions dropwise over 1 h (fast addition resulted in precipitation of the radical). Higher percentage of loading was observed (1.2%–2%). Higher percentage of loading for CMC was attempted. That was interesting to find that either **PTMTC-CMC** or **D-TAM-CMC** conjugates were found to be less soluble in PB (pH 7.4) compared to CMC when the radical content in the CMC conjugates is > 5%.

### 5.3.3. EPR spectroscopy

EPR spectroscopy revealed that the **PTMTC** radical has a single narrow signal with a  $\Delta B_{PP}$  of 0.047 mT (1 mM in PB pH 7.4). After conjugation with CS, line width is drastically increased to 0.460 mT. In contrast, **PTMTC-CMC** conjugate showed only a slight increase ( $\Delta B_{PP} = 0.077$  mT). The same result was observed with **D-TAM-polymer** conjugates. The broader line of the CS conjugate may be caused by high viscosity. The used CS with molecular weight of (200–400 kDa) has a viscosity of 449 mPaS (1% in 1% acetic acid, 20 °C) whereas CMC with molecular weight of 30,000-500,000 has a viscosity of 56 mPas (1% solution in water, 20°C). Viscosity impairs mobility of the radical. EPR line widths of free radicals and trityl-polymer conjugates are listed in **Table 5-2**.

**Table 5-2** EPR line widths of free radicals and trityl-polymer conjugates.

Radical	$\Delta B_{PP}$ (mT)	Solvent	Concentration
<b>PTMTC</b>	0.047	PB (pH 7.4)	1 mM
<b>PTMTC</b>	0.055	mixture of 1% acetic acid and methanol (100:85)	45 $\mu$ M
<b>PTMTC-CS</b>	0.460	mixture of 1% acetic acid and methanol (100:85)	1%
<b>PTMTC-CMC</b>	0.077	PB (pH 7.4)	1%
<b>D-TAM</b>	0.014	PB (pH 7.4)	50 $\mu$ M
<b>D-TAM</b>	0.03	mixture of 1% acetic acid and methanol (100:85)	20 $\mu$ M
<b>D-TAM-CS</b>	0.53	mixture of 1% acetic acid and methanol (100:85)	1%
<b>D-TAM-CMC</b>	0.044	PB (pH 7.4)	1%



The unexpected narrow line width of trityl-CMC conjugate suggested a question whether the trityl radical was covalently bonded to the polymer or it was just a physical mixture. To ensure the chemical reaction between the **PTMTC** and CMC, two experiments were performed with **PTMTC-CMC** conjugate:

- a. **PTMTC** as a free radical, is freely soluble in methanol. **PTMTC-CMC** conjugate was suspended in methanol and was shaken on the end over end apparatus for 2 h. Methanol solution was separated and an EPR spectroscopy was tested. No EPR signal was detected indicating that **PTMTC** is bonded to the polymer backbone.
- b. The second experiment depended on partition of lipophilic radical **29** between MCT and aqueous media. Five samples were prepared; **PTMTC** as free acid, radical **29**, **PTMTC** physically mixed with CMC, radical **29** physically mixed with CMC, and **PTMTC-CMC** conjugate. The five samples were suspended in a mixture of MCT/PB pH 7.4 (1:1, v/v) and were allowed to rotate at the end over end overnight. MCT and PB layers were separated through centrifugation and analysed with EPR spectroscopy. In case of **PTMTC**, **PTMTC** physically mixed with CMC and **PTMTC-CMC** conjugate, the signal was detected at the aqueous layer only. In case of radical **29**, signal was portioned between MCT and PB layers suggesting that the acid chloride radical (**29**) hydrolysed with time into the free acid **PTMTC**.

#### 5.4. Conclusion

The coupling of **D-TAM** and **PTMTC** radicals with CS and CMC, as biopolymers of pharmaceutical interest was achieved. EPR spectra showed that the radical is still active after coupling with the biopolymer. Line widths after coupling with CMC was still narrow.

The effects of a **D-TAM** and **PTMTC** on the growth of fibroblast cells and the phenotype of rat erythrocytes were investigated (see section 9.3) and further investigation will be done to determine the toxicity of the polymer conjugates.

#### 5.5. Syntheses

##### Preparation of the NHS-ester activated forms of the radicals

The trityl radical (50 mg of either **D-TAM** or **PTMTC**) was dissolved in 5 mL of DMSO. A 1:1 molar ratio of NHS and EDC were then added. The reaction mixture was stirred for 1 h in the dark. In case of radical **51**, 50 mg of the radical was dissolved in DMSO and a catalytic amount of TEA was added.

### **Preparation of the trityl-polymer conjugate**

CS (100 mg) was dissolved in 1% (v/v) aqueous acetic acid solution (100 mL) and diluted with 85 mL of MeOH. The radical containing DMSO solution was then added dropwise over 1 h (fast addition resulted in precipitation of the radical). The reaction mixture was stirred for 24 h protected from light, poured into 200 mL of MeOH /ammonia solution (7/3, v/v) with stirring. The precipitated material was filtered, washed thoroughly with distilled water, MeOH, and Et<sub>2</sub>O, and then dried under vacuum to give 90% of trityl-CS conjugate<sup>306</sup>.

CMC (100 mg) was dissolved in PB (100 mL, 50mM, pH 7.4). The radical containing DMSO solution was then added dropwise over 1 h. The reaction mixture was stirred for 24 h protected from light, the solution was dialysed in D45 mm dialysis bags (Closure 8000–120000) against PB (0.05 mol/L, pH 7.4) for 2 days followed by distilled water for another 2 days to remove the unreacted small molecules. The polymer was isolated by lyophilization.<sup>307</sup>.

## 6. Tetraoxatriarylmethyl radicals

### 6.1. Introduction

As described before, Gomberg prepared the first unsubstituted trityl radical <sup>14</sup>, **Fig. 1.5**. The Gomberg radical displayed a complex EPR spectrum (theoretically composed of 196 lines <sup>308</sup>) because of hyperfine interaction with the aromatic hydrogens, **Fig. 6.1A**. Ballester described the synthesis of tetrachloro-TAM radicals <sup>20</sup>, where the aromatic hydrogens are substituted with bulky chlorine atoms. Tetrachloro-TAM radicals have broad line widths because of chlorine atoms <sup>150</sup>, **Fig. 6.1B**. Nycomed Innovation AB reported the synthesis of tetrathia-TAM radicals <sup>22-25,95</sup>. The hyperfine splitting was eliminated through replacement of the aromatic hydrogens with alkylthio atoms. As a result, tetrathia-TAM radicals have single and extremely narrow EPR signal (**Fig. 6.1C**) that are favorable properties for various applications, *e.g.* EPR imaging (EPRI) <sup>56,97</sup>.

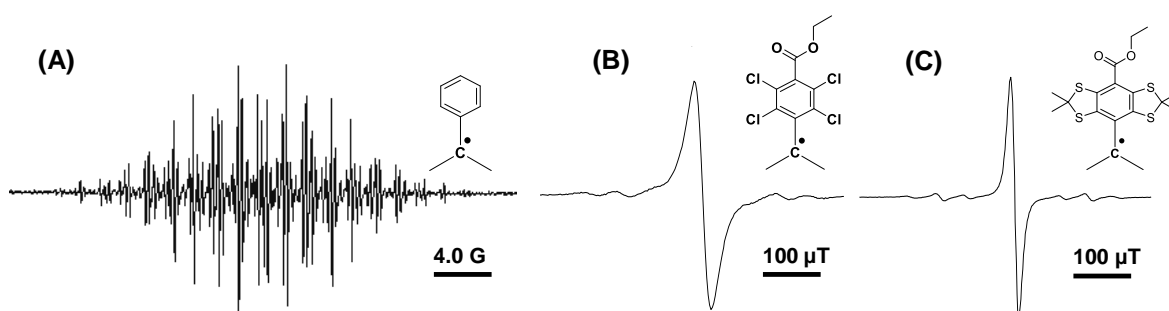


**Fig. 6.1** EPR spectra of trityl radicals. (A) Triarylmethyl (Gomberg radical), copied from <sup>308</sup>; (B) Triethyl ester of tetrachloro-TAM radicals (radical **24**, **Fig. 3.1**) shows broader line width; (C) Triethyl ester of tetrathia-TAM radicals (radical **7**, **Fig. 2.1**) shows narrower line width under ambient conditions.

Tetrathia-TAM radicals are difficult to prepare; the highest difficulty is the synthesis of the starting substance. The very odoriferous *tert*-butyl thiol is needed for the synthesis of the starting tetrakis(*tert*-butylthio)benzene (**Fig. 2.1**), which is difficult to handle in a normal lab environment. The tetraoxatriarylmethyl radicals (tetraoxa-TAM) are structurally related to tetrathia-TAM radicals, with oxygen instead of sulfur. The synthesis of different derivatives of tetraoxa-TAM (**Fig. 6.2A**) was reported in Nycomed Innovation AB patents <sup>24,95</sup>, however it was difficult to reproduce. In 2002, Reddy and co-authors did some improvement regarding the synthesis <sup>28</sup> and showed the EPR spectrum of tetraoxa-TAM substituted with methoxycarbonyl group at the *para* positions of the aromatic rings, **Fig. 6.2B**. Since then tetraoxa-TAM gained

no attention as EPR spin probes. It transpires from the patent, publication and personal information from Dr. Reddy that tetraoxa-TAMs may have stability issues.

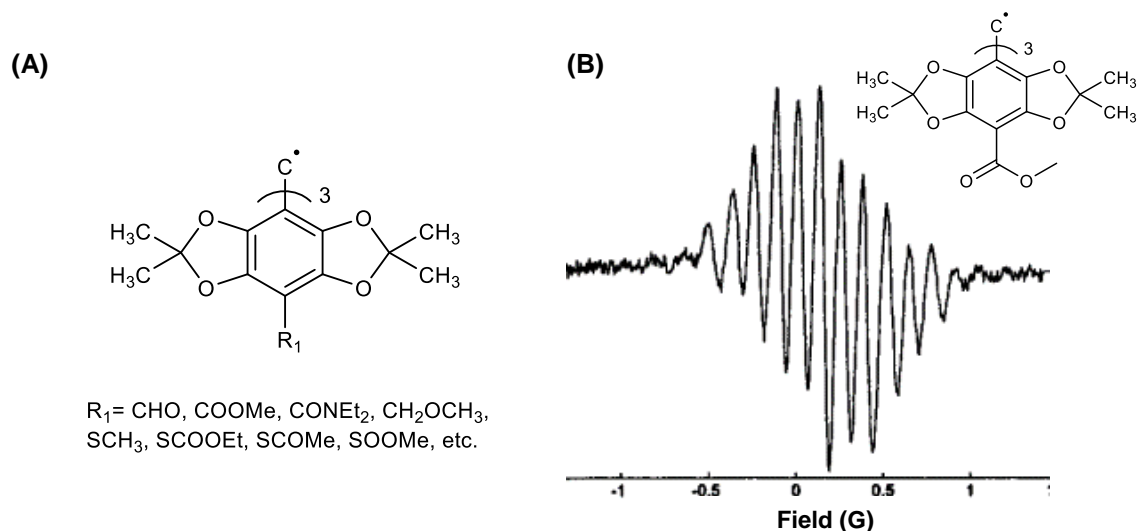


**Fig. 6.2** (A) Different derivatives of tetraoxa-TAM; (B) EPR spectrum of tetraoxa-TAM, when R<sub>1</sub> = COOMe, appears as 10 lines (because of hyperfine coupling with the 9 methoxy protons), with line widths = 44 mG<sup>28</sup>.

Because of the commercial availability of the starting material, 2,5-dihydroxy-1,4-benzquinone (compound **1**, **Fig. 6.3**) as well as the expected narrow line width, synthesis of tetraoxa-TAM derivatives seemed to be worth a trial.

## 6.2. Results and Discussion

The aim was to establish a protocol for the synthesis of tetraoxa-TAM that works reproducibly. Because the lipophilic ester derivatives of both tetrathia-TAM and tetrachloro-TAM radicals (sections **Tetrathiatriarylmethyl radicals** and **Tetrachlorotriarylmethyl radicals**) were very efficient oxygen sensitive spin probes, synthesis of tetraoxa-TAM ethyl ester radical was evaluated, **Fig. 6.3**.

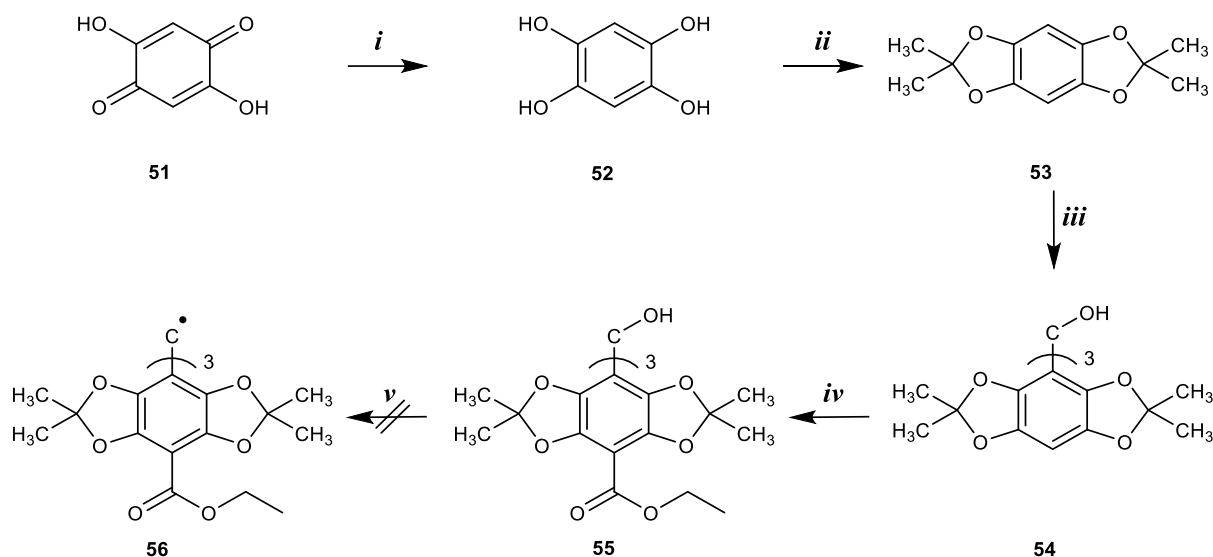


**Fig. 6.3** Synthesis of tetraoxatriarylmethyl ethyl ester radical. Reagents and conditions: **(i)**  $\text{Na}_2\text{S}_2\text{O}_4/37\% \text{HCl}$ ; **(ii)** PPTS/2-Methoxypropene **(iii)**  $n\text{-BuLi}$ , TMEDA and methyl chloroformate; **(iv)**  $n\text{-BuLi}$ , TMEDA and diethyl carbonate ; **(v)**  $\text{BF}_3 \cdot \text{Et}_2\text{O}/\text{SnCl}_2$ .

The first step in the sequence is the reduction of 2,5-dihydroxy-1,4-benzoquinone (**51**) into 1,2,4,5-tetrahydroxybenzene (**52**). Different reducing mixtures such as: Pd catalytic hydrogenation in EtOH under argon<sup>24,28,95</sup>, sodium dithionite ( $\text{Na}_2\text{S}_2\text{O}_4$ ) in conc. HCl<sup>24</sup>, Iron (Fe) in conc. HCl<sup>24</sup> and tin granulate in conc. HCl at 110 °C<sup>309-311</sup>, were used. Reflux of **1** with tin granulate in 37% HCl for 1 h gave 12% yield, and increasing reflux time did not improve the yield. Compound **52** was synthesized in an acceptable yield (50%) on using  $\text{Na}_2\text{S}_2\text{O}_4/37\% \text{HCl}$ , and increasing the reaction time (2 h) enhanced the yield (62%). It was interesting to notice that the white color of **52** became dark grey when left under normal atmosphere, probably it was oxidized to the starting quinone or even polymerized. Compound **52** showed no change in color when kept under argon (the flask was evacuated and flushed with argon three times) till going to the next step.

Compound **52** was further converted into the cyclized arene (**53**). A mixture of acetone/ $\text{P}_2\text{O}_5$  was used to give **53** in 48% yield<sup>16,17</sup>. Recent publications reported the use of 2-methoxypropene and catalytic amount of pyridinium *p*-toluenesulfonate (PPTS) in order to improve the yield<sup>28,309,312</sup>. **Fig. 6.4** shows the suggested mechanism.

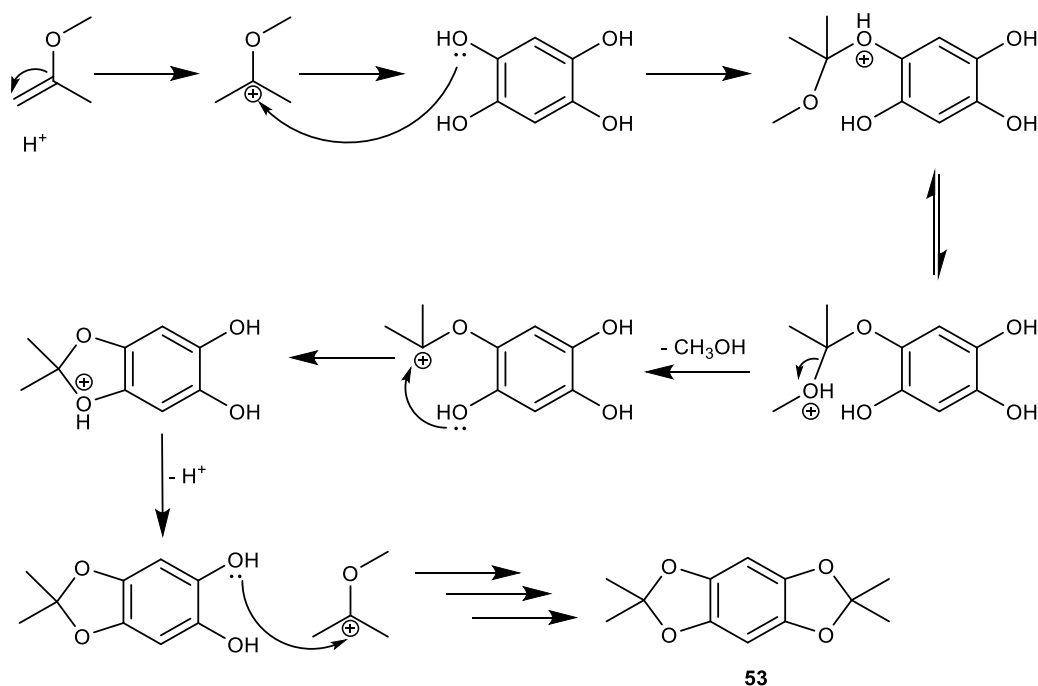


**Fig. 6.4** Suggested mechanism for the synthesis of cyclized arene (**53**) with 2-methoxypropene and PPTS as catalyst.

Slight modification of the molar amounts of the reactants was found to increase the yield to 74%, **Table 6-1**.

**Table 6-1** Modifications on the molar amounts of the reactants to improve the yield of **53**.

Molar ratio of reactants		Yield
51 : 2-methoxypropene (1 <sup>st</sup> portion) : PPTS : 2-methoxypropene (2 <sup>nd</sup> portion)		
1 : 3 : 0.07 : 2.4		56%
1 : 4.4 : 0.11 : 3		74%

Reaction of **53** with *n*-BuLi gave the corresponding trianion, which was converted into the triarylmethanol (**54**), **Fig. 6.5**. Variation of the reaction conditions - based on the patent procedures, other recently published articles<sup>31</sup> in addition to trials to improve the synthesis of TAM radicals - was performed in order to optimize the yield of **54**. **Table 6-2G** are the experimental conditions that gave the highest yield (54%).

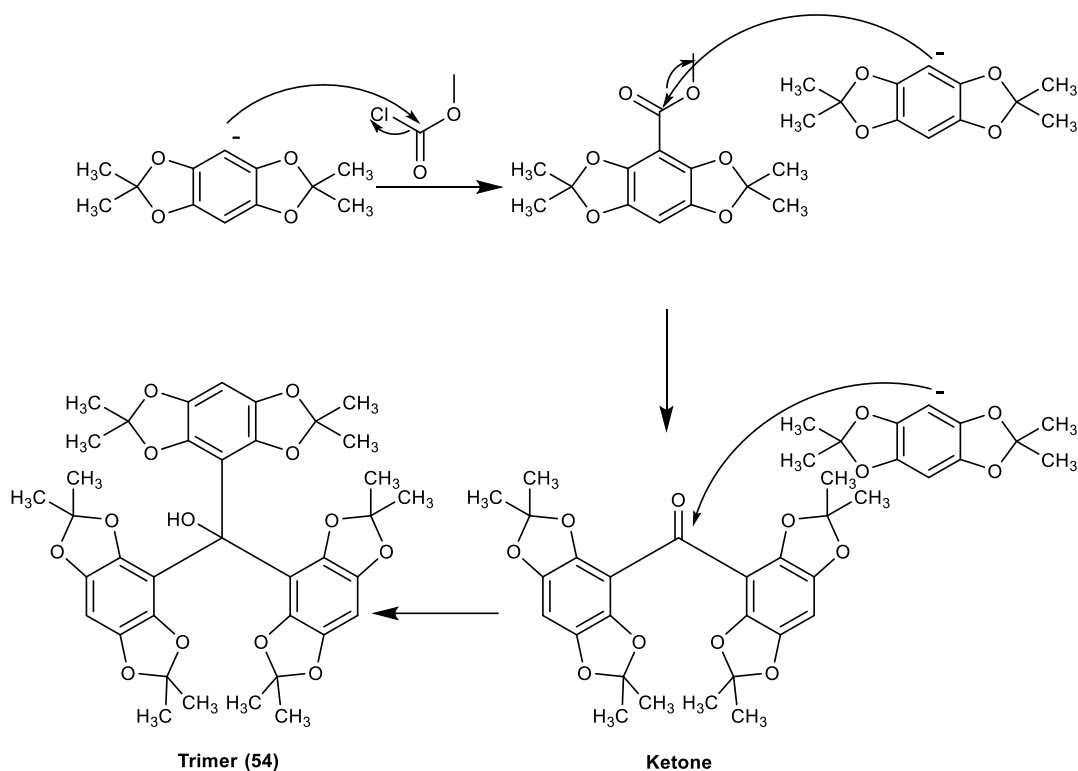


**Fig. 6.5** Synthesis of triarylmethanol (**54**).

**Table 6-2** Optimization of the reaction conditions to enhance the yield of **54**.

	Reagent	Solvent	Temp. (°C)	Time (h)	Yield of <b>54</b>
<b>A</b>	Diethyl carbonate	Toluene	-4	17	8%
<b>B</b>	Methyl chloroformate	Toluene	-4	17	23%
<b>C</b>	Diethyl carbonate	Et <sub>2</sub> O	-4	17	21%
<b>D</b>	Methyl chloroformate	Et <sub>2</sub> O	Room temp.	48	36%
<b>E</b>	Diethyl carbonate	THF	-20	17	13%
<b>F</b>	Methyl chloroformate	Toluene	-4	48	25%
<b>G</b>	Dimethyl carbonate	Toluene	-4	17	54%

Reaction of **54** with ten equivalents of *n*-BuLi and TMEDA at low temperature gave the corresponding trianion that is converted to the trisubstituted ester (**55**) with excess of the reagent (diethyl carbonate or ethyl chloroformate). It can be deduced from **Table 6-3** that the reactivity of tetraoxatriarylmethanol (**54**) is much lower than the sulfur analogue (section 2.3.1). much excess (100 equivalents) of diethyl carbonate were used to afford **55** in 13% yield.

**Table 6-3** Optimization of the reaction conditions to enhance the yield of the trisubstituted ethoxycarbonyl derivative (**55**).

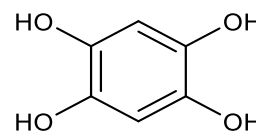
	Reagent	Solvent	Temp. (°C)	Time (h)	Yield %		
					Mono-subst.	Di-subst.	Trisubst. ( <b>55</b> )
<b>A</b>	Diethyl carbonate (10 eq.)	THF	-20	17	17%	2%	-
<b>B</b>	Diethyl carbonate (50 eq.)	THF	-20	17	26%	15%	-
<b>C</b>	Diethyl carbonate (100 eq.)	THF	-20	48	13%	35%	10%
<b>D</b>	Diethyl carbonate (100 eq.)	Hexane, toluene	-10	48	10%	22%	13%
<b>E</b>	Ethyl chloroformate (100 eq.)	THF	-20	17	18%	32%	8%

The conversion of **55** by  $\text{BF}_3 \cdot \text{Et}_2\text{O}$  into the carbocation followed by reduction with  $\text{SnCl}_2$  was expected to provide the lipophilic radical (**56**), as it was previously reported<sup>28</sup> for the trimethyl ester radical, **Fig. 6.2B**. Compound **55** was dissolved in DCM. On adding  $\text{BF}_3 \cdot \text{Et}_2\text{O}$  the solution color turned to brownish-green suggesting the carbocation formation. After addition of  $\text{SnCl}_2/\text{THF}$  the reaction mixture became dark brown. Running an EPR experiment to detect the radical, showed no EPR signal.

### 6.3. Syntheses

#### 1,2,4,5-Tetrahydroxybenzene (**52**).

2,5-Dihydroxy-1,4-benzquinone (**51**) (4 g, 28.55 mmol) was suspended in a mixture of distilled water (50 mL),  $\text{Na}_2\text{S}_2\text{O}_4$  (10 g, 57.47 mmol) and HCl 37% (6 mL, 55.75 mmol). The reaction mixture was stirred for 2 h and then evaporate to dryness. The residue was extracted five times with THF (20 mL). The combined organic layers were concentrated in vacuum. The pure product was crystallized off, separated by filtration, washed with cold THF and dried.



**Yield:** 2.5 g (62%)

**Colour:** White solid

**Molecular formula:**  $\text{C}_6\text{H}_6\text{O}_4$

**Molar mass:** 142.03 g/mol

**Mp:** 200–210 °C

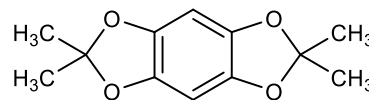


**$^1\text{H}$  NMR:** (400 MHz, d-DMSO)  $\delta$  7.90 (brs, 4H), 6.20 (s, 2H)

**$^{13}\text{C}$  NMR:** (100 MHz, d-DMSO)  $\delta$  137.45, 105.14

**2,2,6,6-Tetramethylbenzo[1,2-*d*:4,5-*d'*]bis[1,3]dioxole (53).**

A solution of **52** (2 g, 14.1 mmol) in toluene (60 mL) was introduced to a round-bottom flask fitted with Dean-Stark apparatus. PPTS (0.4 g, 1.6 mmol) and 2-methoxypropene (6 mL, 62.326 mmol) were added. The mixture was heated to reflux for 3 h. A second portion of 2-methoxypropene (4 mL, 42.22 mmol) was added and heating continued for 12 h. After cooling, the reaction mixture was washed with aqueous NaOH (6 M) and brine, dried over  $\text{Na}_2\text{SO}_4$ , and concentrated in vacuum. The brown oily mixture was treated with petroleum ether (PE) (40–60 °C), white crystals were separated, collect the first crop of the product (1.47 g, 47 %) through suction. The filtrate was collected, and further purified on silica gel eluting with (PE/EA, 100/1).



**Yield:** 0.85 g (27%)

**Colour:** White solid

**Molecular formula:**  $\text{C}_{12}\text{H}_{14}\text{O}_4$

**Molar mass:** 222.09 g/mol

**Mp:** 120–122 °C

**R<sub>f</sub>:** 0.3 (PE/EA, 100/1)

**$^1\text{H}$  NMR:** (400 MHz,  $\text{CDCl}_3$ )  $\delta$  6.31 (s, 2H), 1.63 (s, 12H)

**$^{13}\text{C}$  NMR:** (100 MHz,  $\text{CDCl}_3$ )  $\delta$  140.39, 117.76, 92.72, 25.52

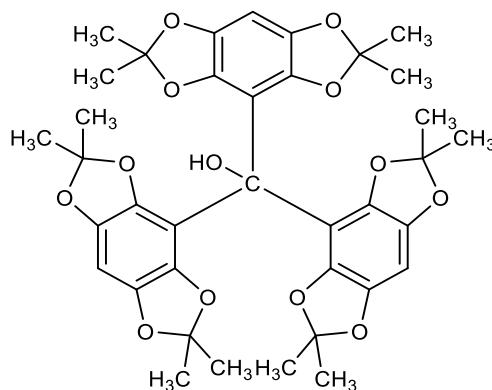
**IR (KBr):** 2987, 1488, 1376, 1327, 1245, 1218, 1153, 1140, 977, 872, 830, 775  $\text{cm}^{-1}$

**MS (ESI):**  $m/z$  222.10  $[\text{M}]^+$

**HRMS (ESI):** calcd. for  $\text{C}_{12}\text{H}_{14}\text{O}_4$   $[\text{M}]^+$  222.089; found 222.089

**Tris(2,2,6,6-tetramethylbenzo[1,2-*d*:4,5-*d'*]bis[1,3]dioxole)-4-yl)methanol (54).**

Compound **53** (3 g, 13.5 mmol) and TMEDA (2 mL, 13.2 mmol) were dissolved in toluene (100 mL) under argon atmosphere and cooled to 0 °C. A solution of 2.5 M *n*-BuLi in *n*-hexane (5.4 mL, 13.5 mmol) was added dropwise, and the reaction mixture was stirred at this temperature for 30 min. Afterwards, the cooling bath was removed, and the mixture was stirred at RT for 2 h. The lithium salt was precipitated, and the



resulting suspension was cooled to 0 °C. Dimethyl carbonate (0.38 mL, 4.5 mmol) was added dropwise, and the reaction mixture was allowed to reach RT overnight. The reaction mixture was poured into saturated aqueous NaHCO<sub>3</sub>; the organic layer was separated and the aqueous layer was extracted three times with DCM. The combined organic layers were washed with brine and dried over MgSO<sub>4</sub>. Solvent was evaporated under vacuum and residue was purified with silica gel eluting with (PE/EA, 9/1). 1.4 g of the starting (**53**) was recovered.

**Yield:** 1.7 g (54%)

**Colour:** Yellow solid

**Molecular formula:** C<sub>37</sub>H<sub>40</sub>O<sub>13</sub>

**Molar mass:** 692.25 g/mol

**Mp:** 220–230 °C (turned black)

**R<sub>f</sub>:** 0.5 (PE/EA, 9/1)

**<sup>1</sup>H NMR:** (400 MHz, d-DMSO) δ 6.44 (s, 3H), 4.25 (s, 1H), 1.41 (s, 36H)

**<sup>13</sup>C NMR:** (100 MHz, d-DMSO) δ 140.1, 139.0, 116.8, 112.6, 91.6, 25.4

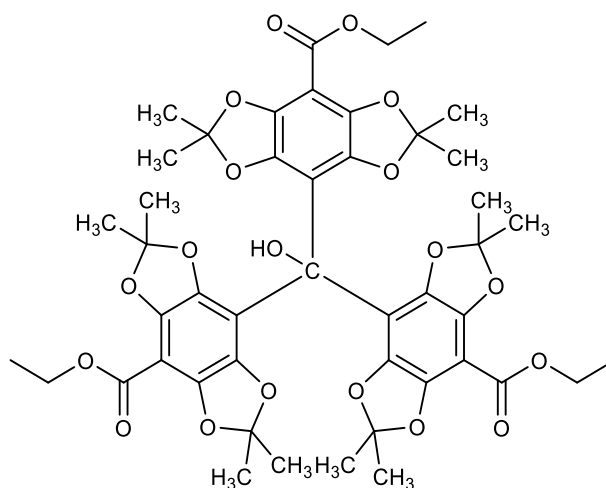
**IR (KBr):** 3565, 2993, 2939, 1446, 1375, 1314, 1151, 988, 915, 835, 802, 774 cm<sup>-1</sup>

**MS (ESI):** *m/z* 715.02 [M+Na]<sup>+</sup>

**HRMS (ESI):** calcd. for C<sub>37</sub>H<sub>40</sub>O<sub>13</sub> [M]<sup>+</sup> 692.246; found 692.248

### Tris(8-ethoxycarbonyl-2,2,6,6-tetramethylbenzo[1,2-*d*:4,5-*d'*]bis([1,3]dioxole)-4-yl)methanol (**55**).

Compound **54** (574 mg, 0.83 mmol) and TMEDA (1.25 mL, 8.3 mmol) were mixed in dry *n*-hexane (5 mL) under argon atmosphere and cooled to 0 °C. A solution of 2.5 M *n*-BuLi in *n*-hexane (3.3 mL, 83 mmol) was added dropwise over 30 min and the mixture was stirred at RT for 3.5 h. Anhydrous toluene (10 mL) was added and the reaction mixture was allowed to stir for an additional



1 h, afterwards it was added portion wise via syringe to a cold (−25 °C, cooling bath temperature) diethyl carbonate (10 mL, 82.9 mmol) diluted with toluene (5 mL). The reaction mixture was allowed to reach RT and stirred overnight. Saturated aqueous solution of NaH<sub>2</sub>PO<sub>4</sub> (10 mL) was added, the organic layer was separated and the aqueous layer was extracted three times with Et<sub>2</sub>O (10 mL). The combined organic layer was washed with water, dried over

MgSO<sub>4</sub>, and the filtrate was passed through short silica plug. The residue was purified with silica gel eluting with (PE/EA, 7/3).

**Yield:** 98 mg (13%)

**Colour:** Yellow solid

**Molecular formula:** C<sub>46</sub>H<sub>52</sub>O<sub>19</sub>

**Molar mass:** 908.31 g/mol

**Mp:** 258–265 °C (turned black)

**Rf:** 0.2 (PE/EA, 7/3)

**<sup>1</sup>H NMR:** (400 MHz, d-DMSO) δ 4.78 (s, 1H), 4.21 (q, *J* = 7.0 Hz, 6H), 1.41 (s, 36H), 1.22 (t, *J* = 7.0 Hz, 9H)

**<sup>13</sup>C NMR:** (100 MHz, d-DMSO) δ 162.6, 140.03, 139.3, 118.3, 115.6, 99.4, 60.8, 25.7, 14.6.

**MS (ESI):** *m/z* 930.98 [M+Na]<sup>+</sup>

**HRMS (ESI):** calcd. for C<sub>46</sub>H<sub>52</sub>O<sub>19</sub> [M]<sup>+</sup> 908.310; found 908.311

## 7. Summary and Outlook

The quantification of oxygen levels *in-vitro* and *in-vivo* is crucial for understanding of many physiological and pathological processes. EPR oximetry is one of various techniques for oxygen measurement with high selectivity, sensitivity, and non-invasiveness. In addition, pH status was found to play a critical role in the physiology of the living organism<sup>119</sup>. Deviations from normal tissue pH are associated with a number of pathological conditions such as neurodegenerative disease<sup>120</sup>, myocardial ischemia<sup>39</sup>, or cancer<sup>121</sup>.

Triarylmethyl (TAM or trityl) radicals are carbon-centered radicals that are used as paramagnetic spin probes. The synthesis of trityl radicals is known to be difficult. The preparation of tetrathia- and tetrachloro-TAM radicals was evaluated. An overview of the successfully synthesized compounds is shown in **Table 7-1**.

The synthesis of tetrathia-TAM radicals is known to be very difficult. From one hand; the preparation of molar amounts of tetrakis(*tert*-butylthio)benzene (compound **1**, **Fig. 2.1**) requires the use of the very odoriferous *tert*-butyl thiol that is added to city gas to detect leakages. From another hand, the subsequent steps including trimerization and introduction of different substituents at the *para* positions are very sensitive to residual moisture in the solvent, temperature and reaction time. In this work, reproducible protocols for the synthesis of different derivatives of tetrathia-TAM radicals were presented. The EPR properties of the synthesized hydrophilic radicals (**C-TAM** and **D-TAM**) were investigated in aqueous media. It was shown that within physiological limits of osmolarity, viscosity, and pH value, there was, for practical purposes, no impact on the EPR line widths of the hydrophilic radicals. The EPR properties of lipophilic radicals (**7**, **8**, **11** and **13**) were explored in oily solutions (MCT and IPM). The non-deuterated lipophilic triethyl esters of **C-TAM** or **D-TAM** (radicals **7** and **11**) showed hyperfine splitting in deoxygenated solutions. Radicals **8** and **13** exhibited single EPR lines with line widths directly proportional to the oxygen concentration. Radical **13** showed a very narrow EPR line under anoxic conditions and high oxygen sensitivity ( $\sim 0.5 \mu\text{T/mmHg}$ ) in addition to better synthetic accessibility than radical **8**. Therefore, solutions of radical **13** in MCT and IPM were encapsulated into NCs. The formed NCs were able to retain the oxygen responsiveness and protect the incorporated radical from reducing agents such as ascorbic acid.

Generally, tetrachloro-TAM radicals have broader line widths compared to tetrathia-TAM radicals because of chlorine splitting, but are distinguished by better synthetic accessibility. Various derivatives of trisubstituted tetrachloro-TAM radicals (radicals **23–29**) were synthesized. The prepared radicals were investigated with EPR spectroscopy. Neither

increasing the number of alkoxy protons, *i.e.* 3 protons in case of **23** or 5 protons in case of **24**, nor increasing their relative distance from the ester (**25**) caused significant effects on line width of the triesters of the tetrachloro-TAM radicals (**23–25**). Radical **26** showed a quartet signal (internal ratio 1:3:3:1) with line widths of approx. 0.044 mT (1 mM solution in DMSO under aerated conditions) and 0.026 mT under anoxic conditions. The trinitro methane (**21**) was reduced to the triamino methane derivative (**22**). The corresponding radical (**30**) is unstable in aerobic environment and it decomposed during purification to the carbocation.

Tetrathia-TAM radicals were used as spin labels for distance measurements<sup>52-54,220</sup>. The tricarboxylic acid radical **PTMTC** was used to synthesize a spin labelled nucleoside. However, the three free carboxyl groups resulted in a series of side products that made the purification difficult. The trimethyl ester (**16**) was used to prepare a tetrachloro-TAM structure with terminal alkyne group (**39**). Conversion to the corresponding radical (**40**) was successfully achieved. Sonogashira coupling between **40** and nucleoside **41** resulted in the formation of cross-coupling product (**42**) and the homocoupling product (**43**). Interestingly, radical **43** was stable and could be separated in a pure form but radical **42** was unstable under atmospheric conditions and could not be separated in a radical form. Sonogashira coupling between one of triester derivatives of tetrathia-TAM radicals (for example radical **7** or **11**) with radical **40** might provide a stable nucleoside that is suitable for distance measurement.

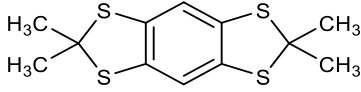
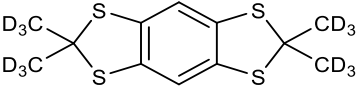
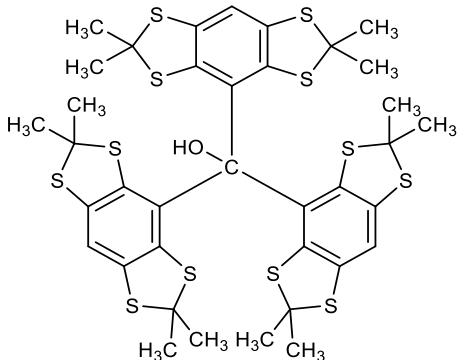
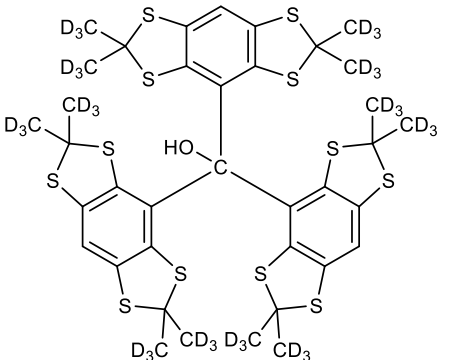
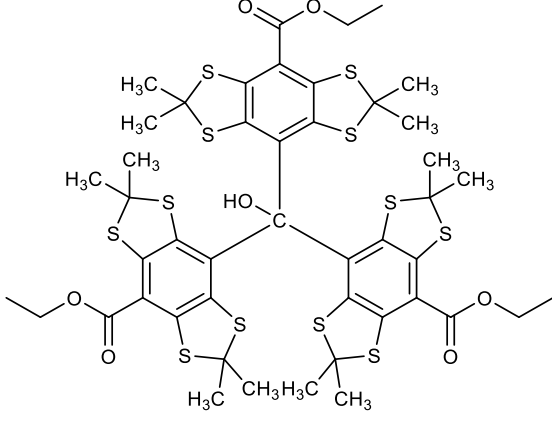
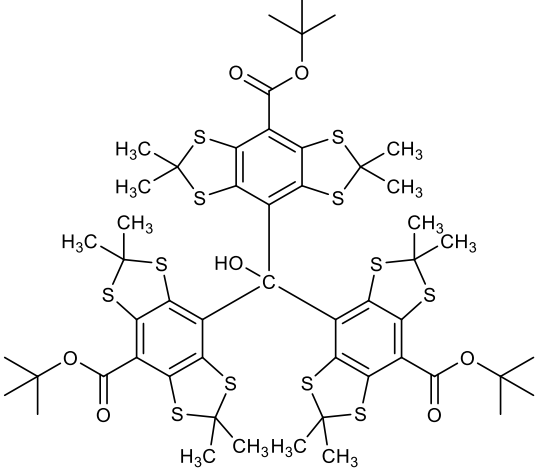
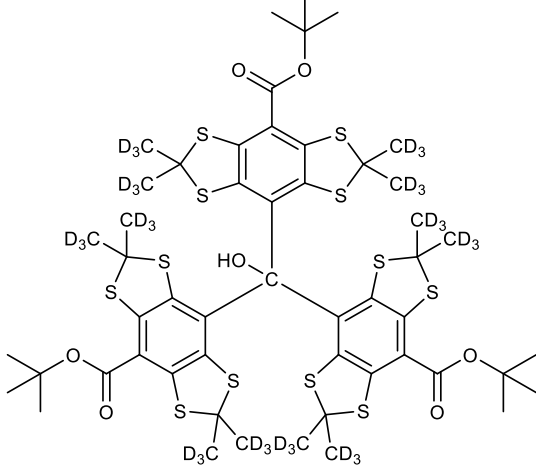
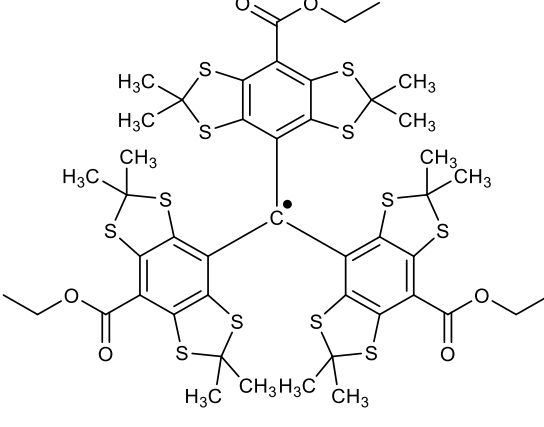
Synthesis of **PTMTC** is reported before, **Fig. 1.33**<sup>179</sup>. However, this sequence is not reproducible and separation of intermediate (4-dichloromethyl perchlorotriarylmethane) is problematic<sup>199</sup>. Synthesis of **PTMTC**, through hydrolysis of the triethyl ester (radical **24**, **Fig. 3.1**) gave reproducibly with high yield the tricarboxylic acid **PTMTC**. The hydrophilic radical **PTMTC** showed very good aqueous solubility (up to 10 mM in PB, pH 7.4) without spin-spin line broadening and promising EPR properties of single narrow line width. The isotopic analogue <sup>13</sup>C-**PTMTC** with 50% <sup>13</sup>C labelling at the methyl radical center was prepared. EPR spectrum showed three lines. The central line is related to the <sup>12</sup>C containing radical. <sup>13</sup>C (nuclear spin = 1/2) split the spectra into doublet peak (high field and low field peaks). The influences of different parameters *e.g.* pH value, viscosity and oxygen content on the EPR spectra were discussed. The <sup>12</sup>C EPR signal line width showed a linear relationship with increasing the oxygen content. Change in viscosity, within the physiological limits, showed no impact on the <sup>12</sup>C EPR signal in contrary to the <sup>13</sup>C doublets. The <sup>13</sup>C doublet peak line widths were dominated by viscosity. This observed differential effects of oxygen content

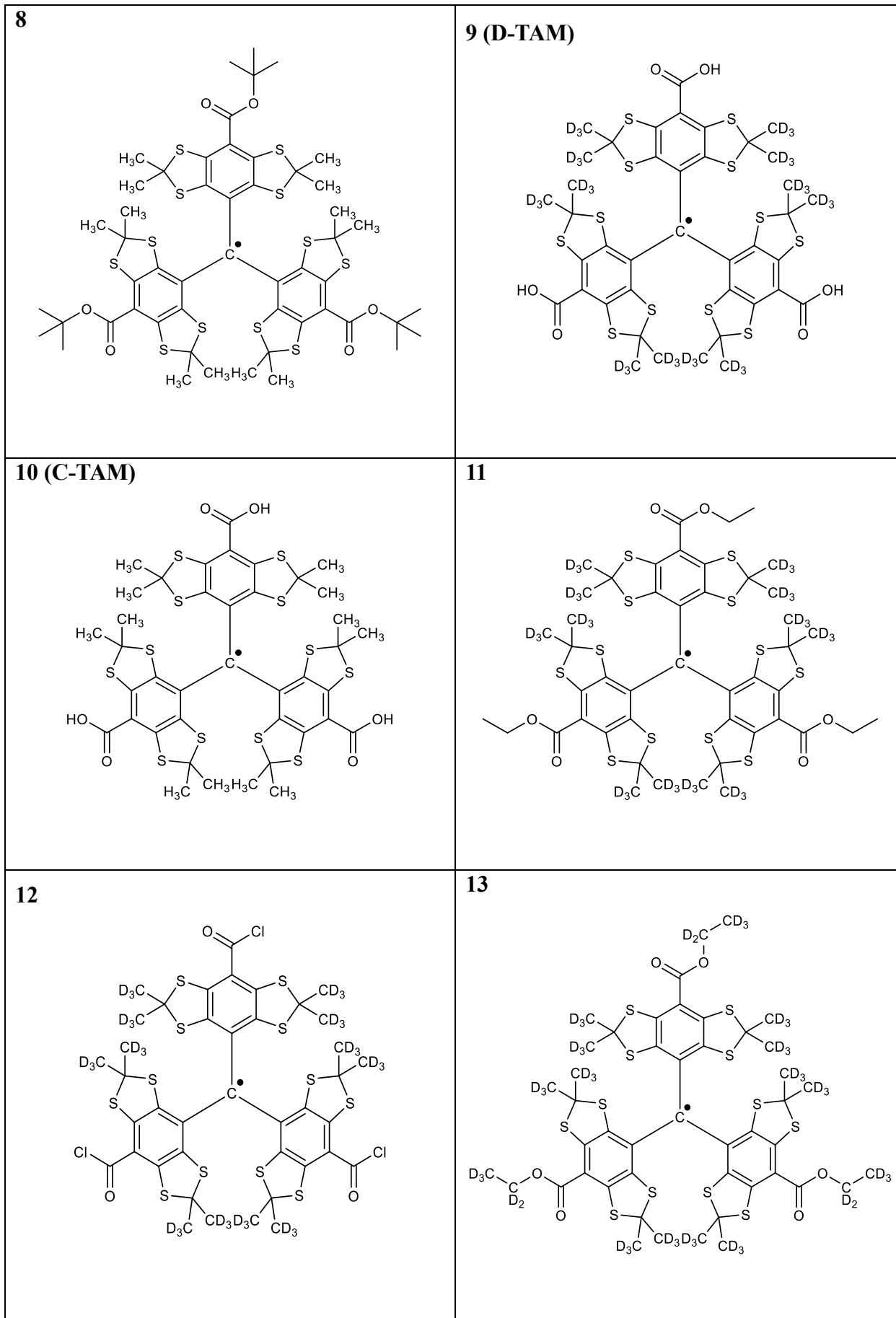
and viscosity on the line widths of the  $^{12}\text{C}$  and the  $^{13}\text{C}$  EPR signals suggest that this mixture of isotopic radicals could gain importance as a probe for both parameters.

Radicals are generally toxic. Linking to polymer scaffold might optimize the properties for the non-invasive monitoring of oxygen and pH gradients by EPRI. The hydrophilic radicals **D-TAM** and **PTMTC** were attached covalently to chitosan and carboxymethyl chitosan as biopolymers of pharmaceutical interest. Further investigation will be done to determine the toxicity of the polymer conjugates.

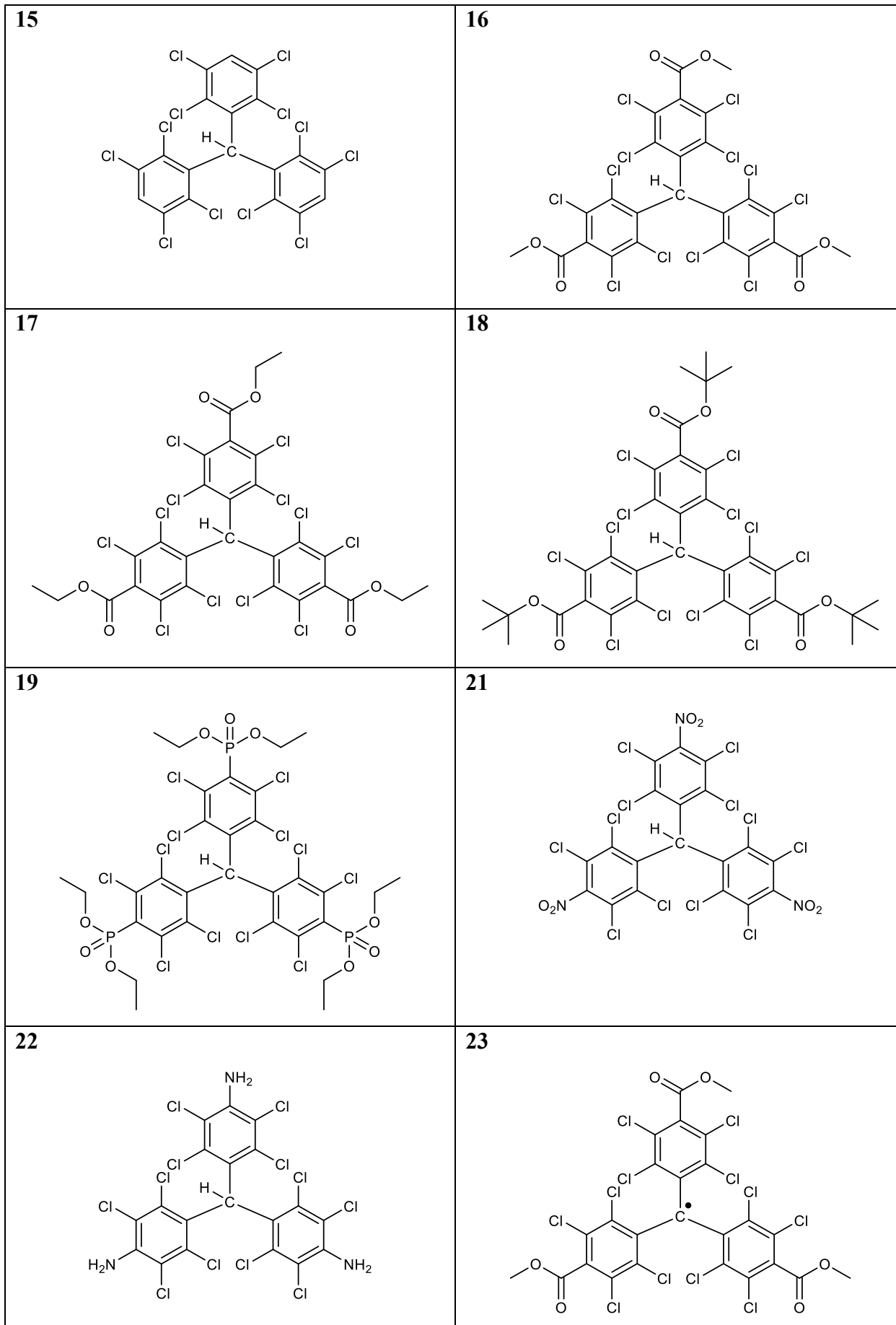
The tetraoxatriarylmethyl radicals (tetraoxa-TAM) are structurally related to tetrathia-TAM radicals, with oxygen instead of sulfur. The synthesis of different derivatives of tetraoxa-TAM (**Fig. 6.2A**) was reported before <sup>24,28,95</sup>. The commercial availability of the starting 2,5-dihydroxy-1,4-benzquinone (compound **1**, **Fig. 6.3**) as well as the expected narrow line width, make tetraoxa-TAM attractive spin probes. Synthesis of tetraoxa-TAM radicals was attempted. Synthesis of starting structures (compounds to **52**, **53** and **54**) was optimized regarding to reaction conditions and yields. Synthesis of triethyl ester (**55**) was achieved successfully. Conversion into the corresponding radical using the commonly used mixture  $\text{BF}_3 \cdot \text{Et}_2\text{O}$  and  $\text{SnCl}_2$  was not successful. After addition of  $\text{BF}_3 \cdot \text{Et}_2\text{O}$ , solution colour changed from yellow to brownish-green suggesting the carbocation formation. A more powerful reducing agent may be needed to achieve radical release.

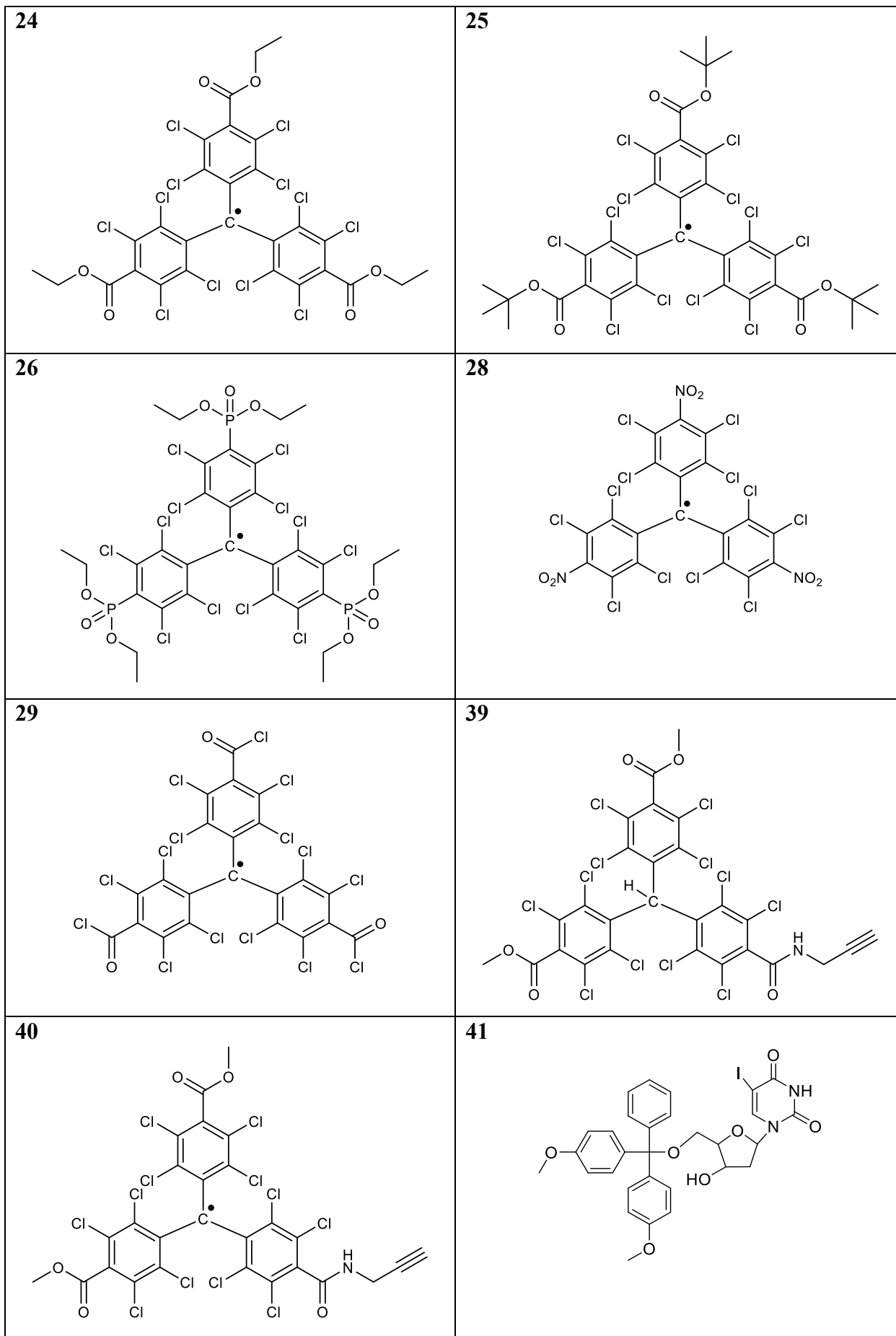
**Table 7-1** Overview of the successfully synthesized compounds.

<p><b>2a</b></p> 	<p><b>2b</b></p> 
<p><b>3a</b></p> 	<p><b>3b</b></p> 
<p><b>4</b></p> 	<p><b>5</b></p> 
<p><b>6</b></p> 	<p><b>7</b></p> 

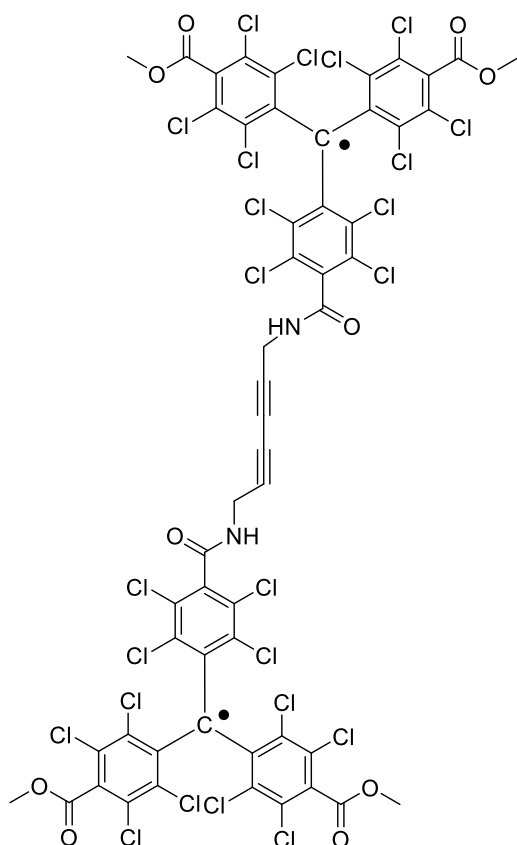




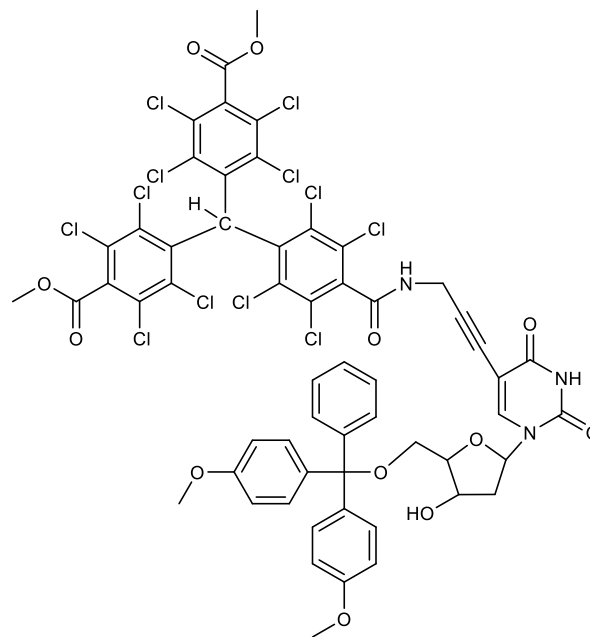




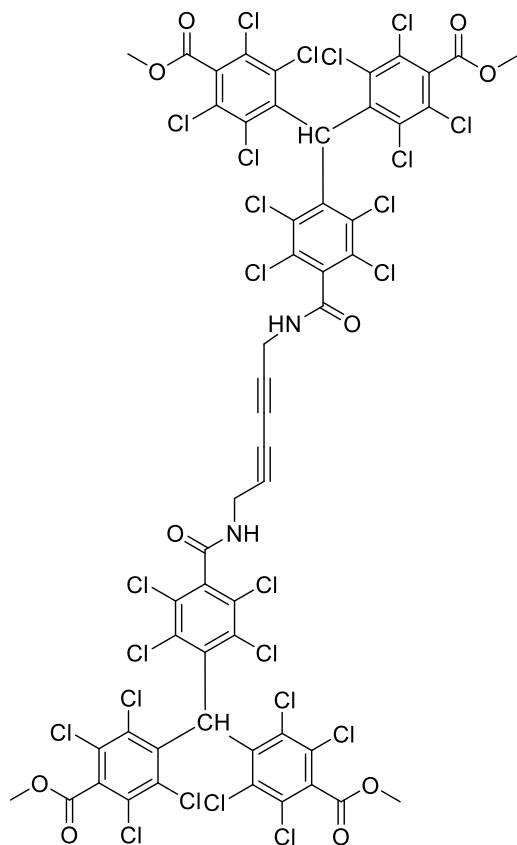
43



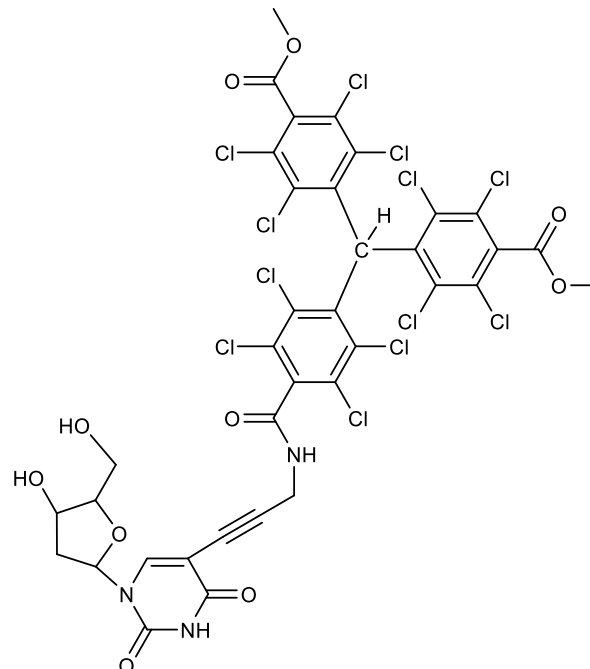
44

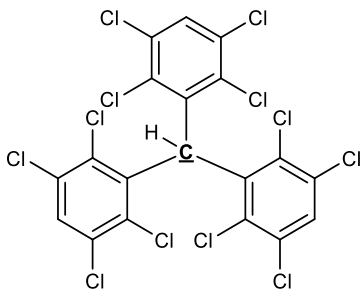
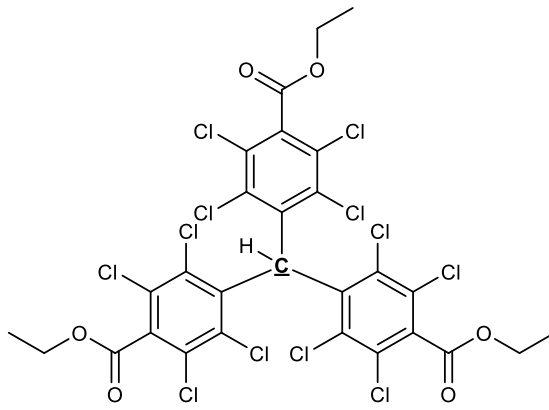
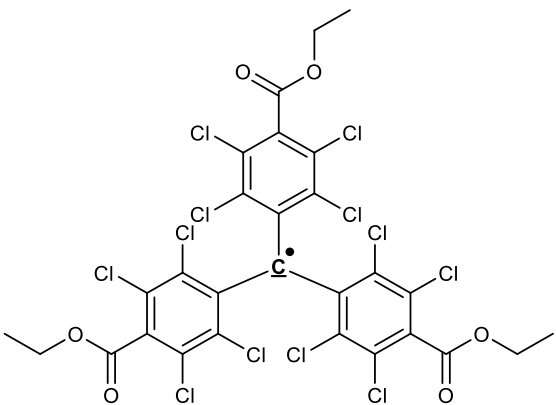
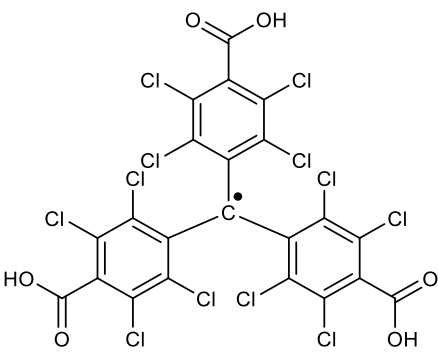
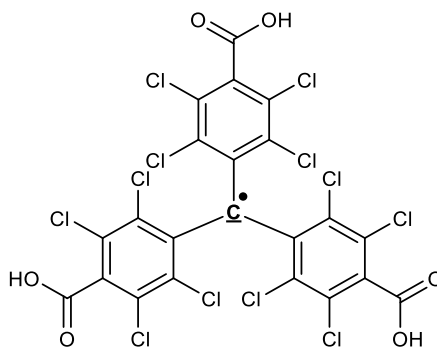
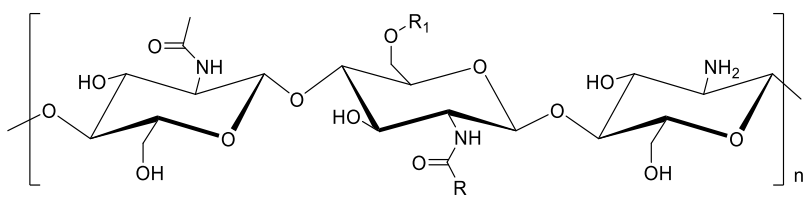


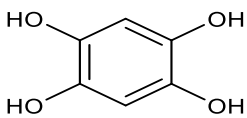
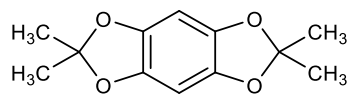
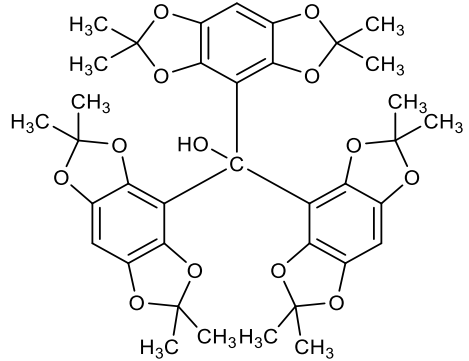
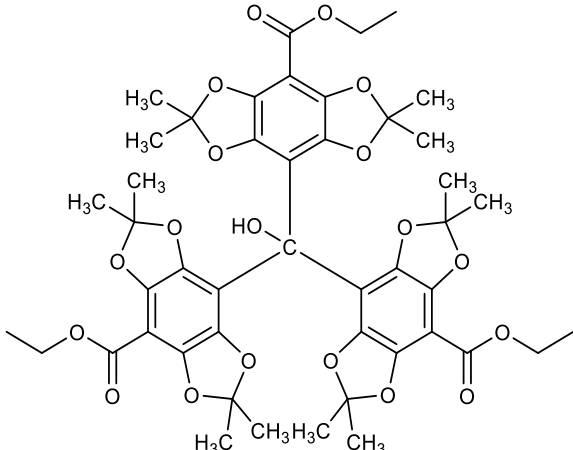
45



46



<p><b>48</b></p> 	<p><b>49</b></p> 
<p><b>50</b></p> 	
<p><b>PTMTC</b></p> 	<p><b><sup>13</sup>C-PTMTC</b></p> 
<p><b>Trityl-polymer conjugates</b></p>  <p><b>PTMTC-CS:</b> R= PTMTC, R<sub>1</sub>= H</p> <p><b>PTMTC-CMC:</b> R= PTMTC, R<sub>1</sub>= CH<sub>2</sub>-COOH</p> <p><b>D-TAM-CS:</b> R= D-TAM, R<sub>1</sub>= H</p> <p><b>D-TAM-CMC:</b> R= D-TAM, R<sub>1</sub>= CH<sub>2</sub>-COOH</p>	

<p><b>52</b></p> 	<p><b>53</b></p> 
<p><b>54</b></p> 	<p><b>55</b></p> 

---

## 8. References

- (1) Zavoisky, E. *J. Phys. USSR* **1944**, *8*, 377.
- (2) Swartz, H. M.; Khan, N.; Buckey, J.; Comi, R.; Gould, L.; Grinberg, O.; Hartford, A.; Hopf, H.; Hou, H.; Hug, E. *NMR Biomed.* **2004**, *17*, 335.
- (3) Carini, M.; Aldini, G.; Orioli, M.; Facino, R. M. *Curr. Pharm. Anal.* **2006**, *2*, 141.
- (4) Brustolon, M. *Electron paramagnetic resonance: a practitioner's toolkit*; John Wiley & Sons, 2009.
- (5) Ahmad, R.; Kuppusamy, P. *Chem. Rev.* **2010**, *110*, 3212.
- (6) Liu, Y.; Villamena, F. A.; Sun, J.; Xu, Y.; Dhimitruka, I.; Zweier, J. L. *J. Org. Chem.* **2008**, *73*, 1490.
- (7) Mäder, K. *Phys. Med. Biol.* **1998**, *43*, 1931.
- (8) Mäder, K.; Bittner, B.; Li, Y.; Wohlauf, W.; Kissel, T. *Pharm. Res.* **1998**, *15*, 787.
- (9) Halpern, H. J.; Chandramouli, G.; Barth, E. D.; Yu, C.; Peric, M.; Grdina, D. J.; Teicher, B. A. *Cancer Res.* **1999**, *59*, 5836.
- (10) Driesschaert, B.; Marchand, V.; Levêque, P.; Gallez, B.; Marchand-Brynaert, J. *Chem. Commun.* **2012**, *48*, 4049.
- (11) Hassan, T. H.; Metz, H.; Mäder, K. *Int. J. Pharm.* **2014**, *477*, 506.
- (12) Williams, B. B.; Halpern, H. J. In *Biomedical EPR, Part A: Free Radicals, Metals, Medicine, and Physiology*; Springer: 2005, p 283.
- (13) Ahmad, R.; Kuppusamy, P. In *Multifrequency Electron Paramagnetic Resonance*; Wiley-VCH Verlag GmbH & Co. KGaA: 2011, p 755.
- (14) Gomberg, M. *JACS* **1900**, *22*, 757.
- (15) Jacobson, P. *Berichte d. D. Chem. Gesellschaft.* **1905**, *38*, 196.
- (16) Lankamp, H.; Nauta, W. T.; MacLean, C. *Tetrahedron Lett.* **1968**, *9*, 249.
- (17) Schmidlin, J. *Berichte d. D. Chem. Gesellschaft.* **1908**, *41*, 2471.
- (18) Janzen, E. G.; Johnston, F. J.; Ayers, C. L. *JACS* **1967**, *89*, 1176.
- (19) Gomberg, M. *JACS* **1901**, *23*, 496.
- (20) Ballester, M. *Pure Appl. Chem.* **1967**, *15*, 123.
- (21) Ballester, M.; Riera-Figueras, J.; Castaner, J.; Badfa, C.; Monso, J. M. *JACS* **1971**, *93*, 2215.

## References

---

- (22) Andersson, S. R., Finn; Rydbeck, Anna; Servin, Rolf; Wistrand, Lars Goeran In *CAPLUS US*, 1996; Vol. 5530140 A 19960625.
- (23) Ardenkjaer-larsen, J. H., Leunbach, Ib 1997; Vol. wo9709633.
- (24) Slashed, R. M. J. O.; Rise, F.; Andersson, S.; Almen, T.; Golman, K. US, 1997; Vol. US5599522A.
- (25) Andersson, S. R., Finn; Rydbeck, Anna; Servin, Rolf; Wistrand, Lars-goran US, 1998; Vol. 5728370 A 19980317.
- (26) Thaning, M. a. P., Göran 1998; Vol. WO9839277.
- (27) Driesschaert, B.; Robiette, R.; Le Duff, C. S.; Collard, L.; Robeyns, K.; Gallez, B.; Marchand-Brynaert, J. *Eur. J. Org. Chem.* **2012**, 2012, 6517.
- (28) Reddy, T. J.; Iwama, T.; Halpern, H. J.; Rawal, V. H. *J. Org. Chem.* **2002**, 67, 4635.
- (29) Dhimitruka, I.; Velayutham, M.; Bobko, A. A.; Khramtsov, V. V.; Villamena, F. A.; Hadad, C. M.; Zweier, J. L. *Bioorg. Med. Chem. Lett.* **2007**, 17, 6801.
- (30) Tormyshev, V. M.; Genaev, A. M.; Sal'nikov, G. E.; Rogozhnikova, O. Y.; Troitskaya, T. I.; Trukhin, D. V.; Mamatyuk, V. I.; Fadeev, D. S.; Halpern, H. J. *Eur. J. Org. Chem.* **2012**, 2012, 623.
- (31) Rogozhnikova, O. Y.; Vasiliev, V. G.; Troitskaya, T. I.; Trukhin, D. V.; Mikhailina, T. V.; Halpern, H. J.; Tormyshev, V. M. *Eur. J. Org. Chem.* **2013**, 2013, 3347.
- (32) Xia, S.; Villamena, F. A.; Hadad, C. M.; Kuppusamy, P.; Li, Y.; Zhu, H.; Zweier, J. L. *J. Org. Chem.* **2006**, 71, 7268.
- (33) Liu, Y.; Villamena, F. A.; Zweier, J. L. *Chem. Commun.* **2008**, 4336.
- (34) Khan, N.; Swartz, H. *Mol. Cell. Biochem.* **2002**, 234, 341.
- (35) Liu, Y.; Song, Y.; Rockenbauer, A.; Sun, J.; Hemann, C.; Villamena, F. A.; Zweier, J. L. *J. Org. Chem.* **2011**, 76, 3853.
- (36) Kutala, V. K.; Parinandi, N. L.; Pandian, R. P.; Kuppusamy, P. *Antioxid. Redox Signal.* **2004**, 6, 597.
- (37) Liu, Y.; Villamena, F. A.; Sun, J.; Wang, T.-y.; Zweier, J. L. *Free Radical Biol. Med.* **2009**, 46, 876.
- (38) Bobko, A. A.; Dhimitruka, I.; Eubank, T. D.; Marsh, C. B.; Zweier, J. L.; Khramtsov, V. V. *Free Radical Biol. Med.* **2009**, 47, 654.
- (39) Komarov, D. A.; Dhimitruka, I.; Kirilyuk, I. A.; Trofimiov, D. G.; Grigor'ev, I. A.; Zweier, J. L.; Khramtsov, V. V. *Magn. Reson. Med.* **2012**, 68, 649.
- (40) Rizzi, C.; Samouilov, A.; Kumar Kutala, V.; Parinandi, N. L.; Zweier, J. L.; Kuppusamy, P. *Free Radical Biol. Med.* **2003**, 35, 1608.

## References

---

- (41) Kutala, V. K.; Parinandi, N. L.; Zweier, J. L.; Kuppusamy, P. *Arch. Biochem. Biophys.* **2004**, *424*, 81.
- (42) Liu, Y.; Song, Y.; De Pascali, F.; Liu, X.; Villamena, F. A.; Zweier, J. L. *Free Radical Biol. Med.* **2012**, *53*, 2081.
- (43) Kutala, V. K.; Kuppusamy, P. *Curr. Top. Biophys.* **2005**, *29*, 129.
- (44) Decroos, C.; Li, Y.; Bertho, G.; Frapart, Y.; Mansuy, D.; Boucher, J.-L. *Chem. Commun.* **2009**, 1416.
- (45) Bobko, A. A.; Dhimitruka, I.; Zweier, J. L.; Khramtsov, V. V. *JACS* **2007**, *129*, 7240.
- (46) Bobko, A. A.; Dhimitruka, I.; Komarov, D. A.; Khramtsov, V. V. *Anal. Chem.* **2012**, *84*, 6054.
- (47) Dhimitruka, I.; Bobko, A. A.; Hadad, C. M.; Zweier, J. L.; Khramtsov, V. V. *JACS* **2008**, *130*, 10780.
- (48) Dhimitruka, I.; Bobko, A. A.; Eubank, T. D.; Komarov, D. A.; Khramtsov, V. V. *JACS* **2013**, *135*, 5904.
- (49) Takahashi, W.; Bobko, A.; Dhimitruka, I.; Hirata, H.; Zweier, J.; Samouilov, A.; Khramtsov, V. *Appl. Magn. Reson.* **2014**, *45*, 817.
- (50) Liu, Y.; Villamena, F. A.; Rockenbauer, A.; Zweier, J. L. *Chem. Commun.* **2010**, *46*, 628.
- (51) Liu, Y.; Villamena, F. A.; Song, Y.; Sun, J.; Rockenbauer, A.; Zweier, J. L. *J. Org. Chem.* **2010**, *75*, 7796.
- (52) Shevelev, G. Y.; Krumkacheva, O. A.; Lomzov, A. A.; Kuzhelev, A. A.; Rogozhnikova, O. Y.; Trukhin, D. V.; Troitskaya, T. I.; Tormyshev, V. M.; Fedin, M. V.; Pyshnyi, D. V. *JACS* **2014**, *136*, 9874.
- (53) Yang, Z.; Liu, Y.; Borbat, P.; Zweier, J. L.; Freed, J. H.; Hubbell, W. L. *JACS* **2012**, *134*, 9950.
- (54) Reginsson, G. W.; Kunjir, N. C.; Sigurdsson, S. T.; Schiemann, O. *Chem. Eur. j.* **2012**, *18*, 13580.
- (55) Talmon, Y.; Shtirberg, L.; Harneit, W.; Rogozhnikova, O. Y.; Tormyshev, V.; Blank, A. *Phys. Chem. Chem. Phys.* **2010**, *12*, 5998.
- (56) Elas, M.; Williams, B. B.; Parasca, A.; Mailer, C.; Pelizzari, C. A.; Lewis, M. A.; River, J. N.; Karczmar, G. S.; Barth, E. D.; Halpern, H. J. *Magn. Reson. Med.* **2003**, *49*, 682.
- (57) Owenius, R.; Eaton, G. R.; Eaton, S. S. *J. Magn. Reson.* **2005**, *172*, 168.
- (58) Yong, L.; Harbridge, J.; Quine, R. W.; Rinard, G. A.; Eaton, S. S.; Eaton, G. R.; Mailer, C.; Barth, E.; Halpern, H. J. *J. Magn. Reson.* **2001**, *152*, 156.



- (59) Rong, C. C.; So, H.; Pope, M. T. *Magn. Reson. Med.* **2005**.
- (60) Murugesan, R.; Cook, J. A.; Devasahayam, N.; Afeworki, M.; Subramanian, S.; Tschudin, R.; Larsen, J. A.; Mitchell, J. B.; Russo, A.; Krishna, M. C. *Magn. Reson. Med.* **1997**, *38*, 409.
- (61) Yamada, K.-I.; Murugesan, R.; Devasahayam, N.; Cook, J. A.; Mitchell, J. B.; Subramanian, S.; Krishna, M. C. *J. Magn. Reson.* **2002**, *154*, 287.
- (62) Mailer, C.; Subramanian, S. V.; Pelizzari, C. A.; Halpern, H. J. *Curr. Top. Biophys.* **2005**, *29*, 89.
- (63) Bobko, A. A.; Dhimitruka, I.; Zweier, J. L.; Khramtsov, V. V. *Angew. Chem.* **2014**, *126*, 2773.
- (64) Golman, K.; Petersson, J. S.; Ardenkjær-Larsen, J. H.; Leunbach, I.; Wistrand, L. G.; Ehnholm, G.; Liu, K. *J. Magn. Reson. Imaging* **2000**, *12*, 929.
- (65) Ardenkjaer-Larsen, J.; Laursen, I.; Leunbach, I.; Ehnholm, G.; Wistrand, L.-G.; Petersson, J.; Golman, K. *J. Magn. Reson.* **1998**, *133*, 1.
- (66) Li, H.; Deng, Y.; He, G.; Kuppusamy, P.; Lurie, D. J.; Zweier, J. L. *Magn. Reson. Med.* **2002**, *48*, 530.
- (67) Efimova, O. V.; Caia, G. L.; Sun, Z.; Petryakov, S.; Kesselring, E.; Samouilov, A.; Zweier, J. L. *J. Magn. Reson.* **2011**, *212*, 197.
- (68) Ardenkjær-Larsen, J. H.; Fridlund, B.; Gram, A.; Hansson, G.; Hansson, L.; Lerche, M. H.; Servin, R.; Thaning, M.; Golman, K. *Proc. Natl. Acad. Sci.* **2003**, *100*, 10158.
- (69) Gallagher, F. A.; Kettunen, M. I.; Day, S. E.; Hu, D.-E.; Ardenkjær-Larsen, J. H. *Nature* **2008**, *453*, 940.
- (70) Krishna, M. C.; English, S.; Yamada, K.; Yoo, J.; Murugesan, R.; Devasahayam, N.; Cook, J. A.; Golman, K.; Ardenkjaer-Larsen, J. H.; Subramanian, S. *Proc. Natl. Acad. Sci.* **2002**, *99*, 2216.
- (71) Gallez, B.; Baudalet, C.; Jordan, B. F. *NMR Biomed.* **2004**, *17*, 240.
- (72) Karlsson, M. N., Roberta; Visigalli, Massimo; Lerche, Mathilde H.; Jensen, Pernille Rose; Tedoldi, Fabio Appl., P. I., Ed. 2014; Vol. WO 2014009240.
- (73) Scott, G. *Antioxidants in science, technology, medicine and nutrition*; Elsevier, 1997.
- (74) D'Angio, C. T.; Finkelstein, J. N. *Mol. Genet. Metab.* **2000**, *71*, 371.
- (75) Finkel, T.; Holbrook, N. J. *Nature* **2000**, *408*, 239.
- (76) Swartz, H. M.; Clarkson, R. B. *Phys. Med. Biol.* **1998**, *43*, 1957.
- (77) Pardini, R. S. *Arch. Insect Biochem. Physiol.* **1995**, *29*, 101.

## References

---

- (78) Teng, C.-L.; Hong, H.; Kiihne, S.; Bryant, R. G. *J. Magn. Reson.* **2001**, *148*, 31.
- (79) Hyde, J. S.; Subczynski, W. K. In *Spin Labeling*; Springer: 1989, p 399.
- (80) Swartz, H. M. *Antioxid. Redox Signal.* **2004**, *6*, 677.
- (81) He, G.; Shankar, R. A.; Chzhan, M.; Samouilov, A.; Kuppusamy, P.; Zweier, J. L. *Proc. Natl. Acad. Sci.* **1999**, *96*, 4586.
- (82) James, P. E.; Jackson, S. K.; Grinberg, O. Y.; Swartz, H. M. *Free Radical Biol. Med.* **1995**, *18*, 641.
- (83) Liu, K.; Gast, P.; Moussavi, M.; Norby, S.; Vahidi, N.; Walczak, T.; Wu, M.; Swartz, H. *Proc. Natl. Acad. Sci.* **1993**, *90*, 5438.
- (84) Presley, T.; Kuppusamy, P.; Zweier, J. L.; Ilangovan, G. *Biophys. J.* **2006**, *91*, 4623.
- (85) Pandian, R. P.; Parinandi, N. L.; Ilangovan, G.; Zweier, J. L.; Kuppusamy, P. *Free Radical Biol. Med.* **2003**, *35*, 1138.
- (86) Clarkson, R.; Odintsov, B.; Ceroke, P.; Fruianu, M.; Belford, R. *Phys. Med. Biol.* **1998**, *43*, 1907.
- (87) James, P. E.; Grinberg, O. Y.; Goda, F.; Panz, T.; O'Hara, J. A.; Swartz, H. M. *Magn. Reson. Med.* **1997**, *38*, 48.
- (88) Jordan, B. F.; Baudalet, C.; Gallez, B. *MAGMA* **1998**, *7*, 121.
- (89) Lan, M.; Beghein, N.; Charlier, N.; Gallez, B. *Magn. Reson. Med.* **2004**, *51*, 1272.
- (90) Goda, F.; Liu, K. J.; Walczak, T.; O'Hara, J. A.; Jiang, J.; Swartz, H. M. *Magn. Reson. Med.* **1995**, *33*, 237.
- (91) Gallez, B.; Bacic, G.; Goda, F.; Jiang, J.; Dunn, J. F.; Swartz, H. M. *Magn. Reson. Med.* **1996**, *35*, 97.
- (92) Velan, S. S.; Spencer, R. G.; Zweier, J. L.; Kuppusamy, P. *Magn. Reson. Med.* **2000**, *43*, 804.
- (93) Burks, S. R.; Bakhshai, J.; Makowsky, M. A.; Muralidharan, S.; Tsai, P.; Rosen, G. M.; Kao, J. P. *J. Org. Chem.* **2010**, *75*, 6463.
- (94) Halpern, H. J.; Yu, C.; Peric, M.; Barth, E.; Grdina, D. J.; Teicher, B. A. *Proc. Natl. Acad. Sci.* **1994**, *91*, 13047.
- (95) Joergensen, M. R., Frode; Andersson, Sven; Almen, Torsten; Aabye, Arne; Wistrand, Lars Goeran; Wikstroem, Haakan; Golman, Klaes; Servin, Rolf; Michelsen, Peter In *PCT Int. Appl.* 1991; Vol. WO 9112024 A1 19910822.
- (96) Matsumoto, K. i.; English, S.; Yoo, J.; Yamada, K. i.; Devasahayam, N.; Cook, J. A.; Mitchell, J. B.; Subramanian, S.; Krishna, M. C. *Magn. Reson. Med.* **2004**, *52*, 885.

- (97) Matsumoto, K. i.; Subramanian, S.; Devasahayam, N.; Aravalluvan, T.; Murugesan, R.; Cook, J. A.; Mitchell, J. B.; Krishna, M. C. *Magn. Reson. Med.* **2006**, *55*, 1157.
- (98) Matsumoto, S.; Hyodo, F.; Subramanian, S.; Devasahayam, N.; Munasinghe, J.; Hyodo, E.; Gadiseti, C.; Cook, J. A.; Mitchell, J. B.; Krishna, M. C. *J. Clin. Invest.* **2008**, *118*, 1965.
- (99) Song, Y.; Liu, Y.; Hemann, C.; Villamena, F. A.; Zweier, J. L. *J. Org. Chem.* **2013**, *78*, 1371.
- (100) Elas, M.; Ahn, K.-H.; Parasca, A.; Barth, E. D.; Lee, D.; Haney, C.; Halpern, H. J. *Clin. Cancer Res.* **2006**, *12*, 4209.
- (101) Wan, X.; Fu, T.-C.; Funk, A.; London, R. E. *Brain Res. Bull.* **1995**, *36*, 91.
- (102) Bardelang, D.; Hardy, M.; Ouari, O.; Tordo, P. In *Encyclopedia of Radicals in Chemistry, Biology and Materials*; John Wiley & Sons, Ltd: 2012.
- (103) Rietjens, I. M.; Steensma, A.; Den Besten, C.; van Tintelen, G.; Haas, J.; van Ommen, B.; van Bladeren, P. J. *Eur. J. Pharmacol. Environ. Toxicol. Pharmacol.* **1995**, *293*, 293.
- (104) Riess, J. G. *Chem. Rev.* **2001**, *101*, 2797.
- (105) Kirsch, P. *Modern Fluoroorganic Chemistry Synthesis, Reactivity, Application*; Wiley Online Library, 2004.
- (106) Bratasz, A.; Kulkarni, A. C.; Kuppusamy, P. *Biophys. J.* **2007**, *92*, 2918.
- (107) Murov, S. L.; Carmichael, I.; Hug, G. L. *Handbook of photochemistry*; CRC Press, 1993.
- (108) Driesschaert, B.; Charlier, N.; Gallez, B.; Marchand-Brynaert, J. *Bioorg. Med. Chem. Lett.* **2008**, *18*, 4291.
- (109) Charlier, N.; Driesschaert, B.; Wauthoz, N.; Beghein, N.; Pr eat, V.; Amighi, K.; Marchand-Brynaert, J.; Gallez, B. *J. Magn. Reson.* **2009**, *197*, 176.
- (110) Dhimitruka, I.; Grigorieva, O.; Zweier, J. L.; Khramtsov, V. V. *Bioorg. Med. Chem. Lett.* **2010**, *20*, 3946.
- (111) Decroos, C.; Li, Y.; Bertho, G.; Frapart, Y.; Mansuy, D.; Boucher, J.-L. *Chem. Res. Toxicol.* **2009**, *22*, 1342.
- (112) Decroos, C.; Li, Y.; Soltani, A.; Frapart, Y.; Mansuy, D.; Boucher, J.-L. *Arch. Biochem. Biophys.* **2010**, *502*, 74.
- (113) Decroos, C.; Prang e, T.; Mansuy, D.; Boucher, J.-L.; Li, Y. *Chem. Commun.* **2011**, *47*, 4805.
- (114) Decroos, C.; Balland, V.; Boucher, J.-L.; Bertho, G.; Xu-Li, Y.; Mansuy, D. *Chem. Res. Toxicol.* **2013**, *26*, 1561.

## References

---

- (115) Tormyshev, V. M.; Rogozhnikova, O. Y.; Bowman, M. K.; Trukhin, D. V.; Troitskaya, T. I.; Vasiliev, V. G.; Shundrin, L. A.; Halpern, H. J. *Eur. J. Org. Chem.* **2014**, 2014, 371.
- (116) Song, Y.; Liu, Y.; Liu, W.; Villamena, F. A.; Zweier, J. L. *RSC Advances* **2014**, 4, 47649.
- (117) Decroos, C.; Boucher, J.-L.; Mansuy, D.; Xu-Li, Y. *Chem. Res. Toxicol.* **2014**, 27, 627.
- (118) Driesschaert, B.; Robiette, R.; Lucaccioni, F.; Gallez, B.; Marchand-Brynaert, J. *Chem. Commun.* **2011**, 47, 4793.
- (119) Kurkdjian, A.; Guern, J. *Annu. Rev. Plant Biol.* **1989**, 40, 271.
- (120) Kingsbury, A. E.; Foster, O. J. F.; Nisbet, A. P.; Cairns, N.; Bray, L.; Eve, D. J.; Lees, A. J.; David Marsden, C. *Mol. Brain Res.* **1995**, 28, 311.
- (121) Gillies, R. J.; Raghunand, N.; Garcia-Martin, M. L.; Gatenby, R. A. *IEEE Eng. Med. Biol. Mag.* **2004**, 23, 57.
- (122) Khrantsov, V.; Grigor'Ev, I.; Foster, M.; Lurie, D.; Nicholson, I. *Cell. Mol. Biol. (Noisy-le-grand)* **2000**, 46, 1361.
- (123) Khrantsov, V. V. *Curr. Org. Chem.* **2005**, 9, 909.
- (124) Khrantsov, V. V. In *Nitroxides - Theory, Experiment and Applications*; Kokorin, A., Ed. 2012.
- (125) Oktyabrsky, O.; Smirnova, G. *Biochem. (Mosc.)* **2007**, 72, 132.
- (126) Hyodo, F.; Soule, B. P.; Matsumoto, K. i.; Matusmoto, S.; Cook, J. A.; Hyodo, E.; Sowers, A. L.; Krishna, M. C.; Mitchell, J. B. *J. Pharm. Pharmacol.* **2008**, 60, 1049.
- (127) Schafer, F. Q.; Buettner, G. R. *Free Radical Biol. Med.* **2001**, 30, 1191.
- (128) Matsumoto, K.-i.; Hyodo, F.; Matsumoto, A.; Koretsky, A. P.; Sowers, A. L.; Mitchell, J. B.; Krishna, M. C. *Clin. Cancer Res.* **2006**, 12, 2455.
- (129) Hyodo, F.; Matsumoto, K.-i.; Matsumoto, A.; Mitchell, J. B.; Krishna, M. C. *Cancer Res.* **2006**, 66, 9921.
- (130) Sies, H. *Free Radical Biol. Med.* **1999**, 27, 916.
- (131) Noda, T.; Iwakiri, R.; Fujimoto, K.; Aw, T. Y. *FASEB J.* **2001**, 15, 2131.
- (132) Khrantsov, V.; Weiner, L.; Berezina, T.; Martin, V.; Volodarsky, L. *Anal. Biochem.* **1989**, 182, 58.
- (133) Khrantsov, V.; Yelinova, V.; Glazachev, Y. I.; Reznikov, V.; Zimmer, G. *J. Biochem. Biophys. Methods* **1997**, 35, 115.
- (134) Roshchupkina, G. I.; Bobko, A. A.; Bratasz, A.; Reznikov, V. A.; Kuppusamy, P.; Khrantsov, V. V. *Free Radical Biol. Med.* **2008**, 45, 312.

## References

---

- (135) Bobko, A. A.; Eubank, T. D.; Voorhees, J. L.; Efimova, O. V.; Kirilyuk, I. A.; Petryakov, S.; Trofimov, D. G.; Marsh, C. B.; Zweier, J. L.; Grigor'ev, I. A. *Magn. Reson. Med.* **2012**, *67*, 1827.
- (136) Waris, G.; Ahsan, H. *J. Carcinog.* **2006**, *5*, 14.
- (137) McCord, J. M.; Roy, R. S. *Can. J. Physiol. Pharmacol.* **1982**, *60*, 1346.
- (138) Shah, A.; Channon, K. *Heart* **2004**, *90*, 486.
- (139) Oberley, L. W. *Free Radical Biol. Med.* **1988**, *5*, 113.
- (140) Valko, M.; Izakovic, M.; Mazur, M.; Rhodes, C. J.; Telser, J. *Mol. Cell. Biochem.* **2004**, *266*, 37.
- (141) Veciana, J.; Ratera, I. *Polychlorotriphenylmethyl Radicals: Towards Multifunctional Molecular Materials*; Wiley, 2010.
- (142) Veciana, J.; Crespo, M. I. *Angew. Chem. Int. Ed. Engl.* **1991**, *30*, 74.
- (143) Ballester, M. *Acc. Chem. Res.* **1985**, *18*, 380.
- (144) Fieser, L.; Fieser, M. *Reagents for organic chemistry*; John Wiley and Sons, New York, 1967.
- (145) Ballester, M.; Molinet, C.; Castañer, J. *JACS* **1960**, *82*, 4254.
- (146) Ballester, M. *Adv. Phys. Org. Chem* **1989**, *25*, 267.
- (147) Ballester, M.; Riera, J.; Castañer, J.; Rovira, C.; Armet, O. *Synthesis* **1986**, *1986*, 64.
- (148) Ballester, M.; Pascual, I. *Tetrahedron Lett.* **1985**, *26*, 5589.
- (149) Perone, R. C. **2012**.
- (150) Falle, H.; Luckhurst, G.; Horsfield, A.; Ballester, M. *J. Chem. Phys.* **1969**, *50*, 258.
- (151) Ballester, M.; Castaner, J.; Riera, J.; Ibanez, A.; Pujadas, J. *J. Org. Chem.* **1982**, *47*, 259.
- (152) Ballester, M.; Riera, J.; Castaner, J.; Rodriguez, A.; Rovira, C.; Veciana, J. *J. Org. Chem.* **1982**, *47*, 4498.
- (153) Armet, O.; Veciana, J.; Rovira, C.; Riera, J.; Castaner, J.; Molins, E.; Rius, J.; Miravittles, C.; Olivella, S.; Brichfeus, J. *J. Phys. Chem.* **1987**, *91*, 5608.
- (154) Luckhurst, G. R.; Ockwell, J. N. *Tetrahedron Lett.* **1968**, *9*, 4123.
- (155) Ballester, M.; Castañer, J.; Pujadas, J. *Tetrahedron Lett.* **1971**, *12*, 1699.
- (156) Gomberg, M.; Cone, L. H. *Berichte d. D. Chem. Gesellschaft.* **1904**, *37*, 3538.
- (157) Schmidlin, J.; Garcia-Banús, A. *Berichte d. D. Chem. Gesellschaft.* **1912**, *45*, 1344.

## References

---

- (158) Ballester, M.; Riera, J.; Castañer, J.; Carreras, C.; Ubierna, J.; Badia, C.; Miravittles, C.; Molins, E. *J. Org. Chem.* **1989**, *54*, 4611.
- (159) Molins, E.; Mas, M.; Maniukiewicz, W.; Ballester, M.; Castaner, J. *Acta. Crystallogr. C.* **1996**, *52*, 2412.
- (160) Ballester, M.; Miravittles, C.; Molins, E.; Carreras, C. *J. Org. Chem.* **2003**, *68*, 2748.
- (161) Ballester, M.; Riera-Figueras, J.; Rodriguez-Siurana, A. *Tetrahedron Lett.* **1970**, *11*, 3615.
- (162) Ballester, M.; de la Fuente, G. *Tetrahedron Lett.* **1970**, *11*, 4509.
- (163) Ballester, M.; Riera, J.; Castañer, J.; Casulleras, M. *Tetrahedron Lett.* **1978**, *19*, 643.
- (164) Ballester, M.; Veciana, J.; Riera, J.; Castaner, J.; Rovira, C.; Armet, O. *J. Org. Chem.* **1986**, *51*, 2472.
- (165) Juliá, L.; Ballester, M.; Riera, J.; Castaner, J.; Ortin, J.; Onrubia, C. *J. Org. Chem.* **1988**, *53*, 1267.
- (166) López, S.; Carilla, J.; Fajarí, L.; Juliá, L.; Brillas, E.; Labarta, A. *Tetrahedron* **1995**, *51*, 7301.
- (167) Ribas, X.; Maspoch, D.; Wurst, K.; Veciana, J.; Rovira, C. *Inorg. Chem.* **2006**, *45*, 5383.
- (168) Ratera, I.; Marcen, S.; Montant, S.; Ruiz-Molina, D.; Rovira, C.; Veciana, J.; Létard, J.-F.; Freysz, E. *Chem. Phys. Lett.* **2002**, *363*, 245.
- (169) Ballester, M.; Riera, J.; Castaner, J.; Rovira, C.; Veciana, J.; Onrubia, C. *J. Org. Chem.* **1983**, *48*, 3716.
- (170) Ballester, M.; Riera, J.; Rodríguez-Siurana, A.; Rovira, C. *Tetrahedron Lett.* **1977**, *18*, 2355.
- (171) Ballester, M.; Castañer, J.; Riera, J.; Veciana, J. *Tetrahedron Lett.* **1978**, *19*, 479.
- (172) Mesa, J. A.; Velázquez-Palenzuela, A.; Brillas, E.; Coll, J.; Torres, J. L.; Juliá, L. *J. Org. Chem.* **2012**, *77*, 1081.
- (173) Ballester, M.; Veciana, J.; Riera, J.; Castañer, J.; Armet, O.; Rovira, C. *J. Chem. Soc., Chem. Commun.* **1983**, 982.
- (174) Ballester, M.; Veciana, J.; Riera, J.; Castañer, J.; Rovira, C.; Armet, O. *Tetrahedron Lett.* **1982**, *23*, 5075.
- (175) Ballester, M.; Pascual, I. *J. Org. Chem.* **1991**, *56*, 4314.
- (176) Torres, J. L.; Carreras, A.; Jiménez, A.; Brillas, E.; Torrelles, X.; Rius, J.; Juliá, L. *J. Org. Chem.* **2007**, *72*, 3750.

## References

---

- (177) Mesa, J. A.; Velázquez-Palenzuela, A.; Brillas, E.; Torres, J. L.; Juliá, L. *Tetrahedron* **2011**, *67*, 3119.
- (178) Dang, V.; Wang, J.; Feng, S.; Buron, C.; Villamena, F. A.; Wang, P. G.; Kuppusamy, P. *Bioorg. Med. Chem. Lett.* **2007**, *17*, 4062.
- (179) MasPOCH, D.; Domingo, N.; Ruiz-Molina, D.; WurSt, K.; Vaughan, G.; Tejada, J.; Rovira, C.; Veciana, J. *Angew. Chem.* **2004**, *116*, 1864.
- (180) Castillo, M.; Brillas, E.; Rillo, C.; Kuzmin, M. D.; Juliá, L. *Tetrahedron* **2007**, *63*, 708.
- (181) Roques, N.; MasPOCH, D.; Domingo, N.; Ruiz-Molina, D.; WurSt, K.; Tejada, J.; Rovira, C.; Veciana, J. *Chem. Commun.* **2005**, 4801.
- (182) Torres, J. L.; Varela, B.; Brillas, E.; Juliá, L. *Chem. Commun.* **2003**, 74.
- (183) Roques, N.; MasPOCH, D.; WurSt, K.; Ruiz-Molina, D.; Rovira, C.; Veciana, J. *Chem. Eur. j.* **2006**, *12*, 9238.
- (184) Banerjee, D.; Paniagua, J. C.; Mugnaini, V.; Veciana, J.; Feintuch, A.; Pons, M.; Goldfarb, D. *Phys. Chem. Chem. Phys.* **2011**, *13*, 18626.
- (185) Gabellieri, C.; Mugnaini, V.; Paniagua, J. C.; Roques, N.; Oliveros, M.; Feliz, M.; Veciana, J.; Pons, M. *Angew. Chem. Int. Ed.* **2010**, *49*, 3360.
- (186) Paniagua, J. C.; Mugnaini, V.; Gabellieri, C.; Feliz, M.; Roques, N.; Veciana, J.; Pons, M. *Phys. Chem. Chem. Phys.* **2010**, *12*, 5824.
- (187) Vigier, F. M.; Shimon, D.; Mugnaini, V.; Veciana, J.; Feintuch, A.; Pons, M.; Vega, S.; Goldfarb, D. *Phys. Chem. Chem. Phys.* **2014**, *16*, 19218.
- (188) Ratera, I.; Veciana, J. *Chem. Soc. Rev.* **2012**, *41*, 303.
- (189) Meenakshisundaram, G.; Eteshola, E.; Blank, A.; Lee, S. C.; Kuppusamy, P. *Biosens. Bioelectron.* **2010**, *25*, 2283.
- (190) Wang, J.; Dang, V.; Zhao, W.; Lu, D.; Rivera, B. K.; Villamena, F. A.; Wang, P. G.; Kuppusamy, P. *Bioorg. Med. Chem.* **2010**, *18*, 922.
- (191) Kutala, V. K.; Villamena, F. A.; Ilangovan, G.; MasPOCH, D.; Roques, N.; Veciana, J.; Rovira, C.; Kuppusamy, P. *J. Phys. Chem. B* **2008**, *112*, 158.
- (192) Grillo, F.; Mugnaini, V.; Oliveros, M.; Francis, S. M.; Choi, D.-J.; Rastei, M. V.; Limot, L.; Cepek, C.; Pedio, M.; Bromley, S. T. *J. Phys. Chem. Lett.* **2012**, *3*, 1559.
- (193) Warwar, N.; Mor, A.; Fluhr, R.; Pandian, R. P.; Kuppusamy, P.; Blank, A. *Biophys. J.* **2011**, *101*, 1529.
- (194) Mesa, J. A.; Lluís Torres, J.; Juliá, L. *Talanta* **2012**, *101*, 141.
- (195) Prior, R. L.; Wu, X.; Schaich, K. *J. Agric. Food. Chem.* **2005**, *53*, 4290.

## References

---

- (196) Mesa, J. A.; Chávez, S.; Fajarí, L.; Torres, J. L.; Juliá, L. *RSC Advances* **2013**, *3*, 9949.
- (197) Frank, J.; Elewa, M.; Said, M. M.; El Shihawy, H. A.; El-Sadek, M.; Müller, D.; Meister, A.; Hause, G.; Drescher, S.; Metz, H.; Imming, P.; Mäder, K. *J. Org. Chem.* **2015**, *80*, 6754.
- (198) Müller, D.; Adelsberger, K.; Imming, P. *Synth. Commun.* **2013**, *43*, 1447.
- (199) Müller, D. PhD thesis, Martin-Luther-Universität Halle-Wittenberg, 2013.
- (200) Kutsche, I.; Gildehaus, G.; Schuller, D.; Schumpe, A. *J. Chem. Eng. Data* **1984**, *29*, 286.
- (201) Battino, R.; Oxford, UK: Pergamon Press: 1981.
- (202) Pandian, R. P.; Raju, N. P.; Gallucci, J. C.; Woodward, P. M.; Epstein, A. J.; Kuppusamy, P. *Chem. Mater.* **2010**, *22*, 6254.
- (203) Liu, K. J.; Grinstaff, M. W.; Jiang, J.; Suslick, K. S.; Swartz, H. M.; Wang, W. *Biophys. J.* **1994**, *67*, 896.
- (204) Meenakshisundaram, G.; Eteshola, E.; Pandian, R. P.; Bratasz, A.; Selvendiran, K.; Lee, S. C.; Krishna, M. C.; Swartz, H. M.; Kuppusamy, P. *Biomed. Microdevices* **2009**, *11*, 817.
- (205) Gallez, B.; Mäder, K. *Free Radical Biol. Med.* **2000**, *29*, 1078.
- (206) Kuethe, J. T. *J. Labelled Compd. Radiopharm.* **2012**, *55*, 180.
- (207) Maspoch, D.; Domingo, N.; Roques, N.; Wurst, K.; Tejada, J.; Rovira, C.; Ruiz-Molina, D.; Veciana, J. *Chem. Eur. j.* **2007**, *13*, 8153.
- (208) Xia, S. PhD thesis, The Ohio State University, 2008.
- (209) Jeschke, G. *Annu. Rev. Phys. Chem.* **2012**, *63*, 419.
- (210) Schiemann, O.; Piton, N.; Mu, Y.; Stock, G.; Engels, J. W.; Prisner, T. F. *JACS* **2004**, *126*, 5722.
- (211) Schiemann, O.; Prisner, T. F. *Q. Rev. Biophys.* **2007**, *40*, 1.
- (212) Hubbell, W. L.; Gross, A.; Langen, R.; Lietzow, M. A. *Curr. Opin. Struct. Biol.* **1998**, *8*, 649.
- (213) Hubbell, W. L.; Cafiso, D. S.; Altenbach, C. *Nat. Struct. Mol. Biol.* **2000**, *7*, 735.
- (214) Becker, C. F.; Lausecker, K.; Balog, M.; Kálai, T.; Hideg, K.; Steinhoff, H. J.; Engelhard, M. *Magn. Reson. Chem.* **2005**, *43*, S34.
- (215) Ding, P.; Wunnicke, D.; Steinhoff, H. J.; Seela, F. *Chem. Eur. j.* **2010**, *16*, 14385.
- (216) Edwards, T. E.; Okonogi, T. M.; Robinson, B. H.; Sigurdsson, S. T. *JACS* **2001**, *123*, 1527.
- (217) Edwards, T. E.; Sigurdsson, S. T. *Nat. Protoc.* **2007**, *2*, 1954.



## References

---

- (218) Schiemann, O.; Piton, N.; Plackmeyer, J.; Bode, B. E.; Prisner, T. F.; Engels, J. W. *Nat. Protocols* **2007**, *2*, 904.
- (219) Cai, Q.; Kusnetzow, A. K.; Hideg, K.; Price, E. A.; Haworth, I. S.; Qin, P. Z. *Biophys. J.* **2007**, *93*, 2110.
- (220) Kunjir, N. C.; Reginsson, G. W.; Schiemann, O.; Sigurdsson, S. T. *Phys. Chem. Chem. Phys.* **2013**, *15*, 19673.
- (221) Tom Brown, D. B., Asha Brown, Tom Brown (Jr) 2005.
- (222) Lee, S. E.; Sidorov, A.; Gourelain, T.; Mignet, N.; Thorpe, S. J.; Brazier, J. A.; Dickman, M. J.; Hornby, D. P.; Grasby, J. A.; Williams, D. M. *Nucleic Acids Res.* **2001**, *29*, 1565.
- (223) Saito, Y.; Shinohara, Y.; Bag, S. S.; Takeuchi, Y.; Matsumoto, K.; Saito, I. *Tetrahedron* **2009**, *65*, 934.
- (224) Borsenberger, V.; Kukwikila, M.; Howorka, S. *Org. Biomol. Chem.* **2009**, *7*, 3826.
- (225) Trybulski, E. J.; Zhang, J.; Kramss, R. H.; Mangano, R. M. *J. Med. Chem.* **1993**, *36*, 3533.
- (226) Brazier, J. A.; Shibata, T.; Townsley, J.; Taylor, B. F.; Frary, E.; Williams, N. H.; Williams, D. M. *Nucleic Acids Res.* **2005**, *33*, 1362.
- (227) Hardwidge, P. R.; Lee, D.-K.; Prakash, T. P.; Iglesias, B.; Den, R. B.; Switzer, C.; Maher Iii, L. J. *Chemistry & biology* **2001**, *8*, 967.
- (228) Nuzzolo, M.; Grabulosa, A.; Slawin, A. M.; Meeuwenoord, N. J.; van der Marel, G. A.; Kamer, P. C. *Eur. J. Org. Chem.* **2010**, *2010*, 3229.
- (229) Yang, X. **2009**.
- (230) Basha, A.; Lipton, M.; Weinreb, S. M. *Tetrahedron Lett.* **1977**, *18*, 4171.
- (231) Sidler, D. R.; Lovelace, T. C.; McNamara, J. M.; Reider, P. J. *J. Org. Chem.* **1994**, *59*, 1231.
- (232) Lipton, M. F.; Basha, A.; Weinreb, S. M. *Org. Synth.*, 49.
- (233) Németh, B. z.; Guégan, J.-P.; Veszprémi, T. s.; Guillemin, J.-C. *Inorg. Chem.* **2012**, *52*, 346.
- (234) Ahlborn, C.; Siegmund, K.; Richert, C. *JACS* **2007**, *129*, 15218.
- (235) Hudson, R. H.; Ghorbani-Choghamarani, A. *Synlett* **2007**, 870.
- (236) Chinchilla, R.; Nájera, C. *Chem. Rev.* **2007**, *107*, 874.
- (237) Sonogashira, K.; Tohda, Y.; Hagihara, N. *Tetrahedron Lett.* **1975**, *16*, 4467.
- (238) Siemsen, P.; Livingston, R. C.; Diederich, F. *Angew. Chem. Int. Ed.* **2000**, *39*, 2632.

- (239) Elangovan, A.; Wang, Y.-H.; Ho, T.-I. *Org. Lett.* **2003**, *5*, 1841.
- (240) Gelman, D.; Buchwald, S. L. *Angew. Chem. Int. Ed.* **2003**, *42*, 5993.
- (241) Liang, Y.; Xie, Y.-X.; Li, J.-H. *J. Org. Chem.* **2006**, *71*, 379.
- (242) Drescher, S.; Becker, S.; Dobner, B.; Blume, A. *RSC Advances* **2012**, *2*, 4052.
- (243) Chinchilla, R.; Nájera, C. *Chem. Soc. Rev.* **2011**, *40*, 5084.
- (244) Stoll, S.; Schweiger, A. *J. Magn. Reson.* **2006**, *178*, 42.
- (245) Weissman, S.; Sowden, J. C. *JACS* **1953**, *75*, 503.
- (246) Sabacky, M.; Johnson, C.; Smith, R.; Gutowsky, H.; Martin, J. *JACS* **1967**, *89*, 2054.
- (247) Williams, B. B.; al Hallaq, H.; Chandramouli, G.; Barth, E. D.; Rivers, J. N.; Lewis, M.; Galtsev, V. E.; Karczmar, G. S.; Halpern, H. J. *Magn. Reson. Med.* **2002**, *47*, 634.
- (248) Elert, G. *The Physics Hypertextbook* **2005**.
- (249) *CRC handbook of chemistry and physics*; 89th edition (Internet Version 2009) ed.; CRC Press/Taylor and Francis, Boca Raton, FL., 2009.
- (250) Haynes, W. M. *CRC handbook of chemistry and physics*; CRC press, 2012.
- (251) Dougan, L.; Bates, S.; Hargreaves, R.; Fox, J.; Crain, J.; Finney, J.; Reat, V.; Soper, A. *J. Chem. Phys.* **2004**, *121*, 6456.
- (252) Pascal, T. A.; Goddard III, W. A. *J. Phys. Chem. B* **2012**, *116*, 13905.
- (253) Burlamacchi, L. *Mol. Phys.* **1969**, *16*, 369.
- (254) Atkins, P.; Kivelson, D. *J. Chem. Phys.* **1966**, *44*, 169.
- (255) Waterman, K. C.; Adami, R. C. *Int. J. Pharm.* **2005**, *293*, 101.
- (256) Cooney, M. J.; Petermann, J.; Lau, C.; Minter, S. D. *Carbohydr. Polym.* **2009**, *75*, 428.
- (257) Peesan, M.; Supaphol, P.; Rujiravanit, R. *Carbohydr. Polym.* **2005**, *60*, 343.
- (258) Felt, O.; Buri, P.; Gurny, R. *Drug Dev. Ind. Pharm.* **1998**, *24*, 979.
- (259) Fan, M.; Hu, Q.; Shen, K. *Carbohydr. Polym.* **2009**, *78*, 66.
- (260) Ilium, L. *Pharm. Res.* **1998**, *15*, 1326.
- (261) Ji, J.; Hao, S.; Wu, D.; Huang, R.; Xu, Y. *Carbohydr. Polym.* **2011**, *85*, 803.
- (262) Manchanda, R.; Nimesh, S. *J. Appl. Polym. Sci.* **2010**, *118*, 2071.
- (263) Ajun, W.; Yan, S.; Li, G.; Huili, L. *Carbohydr. Polym.* **2009**, *75*, 566.

- (264) Zhang, Y.; Zhang, M. *J. Biomed. Mater. Res.* **2001**, *55*, 304.
- (265) Yamane, S.; Iwasaki, N.; Majima, T.; Funakoshi, T.; Masuko, T.; Harada, K.; Minami, A.; Monde, K.; Nishimura, S.-i. *Biomaterials* **2005**, *26*, 611.
- (266) Wang, X.; Yan, Y.; Lin, F.; Xiong, Z.; Wu, R.; Zhang, R.; Lu, Q. *J. Biomater. Sci. Polym. Ed.* **2005**, *16*, 1063.
- (267) Azad, A. K.; Sermsintham, N.; Chandkrachang, S.; Stevens, W. F. *J. Biomed. Mater. Res. Part B Appl. Biomater.* **2004**, *69*, 216.
- (268) Park, C. J.; Clark, S. G.; Lichtensteiger, C. A.; Jamison, R. D.; Johnson, A. J. W. *Acta Biomater.* **2009**, *5*, 1926.
- (269) Gan, Q.; Wang, T.; Cochrane, C.; McCarron, P. *Colloids and Surfaces B: Biointerfaces* **2005**, *44*, 65.
- (270) Lee, J. I.; Kim, H. S.; Yoo, H. S. *Int. J. Pharm.* **2009**, *373*, 93.
- (271) Lee, C.-M.; Jeong, H.-J.; Kim, S.-L.; Kim, E.-M.; Kim, D. W.; Lim, S. T.; Jang, K. Y.; Jeong, Y. Y.; Nah, J.-W.; Sohn, M.-H. *Int. J. Pharm.* **2009**, *371*, 163.
- (272) Saha, T. K.; Ichikawa, H.; Fukumori, Y. *Carbohydr. Res.* **2006**, *341*, 2835.
- (273) Tokumitsu, H.; Ichikawa, H.; Saha, T.; Fukumori, Y.; Block, L. *STP pharma sciences* **2000**, *10*, 39.
- (274) Sun, Y.; Wan, A. *J. Appl. Polym. Sci.* **2007**, *105*, 552.
- (275) Park, J. H.; Cho, Y. W.; Chung, H.; Kwon, I. C.; Jeong, S. Y. *Biomacromolecules* **2003**, *4*, 1087.
- (276) Fu, X.; Huang, L.; Zhai, M.; Li, W.; Liu, H. *Carbohydr. Polym.* **2007**, *68*, 511.
- (277) Chen, X.-G.; Wang, Z.; Liu, W.-S.; Park, H.-J. *Biomaterials* **2002**, *23*, 4609.
- (278) Liu, S.-Q.; Qiu, B.; Chen, L.-y.; Peng, H.; Du, Y.-M. *Rheumatol. Int.* **2005**, *26*, 52.
- (279) Liu, Z.; Jiao, Y.; Zhang, Z. *J. Appl. Polym. Sci.* **2007**, *103*, 3164.
- (280) Jayakumar, R.; Prabakaran, M.; Nair, S. V.; Tokura, S.; Tamura, H.; Selvamurugan, N. *Prog. Mater. Sci.* **2010**, *55*, 675.
- (281) Mourya, V. K.; Inamdar, N. N.; Choudhari, Y. M. *Polym. Sci. Ser. A* **2011**, *53*, 583.
- (282) Dash, M.; Chiellini, F.; Ottenbrite, R. M.; Chiellini, E. *Prog. Polym. Sci.* **2011**, *36*, 981.
- (283) Mourya, V.; Inamdar, N. N.; Tiwari, A. *Adv. Mater. Lett.* **2010**, *1*, 11.
- (284) Harish Prashanth, K. V.; Tharanathan, R. N. *Trends Food Sci. Technol.* **2007**, *18*, 117.
- (285) Rinaudo, M. *Prog. Polym. Sci.* **2006**, *31*, 603.

- (286) Mourya, V.; Inamdar, N. N. *React. Funct. Polym.* **2008**, *68*, 1013.
- (287) Jayakumar, R.; Prabakaran, M.; Reis, R.; Mano, J. *Carbohydr. Polym.* **2005**, *62*, 142.
- (288) Jiao, T. F.; Zhou, J.; Zhou, J.; Gao, L.; Xing, Y.; Li, X. *Iran. Polym. J.* **2011**, *20*, 123.
- (289) Muzzarelli, R. A. *Carbohydr. Polym.* **1988**, *8*, 1.
- (290) de Abreu, F. R.; Campana-Filho, S. P. *Carbohydr. Polym.* **2009**, *75*, 214.
- (291) Vaghani, S. S.; Patel, M. M.; Satish, C. *Carbohydr. Res.* **2012**, *347*, 76.
- (292) Dmitriev, B. A.; Knirel, Y. A.; Kochetkov, N. K. *Carbohydr. Res.* **1975**, *40*, 365.
- (293) Pillai, C. K. S.; Paul, W.; Sharma, C. P. *Prog. Polym. Sci.* **2009**, *34*, 641.
- (294) Zhang, H.; Neau, S. H. *Biomaterials* **2001**, *22*, 1653.
- (295) Kasaai, M. R.; Arul, J.; Charlet, G. *J. Polym. Sci., Part B: Polym. Phys.* **2000**, *38*, 2591.
- (296) Chatelet, C.; Damour, O.; Domard, A. *Biomaterials* **2001**, *22*, 261.
- (297) Kurita, K.; Kaji, Y.; Mori, T.; Nishiyama, Y. *Carbohydr. Polym.* **2000**, *42*, 19.
- (298) Klotzbach, T.; Watt, M.; Ansari, Y.; Minteer, S. D. *J. Memb. Sci.* **2006**, *282*, 276.
- (299) LeHoux, J.-G.; Dupuis, G. *Carbohydr. Polym.* **2007**, *68*, 295.
- (300) Errington, N.; Harding, S.; Vårum, K.; Illum, L. *Int. J. Biol. Macromol.* **1993**, *15*, 113.
- (301) Nordtveit, R. J.; Vårum, K. M.; Smidsrød, O. *Carbohydr. Polym.* **1996**, *29*, 163.
- (302) Lee, K. Y.; Ha, W. S.; Park, W. H. *Biomaterials* **1995**, *16*, 1211.
- (303) Chen, L.; Tian, Z.; Du, Y. *Biomaterials* **2004**, *25*, 3725.
- (304) Chen, X.-G.; Park, H.-J. *Carbohydr. Polym.* **2003**, *53*, 355.
- (305) Montalbetti, C. A. G. N.; Falque, V. *Tetrahedron* **2005**, *61*, 10827.
- (306) Liu, C.-G.; Desai, K. G. H.; Chen, X.-G.; Park, H.-J. *J. Agric. Food. Chem.* **2004**, *53*, 437.
- (307) Jing, H.; Guo, Z.; Guo, W.; Yang, W.; Xu, P.; Zhang, X. *Bioorg. Med. Chem. Lett.* **2012**, *22*, 3418.
- (308) Reusch, W. In *Virtual Text of Organic Chemistry* 1999.
- (309) Filosa, R.; Peduto, A.; Aparoy, P.; Schaible, A. M.; Luderer, S.; Krauth, V.; Petronzi, C.; Massa, A.; de Rosa, M.; Reddanna, P. *Eur. J. Med. Chem.* **2013**, *67*, 269.
- (310) Wawrzinek, R.; Ziomkowska, J.; Heuveling, J.; Mertens, M.; Herrmann, A.; Schneider, E.; Wessig, P. *Chem. Eur. j.* **2013**, *19*, 17349.

## References

---

(311) Wessig, P.; Möllnitz, K. *J. Org. Chem.* **2008**, *73*, 4452.

(312) Chen, F.; Zhang, G.; Hong, Z.; Lin, Z.; Lei, M.; Huang, M.; Hu, L. *Bioorg. Med. Chem. Lett.* **2014**, *24*, 2379.



## 9. Appendices

### 9.1. Materials

All chemicals used for synthesis were purchased from Sigma-Aldrich (Schnelldorf, Germany), Alfa Aesar (Karlsruhe, Germany), VWR (Darmstadt, Germany), Carl Roth (Karlsruhe, Germany), Fisher Scientific (Nidderau, Germany), or Acros Organics (Geel, Belgium) and were used without further purification. Buffer salts were obtained from Gruessing (Filsum, Germany). Medium-chain triglycerides (Pionier<sup>®</sup> MCT) and isopropyl myristate (Pionier<sup>®</sup> IPM) were purchased from Hansen & Rosenthal KG (Hamburg, Germany), Acetone and glycerol were obtained from VWR International (Fontenay-sous-Bois, France). Water was used in double distilled quality. Buffer salts were obtained from Gruessing (Filsum, Germany). <sup>13</sup>C labelled chloroform was purchased from Cambridge Isotope Laboratories Ins.

Chitosan and Carboxymethylchitosan were kindly offered from Heppe Medical Chitosan GmbH, Halle (Saale), Germany. Chitosan 95/500, Degree of deacetylation was 95.2%, molecular weight was 200–400 kDa and viscosity (1% in 1% acetic acid, 20 °C) was 449 mPaS. Carboxymethyl chitosan, Degree of deacetylation was 91.2%, molecular weight was 30–500 kDa and viscosity (1% in water, 20 °C) was 56 mPaS.

### 9.2. General methods for synthesis and analytical characterization

All organic solvents were purified and dried before use and stored over molecular sieve (3 Å). Glassware for reactions under argon atmosphere was oven-dried at 100 °C for 2 h prior use, evacuated, and flushed with argon immediately. The purity of all compounds and the progress of reactions were monitored by thin layer chromatography (TLC) using silica gel 60 F<sub>254</sub> plates (Merck KGaA, Darmstadt, Germany). Visualizations were accomplished with an UV lamp (254 nm) or I<sub>2</sub> stain and the R<sub>f</sub> values given are uncorrected. Purification of the compounds was achieved either by crystallization from appropriate solvents or Flash chromatography. Flash chromatography was performed as follows: (1) Silica gel 60 (Merck, 0.040–0.063 mm) was suspended in appropriate eluent, poured into glass columns of appropriate size and the crude mixture was applied as solid. (2) The purification of compounds via middle pressure liquid chromatography (MPLC) was performed on a PuriFlash 430 (Interchim, Montluçon, France) using pre-packed columns with silica gel of different pore sizes (0.015–0.050 mm) and different quantities (12–30 g silica gel). Melting points (mp) were determined with Boetius apparatus. NMR spectra were recorded on a Varian (now Agilent Technologies, Böblingen, Germany) Inova 500 MHz or an Agilent Technologies VNMR 400 MHz. Chemical shifts (δ) are reported

in parts per million (ppm) relative to the residual non-deuterated solvent peak in the corresponding spectra (chloroform  $\delta = 7.26$ , methanol  $\delta = 3.31$ , DMSO  $\delta = 2.49$ ). The splitting pattern was assigned as follows: s = singlet, bs = broad singlet, d = doublet, t = triplet, q = quartet, m = multiplet and coupling constants (J) are given in Hertz (Hz).  $^{13}\text{C}$  NMR chemical shifts were reported as  $\delta$  values (ppm) relative to the residual non-deuterated solvent peak in the corresponding spectra (chloroform  $\delta = 77.2$ , methanol  $\delta = 49.0$ , DMSO  $\delta = 39.5$ ). NMR spectra were analyzed using MestReNova, version 6.0.2-5475 software. Mass spectrometry (MS): Electron spray ionization (ESI) mass spectra were recorded on a LCQ Classic (Thermo Finnigan, San Jose, California, USA). Electron impact (EI) mass spectra were recorded on an AMD 402 (AMD Intectra GmbH, Harpstedt, Germany) with a medium ionization voltage of 70 eV. Infrared spectra (IR) spectra were recorded on an IFS 28 FTIR spectrometer (Bruker, Billerica, USA) with a Thermo Spectra-Tech ATR unit (Thermo Scientific). IR spectra reported in reciprocal centimeter ( $\text{cm}^{-1}$ ). The samples were analyzed on an orbitrap XL mass spectrometer (Thermo Fisher Scientific) with a resolving power of 100000 at  $m/z$  400, samples were introduced to the MS by static nano-electrospray ionization.

### 9.3. LDH-release and cell activity/proliferation <sup>\*\*\*\*</sup>

Tris(tetrathia- and tetrachloroaryl)methyl radicals (TAMs) are a class of trityl radicals which shows an intense, single and narrow EPR line at concentrations in the  $\mu\text{M}$  range, water solubility (as tricarboxylates) and stability in biological systems. These radicals might be advantageous not only for EPR imaging with monitoring of oxygen concentration and pH, but also for MRT imaging. The present study tested the effects of a deuterated thia TAM tricarboxylic acid (d-TAM) on the growth of fibroblast cells and the phenotype of rat erythrocytes. The study was performed in strong accordance to DIN EN ISO 10993. After cultivation of 3T3 cells (mouse fibroblasts) in cell culture medium supplemented with d-TAM at different concentrations (50, 250 and 500  $\mu\text{M}$ ), the 3T3 and erythrocyte phenotypes did not change. Neither did d-TAM impact functional 3T3 cell membrane integrity (LDH release) and cell activity/proliferation (MTS assay). These results prove d-TAM to be non-cytotoxic and compatible to erythrocytes and suggest d-TAM for further tests *in vivo* to investigate the usefulness for MRT imaging. The chemically related tris(tetrachlorophenyl)tricarboxylic acid did not affect the morphology of both cell types at 50-500  $\mu\text{M}$ , but decreased proliferation with concomitant LDH release at 50 and 250  $\mu\text{M}$ .

---

<sup>\*\*\*\*</sup> These results were presented as abstract: **Biocompatibility of a triarylmethyl (trityl) radical, candidate for MRT contrast media.** 33<sup>rd</sup> DGKMH Jahrestagung 2014, Villingen-Schwenningen (abstract).



#### **9.4. Acknowledgement**

First and foremost, I am thankful for “Allah”, the most gracious and the most merciful.

I would like to express my appreciation and sincere gratitude to Prof. Peter Imming for his continuous support, valuable advices, endless encouragement and great efforts in supervision through the development of this work. Moreover, his great efforts to resolve any trouble I had during my stay in Germany, is highly appreciated by me and my husband Tamer.

My profound thanks are due to Prof. Karsten Mäder for his supervision as well as for providing me lab facilities for the EPR and UV measurements.

I am grateful to Prof. Dariush Hinderberger and Dr. Nadica Maltar Strmecki for their kind co-operation, performing some EPR measurements and a great help in the interpretation of data.

Dr. Hendrik Metz is acknowledged for his guidance in some EPR experiments.

I am indebted to Dr. Simon Drescher for his valuable discussions and suggestions during the work. In addition, Dr. Drescher and Ms. Juliane Frank are acknowledged for carrying out the EPR oximetry studies.

Prof. Mohamed El-Sadek (Zagazig University, Egypt), Dr. Mohamed Mokhtar and Dr. Hosam Eldin Abd Elhamed (Suez Canal University, Egypt) are thanked for their supervision during the first two years of my project.

I would like to express my thanks to Dr. Bernhard Hiebl and Ms. Zhanna Svatko for doing MRT imaging and toxicity studies. Dr. Malte Drescher workgroup (University of Konstanz) is acknowledged for performing the cell lysate study

A special thank is extended to Dr. Dieter Stroehl for NMR measurements, Dr. Christian Ihling for HRMS measurements, Ms. Heike Rudolf for IR measurements, Dr. Juergen Schmidt and Dr. Harry Schmidt for EI-MS measurements. My deep thanks for the nice time, fruitful discussions and cultural exchange I had with the group members: Marcel, Henok, Adrian and Sandra. Adrian Richter and Lisa Lampp are further acknowledged for proof reading of the German abstract. Additionally, my thanks go to the lab technician Ms. Sabine Dobberstein for her kindness, helpfulness and lab assistance.

I thank the Egyptian Ministry of Higher Education and Scientific Research and the Institut fuer Angewandte Dermatopharmazie Halle for the financial support.

My infinite appreciation and thanks to my husband Tamer Hassan for his unlimited support, understanding, encouragement and performing UV measurements. I wish to express my gratitude and appreciation to my parents and brother Mohamed for their prayers, good wishes, and encouragement.

I would like to thank everyone, who helped me either in Egypt or Germany.

## 9.5. Curriculum vitae

### PERSONAL INFORMATION

Name	Marwa Aly El-metwaly Mohamed Elewa
Birth date	16.08.1982 in Port Said, Egypt
Nationality	Egyptian
Marital status	Married

### WORK HISTORY

09. 2009 – 02. 2011	Assistant lecturer, Organic Chemistry Department, Faculty of Pharmacy, Suez Canal University, Ismailia, Egypt.
09. 2004 – 09. 2009	Demonstrator, Organic Chemistry Department, Faculty of Pharmacy, Suez Canal University, Ismailia, Egypt.
Since 07. 2004	Pharmacist in private and hospital pharmacies.

### EDUCATION AND TRAINING

04. 2011 – 09. 2015	PhD student in the workgroup of Prof. Dr. Peter Imming, Institute of Pharmacy, Martin-Luther-University Halle-Wittenberg, Halle (Saale), Germany.
04. 2009	MSc. Pharmaceutical Science (Organic Chemistry), Faculty of Pharmacy, Suez Canal University, Ismailia, Egypt. Title of Master thesis: "Synthesis and Biological Activity of Certain Glycosides Containing Aza Heterocycles".
07. 2004	BSc. Pharmaceutical Science, Faculty of Pharmacy, Suez Canal University, Ismailia, Egypt. Graduation Grade: Excellent with Honors.

## 9.6. List of publications

### 9.6.1. Research articles

- Juliane Frank, Marwa Elewa, Mohamed M. Said, Hosam A. El Shihawy, Mohamed El-Sadek, Diana Müller, Annette Meister, Gerd Hause, Simon Drescher, Hendrik Metz, Peter Imming and Karsten Mäder. **Synthesis, characterization, and nanoencapsulation of tetrathiatriarylmethyl and tetrachlorotriarylmethyl (trityl) radical derivatives – a study to advance their applicability as *in vivo* EPR oxygen sensors.** *J. Org. Chem.* **2015**, *80*, 6754.
- Marwa Elewa, Nadica Maltar Strmecki, Hendrik Metz, Mohamed Mokhtar, Hosam Eldin Abd Elhamed, Mohamed El-Sadek, Juliane Frank, Simon Drescher, Karsten Mäder, Dariush Hinderberger and Peter Imming. **Synthesis and EPR characterization of tris(tetrachlorophenyl) tricarboxylic acid methyl radical and its <sup>13</sup>C labelled analog.** To be submitted.
- Mohamed M. A. Said, Marwa A. El-metwaly, Mohy El-dein Abd el-fattah, and Adel A. El-gendy, **Synthesis of Biologically Active Compounds Based on Indole -2-Carboxylate Scaffold.** *Egypt. J. Biomedical. Sci.* (2009), *30*, 41-53.

### 9.6.2. Conference contributions

- Marwa Elewa, Peter Imming, Hendrik Metz, Zhanna Svatko, M. Knörger and Bernhard Hiebl. **Biocompatibility of a triarylmethyl (trityl) radical, candidate for MRT contrast media.** 33<sup>rd</sup> DGKMH Jahrestagung 2014, Villingen-Schwenningen (abstract).
- Marwa Elewa, Juliane Frank, Karsten Mäder, Simon Drescher and Peter Imming. **Triarylmethyl radicals: Synthesis, EPR characterization and pharmaceutical applications.** DPhG Jahrestagung 2014, Frankfurt (Poster).
- Juliane Frank, Marwa Elewa, Simon Drescher, Mariana Albanez Campos, Peter Imming and Karsten Mäder. **Poly(vinyl acetate) nanocapsules as a carrier for lipophilic oxygen-sensitive EPR spin probes.** 9th World Meeting on Pharmaceutics, Biopharmaceutics and Pharmaceutical Technology 2014, Lissabon, Portugal (Poster).
- Marwa Elewa, Juliane Frank, Simon Drescher, Hendrik Metz, Karsten Mäder and Peter Imming. **Synthesis and EPR measurements of the perchlorotriphenylmethyl-tricarboxylic acid radical (PTMTC) and its <sup>13</sup>C labelled analogue (<sup>13</sup>C-PTMTC).** DPhG Jahrestagung 2013, Freiburg (Poster).
- Marwa Elewa, Diana Müller, Juliane Frank, Sabine Kempe, Simon Drescher, Mohamed El-Sadek, Mohamed Mokhtar, Hosam Eldin Abd Elhamed, Karsten Mäder and Peter Imming. **Synthesis and EPR measurement of perchlorotriphenylmethyl radicals and their conjugates with biopolymers.** 3<sup>rd</sup> International Conference of the Faculty of Pharmacy & 15<sup>th</sup> Scientific Congress of the Association of Pharmacy Colleges in the Arab world 2012, Amman, Jordan (Poster).

### **9.7. Selbständigkeitserklärung**

Hiermit erkläre ich gemäß § 5 der Promotionsordnung der Naturwissenschaftlichen Fakultät I der Martin-Luther-Universität Halle-Wittenberg, dass ich die Ergebnisse der vorliegenden Dissertationsarbeit

**„ Synthesis, EPR characterization and chitosan labelling of triarylmethyl radicals “**

am Institut für Pharmazie der Martin-Luther-Universität Halle-Wittenberg unter Anleitung von Herrn Professor Dr. rer. nat. habil. Peter Imming selbständig erarbeitet und die Dissertation ohne fremde Hilfe verfasst habe. Ich habe keine anderen als die von mir angegebenen Quellen und Hilfsmittel benutzt und die den verwendeten Werken wörtlich oder inhaltlich entnommenen Stellen als solche kenntlich gemacht. Weiterhin habe ich diese Arbeit bisher an keiner in- oder ausländischen Fakultät als Dissertationsschrift vorgelegt.

Halle (Saale), den 30.07.2015

Marwa Elewa, MSc.